international conference

FT 2023

conference proceedings

Darko Lovrec
Vito Tič
Editors

University of Maribor Press

Fluid Power 2023
Fluidna Tehnika 2023

International Conference Fluid Power 2023

Conference Proceedings

Editors
Darko Lovrec
Vito Tič

September 2023

Table of Contents

FLUID POWER TECHNOLOGY AND DEVELOPMENT TRENDS

FRANC MAJDIČ

University of Ljubljana, Faculty of Mechanical Engineering, Ljubljana, Slovenia
franc.majdic@fs.uni-lj.si

Fluid power represents one of the possibilities of controlled energy transfer. Although nowadays especially political actors on a global level strongly push electric drives, hydraulics is still unavoidable. Fluid power also impacts the carbon footprint, so reducing this impact is a very important trend. From a hydraulics perspective, this can be achieved by improving the efficiency of individual components. The average overall efficiency of hydraulic systems is between 23 % and 30 %, so it is necessary to analyse in depth the causes of this situation and take action. Users of hydraulic components want to calculate the service life of each hydraulic component, similar to bearings. It is also a modern trend to set up digital twins, i.e. numerical models and measurement and control systems that use machine learning to tell the user the current state of the system. The use of computer simulations and 3D printing is also very important.

1   Introduction

Fluid power is the generation, transmission, and control of power through the use of pressurised fluids. Fluid power technology is continuously developing according to all other technical improvements from digitalisations, low energy consumption, to full diagnostic, green and smart. For decades there has been competition between electric and hydraulic drives, today the electric ones are particularly exposed. Global political trends are trying to convince that electric drives are the only solution for our future, which will be green and progressive. Despite all this, hydraulic drives have remained and will remain, as they are constantly improved and adapted to global trends. Today, it is impossible to imagine heavy construction, agricultural, forestry, mining, marine, aviation, iron, woodworking and other machines without hydraulic drives. They are particularly suitable for heavy loads, fast and precise positioning, etc. Advantages of fluid power – hydraulics are: high power density – small volume of components, good damping of dynamic loads, simple and reliable protection of the system against overload, easy change of the direction of movement, simple adjustment of force or moment, fast response, large rigidity, etc.

Fluid power is evolving in multiple ways: fluids, components, materials, technologies, alternative technologies - 3D printing, mechatronics, digitalization, engineering diagnostics, carbon footprint, soft robotics, humanoid robotics, remote learning, internet of things, etc. In hydraulics, there are other obstacles on the road to improvement: higher production costs, high system complexity, implementation effort, incomplete use of digital solutions, etc.

The field of fluid power is also linked to the effects of climate change, which indirectly cause natural disasters such as higher temperatures, hurricanes, tornadoes, floods, etc. From 1890 to today [1], the ambient temperature in Europe has risen by an average of 1,6 °C (Fig. 1).

The environment, therefore, requires quick and effective action so that we do not suffer even greater disasters. Experts warn that an increase in the average environmental temperature of only 2 °C in the next ten years can cause a complete melting of the Arctic ice (Fig. 2) [2], that up to 99 % of tropical coral reefs can disappear, that river floods can increase by 170 % (as was the case in Slovenia this August), that sea levels can rise by more than a meter.
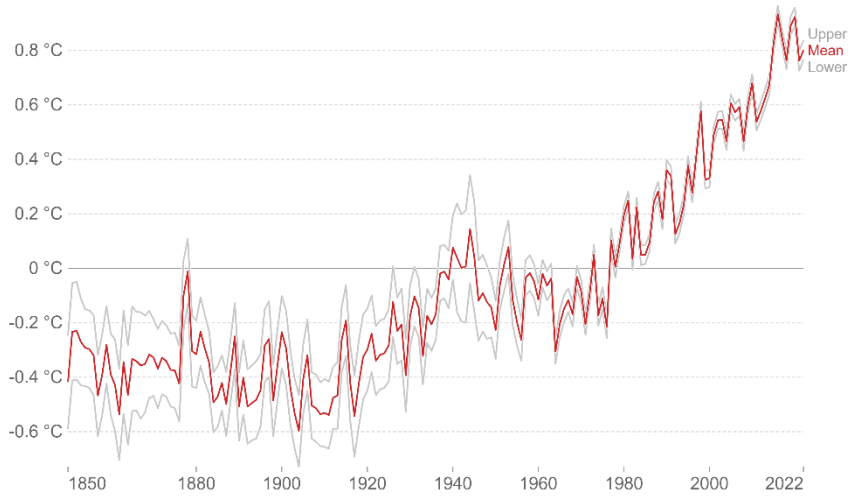
Source: Met Office Hadley Centre (HadCRUT5) OurWorldInData.org/co2-and-greenhouse-gas-emissions • CC BY
Note: The gray lines represent the upper and lower bounds of the 95% confidence intervals.

Figure 1: Change of global average land-see temperature during the years [1]
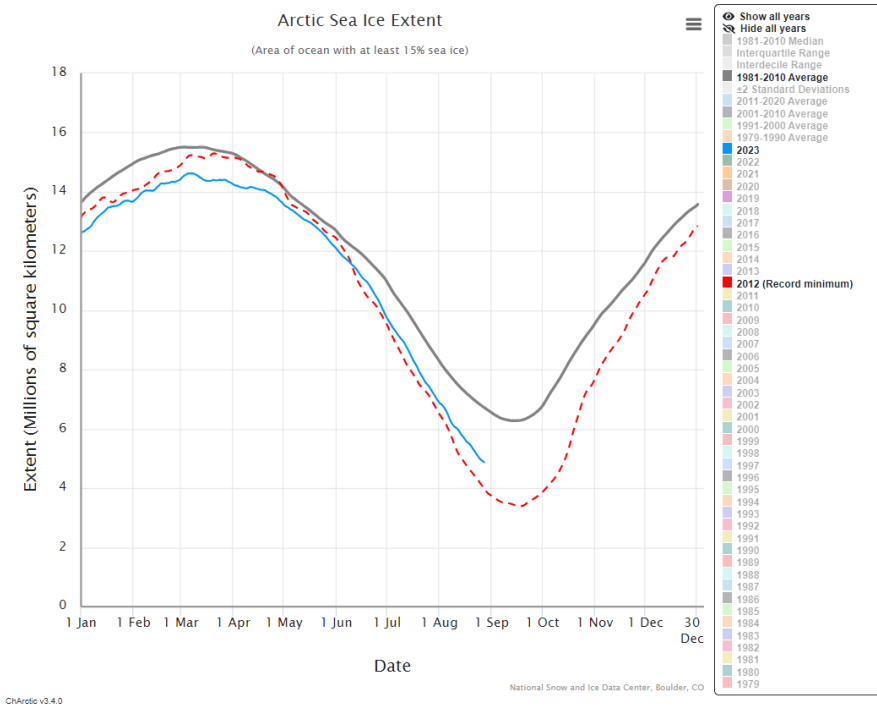
Figure 2: Change of Artic Sea Ice [2]

2 Increasing energy efficiency

Fluid power consumes between $66 \cdot 10^{10}$ kWh and $88 \cdot 10^{10}$ kWh annually, of which 40 % is used by mobile machinery, 56 % by industrial hydraulics and 3 % by aviation. With the above amount of energy consumed annually, hydraulic systems produce between 310 and 380 million metric tons (MMT) of carbon dioxide. According to the British Fluid Power Association, the efficiency of downstream fluid power systems ranges from 23 % to 30 % [3].

Hydraulic systems produce kinetic energy in the form of flow and potential energy in the form of pressure. Internal tribological contact between movable and stationary elements inside of hydraulic components (mostly pumps and valves) do not have sealings, but very low gap. Pressure difference in gaps occurs internal leakage, where hydraulic pressure energy converts into higher fluid temperature. Inadequate, degraded cleanliness of the hydraulic fluid affects more wear and increases the gap between two elements. As internal leakage through the gaps increases, the volumetric efficiency of the observed component decreases [4].

Digital hydraulic valves enable energy-efficient use in position and pressure control [5]. Such digital valves can be found in many industry branches. They are characterised by fast regulation and little or no internal leakage because a seat valve is used (Fig. 3). It also allows energy recuperation and can be used in many applications, such as cranes, forklifting trucks, etc.

Due to internal leakage in hydraulic components and pressure differences in flow through hydraulic lines and components, hydraulic energy is converted to heat. Heating the hydraulic fluid changes its properties, which is not desirable. Therefore, high-quality heat dissipation is very important. New high-quality cooling solutions are constantly being developed for this purpose. of heat dissipation from the hydraulic fluid to the environment [6].

3 Improving system reliability

Reliability for hydraulic **fluids** include viscosity, wear protection, thermal stability, corrosion inhibition, foam resistance, demulsibility (ability to release water), oxidation life and cleanliness. Pressure-dependent fluid properties, which include

bulk modulus, density and traction, can have a large effect on hydraulic system efficiency [4, 7, 8].
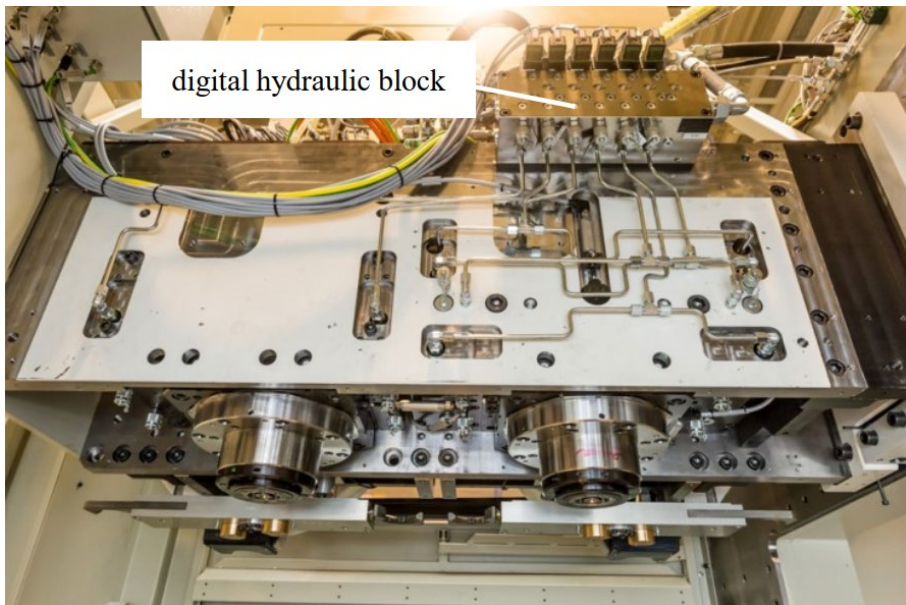
Figure 3: Micro-positioning system with digital valves [5]

3.1 Predicting of lifetime components in connection with cleanliness of hydraulic fluid

The reliability and service life of hydraulic components depend heavily on their working conditions, especially on the cleanliness of the hydraulic fluid used. Many experts worldwide are engaged in determining the service life of individual hydraulic components as a function of cleanliness. Real wear particles with their technical properties (hardness, toughness, ...) migrate with the hydraulic fluid and wear the sealing sliding surfaces of the components. Because it is difficult to obtain real wear particles and because such tests take a long time, research is currently underway to determine the acceleration factor of sustained wear tests using an abrasive-aggressive standard test powder (MTD) [9] (Fig. 4). Novak et al. for the first time investigated the wear of a hydraulic gear pump with external gearing separately with test dust and with wear particles [10].
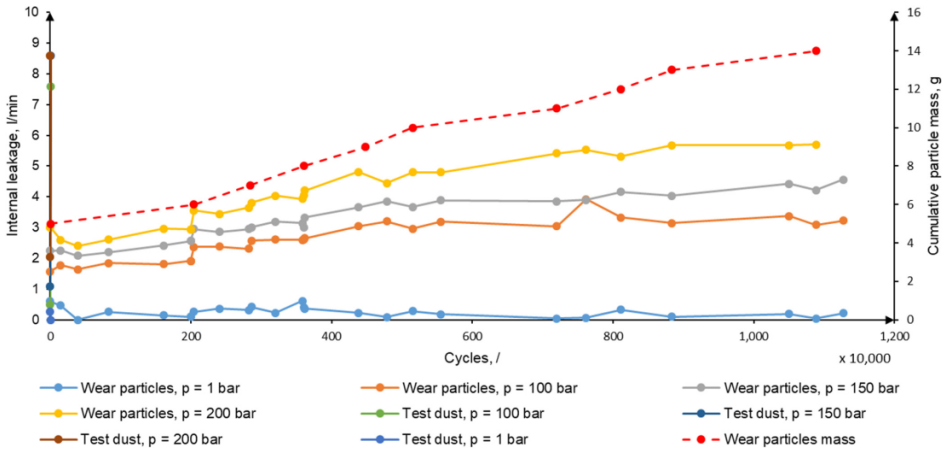
Figure 4: Comparison of volumetric efficiencies of hydraulic pump at different operation pressure, test dust and wear particles [9]

3.2   Opportunity for condition monitoring and predictive maintenance over digital twins & virtual sensors

Monitoring the condition of hydraulic components and systems can save a lot of money due to the high probability of avoiding failures. Damage/wear can be detected at an early stage so that early action can be taken on this basis to prevent the worst from happening. With proper condition monitoring, we can detect failures of individual parts of the observed hydraulic component. American researchers [11] have developed a method for detecting a worn valve plate (Fig. 5) of a variable displacement axial piston pump that reduces the number of sensors required to five.
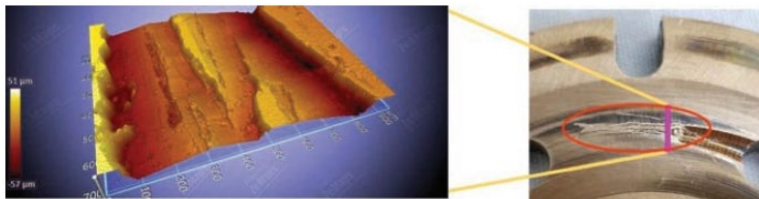
Figure 5: Valve plate with severe damage [11]

To successfully detect the valve plate failure, they measured the inlet and outlet pressures, drain pressure, the number of revolutions of the drive shaft, and the actual flow rate at the pump's outlet pressure port.

4 Building intelligent systems

Trends in the development of fluid power are strongly oriented toward complete digitization in several areas [4]:

- Industry 4.0 (cyber-physical systems, IoT)
- Fusion of physical machines and embedded systems
- Digital twin / digital shadow of machines, systems, processes
- Big Data and advanced data analytics, etc.
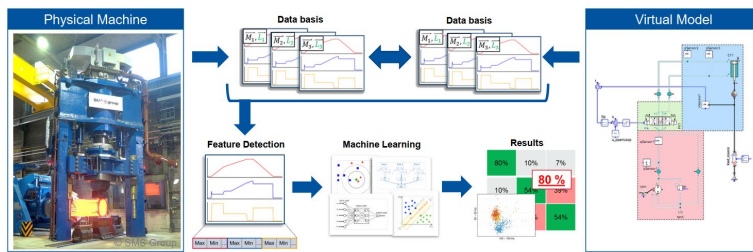
Figure 6: Hydraulic press digital twin [4]

5 Reducing the size and weight of components

Size and weight of materials can be reduced by various approaches. To name a few:

- new, alternative materials,
- shape optimization and iterative processes,
- 3D printing.

New and alternative materials

First, the tendencies of using new materials are divided into groups according to their definition or application. Here we divide them into base materials and materials used for coating. Since most hydraulic components are made of metals and metal alloys, the tendencies focus on improving the chemical structure of existing materials. This is achieved by creating the perfect mix of raw materials and combining them (melting) to create more durable materials that can better withstand stresses and, if possible, reduce the weight of the final structure [12]. In relation to

metallic structures, many studies and thus development of coating layers have been carried out recently. The main function of coatings is to better resist corrosion, erosion and cavitation. Different materials and alloys bring a wide range of different coating properties, which must be very well understood in order to select the right coating for a particular application. Coatings can be classified according to the initial state of the coating material:

- Vapor phase: chemical vapor deposition (CVD) and physical vapor deposition (PVD) (Fig. 7) both use a plasma as the main energy source for depositing materials
- Solution state: electrochemical deposition, salt-gel, …
- Molten (or partially molten) state: laser deposition, welding, …

Materials used for coatings include hard and soft coatings, which are mostly polymers. Metals used for coating applications: molybdenum disulfite, titanium nitride, nickel, chromium, copper, silver, gold, cadmium, platinum, indium and others. As mentioned earlier, some coatings that are highly wear resistant are not based on metals, but are mostly polymers. To name a few: PTFE, polyamides, elastomer coatings and others.

Figure 7: PVD coated gear [13]

Some polymer materials can also be used as stand-alone materials: Polyamides, polyester resins, PEEK, UHMWPE, POM, PTFE, and others.

We can hardly talk about new materials without talking about carbon-based materials. The widely used carbon fibers combined with polyester resins can be either in an organized form as a fabric or in a chaotic state with fibers randomly

distributed in the volume, which is called forged carbon fibers. Carbon allows structures to withstand large loads while keeping weight to a minimum. Many studies have also been conducted on carbon nanostructures in the form of nanotubes [14]. These studies have shown that nanotubes can withstand the highest loads measured up to now, more than any other known materials.

Shape optimization and iterative processes

Shape optimization is an old process of removing unnecessary volume of initial material to reduce the mass of the structure. This can be, has been, and in some cases is done by hand. However, knowing how much material can be removed to make the structure withstand the applied loads and strains is a very complex numerical process. Basically, it's a question of "how much is too much". Human instinct is incapable of such operations, so computers have had to be used to achieve optimal results. The use of modern software to determine the optimum shape and mass to be removed based on loads and constraints with a known initial volume is called topology optimization. In this type of shape optimization, finite element methods are used to calculate the stresses that occur in the volume of material to determine where and how much material can be safely removed so that the object can still perform its intended tasks [15].

In a slightly different approach, the iterative methods are not limited by the initial volume and can produce a variety of different solutions to the same problem, allowing the designer to choose the optimal one. Typically, different solutions are compared based on strength, the material used, and the overall shape that must meet the requirements or constraints. One such process is generative design [16]. Generative designs are also distinguished by their purpose. Solutions can be purely structural, but in some cases it is the internal structure that needs to be optimised for fluid flow. This is then generative design, which incorporates CFD as part of the solution to reduce the pressure drop through the structure through which the fluid flows.

3D printing

Directly related to the previous subsection on optimization, some structures are impossible or to complex to produce using the subtractive manufacturing techniques known and used so far [17]. For these structures, 3-dimensional printing of materials is used. Since firstly introduced and patented 1970, 3D printing has become almost

an industry in itself (Fig. 8), supporting other processes where possible and where other processes fall short [18]. Printing a wide variety of polymers and metals, this type of manufacturing can be used to produce complex internal geometries and closed structures, which is important in the field of hydraulics [19].
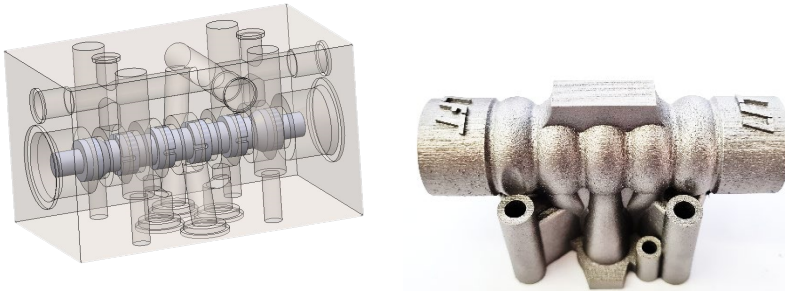
Figure 8: Comparison of conventional (left) and 3D printed (right) Hydraulic valve [20]

6   Reduction of negative impacts on the environment

It is almost impossible to define all the impacts that hydraulic systems have on the environment during and after their life cycle. However, it is important that engineers are at least aware of the main pollutants that affect the environment of hydraulic systems. In this way, it is possible to reduce these impacts in order to minimize them and, consequently, the negative consequences for the environment [21].

In the context of hydraulics, there are several influences that have a negative impact on the environment:

- – Reduced air quality,
- – Noise and vibration,
- – Soil and ground pollution,
- – Ground and underground water pollution, etc.

Since all of these environmental impacts are directly related to human health and well-being, engineers should consider environmental impacts when designing new hydraulic systems. While vibration and noise reductions are related to system operation, soil contamination and contamination of the earth are due to improper

disposal of fluids and structures. Recycling as many materials as possible can only be achieved if the system is designed for reuse in the first place. For example, the automotive industry has begun to reduce the use of non-recyclable materials, especially plastics [20].

Dealing with noise and vibration normally requires some type of enclosure. However, this is changing in the case of hydraulic systems as they present new challenges in terms of maintenance, retrofitting, heat dissipation, etc…

Improving air quality has become an ongoing debate about "how to", but we have yet to move from words to action. Similar to soil and land pollution, air pollution is not only associated with equipment when it is in operation. The manufacture, transport of parts and the improper disposal of components and fluids can also have a major impact on the environment, so we must always look at the entire life cycle to understand the big picture.

7 Conclusions

This paper provides an overview of the current state of development and guidelines for fluid power. One of the biggest global problems is the warming of the atmosphere, to which fluid power also contributes. It produces an average of 345 million metric tons of carbon dioxide per year. The situation can be improved by lower consumption and better hydraulic efficiency, which averages only 26%. The main trends in hydraulics are digitalization, digital twins, advanced automation, reliability improvement, ability to predict component life depending on operating parameters, advanced numerical simulations, building intelligent self-learning hydraulic systems, Big Data management and storage, green technologies, advanced green hydraulic fluids, new advanced materials, additive technologies – 3D printing, etc.

With further development in the above directions, fluid power will by no means die out, but will continue to be used in the future and compete with electric and other drives.

References

[1]   Our World in Data. (2023). Global average land-sea temperature anomaly relative to the 1961-1990 average temperature, Source*: https://ourworldindata.org/grapher/temperature-anomaly*, Last visited: 31. 08. 2023

[2]   Earth observatory. (2023). World of Change: Arctic Sea Ice. Source: *https://earthobservatory.nasa.gov/world-of-change/sea-ice-arctic.* Last visited: 31. 08. 2023

[3]   Michael, P., McGuire, N., (2020). Getting the Most Efficiency Out of Hydraulics, Power & Motion, Source: *https://www.powermotiontech.com/print/content/21125703*, Last visited: 30. 08. 2023

[4]   Schmitz, K. (2022). The potential of fluid power technology, *13th IFK*

[5]   Winkler, B. (2017). Recent advantages in digital hydraulic components and applications. *The Ninth Workshop on Digital Fluid Power, September 7-8, 2017, Aalborg, Denmark*

[6]   Lipnicky, M., Brodnianska, Z. (2023). Z. Enhancement of Heat Dissipation from the Hydraulic System Using a Finned Adaptive Heat Exchanger, *Applied Science, 13*, 5479

[7]   Lovrec, D., Kalb, R., Tič, V. (2023). Application areas of ionic hydraulic fluids. *Chemical engineering & technology,* vol. 46, iss. 1, 14-20. ISSN 1521-4125. doi: 10.1002/ceat.202200368.

[8]   Lovrec, D., Tič, V. (2022). The importance of the electrical properties of hydraulic fluids. *Industrial Lubrication and Tribology.* vol. 74, iss. 3, 302-308. ISSN 0036-8792. doi: 10.1108/ILT-06-2021-0218

[9]   Novak, N., Trakovski, A., Kalin, M., Majdič, F. (2023). Degradation of Hydraulic System due to Wear Particles or Medium Test Dust, *Appiled Sciences*, 13, 7777

[10]   Novak, N., Trakovski, A., Polajnar, M., Kalin, M., Majdič, F. (2023). Wear of hydraulic pump with real particles and medium test dust, *Wear*, 532-533 (2023) 205101

[11]   Keller, N., Sciancalepore, A., Vacca, A. (2022). Demonstrating a Condition Monitoring Process for Axial Piston Pumps with Damaged Valve Plates, *International Journal of Fluid Power, Vol. 23 2*, 205–236

[12]   Quaranta E., Davies P. (2021). Emerging and Innovative Materials for Hydropower Engineering Applications: Turbines, Bearings, Sealing, Dams and Waterways, and Ocean Power, *Engineering, Volume 8,* ISSN 2095-8099, https://doi.org/10.1016/j.eng.2021.06.025.

[13]   Strmčnik, E. (2020). *Vplivni parametri na delovanje orbitalnega hidravličnega motorja na vodo,* doctoral dissertation. University of Ljubljana, Faculty of Mechanical Engineering.

[14]   Gupta, N., Gupta, S.M. & Sharma, S.K. (2019) Carbon nanotubes: synthesis, properties and engineering applications. *Carbon Lett. 29*, 419–447. https://doi.org/10.1007/s42823-019-00068-2

[15]   Woon, S., Querin, O. & Steven, G. (2001) Structural application of a shape optimization method based on a genetic algorithm. *Struct Multidisc Optim. 22*, 57–64. https://doi.org/10.1007/s001580100124

[16]   Gunpinar, E., Coskun, U. C., Ozsipahi, M., Gunpinar, S. (2019). A Generative Design and Drag Coefficient Prediction System for Sedan Car Side Silhouettes based on Computational Fluid Dynamics, *Computer-Aided Design, Volume 111*, Pages 65-79, ISSN 0010-4485, https://doi.org/10.1016/j.cad.2019.02.003.

[17]   Ngo, T. D., Kashani, A., Imbalzano, G., Nguyen, K.T.Q., Hui, D. (2018) Additive manufacturing (3D printing): A review of materials, methods, applications and challenges. *Compos. Part B Eng. 143*, 172–196.

[18]   Zhu, Y., Yang, Y., Lu, P., Ge, X., Yang, H. (2019). Influence of surface pores on selective laser melted parts under lubricated contacts: a case study of a hydraulic spool valve. *Virtual Phys. Prototyp. 2759*, 1–14.

[19]   Aidro Hydraulics (2023): Additive manufacturing Aidro: 3d printing for hydraulic components, AMES valves, Source: *https://aidro.it/additive-manufacturing/* , Last visited: 30. 08. 2023.

[20]   Bartolj, J. (2022). Razvoj 4/3 proporcionalnega potnega ventila za izdelavo s postopkom 3D tiska kovin. Diploma thesis. University of Ljubljana, Faculty of Mechanical Engineering.

[21]   Artiola, J.F., Walworth, J.L., Musil, S.A., Crimmins, M.A. (2019). Chapter 14 - Soil and Land Pollution, Editor(s): Mark L. Brusseau, Ian L. Pepper, Charles P. Gerba, *Environmental and Pollution Science (Third Edition),* Academic Press, 219-235, ISBN 9780128147191, https://doi.org/10.1016/B978-0-12-814719-1.00014-8.

LEGAL REQUIREMENTS OF HYDRAULIC POWER UNITS

TADEJ TAŠNER
HAWE Hidravlični sistemi d.o.o., Štore, Slovenia
t.tasner@hawe.si

With the growing complexity of modern machinery and in order to ensure their safe and reliable operation, a lot of legal directives, regulations and standards have been published throughout the world. Mechanical engineers often struggle which have to be followed and when. This article focuses on the legal requirements which are applicable to hydraulic power units and their components in the European Single Market. In European Union the fundamental mandatory directive is Machinery Directive (2006/42/EC) which promotes the free movement of machinery within the single market and guarantees a high level of protection for EU workers and citizens. Which part of Machinery Directive is important for hydraulic power units and which other directives also apply will be described on the following pages. (This article was partially prepared before the new Machinery Regulation (Regulation (EU) 2023/1230) was published).

1 Introduction

There are a number of different regulations worldwide that have to be followed. Which of them are applicable is mainly defined by the location where the machine will be used at. As there are too many regulations available this article will focus on the regulations that are applicable when a machine will used in the European Union (EU).

The basic steps when determining which regulations are applicable for our product the following steps are recommended [1]:

1. **Product Classification:** Begin by classifying your product into its appropriate category or sector. Different types of products fall under specific regulations. For example, medical devices, machinery, electrical products, toys, and cosmetics each have their own set of regulations.
2. **Research Directives and Regulations:** Identify the relevant directives or regulations that pertain to your product category. For instance, machinery may fall under the Machinery Directive (2006/42/EC), medical devices under the Medical Devices Regulation (MDR), and so on.
3. **Check Harmonized Standards:** Harmonized standards are technical specifications that provide a presumption of conformity with EU regulations. Check if there are any harmonized standards applicable to your product category. Harmonized standards are listed on the European Commission's official website or in the directives that apply to your product.
4. **Use Online Resources:** There are various online resources provided by the EU, such as the "Your Europe" portal or the "New Approach" website, that offer guidance on product regulations and requirements.
5. **Consult Notified Bodies:** Each EU member state has a designated authority responsible for overseeing product compliance. These authorities can provide guidance on which regulations apply to your product. (List of notified bodies can be found in NANDO database: https://webgate.ec.europa.eu/single-market-compliance-space/#/notified-bodies)
6. **Seek Legal and Regulatory Experts:** If you're uncertain about the applicable regulations, consider seeking advice from legal or regulatory experts who specialize in EU product compliance.

2   List of regulations applicable to hydraulic power units

The following directives and regulations apply to most of the hydraulic power units and when:

Table 1

Name (abbr.)	Number	Applies to
Machinery Regulation[1]	2023/1230	all machinery (all hydraulic power units)
Machinery Directive	2006/42/EC	all machinery (all hydraulic power units)
Pressure Equipment Directive (PED)	2014/68/EU	hydraulic power units with built in pressure equipment
Ecodesign Regulation	2019/1781	hydraulic power units using electric motors or variable speed drives
Low Voltage Directive (LVD)	2014/35/EU	hydraulic power units operating with input/output voltage between 50 and 1000 VAC or 75 and 1500 VDC
Electromagnetic Compatibility (EMC) Directive	2014/30/EU	hydraulic power units using electrical or electronic devices which may generate electromagnetic disturbances
ATEX Directive	2014/34/EU	hydraulic power units used in potentially explosive atmospheres
Registration, Evaluation, Authorisation and Restriction of Chemicals (REACH) Regulation	EC 1907/2006	all materials (all hydraulic power units)
Restriction of Hazardous Substances (RoHS) Directive	2011/65/EU	hydraulic power units using electrical or electronic equipment (EEE)
Waste Electrical and Electronic Equipment (WEEE) Directive	2012/19/EU	hydraulic power units using electrical or electronic equipment (EEE)

The machinery directive is mutually exclusive with PED, LVD and EMC Directives in terms of putting CE mark on the partly completed machinery, however the directives have to be followed and risks from all directives have to be taken into account when performing risk assessment of machinery. The only directive that supersedes the Machinery Directive is ATEX Directive and also the only case where CE mark is issued to hydraulic power units.

3   Directives and regulations in detail

This chapter will briefly describe each directive and present the part that applies to the hydraulic power units.

---

[1] Updated version of the Machinery Directive. (see chapter 3.1)

3.1   Machinery Regulation (2023/1230)

Machinery Regulation was published on 29. 06. 2023 and will enter into force on 20.01.2027. Machinery Regulation extends and updates Machinery Directive which is therefore repealed. Because of lack of time to study the regulation in detail only the most important changes from the machinery directive are pointed out. These are:

- A machine's operating instructions only need to be available digitally.
- Substantial modification of the machine is defined. Makes user the manufacturer with all the obligations that entails.
- Different conformity assessment procedures for different categories of machinery.
- Some paragraphs were amended.
- The definition of 'machine or related product' was expanded and now includes cobots – machines without programming or application. [2, 3]

3.2   Machinery Directive (2006/42/EC)

The main European directive concerning machinery and certain parts of machinery is Machinery Directive (2006/42/EC). Intent of the directive is to ensure a common safety level in machinery placed on the market or put in service in all member states and to ensure freedom of movement within the EU by stating that "member states shall not prohibit, restrict or impede the placing on the market and/or putting into service in their territory of machinery which complies with [the] Directive". [4]

The Machinery Directive also applies to some other countries which are members of the European Single Market and are not part of the EU or European Economic Area (EEA). These countries include Norway, Iceland, Switzerland, Lichtenstein, Turkey, Andorra and San Marino. (European Commission, 2019)

This means that any machinery, safety component, interchangeable equipment, or accessory placed on the market within the EU must comply with the requirements outlined in the directive. It applies to both manufacturers based within the EU and those outside the EU who intend to sell machinery within the EU market. Non-EU

countries might have their own regulations and standards for machinery safety, but the Machinery Directive specifically applies to the EU member states.

Machinery Directive distinguishes between complete machinery and partly complete machinery [4]:

- **Complete machines** are those that are designed and constructed to perform a specific function on their own. They can be used as standalone equipment without the need for additional parts or modifications. These machines must meet the essential health and safety requirements outlined in the Machinery Directive before they can be placed on the EU market. Manufacturers of complete machines are responsible for ensuring that their products comply with the directive. This includes conducting risk assessments, designing machines with safety in mind, providing appropriate documentation, and affixing the CE marking to indicate compliance. The CE marking signifies that the machine meets the necessary standards and can be legally sold within the EU.
- **Partly complete machines** are components or sub-assemblies that are not capable of performing a specific function by themselves. They need further assembly, modification, or addition of other components to become functional machines. These components might include engines, frames, control systems, or other parts that, when combined, create a functioning machine. Incomplete machines are also subject to the Machinery Directive, although their requirements are slightly different. Manufacturers of incomplete machines must provide information on the intended use of the components and any potential risks associated with their assembly. This information helps the end user, who will complete the assembly, to understand how to safely integrate the incomplete machine into a complete and functional unit.

As it can be seen hydraulic power units in almost all cases fall into category of partly complete machines, therefore a closer look to obligations of manufacturer of partly completed machinery [6] (differences to complete machinery are in italic):

1. Identify the relevant product Directives/Regulations.
2. Identify the applicable requirements of the Directives/Regulations.
3. Identify an appropriate route to conformity.

4. Identify the relevant Harmonised Standards to which product could be designed.
5. Identify any other relevant Standards to which the product could be designed (if necessary).
6. Design the product to the requirements of the Standards.
7. Ensure the design of the product meets the requirements of the appropriate Directive/Regulation.
8. Ensure the product is marked as per the requirements of the identified Directives/Regulations/Standards.
9. Assembly Instructions (*Operating and Maintenance Instructions*) meet the requirements of the identified Directives/Regulations/Standards.
10. Complete and Document a Product Risk Assessment (It is advised that the Harmonised Standard EN ISO 12100:2010 is used for guidance).
11. Take action against any issues identified in the Risk Assessment.
12. Assess the product against the requirements of the appropriate Standards.
13. Assess the product directly against the requirements of the appropriate Directives/Regulations.
14. Take an action against any non-conformities identified in the Standard/Directive/Regulations Assessments. (Actions taken should be documented where necessary)
15. Compile the Technical File which consists of:
    a. description of partly completed machinery and its intended function,
    b. risk assessment documentation (requirements, protective measures),
    c. drawings and Schemes,
    d. references of the applied harmonized standards,
        e. description of applied technical specifications,
        f. calculation reports and test results to verify conformity of the machine,
        g. assembly instructions (*Operating and Maintenance Instructions),*
        h. *Declarations of incorporation for included partly completed machinery*
16. Produce and Sign the 'Declaration of Incorporation' ('*EC declaration of conformity*') and
17. *Display CE mark on the product.*

If the product is classed as Partly Completed Machine only the Declaration of Incorporation and Assembly Instructions are required to be supplied to demonstrate conformity to a third party. Also the CE Mark must NOT be attached to the Partly

Completed Machine (Exception: if the partly complete machinery falls under ATEX directive – it must be CE marked according to ATEX directive).

The most important harmonized standards for safety of machinery and hydraulic power units referred to from machinery directive are [7]:

– EN ISO 4413:2010 - Hydraulic fluid power – General rules and safety requirements for systems and their components (ISO 4413:2010)
– EN ISO 4414:2010 - Pneumatic fluid power – General rules and safety requirements for systems and their components (ISO 4413:2010)
– EN ISO 12100:2010 - Safety of machinery – General principles for design – Risk assessment and risk reduction
– EN ISO 16092-3:2018 - Machine tools safety - Presses - Part 3: Safety requirements for hydraulic presses (ISO 16092-3:2017)
– EN IEC 62061:2021 - Safety of machinery - Functional safety of safety-related control systems
– EN 693:2001+A2:2011 – Machine tools – Safety – Hydraulic presses
– EN 982:1996+A1:2008 - Safety of machinery – Safety requirements for fluid power systems and their components – Hydraulics
– EN 983:1996+A1:2008 - Safety of machinery – Safety requirements for fluid power systems and their components – Pneumatics
– EN 12622:2009+A1:2013 - Safety of machine tools – Hydraulic press brakes
– EN 14673:2006+A1:2010 - Safety of machinery - Safety requirements for hydraulically powered open die hot forging presses for the forging of steel and non-ferrous metals

3.3   Pressure Equipment Directive (PED) (2014/68/EU)

The Pressure Equipment Directive (PED) is a European Union directive that establishes rules and regulations for the design, manufacturing, testing, and conformity assessment of pressure equipment. The directive was introduced to ensure a high level of safety for pressure equipment, which includes items such as vessels, piping, boilers, pressure accessories, and assemblies. Pump housings, manifolds etc. are not considered pressure vessels according to PED in any case. [8] Pressure vessels used in hydraulics are hydraulic accumulators and piping. If they fall

under the PED can be determined from Annex II of the PED. For hydraulic power units the following tables are applicable (Considering mineral oil and nitrogen are in fluid group 2): Table 2 – gas side of the accumulator; Table 4 – fluid side of the accumulator; Table 7 – gas side piping and Table 9 – fluid side piping (Figure 1).
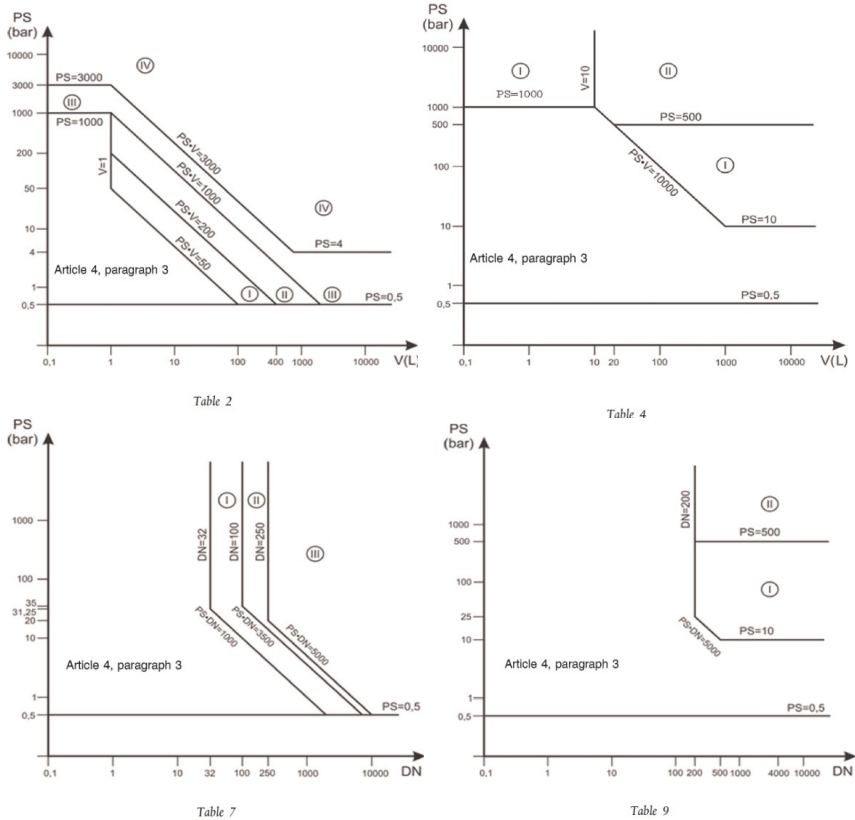
Figure 1: PED categories for pressure vessels and piping for fluid group 2 [8]

Accumulators must be checked on the gas side and on the oil side. The gas side is always stricter, therefore all accumulators greater than 1 l or P*V>50 bar l fall under PED. From Table 7 we can see that in rare cases piping on the gas side could fall under PED (DN>32 mm and p*DN>1000 bar mm) and therefore be PED certified (the PED certification procedure is not in scope of this article). Piping on the oil side almost never falls under ped as diameters greater than DN200 at pressures greater than 10 bar are rarely used in hydraulics. [8]

When an accumulator falls under PED, it must be purchased with valid PED certificate and adequately protected using a PED certified safety pressure relief valve.

How to properly protect the hydraulic accumulators is described in EN 14359 with circuit examples in Annex C [9]. Each accumulator must have a manual valve to be disconnected from the system, one ball valve to empty it back to tank and must be directly connected to PED certified safety pressure relief valve, which must not be used as a main system pressure relief valve at the same time as shown in Figure 2. When multiple accumulators are used in parallel there is no need to have a separate ball valve and safety pressure relief valve for each accumulator. A pressure gauge which cannot be disconnected from the accumulator by means of a ball or a check valve must be included so that the actual accumulator pressure may be read out before starting maintenance work on the machine.
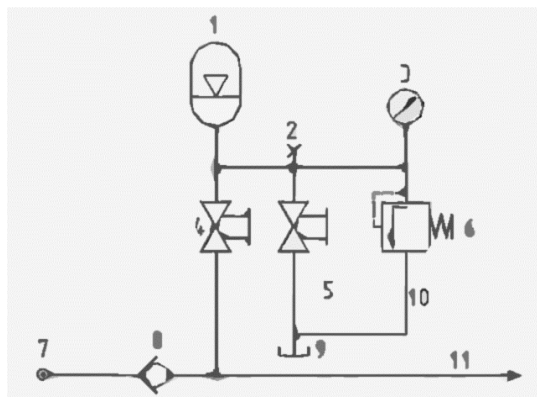
Figure 2: Basic accumulator protection circuit [9][9]

One important thing to note is that hydraulic power unit as partly completed machine does not fall directly under PED directive and thus must not be CE marked, because it only uses components with PED certificate.

3.4   Ecodesign Regulation (2019/1781)

Ecodesign Regulation limits the use of inefficient motors and variable frequency drives. Therefore it applies to all hydraulic power units using AC electric motors. Minimum energy efficiency required by the regulation for motors is depicted in Figure 3 and was applied according to the following timetable [10]:

- from 1 July 2021:
    - o the energy efficiency of three-phase motors with a rated output equal to or above 0,75 kW and equal to or below 1000 kW, with 2, 4, 6 or 8 poles, which are not Ex eb increased safety motors, shall correspond to at least the IE3
    - o the energy efficiency of three-phase motors with a rated output equal to or above 0,12 kW and below 0,75 kW, with 2, 4, 6 or 8 poles, which are not Ex eb increased safety motors, shall correspond to at least the IE2
    - o the power losses of variable speed drives rated for operating with motors with a rated output power equal to or above 0,12 kW and equal to or below 1000 kW shall not exceed the maximum power losses corresponding to the IE2 efficiency level
- from 1 July 2023:
    - o the energy efficiency of Ex eb increased safety motors with a rated output equal to or above 0,12 kW and equal to or below 1000 kW, with 2, 4, 6 or 8 poles, and single-phase motors with a rated output equal to or above 0,12 kW shall correspond to at least the IE2.
    - o the energy efficiency of three-phase motors which are not brake motors, Ex eb increased safety motors, or other explosion-protected motors, with a rated output equal to or above 75 kW and equal to or below 200 kW, with 2, 4, or 6 poles, shall correspond to at least the IE4.
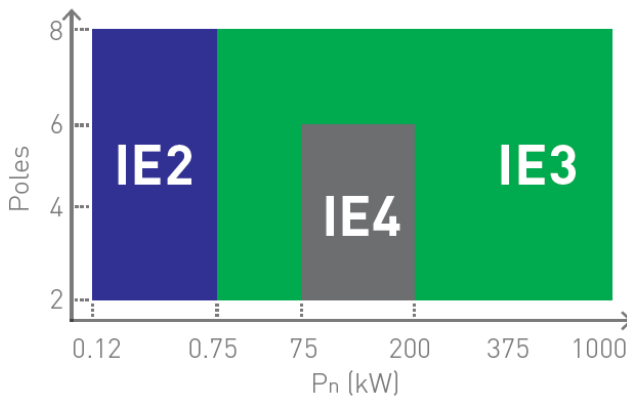
Figure 3: Current (after 1 July 2023) minimal motor efficiency classes for three phase motors
[11]

3.5 Low Voltage Directive (LVD) (2014/35/EU) and Electromagnetic Compatibility (EMC) Directive (2014/30/EU)

Hydraulic power units do not directly fall under Low Voltage Directive [12] and Electromagnetic Compatibility Directive [13], therefore they cannot bear CE mark as required by LVD and EMC. If the components that fall under LVD (input/output voltage between 50 and 1000 VAC or 75 and 1500 VDC) or EMC (electronics emitting electromagnetic noise) are used they must have applicable certificates available, so that they may be used in the EU. Although when only the Machinery Directive applies the risks from other directives still has to be taken into account.

One special case that often causes confusion in practice is the CE marking of the electrical cabinets, which are often part of hydraulic power units. To clarify the topic we need to distinguish between who is the manufacturer of the electrical cabinet and the machine. [14]

- **Machine manufacturer is the cabinet builder for his own machine:** No CE marking on electrical cabinet required as the electrical cabinet is not placed separately on the market, therefore only machinery directive applies.
- **Cabinet builder builds the cabinet according to manufacturer's technical documents:**
  Cabinet builder is not deemed to be the manufacturer in this case, so no CE marking on electrical cabinet required as the electrical cabinet is not placed separately on the market, therefore only machinery directive applies.
- **Cabinet builder designs and builds the cabinet for the machine manufacturer:**
  Cabinet builder is responsible for compliance with EU regulations. There are multiple cases:
  a. **Cabinet does not contain safety functions,** therefore does not fall under machinery directive and therefore needs to follow LVD, EMC and other directives and thus has to be CE marked.
  b. **Cabinet contains safety functions:**
     i. **When safety functions are implemented entirely by the use of safety components,** the cabinet does not fall under machinery directive and therefore needs to follow LVD, EMC and other directives and thus has to be CE marked. All the information regarding the safety

components have to be transferred from the cabinet builder to machine manufacturer.

ii. **When safety functions are implemented by the use of normal components,** the cabinet falls under machinery directive and the cabinet builder has to follow the machinery directive for partly complete machinery.

3.6　ATEX Directive (2014/34/EU)

This directive applies to manufacturers, distributors, and importers of equipment and protective systems intended for use in potentially explosive atmospheres within the European Economic Area (EEA). It also includes components necessary for the safe operation of such equipment.

The directive classifies equipment into different categories based on the level of protection required. Categories are divided into equipment intended for use in Zones 0, 1, 2 (gas/vapor environments) or Zones 20, 21, 22 (dust environments) in terms of their potential explosive nature. The categories help determine the level of conformity assessment required.

Manufacturers are required to carry out additional risk assessment procedure applicable to explosive atmospheres. Primary hazards (potential ignition sources) in explosive atmospheres include (EN ISO 80079-36 Table B.1): hot surfaces, mechanically generated sparks, flames and hot gases, electrical sparks, electrical stray currents and cathodic corrosion protection, static electricity, lightning strike, electromagnetic waves, ionizing radiation, high-frequency radiation, ultrasonic waves, adiabatic compression, chemical reactions. All of those hazards have to be considered along with the applicable ATEX zone and materials present. Using ATEX certified components (motors, level indicators, sensors, paint, materials, etc.) simplifies the risk assessment process and reduces number of potential ignition sources.

When a hydraulic power unit conforms to ATEX Directive it has to be CE marked along with the appropriate ATEX classification. [15]

Important standards for ATEX are:

– EN 1127-1: "Explosion prevention and protection. Part 1: Basic concepts and methodology"
– EN ISO 80079-36: "Explosive atmospheres. Part 36: Non-electrical equipment for explosive atmospheres. Basic method and requirements"
– EN ISO 80079-37: "Explosive atmospheres. Part 37: Non-electrical equipment for explosive atmospheres. Non-metallic"
– IEC 60079-0: "Explosive atmospheres. Part 0: General requirements"

These standards provide guidelines and requirements for ensuring safety in explosive atmospheres, including methods for preventing and protecting against explosions and other related hazards.

3.7 Registration, Evaluation, Authorisation and Restriction of Chemicals (REACH) Regulation (EC 1907/2006)

REACH primarily focuses on the registration, evaluation, authorization, and restriction of chemical substances and their impact on human health and the environment. It doesn't directly regulate machines or their mechanical parts. [16] However, there are scenarios where REACH could indirectly affect machines and their parts:

1. **Substances in Machines:** If a machine or its parts contain chemical substances that are subject to REACH regulations, the manufacturers of those substances or articles may have obligations under REACH. For instance, if a machine's components contain substances of very high concern (SVHCs) in concentrations above 0.1 % by weight, there might be communication requirements down the supply chain about their presence.
2. **Materials Used:** If the manufacturing of machines involves the use of chemicals, whether for surface treatments, coatings, lubrication, or other purposes, the manufacturers of those chemicals must comply with REACH requirements.
3. **Importers and Manufacturers:** Companies importing or manufacturing machines within the EU may need to consider REACH if their machines contain substances in quantities above 1 ton per year. While the main focus

of REACH is on chemical substances, these substances can be used in various ways in the production of machines.

4. **Articles Containing SVHCs:** If machines or their parts contain substances of very high concern (SVHCs) above the 0.1 % threshold, downstream users might have communication obligations to inform their customers about the presence of these substances. This is especially relevant if the substances are intended to be released during normal use.

5. **REACH Compliance of Components:** Manufacturers of machines might request information about the chemical substances used in the components they purchase to ensure compliance with REACH regulations. This is to ensure that no restricted or unauthorized substances are present.

6. **End-of-Life Considerations:** REACH regulations can affect the disposal and recycling of machines containing certain chemical substances, especially substances that are restricted or require authorization. Proper management and communication about these substances become important during the end-of-life phase of machines.

It's important to understand that REACH is primarily concerned with chemical substances and their impact on human health and the environment. While REACH may not directly regulate machines and their parts as mechanical entities, the chemical components within those machines could fall under REACH's scope depending on their properties and usage. REACH obliges manufacturers to get the information about the SVHCs in parts used to build the machine, combine those information and pass it on to the machine builder or end user.

3.8 Restriction of Hazardous Substances (RoHS) Directive (2011/65/EU) and Waste Electrical and Electronic Equipment (WEEE) Directive (2012/19/EU)

Similarly as with LVD and EMC Directive, hydraulic power units do not fall directly into this directives, but some demanding customers may want information that all Electrical and Electronic Equipment (EEE) that is used on the hydraulic power unit are RoHS compliant. RoHS restricts the use of certain hazardous substances in quantities larger than 0,1 %[2](mass) in EEE in order to protect human health and the environment. These substances are: Lead (Pb), Mercury (Hg), Cadmium (Cd),

---

[2] Except for cadmium for which the limit is 0,01 %

Hexavalent Chromium (Cr6+), Polybrominated Biphenyls (PBB), Polybrominated Diphenyl Ethers (PBDE). [17]

The Waste Electrical and Electronic Equipment (WEEE) Directive is a European Union regulation that aims to minimize the environmental impact of electrical and electronic equipment waste. It establishes guidelines for the collection, recycling, and disposal of such waste to reduce its impact on the environment and human health. WEEE Directive requires users of EEE to increase recycling awareness by mentioning in the assembly instructions that the partly complete machinery also includes EEEs which must be disposed separately from unsorted municipal waste. [18]

7 Conclusion

In conclusion, European directives play a pivotal role in harmonizing regulations and standards across the European Union (EU) member states, facilitating the free movement of goods and promoting safety, health, environmental protection, and consumer rights. These directives cover a wide range of industries and topics, ensuring that products placed on the EU market adhere to common requirements, enhancing market efficiency, and fostering cross-border trade.

Each directive is tailored to address specific challenges within its respective domain, outlining essential requirements, conformity assessment procedures, and obligations for manufacturers, importers, and distributors. The Machinery Directive stands out as a cornerstone within the framework of European directives, playing a pivotal role in ensuring the safety of machinery and equipment placed on the market and used within the European Union (EU). With a focus on harmonization, risk reduction, and enhanced consumer protection, the Machinery Directive embodies the principles of standardization and cooperation among member states.

The Machinery Directive addresses a broad spectrum of machinery, ranging from industrial equipment to consumer products, imposing stringent requirements that encompass design, manufacturing, and operation. By establishing essential health and safety requirements, the directive sets the groundwork for risk assessment and mitigation, promoting the development of safer, more reliable machinery.

Manufacturers bear a significant responsibility in complying with the Machinery Directive, conducting thorough risk assessments, adhering to essential requirements, and employing recognized safety standards. The CE marking, affixed upon successful conformity, is a testament to a product's compliance with the directive's stipulations, thereby fostering consumer confidence and facilitating trade across EU borders.

Conformity assessment procedures outlined in the directive facilitate consistent evaluation processes while acknowledging the varying degrees of risk posed by different machinery. Involvement of notified bodies, when necessary, ensures an additional layer of oversight and expertise.

However, the directives are not a static entities. They adapt to technological advancements and emerging risks, ensuring that its regulations remain current and relevant. Stakeholders must remain vigilant, staying informed about updates and revisions, and actively participating in the dialogue surrounding machinery safety. The directives underscore the EU's commitment to safeguarding the welfare of its citizens, promoting workplace safety, and fostering a competitive market environment. It bridges the gap between innovation and responsibility, emphasizing that progress can coexist with precaution.

References

[1] Your Europe, "CE marking," European Union, 08 05 2023. [Online]. Available: https://europa.eu/youreurope/business/product-requirements/labels-markings/ce-marking/index_en.htm. [Accessed 18 8 2023].

[2] Mensura, "A glance at the new Machinery Regulation: What do you need to know?," 05 06 2023. [Online]. Available: https://www.mensura.be/en/blog/een-blik-op-de-nieuwe-machineverordening-wat-moet-je-weten. [Accessed 18 08 18].

[3] The European Parliament and the council of the European Union, "REGULATION (EU) 2023/1230 OF THE EUROPEAN PARLIAMENT AND OF THE COUNCIL of 14 June 2023 on machinery and repealing Directive 2006/42/EC of the European Parliament and of the Council and Council Directive 73/361/EEC," *Official Journal of the European Union*, no. L165, pp. 1-102, 2023.

[4] The European Parliament and the council of the European Union, "Directive 2006/42/EC of the European Parliament and of the Council of 17 May 2006 on machinery, and amending Directive 95/16/EC (recast)," *Official Journal of the European Unio*n, vol. 157, pp. 24-86, 2006.

[5] European Commission, "Guide to application of the Machinery Directive 2006/42/EC," 2019.

[6] CE Marking Association, "CE Marking Guidance: Partly Completed Machinery," 12 2014. [Online]. Available: https://www.cemarkingassociation.co.uk/docs/guidance/partly-completed-machinery.pdf. [Accessed 19 08 2023].

[7] EUROPEAN COMMISSION, "Directive 2006/42/EC on Machinery - summary list as pdf document," 10 01 2023. [Online]. Available:

https://ec.europa.eu/docsroom/documents/52774/attachments/1/translations/en/renditions/native. [Accessed 19 08 2023].

[8] The European Parliament and the council of the European Union, "DIRECTIVE 2014/68/EU OF THE EUROPEAN PARLIAMENT AND OF THE COUNCIL of 15 May 2014 on the harmonisation of the laws of the Member States relating to the making available on the market of pressure equipment," *Official Journal of the European Union*, no. L189, pp. 164-259, 2014.

[9] EN 14359:2011-04, "Gas-loaded accumulators for fluid power applications".

[10] THE EUROPEAN COMISSION, "COMMISSION REGULATION (EU) 2019/1781 of 1 October 2019 laying down ecodesign requirements for electric motors and variable speed drives pursuant to Directive 2009/125/EC of the European Parliament and of the Council, amending Regulation (EC) No 641/2009..," *Official Journal of the European Union*, no. L272, pp. 74-94, 2019.

[11] Bennett Electrical Ltd., "Electric Motor Efficiency Regulations changes 1st July 2021," [Online]. Available: https://www.bennettelectrical.com/electric-motor-efficiency-regulations/#:~:text=The%20IE3%20standard%20will%20be,duty%20cycles%20S1%20and%20S3.. [Accessed 19 8 2023].

[12] THE EUROPEAN PARLIAMENT AND THE COUNCIL OF THE EUROPEAN UNION, "DIRECTIVE 2014/35/EU OF THE EUROPEAN PARLIAMENT AND OF THE COUNCIL of 26 February 2014 on the harmonisation of the laws of the Member States relating to the making available on the market of electrical equipment designed for use within certain voltage lim," Official Journal of the European Union, no. L96, pp. 357-374, 2014.

[13] THE EUROPEAN PARLIAMENT AND THE COUNCIL OF THE EUROPEAN UNION, "DIRECTIVE 2014/30/EU OF THE EUROPEAN PARLIAMENT AND OF THE COUNCIL of 26 February 2014 on the harmonisation of the laws of the Member States relating to electromagnetic compatibility," *Official Journal of the European Union*, no. L96, pp. 79-106, 2014.

[14] ZVEI, "Placing on the market and CE marking of switchgear cabinets for machines," 05 11 2018. [Online]. Available: https://www.zvei.org/fileadmin/user_upload/Presse_und_Medien/Publikationen/2019/Maerz/ZVEI-Position_Entwurf_Schaltschrank_fuer_Maschinen_2018-11-05_enEnglisch_JEH__003_.pdf. [Accessed 19 08 2023].

[15] THE EUROPEAN PARLIAMENT AND THE COUNCIL OF THE EUROPEAN UNION, „DIRECTIVE 2014/68/EU OF THE EUROPEAN PARLIAMENT AND OF THE COUNCIL of 15 May 2014 on the harmonisation of the laws of the Member States relating to the making available on the market of pressure equipment," *Official Journal of the European Union*, št. L189, pp. 164-259, 2014.

[16] THE EUROPEAN PARLIAMENT AND OF THE COUNCIL, "Regulation (EC) No 1907/2006 of the European Parliament and of the Council of 18 December 2006 concerning the Registration, Evaluation, Authorisation and Restriction of Chemicals (REACH)," Official Journal of the European Union, no. L396, pp. 1-856, 2006.

[17] THE EUROPEAN PARLIAMENT AND THE COUNCIL OF THE EUROPEAN UNION, "DIRECTIVE 2011/65/EU OF THE EUROPEAN PARLIAMENT AND OF THE COUNCIL of 8 June 2011 on the restriction of the use of certain hazardous substances in electrical and electronic equipment," *Official Journal of the European Union*, no. L174, pp. 88-110, 2011.

[18] THE EUROPEAN PARLIAMENT AND THE COUNCIL OF THE EUROPEAN UNION, "DIRECTIVE 2012/19/EU OF THE EUROPEAN PARLIAMENT AND OF THE COUNCIL of 4 July 2012 on waste electrical and electronic equipment (WEEE)," *Official Journal of the European Union*, no. L197, pp. 38-71, 2012.

WAVE PROPAGATION IN HYDRAULIC TRANSMISSION LINES - STATE OF THE ART IN EFFICIENT SIMULATION MODELS

BERNHARD MANHARTSGRUBER

Johannes Kepler University, Institute of Machine Design and Hydraulic Drives, Linz, Austria
bernhard.manhartsgruber@jku.at

Transmission lines are the most simple elements in a fluid power system from the point of view of traditional fluid power system design, simply connecting two individual ports of different components without introducing any additional dynamic effects. In reality, this wishful thinking works only when the system operates quasi-statically with respect to the time constants of wave propagation across the lines. An increasing number of industrial applications faces problems by pushing fluid power systems to operating frequencies high enough to excite significant dynamic effects in transmission lines. In order to mitigate these problems in a model-based systems engineering framework, efficient computational methods for the modelling and simulation of hydraulic transmission lines are crucial. This paper gives an overview of the state of the art in computationally efficient simulation models with a special emphasis on very compact low order models.

1   Intruduction

Fluid power technology relies on a small number of basic working principles. First of all, the displacement principle used in hydraulic pumps and motors (including hydraulic cylinders for translator motion). Secondly, the resistance principle used in various valves for control purposes. For basic system design, the story already ends here, and the designers of hydraulic drive systems apply the same principles that were used for conceiving Joseph Bramah's hydraulic press invention in 1795 or Kepler's gear pump invented around 1600. For all these concepts, the hydraulic fluid may be regarded as a mass-less and incompressible ideal medium for transmitting the hydrostatic pressure without adding any dynamic effects to the system. The friction losses of the viscous fluid in pipelines and hoses are however included in classical fluid power system design. There is abundant literature on the so-called minor pressure losses due to long lines and various fittings for branching and connecting these line elements. From the point of view of the hydraulic design engineer, the simple line representing a pipeline connection in a circuit schematic represents an almost ideal connection between two points in the fluid power system: The pressures at these end points are assumed equal except for a pressure loss depending on the flow. This pressure loss is kept small by a proper dimensioning of the line diameter according to line length and expected flow rates.

The described engineering approach neglects pipeline dynamics and in most cases, this is perfectly justified because of the hydrostatic nature of fluid power systems. In some cases, however, either the mass inertia of the oil column in the lines or the wave propagation effect caused by the interplay of inertia and compressibility can cause severe problems.

These effects are known at least since the days of ancient Rome when supply lines for potable water were equipped with devices against the water hammer phenomenon which was mathematically explained by Joukowsky in the late 19th century.

The first approaches for analysis and design of pipeline systems under the influence of fast dynamic processes have been graphical methods in characteristic coordinates, later on computer codes where developed in order to solve systems of partial differential equations. All of these methods are typically regarded as out of scope for

the fluid power design engineer and their use has been restricted to two groups of special cases: The first case arises when a system is dimensioned with classical knowledge of hydrostatic behaviour, but some dynamic effects result in malfunction and some sort of trouble-shooting is needed. The second possibility arises, when known hydrostatic solutions are pushed to higher and higher operating frequencies resulting in wave propagation in lines becoming important at some point. Section 3 of this paper will give industrial application examples for both cases.

During the last three or four decades both the broad availability of computer systems capable of numerical simulation and the mathematical modelling skills of mechanical and electrical engineers have improved dramatically. The symbiosis of mechanical and electrical engineering together with computer science, now known as mechatronics and the new paradigm of model-based systems engineering have led to new possibilities in hydraulic circuit design. Computer based simulation systems are increasingly used in system dimensioning. In order to be helpful in the system design phase, these simulation tools need to be easy to understand and use and they must be computationally efficient resulting in very small simulation times.

However, most numerical simulation models for wave propagation available in applied mathematics and engineering literature are either more or less the complete opposite of a fast and computationally efficient tool, or they are over-simplified and fail to capture the real system behaviour with sufficient accuracy.

The remainder of this paper is organised as follows: Section 2 contains a brief overview on the state of the art in hydraulic transmission line modelling and simulation, with a special emphasis on the trade-off between computational efficiency and accuracy of the models. Section 3 presents an example from industrial applications where the dynamics of transmission line plays an important role. Section 4 contains some conclusions.

2   Overview on the state of the art in transmission line modelling

2.1   Modelling assumptions

In the most simple case, a perfectly cylindrical (and thus straight) pipe with a length much bigger than its diameter is passed through by a weakly compressible liquid

with Newtonian fluid friction behaviour. The pipe walls are assumed rigid and the temperature is assumed to be constant. Then, the unknowns are the three-dimensional flow velocity and the scalar values of pressure and density inside the pipe. A material law like

$$\rho = \rho_0 \cdot \left(1 + \frac{p - p_0}{K}\right) \tag{1}$$

links the density ρ to the pressure p with a reference density ρ_0 given at a reference pressure p_0. The kinematic viscosity ν is assumed with a constant value due to the constant fluid temperature in this model.
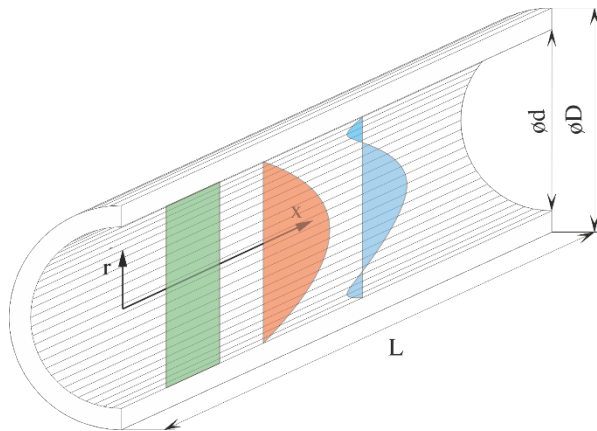
Figure 1: Cylindrical pipe geometry with radial and axial coordinates as well as various assumptions on the axial velocity profile: Plug flow (green), Parabolic Hagen-Poiseuille profile (red), dynamic flow profile under frequency-dependent friction (blue).
Source: own.

When it comes to describing the flow velocity inside the pipe, the Navier-Stokes equations from fluid mechanics must be somehow adapted to the problem at hand. The cylindrical geometry of the pipe calls for the use of a cylindrical coordinate system (axial coordinate r, radial coordinate r, circumferential angle) for formulating the equations of motion for the fluid. In general, this would result in three equations for the momentum balances in axial, radial and circumferential direction. It is common sense in the fluid power community to disregard any swirl flow in the pipe, i. e. to set all circumferential velocity components zo zero a priori. Also the flow

velocity in radial direction is omitted in most models and the pressure in the pipeline is assumed to be independent of the radial coordinate at any given axial position and time. All these assumptions result in a problem for the unknown distributions of pressure p and velocity in axial direction

$$p = p(x,t), u = u(x,r,t) \tag{2}$$

of the form

$$\frac{\partial u}{\partial t} + u\frac{\partial u}{\partial x} = -\frac{1}{\rho}\frac{\partial p}{\partial x} + \nu\left(\frac{1}{r}\frac{\partial u}{\partial r} + \frac{\partial^2 u}{\partial r^2}\right) + \frac{4\nu}{3}\frac{\partial^2 u}{\partial x^2}, \tag{3a}$$

$$\frac{\partial p}{\partial t} + u\frac{\partial p}{\partial x} = -K\frac{\rho}{\rho_0}\frac{\partial u}{\partial x}. \tag{3b}$$

The first equation (3a) comes from the axial component of the Navier-Stokes momentum balance equation. The second one (3b) is motivated by mass conservation. The parameters in these equations are the fluid density at ambient pressure ρ_0, the kinematic viscosity ν and the bulk modulus K.

At the rigid pipe wall, the flow velocity needs to be zero to fulfil the no-slip condition known from fluid mechanics. A number of over-simplified models disregard this condition by neglecting any viscous friction effects and assuming a so-called plug flow with a constant flow velocity over the whole pipe diameter as shown by the rectangular flow profile in Figure 1 (in green colour). This approach was useful in early water-hammer analysis for hydro-power plants.

In the next level of model complexity the flow profile is assumed to always have a parabolic shape as in the stationary laminar flow case (shown in red colour in Figure 1). Such models are very popular among engineers, because the partial differential equation system (3) can be simplified strongly by a set of easy to understand arguments:

- Following the ancient "divide et impera" principle, the pipeline is divided into a number of identical sections in axial direction.
- Within such a section, the velocity is assumed equal to the parabolic profile in radial direction and with a linear gradient in axial direction:

$$u(x,r,t) = \left(u_0(t) \cdot \left(1 - \frac{x}{L}\right) + u_1(t) \cdot \frac{x}{L}\right) \cdot \left(1 - \frac{r}{R}\right)\left(1 + \frac{r}{R}\right)$$

- For the pressure, a linear axial gradient is used:

$$p(x,t) = p_0(t) \cdot \left(1 - \frac{x}{L}\right) + p_1(t) \cdot \frac{x}{L}$$

- The density variations of the hydraulic liquid are small, so the assumption $\frac{\rho}{\rho_0} \approx 1$ simplifies eq. (3b).

Substitution of all these assumptions into eqs. (3), averaging the first equation over the cross sectional area $\left(\frac{1}{R^2\pi} \int_0^R \ldots \, 2\pi r \, dr\right)$ and integrating both equations from 0 to L over x yields a simple system of ordinary differential equations

$$\dot{u}_0 + \dot{u}_1 + \frac{2}{3L}(u_1 + u_0)(u_1 - u_0) = \frac{4}{\rho_0 L}(p_0 - p_1) - \frac{8\nu}{R^2}(u_1 + u_0)$$

$$\dot{p}_0 + \dot{p}_1 + \frac{(u_1 + u_0)(p_1 - p_0)}{2L} = -\frac{K}{L}(u_1 + u_0)$$

For the pressures and flow velocities at start (index 0) and end (index 1) of a section. This concept simply needs to be rolled out for N sections, so the second section will have indices 1 and 2, up to the last section with indices N-1 and N. Concepts more or less similar to this are found in a number of commercial simulation software packages including SimScape Fluids.

This simple approach of the segmented pipeline is quite sufficient for simple simulation tasks with low requirements on model fidelity. When it comes to questions where a precise modelling of the real physical behaviour of a viscous, compressible liquid in a pipeline is needed, the assumption of the radial velocity distribution always staying in a parabolic shape is not helpful. The real flow shows a behaviour, where the flow in the core of the pipeline can transiently have an opposite direction as compared to the boundary layer. The profile shown in blue colour in Fig. 1 depicts such an example. The reason for this can be found in a difference between the core flow which is mainly influenced by inertia effects and the boundary layer where the influence of viscous friction is stronger.

Mathematical models taking this dynamic, so-called frequency dependent friction effect into account [4] and software implementations of these models can be found in [2] where a method of characteristics is employed or in [3] where the transmission line matrix method is used. A very compact low order model has been presented in [4].

3   Example

3.1   Pump with long suction line

The example is motivated by the failure of a large hydraulic pump with long suction line. The damaged pump was one of several 1000 cc axial piston units sharing a common suction line. This line was kept on an elevated suction pressure by a feed pump and a pressure limit valve. The damage in the axial piston pump turned out to be induced by cavitation due to strong pressure oscillations in the suction line.

The plant operators reported about the occurrence of strong cavitation noise depending on several factors. First of all, the oil temperature during start-up of the plant: The problem would typically never occur after a cold start of the hydraulic system and it would also not develop when the plant was warming up during continuous operation of the pumps. If, however, the plant was shut down for a short time and then restarted with warm oil conditions, there was a chance of ending up in a situation with strong cavitation. A cavitation-free operation mode could be reached "with good luck" by several start-up trials. And additionally, the problem seemed to occur most likely on the last of three pumps along the common suction line, i. e. the pump with the lowest mean pressure level during operation of all units.

In order to find out, whether the start-up conditions could decide about two different final operation states, one with and one without cavitation, a computer simulation model is built. The focus is not on precisely reproducing the real system behaviour, but on explaining the mechanism that enables at least two different operating conditions for the same pump, at the same speed of rotation and with the same hydraulic load.

For starting up the large 1000 cc constant displacement units, a dedicated start-up hydraulic system is used with a boost pressure pump operated at a 50 bar pressure level and delivering a flow large enough to drive the pump in motor mode and accelerate it together with the inertia of its electrical motor to a speed near the operating speed, in this case 993 rpm. For the model presented here, the dynamics of the large asynchronous induction motor is neglected completely and a simple grid-synchronous speed assumption is used. Figure 2 shows the axial piston pump taking in fluid either in motoring model from a 50 bar start pressure supply or in pumping mode from a long suction line with a 5 bar constant feed pressure at the end. The left half of the Simulink schematics shows the modelling of the angular speed during the start-up phase. The R-S flip-flop block is initially switched on and the torque generated by the pump in motoring mode accelerates the rotary inertia modelled by the single integrator block. The output of this integrator is fed as angular speed back to the pump model. Once the angular speed reaches the synchronous grid speed of 1000 rpm, the flip-flop is reset resulting in the angular speed becoming constant at 1000 rpm, the 50 bar start pressure being cut-off by a switching valve and the load on the high pressure side being increased by reducing the valve opening of the load orifice.
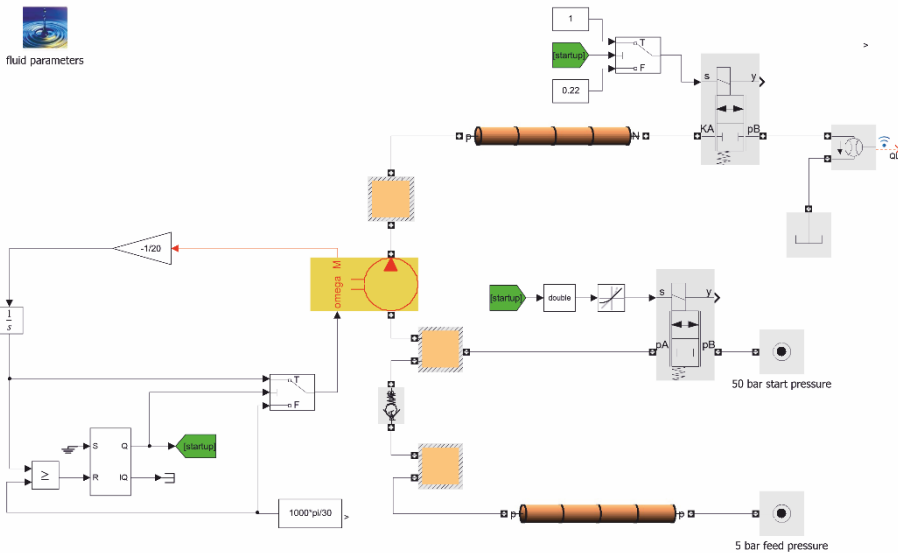
Figure 2: Model of pump with long suction line (MATLAB/Simulink).
Source: own.

The axial piston pump is modelled with nine individual pistons located relative to the crank angle according to

$$\varphi_i = \varphi - i \cdot \frac{2\pi}{9}, \quad i = 0..8$$

The chamber volumes are

$$V_{c,i} = A_p \cdot (h_0 + r + r \cdot \cos \varphi_i)$$

and the pressure build-up in the chambers is described by orifice equations and the compressibility law as

$$\dot{p}_{c,i} \frac{V_{c,i}}{K} = -\dot{V}_{c,i} + \alpha A_{in}(\varphi_i) \sqrt{\frac{2(p_{in} - p_{C,i})}{\rho}} - \alpha A_{out}(\varphi_i) \sqrt{\frac{2(p_{C,i} - p_{out})}{\rho}}$$

$$\dot{p}_{in} \frac{V_{in}}{K} = Q_{in} - \sum_{i=0}^{8} \alpha A_{in}(\varphi_i) \sqrt{\frac{2(p_{in} - p_{C,i})}{\rho}},$$

$$\dot{p}_{out} \frac{V_{out}}{K} = \sum_{i=0}^{8} \alpha A_{out}(\varphi_i) \sqrt{\frac{2(p_{C,i} - p_{out})}{\rho}} - Q_{out}$$

with opening functions shaped like in Figure 3.
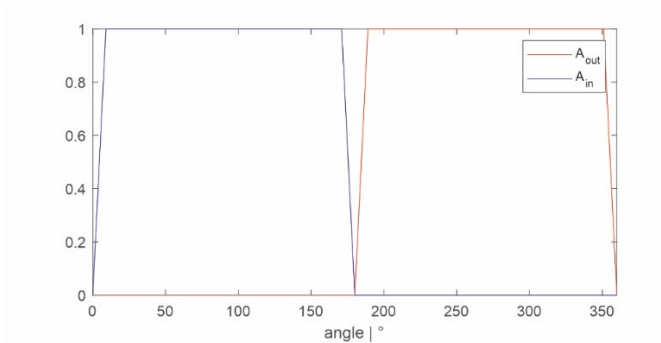
Figure 3: Opening functions (scaled by max. area value).
Source: own.

The modelling of the switching valve for cutting off the 50 bar supply pressure is a done by an orifice equation controlled by an opening function $u_{cut}(t)$ and the check valve between the suction line and the pump also by an orifice equation with an opening that reacts to the pressure differential without dynamics between a crack pressure p_{cr} where the check valve starts to open and a full opening pressure p_{fo} where the full orifice opening is reached. Together the two valve models result in the flow

$$Q_{in} = u_{cut} \cdot Q_{cut} \sqrt{\frac{50 \, \text{bar} - p_{in}}{\Delta p_n}}$$

$$+ Q_{check} \sqrt{\frac{p_{Suc} - p_{in}}{\Delta p_n}} \begin{cases} 0 & p_{Suc} - p_{in} < p_{cr} \\ \dfrac{p_{Suc} - p_{in} - p_{cr}}{p_{fo} - p_{cr}} & else \\ 1 & p_{Suc} - p_{in} > p_{fo} \end{cases}$$

The pressure $p_{Suc}(t)$ is output by the transmission line model. On the delivery side, a transmission line model connects the volume V_{out} to a load orifice and further back to tank pressure.

3.2 Transmission line modelling by method of characteristics

The initial goal for this paper was to compare different modelling approaches for their ability to explain the phenomenon of operating conditions depending on the start-up procedure observed in the real plant. Unfortunately, only one of the models resulted in a good match between model and reality at acceptable simulation times. This was the Zielke-Suzuki [1, 2] method of characteristics. This method is known to be very accurate but computationally inefficient due to the discretization approach with a detailed friction model being applied over and over again at each node of the axial grid along the pipeline.

The reason, why the other models [3, 5] did not perform well was found in their inefficient coupling with boundary conditions algebraically coupling the pressure with the flow rate at the boundary. Figures 4 and 5 show the results for two different values of the switching time of the valve cutting off the 50 bar start pressure supply.
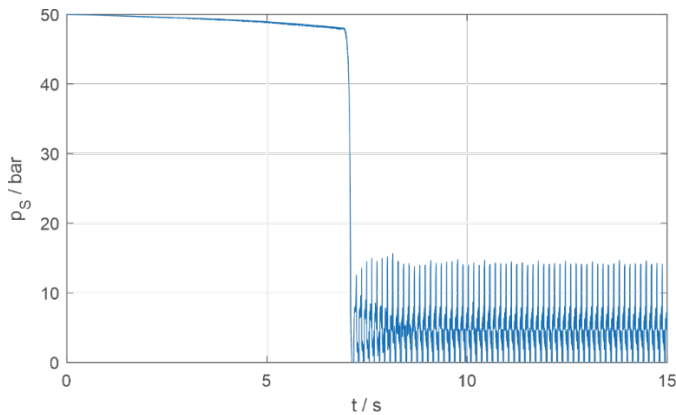
Figure 4: Pressure at pump intake during start-up and shortly thereafter, 200 milliseconds switching time at the cut-off valve.
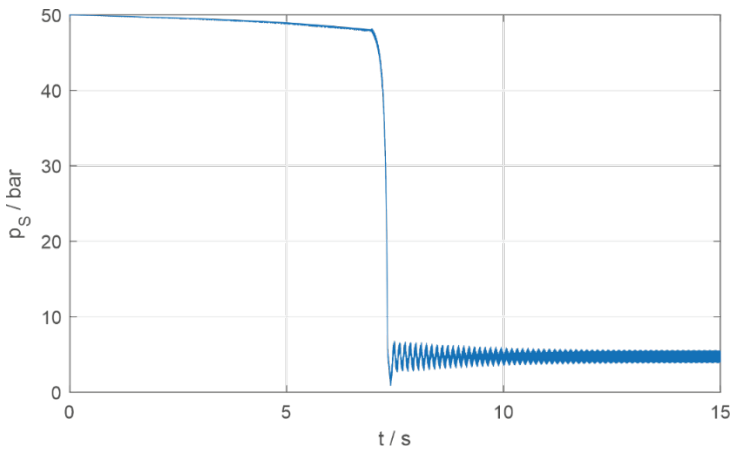
Source: own.

Figure 5: Pressure at pump intake during start-up and shortly thereafter, 500 milliseconds switching time at the cut-off valve.

Source: own.

4   Conclusions

For an industrial example with high demands on the transmission line model fidelity, a benchmark example has been shown. The classical method of characteristics in an implementation with efficient treatment of valve boundary conditions shows

excellent results in explaining the interesting plant behaviour of the final period pressure pulsations at the pump intake having two different amplitudes depending on the switching time between start-up and suction pressure. More modern and theoretically more efficient models failed in the first attempt due to unsolved problems with valve boundary conditions. Further work is under way to resolve this.

References

[1]   Zielke, W. (1966). *Frequency dependent friction in transient pipe flow*. PhD thesis, University of Michigan Ann Arbor

[2]   Suzuki, K., Taketomi, T., and Sato, S. (1991). Improving Zielke's Method of Simulating Frequency-Dependent Friction in Laminar Liquid Pipe Flow. *ASME. J. Fluids Eng*. 113(4): 569–573. doi.org/10.1115/1.2926516

[3]   Johnston N., Pan M., Kudzma S. (2014). *An enhanced transmission line method for modelling laminar flow of liquid in pipelines*. Proceedings of the Institution of Mechanical Engineers, Part I: Journal of Systems and Control Engineering. 228(4):193-206. doi:10.1177/0959651813515205

[4]   Goodson R. E., Leonard R. G. (1972) *A survey of modeling techniques for fluid line transients*. J Basic Eng: T ASME 94(2): 474–482.

[5]   Manhartsgruber, B. "H2-Optimal Low Order Transmission Line Models." Proceedings of the ASME/BATH 2019 Symposium on Fluid Power and Motion Control. ASME/BATH 2019 Symposium on Fluid Power and Motion Control. Longboat Key, Florida, USA. October 7–9, 2019. V001T01A044. ASME. https://doi.org/10.1115/FPMC2019-1688

Tool for the Design and Simulation of Hydrostatic Bearings in Machine Tools

Edler Jörg

Graz University of Technology, IFT, Graz, Austria
joerg.edler@tugraz.at.

Hydrostatic Bearings, in addition to ball bearings and sliding guides, represent a possibility for machine tools to bear moving parts precisely. Compared to the aforementioned types of bearings, hydrostatic bearings are nearly frictionless, have no stick-slip effect, and exhibit very good damping behavior. However, hydrostatic bearings have higher costs due to the complex construction involved. In order to support a hydrostatic bearing with a constant pressure support, a pre-throttle is required. The type of pre-throttling used results in different characteristics of the bearing. A design tool has been developed to characterize various methods of pre-throttling hydrostatic bearing arrangements for machine tools. This tool allows for the selection of the type of pre-throttling, the geometric dimensions of the bearing, and real or assumed load cycles. As a result, the actual behavior of the bearings in the machine tool can be determined during the design phase.

1   Intruduction

oiseuille Equation, a linear pressure drop across the gap is assumed, as illustrated in Figure 2. This assumption holds true for rectangular pockets, with the exception of the corners of the pockets.

A hydrostatic bearing can exclusively withstand pressure forces on the bearing. To accommodate both tensile and pressure forces, two hydrostatic bearings must be employed (see Figure 1. As a result, the tool slide is clamped and maintained at the center of the two bearings, disregarding its own weight.
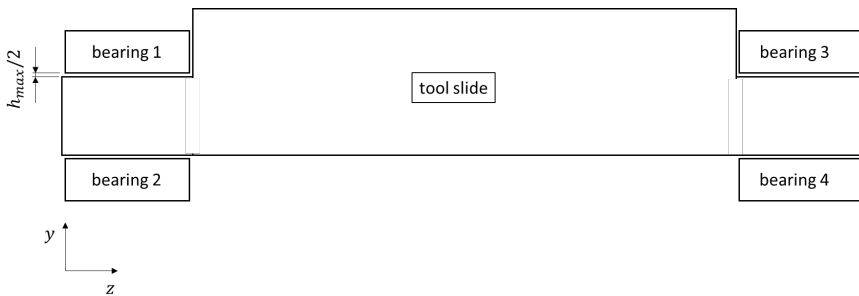
Figure 1: Sketch tool slides of a machine tool.
Source: own

For linear tool slides, mostly rectangular pockets are used. The characteristics of the bearing can be described by the Hagen-Poiseuille Equation for rectangular pockets (see Equation 1). This equation establishes the relationship between the flow rate Q through the bearing, the pressure drop across the bearing Δp, and the geometric dimensions of the bearing b, h, and l. It is notable that the gap height h enters the flow equation with a cubic exponent, and the viscosity η also influences the flow. While the gap height depends on the load and the type of pre-throttling, the viscosity depends on the medium and its temperature.

$$Q = \frac{b\,h^3\,\Delta p}{12\,\eta\,l} \tag{1}$$

To support a tool slide in one direction (x, y or z direction), at least three bearings are necessary; normally, four bearings are used. Therefore, the bearing arrangement for one direction consists of a total of 8 hydrostatic bearings, which are combined into four bearing units (see Figure 2). The forces on the individual bearing units can

be determined by establishing static equilibrium. To describe the mathematical relationships, only one bearing unit is considered. Figure 2 shows a sketch of a hydostatic bearing and the pre-throttle. The pre-throttle is neccessary to reduce the system pressure of the constant pressure system to the load pressure of the bearing. This system is known in electrical engineering as a voltage divider.
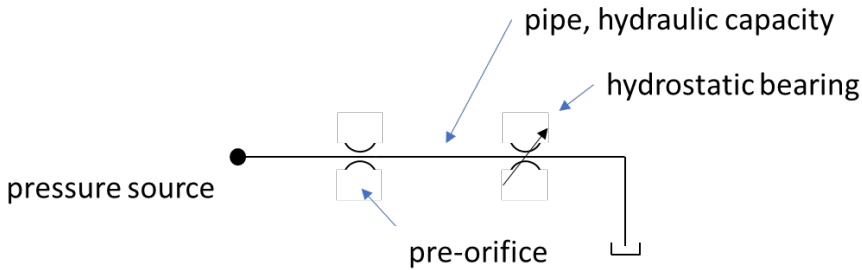
Figure 2: Hydraulic circuit diagram, hydrostatic bearing.
Source: own

The result is a system with a constant pre-throttle (not when a progressive quatity regulator is used) and a variable throttle (hydrostatic bearing). Which type of throttling is used has an affect on the behavior of the hydrostatic bearing. Four different possibilities for pre-throttling can be distinguished:

- – by a capillary,
- – by a throttle,
- – by a orifice,
- – by a progressive flow regulator.

Each of the four different types of throttling has distinct characteristics, leading to varying behavior in response to load changes of the hydrostatic bearing.

The capillary can be regarded as a thn tube with a laminar flow inside. The flow depends on the pressure drop and on the viscosity of the fluid, see Equation 2. This provides an advantage when the temperature of the medium is changing, as the flow through the hydrostatic bearing is also dependent on viscosity.

$$Q = \frac{\pi\, r^4 \Delta p}{8\, \eta\, l} \tag{2}$$

If an orifice is used as a pre-throttle, the flow depends on the geometry of the orifice and the density of the fluid. Additionally, the pressure drop across the orifice follows a quadratic relationship in the equation (refer to Equation 3). One advantage of using an orifice is that it can be placed very close to the hydrostatic bearing, thereby minimizing the dead volume between the orifice and the hydrostatic bearing.

$$Q = \alpha \, A \sqrt{\frac{2 \, \Delta p}{\varrho}} \tag{3}$$

When achieving a load-independent gap height, a progressive flow regulator must be employed. The flow through the hydrostatic bearing then follows the characteristic outlined in Equation 1. In our case, a flow compensator is utilized, as presented by Mörwald [7]. This involves a variable cylindrical annular throttle. The length of this throttle depends on the force equilibrium between a spring and the pressure on the face side of the spool. The gap height is variable and needs to be calculated separately for each distinct hydrostatic bearing.

The shape of the spool can not be calculated analytical, it must be calculated discret. Base of the eauation is the force equilibrium in the spool of the progressive flow regulator. To each pressure drop over the spool a position of the spool is given. Beginning with a start discredization (zero overlab gives a divition by zero) and the equation of continuity each new gab height can be calculated out of the old gab height and the next discret step. Therefore it is necessary to calculate the pressure drop to the last step then the difference between the pressure drop of the last step and the aktualy absolute pressure drop. With this result the new gap height of the aktual step can be calculated.

The actual fow for each step can be calculated with Equation 4. The pressure drop will be quantsized with the same number as the quantization of the maximum stroke of the spool.

$$Q_i = \frac{b \, h^3 \Delta p_{b,i}}{12 \, \eta \, l} \tag{4}$$

Now the pressure drop of the progressive flow regulator must be calculated.

$$\Delta p_{pfr,i} = p_p - \Delta p_{b,i} \tag{5}$$

The nex step is to calculate under the assumption that the flow in each quatization is the same the pressure drop to the last step of calculation $i - 1$,

$$\Delta p_{pfr,n=i-1} = \sum_{n=1}^{i-1} \frac{12 \, Q_i \, \eta \, \Delta l}{d_{spool} \, \pi \, h_n^3} \tag{6}$$

where d_{spool} is the diameter of the spool and h_n is the gap height of the discrete gap.

In the next step the pressure drop of the actual step van be calculated.

$$\Delta p_{pfr,n=i} = \Delta p_{pfr,i} - \Delta p_{pfr,n=i-i} \tag{7}$$

At last the gap height of the actual step i must be calculated.

$$h_i = \sqrt[3]{\frac{12 \, Q_i \, \eta \, \Delta l}{d_{spool} \, \pi \, \Delta p_{pfr,n=i}}} \tag{8}$$

The result of this calculation is exemplary shown in Figure 3. In this case is the diameter of the spool 6 mm and the stroke also 6 mm.
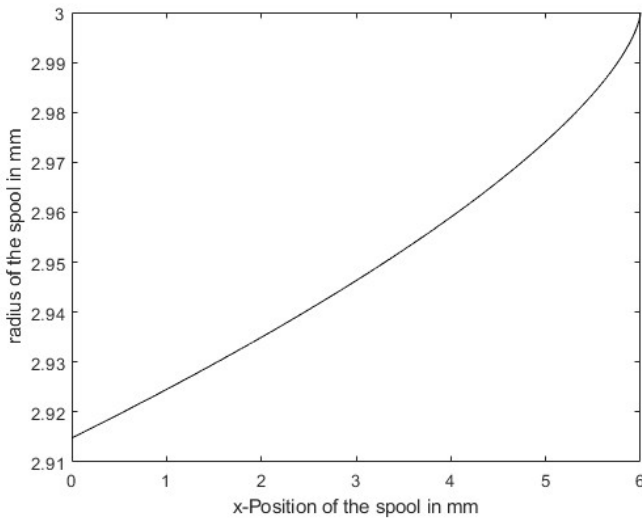
Figure 3: Shape of the gap between spool and housing of the progressive flow controller.
Source: own

To describe the transfer behavior of a hydrostatic bearing a hydraulic-mechanical model must be developed. The hydraulic part of the system will be described with hydraulic resistances, capacitances and inductances. The mechanics of the hydrostatic bearing will be described with Newton's law of motion. In Figure 4 can be seen the model of a hydrostatic bearing consisting of the hydraulic network and the mechanic which is described in [7].
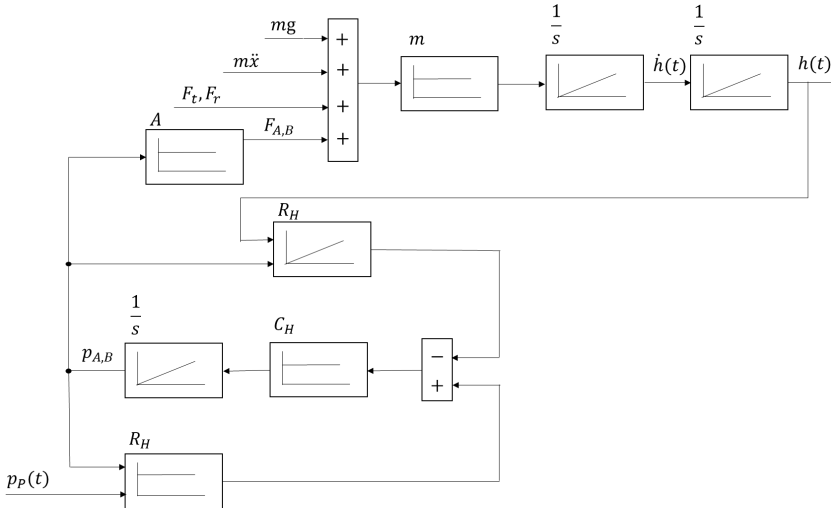
Figure 4: Equivalent circuit, hydrostatic bearing.
Source: [8]

This system is implemented in the Siemens AMESIM software to construct both the hydraulic and mechanical components of a hydrostatic bearing system. The oil volume between the pre-throttle and the hydrostatic bearing is also considered.

3   Model

The AMESIM model consists of different parts. The first one is comprised of the global variables. These variables define the general conditions of the system. A distinction is made here between geometric variables and hydraulic variables. The geometric variable defines the dimensions of the bearings, and the hydraulic variables define the hydraulic conditions.

After defining the global variables, the type of pre-throttling is selected. The precise geometric dimensions of the capillary or orifice are not necessary. The following step involves calculating the exact dimensions of the capillary orifice, which is achieved through the optimization algorithm of the AMESIM software. In situations where a progressive flow controller is employed, the geometry of the spool must be calculated. This task is accomplished using a second software tool, Matlab.
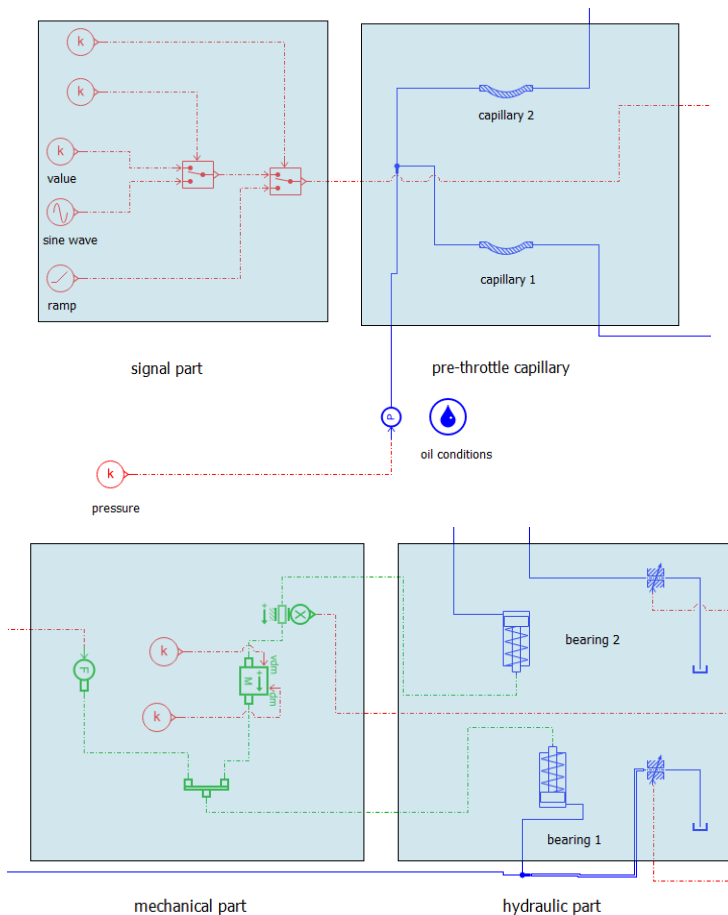
Figure 5: Model of the system hydrostatic beraing with a capillary as pre-throttle.
Source: own

Figure 5 depicts the model for the system with the capillary used as a pre-throttle. The model comprises four parts: the signal part, where the load on the bearing can be selected; the pre-throttle part; the mechanical part of the bearing; and the

hydraulic part of the bearing. The hydraulic part of the bearing is divided into a hydraulic cylinder that manages the forces on the bearing, and the bearing gap which generates the oil flow through the bearing.

For the other two versions of the pre-throttle, only the pre-throttle block is displayed in Figure 6. The shape of the control edge of the progressive flow controller is pre-calculated using Matlab, and the flow characteristic is integrated into the sub-model, as depicted in the left part of Figure 6.
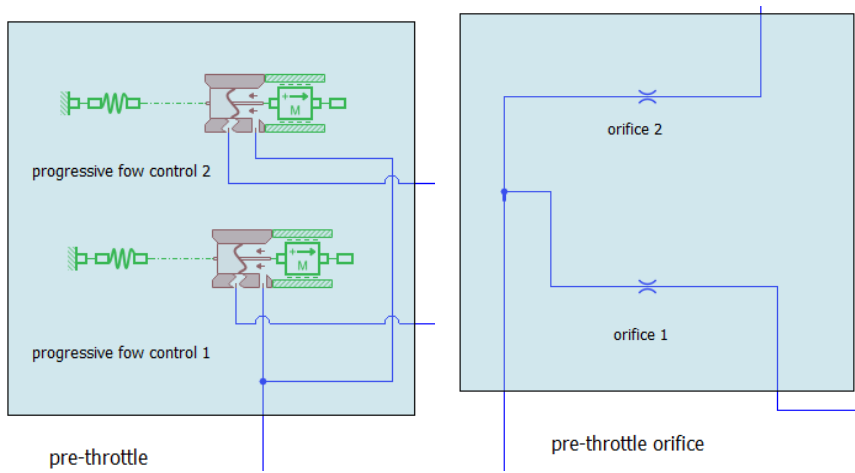
Figure 6: The different models for the pre-throttles.
Source: own

4   Results

To compare the various versions of pre-throttle in the hydrostatic bearings, two diagrams are employed. The first one illustrates the bearing gap in relation to the bearing load (Figure 7). It can be observed that using the capillary and the orifice as pre-throttles results in a variable gap height based on the bearing load. The profile of the gap height varies. On the other hand, the progressive flow controller maintains a consistently ideal gap across the middle of the two bearings, although some oscillations are visible in the curve. These oscillations stem from the spring-mass system of the progressive flow controller.

Figure 7: Compatison of the gap height over the load of tifferent types of pre-throttles
Source: own

In the second figure, Figure 7, a dynamic load with a frequency of 25 Hz is applied to the bearing. In this scenario, the two conventional pre-control versions result in an oscillating gap over the bearing's operational time. The amplitude of the gap oscillation is smaller when using the orifice as the pre-control method.

This can also be observed in Figure 6, where the curve's slope is shallower. Additionally, the progressive flow controller yields an oscillating gap with a significantly smaller amplitude. This outcome is due to the mass of the spool within the progressive flow controller.
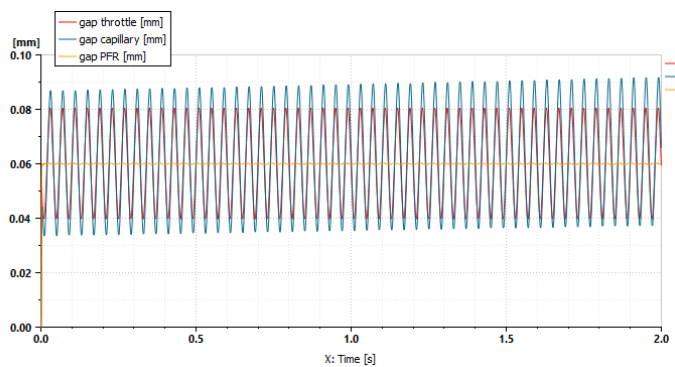
Figure 9: Comparison of the gap height with a dynamic load
Source: own

References

[1]   Koc, E.; Hooke, C.J.: Considerations in the design of partially hydrostatic slipper bearings; *Tribology International*; Volume 30, Issue 11, page 815-823; 1997

[2]   Achten, P, Mommers, R, Potma, J, & Achten, J. "Experimental Investigation of a Hydrostatic Bearing Between Barrels and Port Plates in Floating Cup Axial Piston Pumps." *Proceedings of the BATH/ASME 2020 Symposium on Fluid Power and Motion Control. BATH/ASME 2020 Symposium on Fluid Power and Motion Control.* Virtual, Online. September 9–11, 2020. V001T01A003. ASME.

[3]   Gold, S.; Weber, J: New Plain Bearing Concept for Support of the Propeller Shaft in Pod-drives of Large Ships; *8. Internationales Fluidtechnisches Kolloquium*, proceedings; Dresden; 2012

[4]   Y. Altintas, A. Verl, C. Brecher, L. Uriarte, G. Pritschow: Machine tool feed drives, *CIRP Annals*, Volume 60, Issue 2, 2011, Pages 779-796

[5]   Dmytro Fedorynenko, Rei Kirigaya, Yohichi Nakao: Dynamic characteristics of spindle with water-lubricated hydrostatic bearings for ultra-precision machine tools; *Precision Engineering*, Volume 63, 2020, Pages 187-196

[6]   Steffan M, Haas F, Zopf P, Edler J. Optimierung der Schleifbearbeitung mittels OPC UA: Neue Prozessregelung zur Vermeindung von thermischer Randzonenschädigung. *Zeitschrift für wirtschaftlichen Fabrikbetrieb.* 2017 Mar 1;112(3/2017):137

[7]   Mörwald G, Edler J, Tic V. Calculation of Control Edges with Simulation; *International conference Fluid Power: Conference Proceedings;* Maribor, 2015, S. 249-254

[8]   Edler, J. & Steffan, M.: Verification of a simulation model to predict the transmission behavior of hydrostatic bearing on machine tools, *International conference Fluid Power: Conference Proceedings;* Maribor, 2017, S. 175-184

A Simulation Study on the Feasibility of Valve Spool Stabilization Under the Influence of Spool Core Elasticity

Simon Leonhartsberger
Bernhard Manhartsgruber

Johannes Kepler University, Institute of Machine Design and Hydraulic Drives, Linz, Austria
simon.leonhartsberger@jku.at, bernhard.manhartsgruber@jku.at

Spool valves suffer from friction between spool and sleeve when the spool is not radially stabilized in a central position but unstably moves outwards and touches the sleeve or housing. Circumferential grooves for pressure equalization are a classical remedy for the problem offering some relief but not a real solution for stabilizing the spool in the middle. The use of conical geometries offering a stabilizing mechanism has been suggested repeatedly in the fluid power literature and a few very elegant solutions for generating these geometries solely from pressure induced elastic deformations of initially cylindrical geometries have been published. Some of these proposals are based on strongly simplified models assuming a rigid cylindrical core of the spool surrounded by elastically modelled lands deforming under pressure. The geometry of these lands typically assumes an initially perfect cylindrical geometry. The purpose of this paper is to look into the situation when the first assumption is dropped. What if the whole spool is modelled with elastic deformation? This question is answered by a simulation model based on finite element analysis combined with a solution of the Reynolds equation for the pressure in the gap between spool and sleeve.

1   Intruduction

Spool valves are one of the most common elements used in fluid power circuits. As several variable orifices can be integrated in a single spool and sleeve assembly this valve design allows for the complete directional control of a hydraulic cylinder or motor by just one moving element and thus, by a single mechanical or electromechanical control input. This geometrical design flexibility comes at the expense of demanding manufacturing tolerances in order to fit the spool precisely enough into the sleeve or housing to prevent excessive leakage. If the cylindrical shapes of the two parts differ too much from the ideal geometry due to manufacturing errors or pressure-induced deformations, the friction on the spool becomes a severe issue making precise spool positioning impossible in proportional or servo control applications.

The friction effects on the spool are known to be sensitive to the pressure field in the gap [1]. Asymmetries in this pressure distribution may result in the spool being pushed out of its centre position with an increase due to more pronounced mixed friction or even pure metallic contact at the smaller gap side. A classical countermeasure against pronounced pressure asymmetries along the circumference of the gap is known in the form of circumferential grooves on the cylindrical lands of the spool.

A further important mechanism is related to the stabilizing or destabilizing process of conical sealing gaps depending on the convergence or divergence of the gap from the high-pressure side to the low-pressure side. The principle is long known from hydraulic servo-cylinders with deliberately manufactured precise gaps with tiny cone angles [2]. The effect may also occur in spool valve geometries by deviations from the ideal cylindrical manufacturing or by a pressure-induced elastic deformation [3, 6]. Recently, the design rules for getting a stabilizing pressure-induced deformation from simple-to-manufacture geometries has come into focus. In [4] the effect is studied for an elastically deforming sealing land on a rigid spool core. In the present paper, this study is expanded for the fully elastic spool.

S. Leonhartsberger, B. Manhartsgruber: *A Simulation Study on the Feasibility of Valve Spool Stabilization Under the Influence of Spool Core Elasticity*

55

2   Problem modelling

To provide the possibility to retrace the process described in this paper this chapter sketches the most relevant modelling parameters. Next to the basic geometry parameters and material properties the loads and boundary conditions are in focus.

2.1   Fundamental geometry and material parameters

The geometry consists of two lands which are connected by a rod and guided in a rigid pipe.
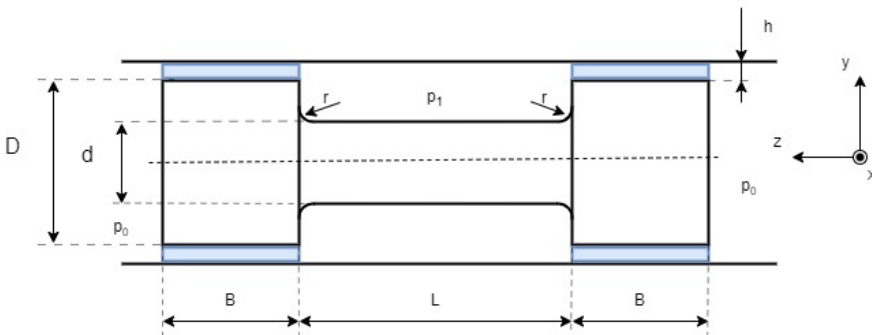
Figure 1: General problem setup.

Surce: own.

Table 1: Geometric and material parameters

symbol	name	value
h	gap height	10 µm
D	outer spool diameter	12 mm
d	inner spool diameter	6 mm
B	land width	10 mm
l	rod width	20 mm
r	radius	1 mm
p_0	outer pressure	1 bar
p_1	inner pressure	200 bar
E	Young's modulus of steel	210 e3 N/mm²
μ	Poisson's ratio	0.3
ν	fluid viscosity	34.4 mm²/s

Figure 1 sketches a cut through the rotationally symmetric setup, while widely overrepresenting the height of the fluid gap. Along the simulations the width of the lands B is varied along with the diameter of the rod connecting both lands. All solid

deformable parts are assumed to be made from steel; the parameters of the fluid can be taken from table 1.

2.1   Simulation setup in Abaqus

In order to maximize the efficiency and reduce calculation time a symmetric boundary condition is set and therefore the number of elements can be halved. As the reaction to a small displacement along the z-axis and tilting around the   x-axis shall be examined, the according displacements have to be introduced. To avoid distorted mesh elements the outer areas of the lands are separated into extra sections with different mesh-controls as noticeable in Figure 2. As the pipe is modelled as a rigid body, the boundary conditions are applied directly to the elements of the fluid gap. Special attention comes to modelling the fluid gap, as described in the following section.
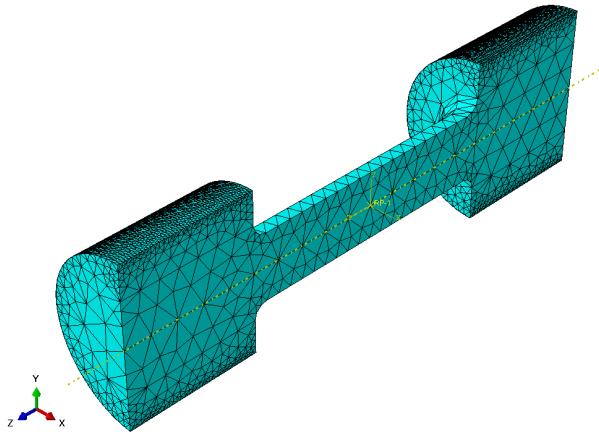
Figure 2: General problem setup.
Surce: own.

2.1.1   Reynolds user-element

Finite element methods require that the dimensions of an element don't differ too much to obtain numeric stability and acceptable convergence rates. Therefore, in case of hexahedral elements, cubes would be the preferred case. Assuming the radial direction is resolved with five elements one fluid gap would contain about 500.000 elements, resulting in an unbearable computing effort.

S. Leonhartsberger, B. Manhartsgruber: A Simulation Study on the Feasibility of Valve Spool Stabilization Under the Influence of Spool Core Elasticity

57

The pressure along the z-axis provides valuable insight. The pressure along the radius is of little interest and can be assumed constant due the small gap height. Furthermore, the inertial forces of the fluid are negligible, the geometry can be unreeled onto a flat plane and hydraulic oil behaves like a Newtonian fluid. As a result, the Reynolds-equation can be used, to implement a so-called user-element in Abaqus. The theoretical and mathematical derivation can be found in [5].

2.1.2 Boundary conditions and external forces

The fluid elements need to be tied onto the spool and pinned at their outer radius. Pressure is applied as an external load onto the surfaces of the spool. In addition, these pressures have to be implemented as boundary conditions for the fluid gaps.

The introduction of the displacement takes place over a coupling with decreasing weighting over the influence radius at the middle of the spool. Thus, unrealistic stresses and supporting effects in the areas of interest can be avoided. After the pressures are applied the spool will be shifted parallelly by 0.5 μm along the z-axis and afterwards rotated by 10^{-5} radians around the x-axis. Additionally, a contact between spool and pipe is introduced, therefore a minimal height of the user-element can be guaranteed and the acquisition of the height values simplifies. The gap pressure is read directly form the output database and visualized in a different program.

3 Analysis and interpretation of the simulation results

Along with the course of pressure and deformation the stability is evaluated depending on the geometry. The simulation was performed for a variety of parameter combinations of the spool width *B* and the inner diameter *d.*

3.1 Deformation and pressure course

Figure 3 shows the deformed spool with a deformation scale factor of 30000. The deformation decreases while going from high to low pressure.
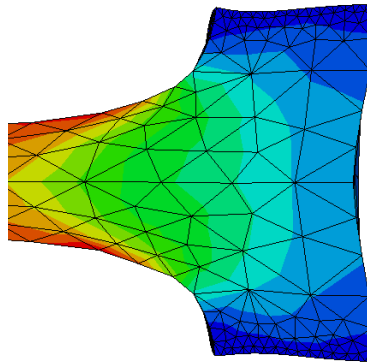
Figure 3: Elastic deformed spool with a width B of 5 mm (deformation scale factor 30000)
Surce: own.

The pressure course over the length of the spool is dominated by the linear pressure gradient resulting of the boundary conditions; comparable as it would occur using an ideal cylindrical gap without eccentricity or tilt. Therefore, the pressure gradient is subtracted from the solution before visualisation. Figure 4 shows the unrolled pressure over the radius and angle. As the symmetry boundary condition applies to the pressure as well, the angle is limited by $\pm 90°$. Due to the pressure boundary conditions the derivation is zero at both borders of the cylinder. The coordinate system of figure 1 applies and has its origin in the middle of the spool.
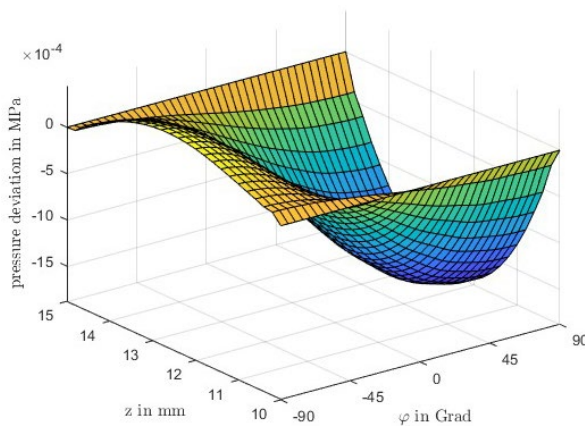
Figure 4: pressure deviation compared to the ideal cylindrical fluid gap without eccentricity or tilt; $B =$ is 5 mm, d = 5
Surce: own.

S. Leonhartsberger, B. Manhartsgruber: A Simulation Study on the Feasibility of Valve Spool Stabilization Under the Influence of Spool Core Elasticity

59

3.2   Determination of stable areas

To determinate conditions for stability the simulation was performed for a variety of parameter combinations of the spool width B and the inner diameter d. This way the development of the reaction force and the momentum as in figure 5 and a stability map as in figure 6 can be derived.
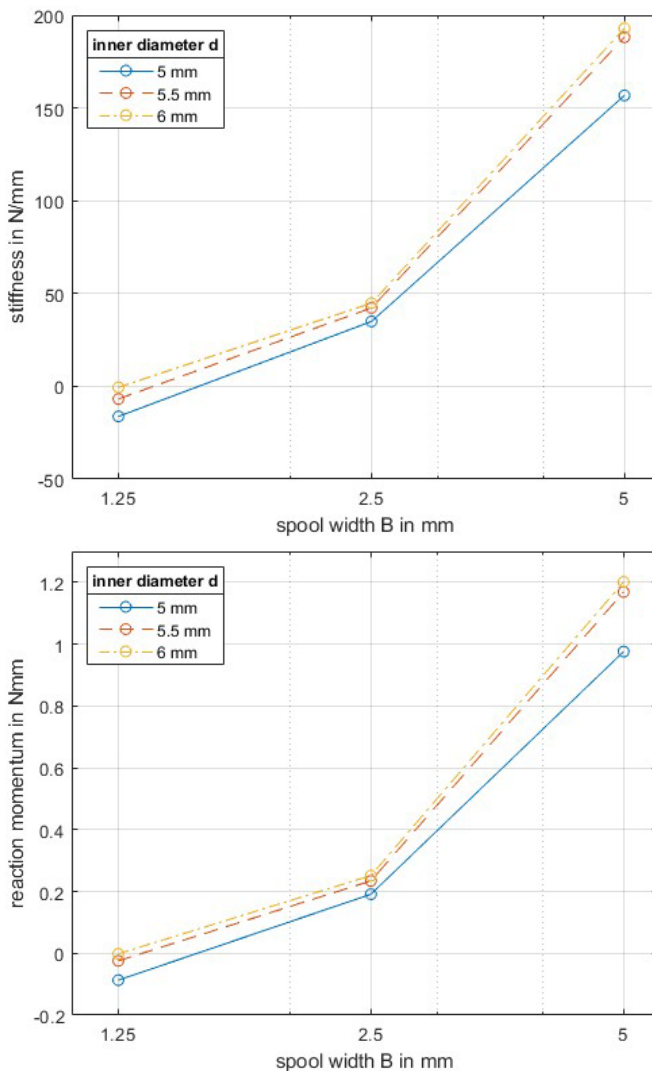
Figure 5: Reaction force and momentum in dependency of the spool width B
Source: own.

For a given rod diameter the system gets instable if the width gets too small. As figure 3 displays the stability depends from the inner diameter. The courses of the reaction forces and the reaction momentums look similar.
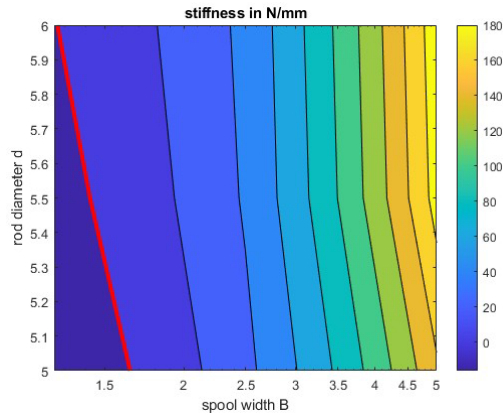
Figure 6: Stability criteria with red marked stability limit
Source: own.

3.3   Conclusion

In this paper the theory can be supported, that the width of the rod has major influence on the stability of the spool; the diameter of the rod has only little impact. In contrary to previous papers, the stabilizing effect can be shown to occur also if the rod is modelled as an elastic body.

References

[1]   Merritt, Herbert E. (1991) *Hydraulic Control Systems*, John Wiley & Sons
[2]   Blackburn, J. F. (1960) Fluid Power Control, Wiley, New York
[3]   Winkler, B., Mikota, G., Scheidl, R., Manhartsgruber, B. (2005) Modelling and Simulation of the Elastohydrodynamic Behavior of Sealing Gaps. Australian Journal of Mechanical Engineering 2(1), 86-72
[4]   Scheidl, R., Manhartsgruber, B. (2023) Spool Valve Stability and Sealing Land Derformation, to appear in Proceedings of NSHP 2023, International Conference on Hydraulic and Pneumatic Drives and Controls, Piechowice, Poland, October 11-13, 2023
[5]   Gradl, Chr.: Hydraulic stepper drive: Conceptual study, design and experiments. PhD thesis, Johannes Kepler University Linz, 2017.
[6]   Scheidl, R., Resch, M., Scherrer, M., & Zagar, P.: An approximate, closed form solution of sealing gap induced lateral forces for imperfect sealing land geometries. In Advances in Hydraulic and Pneumatic Drives and Control 2020 (pp. 102-111). Springer International Publishing. (2021).

The Influence of the Tilt Angle of the Inclined Plate on the Gradient of the Pressure Increase in the Piston-axial Pump Cylinder

Andrzej Banaszek,[1] Predrag Dašić,[2]
Raul Turmanidze[3]

[1] West Pomeranian University of Technology, Szczecin, Poland
andrzej.banaszek@zut.edu.pl
[2] Akademija strukovnih studija Šumadija (ASSŠ) – Odsek Trstenik, Trstenik, Seriba
dasicp58@gmail.com
[3] Georgian Technical University (GTU), Faculty of Transportation and Mechanical
Engineering, Tbilisi, Georgia
inform@gtu.ge

Piston-axial pumps play a crucial role in various industrial and mechanical systems, where the efficient conversion of mechanical energy into fluid pressure is essential. This study investigates the impact of the tilt angle of an inclined plate on the gradient of pressure increase within a piston-axial pump cylinder. By systematically altering the tilt angle of the inclined plate, the research aims to uncover how this parameter influences the distribution of pressure gradients along the piston's axial movement. The findings from this investigation are expected to enhance our understanding of fluid dynamics within such pumps and provide insights into optimizing their design and performance.

1   Intruduction

Piston-axial pumps are widely utilized in applications where controlled fluid flow and pressure generation are vital, including hydraulic systems, automotive engines, and various industrial processes. These pumps feature a reciprocating piston that drives fluid through a cylinder, creating pressure gradients that facilitate fluid movement. The efficiency and effectiveness of such pumps are influenced by numerous factors, including the geometric and operational parameters of their components.
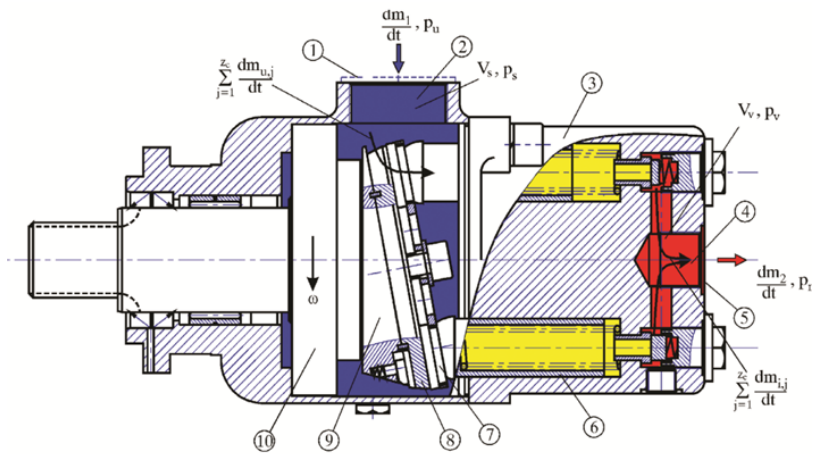
1 – Connection of the suction pipeline, 2 – Suction space of the pump, 3 – Cylinder block,
4 – Discharge space of the pump, 5 – Connection of discharge pipeline, 6 – Piston,
7-Switchboard, 8 – Slantwise panel, 9 – Drive shaft, 10 – Bearing of the drive shaft of the pump

Figure 1: Construction and control spaces of axial piston pump.
Source: own.

One such component is the inclined plate situated within the pump cylinder. This inclined plate can impact the distribution of pressure gradients along the axial movement of the piston. The tilt angle of the inclined plate, defined as the angle between the plate's surface and the horizontal axis, is a critical parameter that can potentially influence the fluid dynamics within the pump.

Understanding the relationship between the tilt angle of the inclined plate and the resulting pressure gradient distribution is essential for optimizing pump performance. This study aims to systematically investigate this relationship to

A. Banaszek, P. Dašić, R. Turmanidze: The Influence of the Tilt Angle of the Inclined Plate on the Gradient of the Pressure Increase in the Piston-axial Pump Cylinder

63

provide insights into the underlying mechanisms governing the fluid dynamics within piston-axial pump cylinders.

2 Methodology

The experimental setup consists of a piston-axial pump cylinder with an inclined plate positioned at a specific tilt angle. A fluid medium is circulated through the pump, and the pressure increase along the axial movement of the piston is measured using pressure sensors placed strategically within the cylinder. The experiments are conducted by varying the tilt angle of the inclined plate while keeping other parameters constant.

Figure 2: **A detail of drive shaft bearing.**
Source: own.

The collected pressure data are analysed to determine the pressure gradient along the axial direction for each tilt angle. Statistical analysis techniques are employed to assess the significance of the observed variations and correlations between the tilt angle and pressure gradient.

3 Results

The results of the experiments reveal a clear relationship between the tilt angle of the inclined plate and the gradient of pressure increase along the piston's axial movement. Different tilt angles lead to distinct pressure gradient profiles, indicating that the fluid dynamics within the pump cylinder are influenced by this parameter.
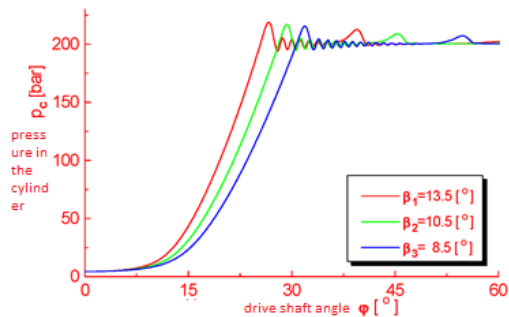
Figure 3: Impact of the angle β of the slope of slantwise plate to the gradient of pressure increase in the cylinder, p_c.
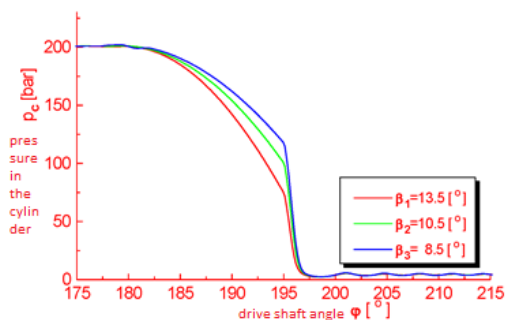
Source: own.

Figure 4: Impact of the angle β of the slope of slantwise plate to the gradient of pressure increase in the cylinder, p_c.
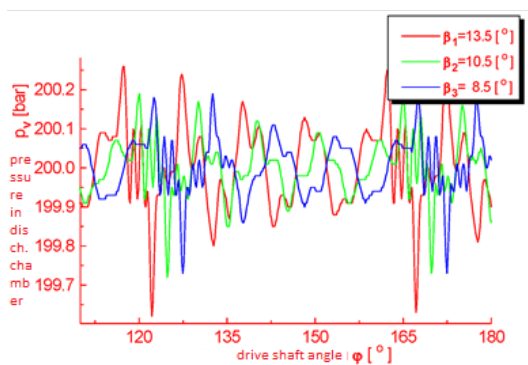
Source: own.

Figure 5: Impact of the angle β of the slope of slantwise plate to the pressure flow in the discharge chamber, p_v.

Source: own.

A. Banaszek, P. Dašić, R. Turmanidze: The Influence of the Tilt Angle of the Inclined Plate
on the Gradient of the Pressure Increase in the Piston-axial Pump Cylinder

65

Changing the angle of inclination of the inclined plate affects the gradient of pressure rise and fall in the cylinder, so that larger values of the angle correspond to steeper gradients of pressure rise, fig.3, and gentler pressure drop gradients, Figure 4. The angle of inclination of the inclined plate affects the flow of pressure in the pressure chamber so that at larger values of the angle, the pressure pulsation is greater, Figure 5.

The observed variations in pressure gradients emphasize the importance of the inclined plate's tilt angle in shaping the flow patterns and pressure distribution within the piston-axial pump cylinder. The findings suggest that optimizing the tilt angle could potentially enhance pump efficiency, reduce energy consumption, and minimize undesirable flow phenomena such as cavitation.

3   Conclusion

This study highlights the significance of the tilt angle of the inclined plate in a piston-axial pump cylinder and its influence on the gradient of pressure increase along the piston's axial movement. The results provide valuable insights for engineers and researchers working on pump design and optimization, contributing to the development of more efficient and effective piston-axial pumps for various applications. Further research can delve into the intricate fluid dynamics mechanisms underlying these observations, enabling a deeper understanding of the interactions between geometric parameters and pump performance.

References

[1]   Petrovic R.: Matematičko modeliranje i identifikacija parametara višecilindričnih klipno-aksijalnih pumpi, doktorska teza, Mašinski fakultet Univerziteta u Beogradu, Beograd 1999.
[3]   Ivantysyn, J., Ivantysynova, M. (2001): „Hydrostatic Pumps and Motors. Principles, Design, Performance, Modelling, Analysis, Control and Testing". First English Edition. New Delhi, India: Akademia Books International
[4]   Jankov R.: „Matematičko modeliranje strujno - termodinamičkih procesa i pogonskih karakteristika dizel - motora, - kvazistacionarni modeli-„ I deo, Naučna knjiga, Beograd, 1984.
[5]   Jankov R., Tomić M., Štavljanin M.: „ Istraživanje kibernetičkih metoda projektovanja i razvoja sistema ubrizgavanja dizel motora", Naučnoistraživački projekat - II faza, Mašinski fakultet, Beograd, 1986.
[6]   R. Petrović, R. Jankov, R. Slavković, M. Živković: primena inženjerskih softvera u PPT Namenska, Trstenik „Software package AKSIP za proračun, identifikaciju i optimizaciju parametara aksijalnih klipnih pumpi", Završni izveštaj Projekata, evidencioni broj 1.5.1208, Ministarstvo za nauku i tehnologiju Republike Srbije u periodu 1996 do 1997. godine

[7]   R. Petrović, M. Živković, R. Slavković,: primena inženjerskih softvera u PPT Namenska „Software package RADIP za proračun, identifikaciju i optimizaciju parametara radijalnih klipnih pumpi", Završni izveštaj Projekta, evidencioni broj MIS. 3.07.0090.A, oblast: Mašinstvo i inženjerski softver, Ministarstvo za nauku, tehnologije i razvoj, u periodu 2002-2004. godine, rukovodilac projekta doc.dr Radovan Petrović, Mašinski fakultet Kraljevo.

[8]   R. Petrović, M. Živković, R. Slavković,: primena inženjerskih softvera u PPT Namenska „Software package KRILP za proračun, identifikaciju i optimizaciju parametara krilnih pumpi", Završni izveštaj Projekta, evidencioni broj TR 6371A, oblast: Inženjerski softver, Ministarstvo za nauku, tehnologije i razvoj, u periodu 2005-2007. godine, rukovodilac projekta dr Radovan Petrović vanredni profesor, Mašinski fakultet Kraljevo

[9]   R. Petrović, M. Živković, R. Slavković,: primena inženjerskih softvera u PPT Namenska „Software package CILHI za proračun, identifikaciju i optimizaciju parametara hidrauličnih cilindara", Završni izveštaj Projekta, evidencioni broj TR 12001, oblast: Inženjerski softver, Ministarstvo za nauku, tehnologije i razvoj, u periodu 2008-2010. godine, rukovodilac projekta dr Radovan Petrović vanredni profesor, Mašinski fakultet Kraljevo

[9]   R. Petrović, " Mathematical Modeling and Experimental Verification of Operating Parameters of Vane Pump With Double Effect", " STROJNIŠKI VESTNIK" – Journal of Mechanical Engineering, Vol.5, No1, p.26-32, Univerza v Ljubljani, Fakulteta za strojništvo, Ljubljana, Slovenia.

[10]   R. Petrović (2009): Mathematical Modelling and Experimental Research of Characteristic Parameters of Hydrodynamic Processes in an axial piston Pump, " STROJNIŠKI VESTNIK" – Journal of Mechanical Engineering, Vol.55, No4, p.224-229 , Univerza v Ljubljani, Fakulteta za strojništvo, Ljubljana, Slovenia

[11]   A. Banaszek, R. Petrović, " Calculations of the unloading operation in case of liquid cargo service with high density on modern product and chemical tankers equipped with hydraulic submerged cargo pumps", " STROJNIŠKI VESTNIK" – Journal of Mechanical Engineering, volume 56, (2010), number 3, p., Ljubljana, March 2010, ISSN 0039-2480, Univerza v Ljubljani, Fakulteta za strojništvo, Ljubljana, Slovenia

[12]   B .Obrović, S. Savić, R. Petrović, „Ionized gas boundary layer on bodies of revolution in the presence of magnetic field", „TEHNIČKI VJESNIK – TECHNICAL GAZETTE"- Journals by scientific areas, volume 17, (2010), number 1, p. 35-42, Osijek, March 2010, ISSN 1330-3651, Faculty of Mechanical Engineering in Slavonski Brod, Faculty of Electrical Engineering in Osijek, Faculty of Civil Engineering in Osijek, Croatia

Optimization of Axial Piston Water Pumps in the Development Phase

Slobodan Savić,[1] Nenad Todić,[1] Stefan Cvejić[2]

[1] University of Kragujevac, Faculty of Engineering, Kragujevac, Serbia
ssavic@kg.ac.rs, ntodic@gmail.com
[2] University "Union-Nikola Tesla" of Belgrade, Faculty of Information Technology and Engineering, Belgrade, Serbia
etfot1@gmail.com

On the basis of theoretical and experimental studies, the appropriate structure of the sliding contact in the framework of the water hydraulic axial piston pump was designed. Load experiments for the developed water hydraulic axial piston pump were carried out on a water hydraulic component test installation. Experimental test results show that the volumetric efficiency and noise characteristics of the water hydraulic piston axial pump are significantly improved under hydrodynamic lubrication conditions compared to dry lubrication conditions. The conclusions obtained from these studies are very significant for further research and development of piston axial pumps of water hydraulics.

1   Intruduction

Axial piston water pumps serve as crucial components for water circulation, supply, and pressure generation in a wide array of applications. To meet the growing demand for efficient and reliable water transport, optimizing these pumps during their development phase is of paramount importance. This study focuses on identifying and addressing critical aspects that contribute to achieving enhanced pump performance, reliability, and longevity.

An important factor that defines the working characteristics of the pump is represented by different pairs of friction inside the pump. The most important couple is the sliding contact between the shaft and the bearings. In this connection, we note two important factors in the operation of the piston-axial pump of water hydraulics, lubrication and wear, as well as sealing and leakage. Various experiments were conducted using sliding contact components manufactured from PEEK material with different compositions. It was concluded that PEEK þ 10wt % CF, 10wt % polytetrafluoroethylene (PTFE) and 10wt % graphite give the most favourable properties for sliding contact operation under dry friction conditions.
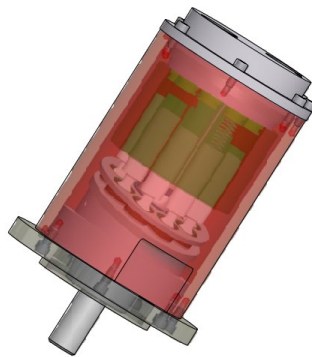
Figure 1: Axial piston water pump.
Source: own.

The wear mechanism of PEEK radial bearings operating in dry conditions was determined. The wear characteristics of EP and PEEK materials that can be used for sliding bearings inside piston-axial pumps of water hydraulics in conditions lubricated by dry and abrasive media were experimentally studied. It was found that the tested results differed significantly with different working fluids.

2 Key Parameters for Optimization

2.1 Piston Geometry

The geometry of pistons in axial piston pumps significantly influences fluid flow dynamics and efficiency. Optimizing parameters such as piston diameter, stroke length, and crown profile can lead to improved hydraulic efficiency and reduced frictional losses.

2.2 Cylinder Arrangement

The arrangement of cylinders within the pump, whether inline or swashplate, impacts the volumetric efficiency and overall performance. Evaluating the pros and cons of each arrangement and determining the optimal choice based on the specific application requirements is crucial.

2.3 Fluid Dynamics

Understanding the flow patterns and pressure distribution within the pump is essential for optimization. Computational Fluid Dynamics (CFD) simulations can provide insights into the effects of design changes on fluid behaviour, helping identify areas for improvement.

2.4 Material Selection

Choosing appropriate materials for pump components is vital to ensure durability and reliability. Materials must withstand the pressures, temperatures, and wear associated with pump operation while maintaining dimensional stability.

3 Results

The results of optimizing the parameters of the hydrodynamic processes of the axial piston pump are shown diagrammatically in Figure 2 (a to f) for different operating modes and for those used in experimental research.
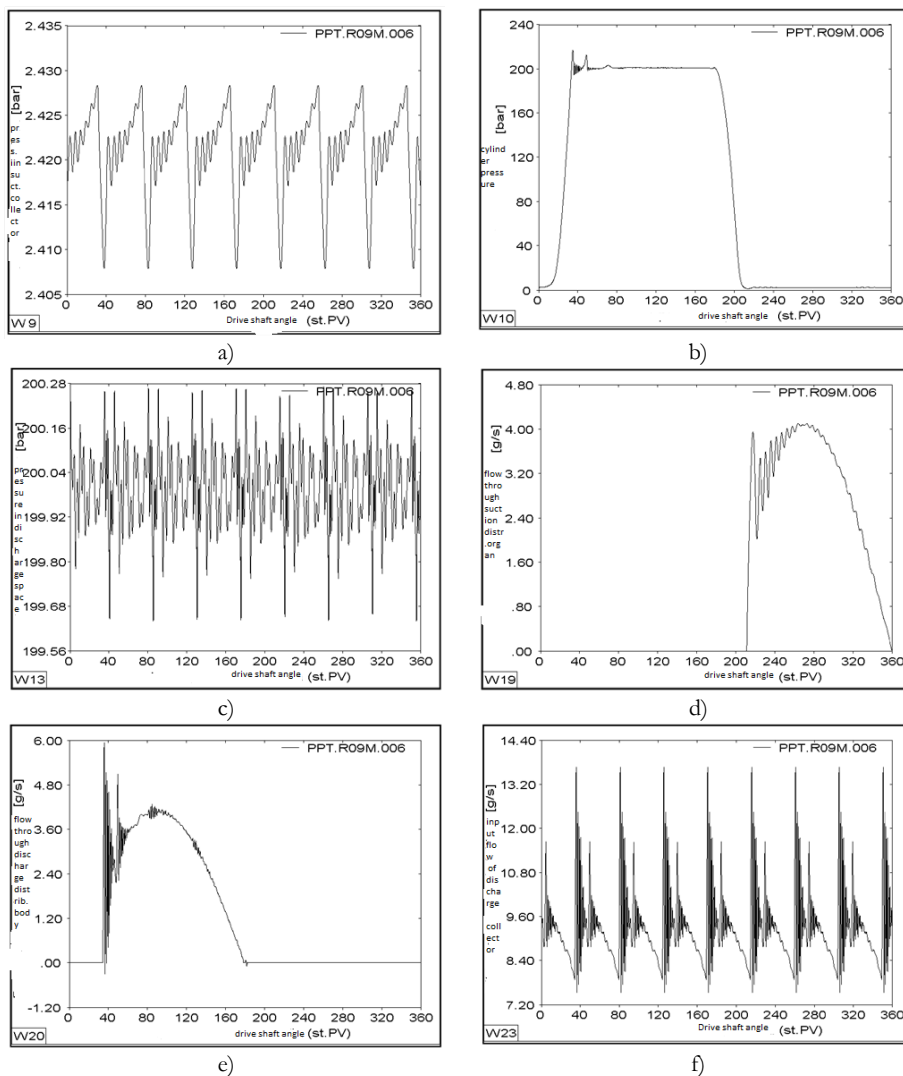
Figure 2 (a to f): Diagrams of characteristic parameters of the axial piston pump, for the operation regime: n = 875.6 min^{-1} and p = 200 bar.

Source: own.

From the diagrams in Figure 2, we can observe great similarity: pressure flow in the suction collector, pressure in the cylinder, pressure in the discharge chamber, flow through suction distribution body and flow through suction collector depending on the angle of a drive shaft in case of different operating modes of the axial piston pump.

The Table 1 shows numerical values of the initial and four optimized parameters of the axial piston pump, which significantly affect the level of cylinder delivery η_c.

Table 1: Initial and optimized numerical values of the four parameters, hydrodynamic processes of the axial piston pump

No	Name of the parameter	Analytical expression	Computer program	Dimension	Numerical values	
					initial	optimal
1.	Suction pressure	p_u	PU	Pa	2.68E5	2.71E5
2.	Parietal radius of the suction opening of distribution panel	R_2	R2U	m	5.1E-2	4.5E-2
3.	Angle of the suction phase beginning	a_2	ALM2G	°	29.77	27.1
4.	Spring rigidity of discharge valve	c_v	CVI	N/m	1104.7	1160

Value of discharge chamber, suction chamber volume, as well as the length of discharge pipeline do not have a significant effect on the maximum coefficient of cylinder delivery η_c. In further analysis, the attention is paid to the impact of initial and optimized parameters to the maximum coefficient of cylinder delivery η_c, for different operating regimes of the axial piston pump, which is shown in Table 2.

Table 2. Values of cylinder delivery coefficient η_c in case of initial and optimized parameters of axial piston pump for different operating regimes

No	Operating regime		Values of cylinder delivery coefficient η_c %		
	p bar	$n min^{-1}$	Initial parameters	7 optimized parameters	4 optimized parameters
1.	50	800	93.6	96.2	95.8
2.	160	800	86.6	93.1	92.6
3.	180	800	85.3	92.1	91.7
4.	180	1000	85.3	92.1	91.7
5.	200	800	84.1	91.4	90.65
6.	200	875.6	84.1	91.4	90.65
7.	200	1000	84.1	91.4	90.65

4   Conclusion

Comparing the results of optimized parameters to the initial ones, the requirements for the analysis of the parameters of the construction of the distribution of working fluid are obvious in case when looking for an optimal solution to the construction of axial piston pump.

Optimizing axial piston water pumps during the development phase involves a comprehensive approach that considers various design and operational parameters. By focusing on piston geometry, cylinder arrangement, fluid dynamics, and material selection, engineers and researchers can create high-performance pumps that meet the demands of diverse applications. Embracing iterative design, simulation tools, and multi-objective optimization ensures the development of efficient, reliable, and robust axial piston water pumps for modern industries.

References

[1]   R. Petrović ,“ Mathematical Modeling and Experimental Research of Characteristic Parameters of Hydrodynamic Processes in an axial piston Pump”, “ STROJNIŠKI VESTNIK” – Journal of Mechanical Engineering, Vol.55, No4, p.224-229 , Univerza v Ljubljani, Fakulteta za strojništvo, Ljubljana, Slovenia

[2]   R.Petrović, J.Pezdirnik, A.Banaszek „Mathematical Modeling and Experimental Research of novel seawater hydraulic axial piston pump” p.459-469, ISBN=978-952-15-2521-6(Vol.4), The Twelfth Scandinavian International Conference on Fluid Power, May 18-20, 2011, Tampere, Finland

[3]   R.Petrović, J.Pezdirnik, A.Banaszek ,“Influence of Compressibility of Working Fluid on Hydrodynamic Processes in The Axial Piston Pump With Combined Distribution/Flow of Working Fluid”, Proceedings of the 2011 International Conference on Fluid Power and Mechatronics, IEEE Catalog Number: CFP1199K-CDR ISBN: 978-1-4244-8449-2,p.335-339, 17 – 20 August 2011 Beijing, China

[4]   Wang, Y. X., Wang, L. P., and Xue, Q. J. (2011), **"**Improvement in the Tribological Performances of Si3N4, SiC and WC by Graphite-Like Carbon Films under Dry and Water-Lubricated Sliding Conditions,**"** Surface and Coatings Technology, 205(8–9), pp 2770–2776

[5]   Wang, Y., Liu, Y., Wang, Z. et al. Surface roughness characteristics effects on fluid load capability of tilt pad thrust bearings with water lubrication. Friction 5, 392–401 (2017). https://doi.org/10.1007/s40544-017-0153-y

[6]   Andrade, T. F., Wiebeck, H., & Sinatora, A. (2019). Tribology of natural Poly-Ether-Ether-Ketone (PEEK) under transmission oil lubrication. Polímeros: Ciência e Technologies, 29(2), e2019026.https://doi.org/10.1590/0104-1428.14416

[7]   Dong W, Nie S, Zhang A. Tribological behavior of PEEK filled with CF/PTFE/graphite sliding against stainless steel surface under water lubrication. Proceedings of the Institution of Mechanical Engineers, Part J: Journal of Engineering Tribology. 2013;227(10):1129-1137. doi:10.1177/1350650113481416

A CONTRIBUTION TO RESEARCH INTO THE DESIGN AND ANALYSIS OF A HYDRAULIC ROBOTIC ARM

ALMIR OSMANOVIĆ, ELVEDIN TRAKIĆ, SALKO ČOSIĆ, MIRZA BEČIROVIĆ

University of Tuzla, Faculty of Tuzla, Tuzla, Bosnia and Herzegovina
almir.osmanovic@untz.ba, elvedin.trakic@untz.ba, salko.cosic@untz.ba, mirzabecirovic80@gmail.com

Hydraulic robotic arms have a wide range of applications. It utilizes hydraulic power, which involves the use of pressurized fluid to generate and control movements. Hydraulic robotic arms consist of several components, including hydraulic cylinders, pumps, valves, and actuators. The advantage of using hydraulic systems in robotic arms is their ability to generate high forces and torque, enabling the arm to lift heavy loads. Hydraulic systems also provide smooth and precise control over movements, allowing for precise positioning and manipulation of objects. However, hydraulic systems can be more complex and require additional maintenance compared to other types of robotic arm mechanisms. In order to analyze the structural integrity of the hydraulic robotic arm were created a kinematic model. For complemented the design analysis process was created cad model, allowing simulations and analysis of the robot for view the motion of each link and characterize their dynamics.

1 Intruduction

Robot is an important element in today's production and assembly. A hydraulic robotic arm is a mechanical device that mimics the movements and functions of a human arm using hydraulic systems. Hydraulic robotic arms have a wide range of applications. They are commonly used in industrial settings for tasks such as heavy lifting, assembling, welding, and material handling. They can also be found in construction equipment. Additionally, hydraulic robotic arms have been used in medical fields for surgical procedures and rehabilitation. A hydraulic robotic arm typically consists of several interconnected segments, often referred to as links or joints. Hydraulic actuators are the key components responsible for moving the joints of the robotic arm. They usually consist of a hydraulic cylinder and motors. Hydraulic fluid is used to transmit force from the actuators to the joints. The movement of the hydraulic robotic arm is controlled by a hydraulic control system. Valves are used to regulate the flow of hydraulic fluid to different actuators, enabling precise control over the arm's movement. To make the robotic arm more intelligent and adaptable, sensors can be integrated into the system. These sensors can provide feedback on the arm's position, force exerted, and other relevant data. This feedback can be used to adjust the arm's movements and ensure accurate and safe operation.

Figure 1: Hydraulic robotic manipulator.
Source: own.

2 Structure of hydraulic robot arm

The structure of a hydraulic robot arm can vary widely depending on its intended purpose and complexity. However, the key components and structure commonly found in hydraulic robots are base, hydraulic elements, sensor and control elements.

The base serves as the foundation of the robot and provides stability and support. It often contains the hydraulic reservoir, pump, and control systems. Depending on the robot's design, it may have multiple joints and segments to enable various degrees of freedom and movements. Hydraulic robots are equipped with end effectors or tools that allow them to interact with their environment. These tools can include grippers, welding torches, cutting tools, or any other devices relevant to the robot's intended tasks. The task of the structure of hydraulic robotic arm is to realize the necessary movement of the robot gripper during the implementation of the work task. This means that it is necessary for the gripper to achieve the planned position and orientation at each point of the path, as well as the appropriate speed and acceleration.

The following figure will show the movement of the hydraulic robot arm when transferring a rectangular object from the stand to the work table. The robotic arm is positioned above the object of manipulation and grasps it with a two-finger gripper.
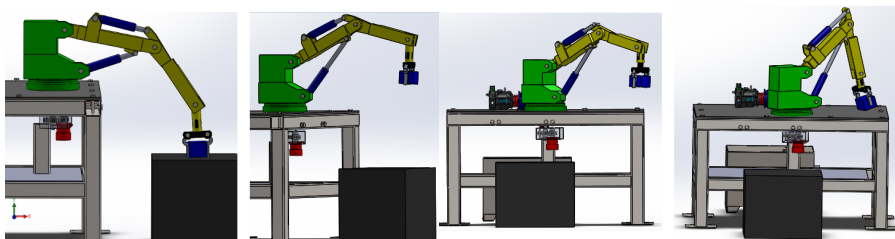
Figure 2: Designed hydraulic robotic arm. Lifting objects and placement object.
Source: own.

3   Components of a robotic arm

The representation of the flow of energy through the hydraulic system of robotic arm is presented in Figure 3. The diagram shows that at the beginning there is a source of mechanical energy, and that finally, the series of energy conversions ends again with mechanical energy (the hydraulic motor or cylinder provides a torque or force that drives the load). Therefore, the hydraulic system has the role of an energy transmitter.
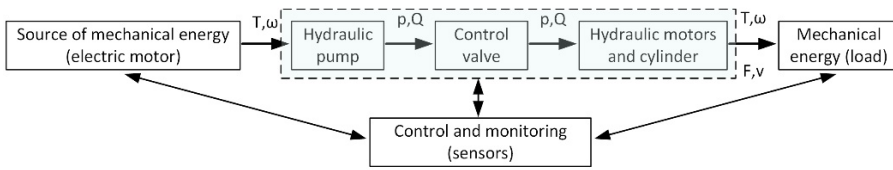
Figure 3: Energy flow through the hydraulic system.
Source: own.

Hydraulic system consists of a hydraulic motor and two hydraulic cylinders. The hydraulic motor has the role of rotating the entire robot. Hydraulic cylinders are used for translational movements of hydraulic arm segments. The cylinder that drives the first segment of the arm has a stroke of 255 mm, and the cylinder that drives the second segment has a stroke of 305 mm. The following figure shows the hydraulic diagram of the entire system with all components. As can be seen, the executive elements of this system are a hydraulic motor and two hydraulic cylinders.
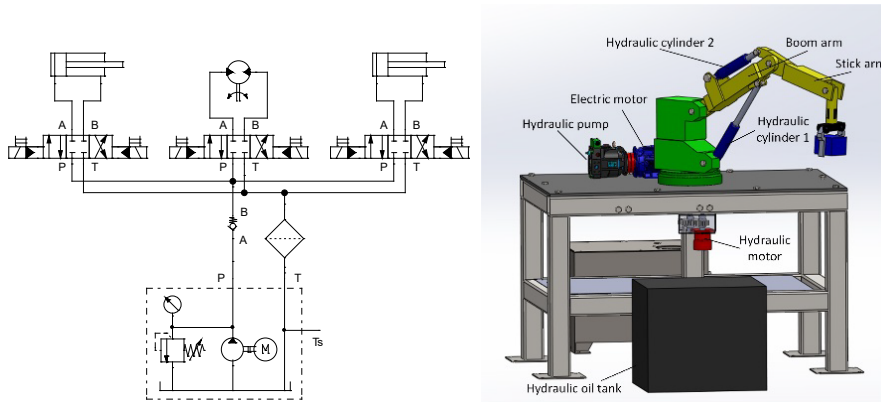
Figure 4: Hydraulic diagram of the robotic arm and main elements.
Source: own.

A hydraulic cylinder is a mechanical actuator that converts hydraulic energy (the pressure of hydraulic fluid) into linear mechanical force and motion. Hydraulic cylinders can be integrated into the joints of robotic arms to provide controlled and powerful movement. They are particularly useful in applications where the robot needs to lift heavy objects, as hydraulic cylinders can generate substantial force while

maintaining precise control over the motion. Table 1 shows all the data that will be subsequently used to create the mathematical model.

<p align="center">Table 1: Data for hydraulic cylinders</p>

	Hydraulic cylinder 1	Hydraulic cylinder 2
Piston surface of cylinder	$A_{11} = \dfrac{D_1^2 \cdot \pi}{4}$ $A_{11} = 1962,5 \ [\text{mm}^2]$	$A_{12} = \dfrac{D_1^2 \cdot \pi}{4}$ $A_{12} = 1453,8 \ [\text{mm}^2]$
Rod surface of cylinder	$A_{21} = \dfrac{(D_1^2 - d_1^2) \cdot \pi}{4}$ $A_{21} = 945.5 \ [\text{mm}^2]$	$A_{22} = \dfrac{(D_1^2 - d_1^2) \cdot \pi}{4}$ $A_{22} = 945.1 \ [\text{mm}^2]$
	Hydraulic system requires a extraction speed v_1=50 [mm/s] for cylinder 1	Hydraulic system requires a extraction speed of v_2=30 [mm/s] for cylinder 2.
Travel time for the total stroke	$v_{i1} = \dfrac{l_1}{t_1} \rightarrow t_1 = 5,1 \ [s]$	$v_i = \dfrac{l_2}{t_2} \rightarrow t_2 = 10,1 \ [s]$
Required amount of oil for the given speed	$Q_{c1} = v_{i1} \cdot A_{11}$ $Q_{c1} = 98125 \ \left[\dfrac{\text{mm}^3}{\text{s}}\right]$	$Q_{c2} = v_{i2} \cdot A_{12}$ $Q_{c2} = 58830 \ \left[\dfrac{\text{mm}^3}{\text{s}}\right]$
Connecting rod retraction speed	$v_{u1} = \dfrac{Q_{c1}}{A_{21}} = 103.8 \ [\text{mm/s}]$	$v_{u2} = \dfrac{Q_{c2}}{A_{22}} = 62.3 \ [\text{o}]$
Selected:	$\varnothing 50/36x255$	$\varnothing 50/36x305$

A hydraulic motor is a mechanical device that converts hydraulic pressure and fluid flow into rotational mechanical power. Hydraulic motors can be integrated into the joints of a hydraulic robot to provide rotational motion. This allows the robot to achieve different degrees of freedom and perform various movements. Hydraulic motors can be used to rotate specific components or manipulators attached to the robot. This rotation can help orient the end effector, tool, or sensor for precise positioning and interaction with the environment. Table 2 shows all the data for hydraulic motor that will be subsequently used to create the mathematical model.

Hydraulic pump creates pressure that drives the hydraulic actuators, such as hydraulic cylinders or hydraulic motors, which move the robotic arm or other components. The pump's flow rate and pressure are carefully controlled to ensure precise and controlled motion of the robotic arm or other parts. This control is essential for accurate positioning, movement, and interaction with the robot's environment.

Table 2: Data for hydraulic motor

Maximum angular speed	$\omega_{Rmax} = 160$ [rad/s]
Max. revolutions of the rotary joint of the robot	$n_{max} = \dfrac{\omega_{R\,max}}{2\pi} = 25$ $[rpm]$
The transmission ratio of the reducer	$i = \dfrac{n_{M\,max}}{n_{R\,max}} = 20$
Max. revolutions of the hydraulic motor	$n_{Mmax} = i \cdot n_{R\,max} = 500$ [rpm]
Selected hydraulic motor	
Maximum starting pressure	$p_{smax} = 280$ [bar]
Maximum working pressure	$p_{rmax} = 210$ [bar]
Working volume	$V = 16.5$ [cm³]
Maximum rotation speed	$n = 3000$ [rpm]
The flow required for this hydraulic motor	$Q_M = n_{M\,max} \cdot V = 8.25$ [l/min]

There are different types of hydraulic pumps commonly used in hydraulic robots, including gear pumps, vane pumps, piston pumps, and more.

Table 3: Data for hydraulic pump.

Total flow for all components in the hydraulic system	for cylinder 1: $Q_{c1} = 5.88$ [l/min] for cylinder 2: $Q_{c2} = 3.53$ [l/min] hyd. motor: $Q_m = 8.25$ [l/min] $Q_{max} = Q_{c1} + Q_{c2} + Q_{c3} = 17.66$ [l/min]
Vane hydraulic pump is selected with the following characteristic:	
Maximum pressure	$p_{max} = 137$ [bar]
Maximum flow	$Q_{max} = 30$ [l/min]
Working volume	$V = 16.4$ [cm³]
Maximum rotation speed	$n_{max} = 1800$ [rpm]
Required rotation speed for this pump	$n = \dfrac{Q}{V} = 1075$ [rpm]

While hydraulic systems are often associated with hydraulic actuators like cylinders and motors, electric motors are also commonly used in combination with hydraulic systems for different parts of a robot. One common application of electric motors in hydraulic robots is to drive hydraulic pumps. An electric motor can provide the necessary rotational power to drive the pump, pressurize the hydraulic fluid, and initiate movement in the hydraulic system. Electric motors offer precise speed and torque control, which can be advantageous when combined with hydraulic systems. Electric motors can drive hydraulic pumps at varying speeds, allowing for finer control over the hydraulic system's performance. Today, some of the following types of electric motors are most often used in robotics: DC Motors; AC motor; stepper Motors. In this work, an AC asynchronous motor will be used. An AC asynchronous

motor, commonly known as an induction motor, is a type of electric motor that operates on alternating current (AC) and is widely used in various industrial and commercial applications due to its simplicity, robustness, and reliability. According to the design task, an alternating three-phase asynchronous cage motor was selected, with power of 7.5 kW, and the speed of the motor is 1440 rpm.

Valves are devices used to control or regulate the start, stop, direction, and flow of pressurized fluid supplied by a hydraulic pump. Distributors and servo valves will be used for this hydraulic system to control and position the executive elements of the hydraulic system. A servovalve is a critical component in a hydraulic system that controls the flow of hydraulic fluid with high precision. Many servovalves operate in a closed-loop system, where feedback sensors provide information about the current position, velocity, or force of the actuator. For this hydraulic system is selected servo valve has the following characteristics: Maximum pressure p_{max} = 315 bar; maximum flow Q_{max}=48 l/min.

Sensors are vital components in hydraulic robots as they provide critical feedback about various parameters, allowing the control system to monitor, adjust, and optimize the robot's performance. Sensors enable the robot to interact with its environment, perform tasks accurately, and ensure safe operation. Robotic system use devices for measuring translational and rotational movements called encoders, then sensors for measuring pressure, as well as a turbine flowmeter.

Finishing devices for a robotic arm refer to tools, attachments, or components that are added to the end effector (gripper or tool) of the robot arm. These devices are designed to perform specific tasks that are often the final steps in a process. The choice of finishing devices depends on the application and industry in which the robotic arm is being used. A gripper is a type of end effector commonly used in robotic arms to grasp, hold, and manipulate objects. Grippers come in different types, each suited for specific applications. Three-Finger Gripper consist of three fingers that move radially to encircle an object. They offer versatility and can grasp a wide range of object shapes and sizes. Two-Finger Grippe, similar to a three-finger gripper, has two fingers that move to grasp an object. It's suitable for tasks where objects have simple shapes and sizes. Vacuum Grippe use suction to hold objects. They are effective for grasping objects with smooth and flat surfaces, such as sheets of material or boxes.
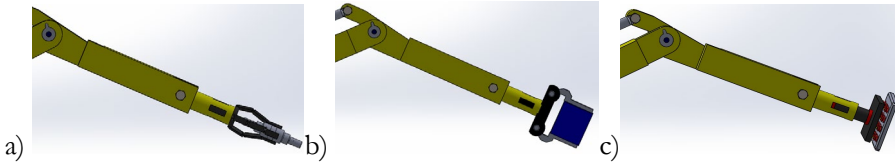
Figure 5: Gripper with two fingers a), three-finger b) and Vacuum gripper c).
Source: own.

4 Modelling of hydraulic robot arm

Hydraulic robotic arm is defined using the hydraulic manipulator equation that includes inertial, gravitational, centrifugal, and external forces acting on the motion dynamics. This model is derived as a function of angles and moments. The base coordinate system $x_0 y_0 z_0$ is defined in the $x_0 y_0$ plane, which represents the base, and the z_0 axis is the axis around which the robot manipulator rotates. The joint angle q_1 is defined as the angle from the x_0 axis to the x_1 axis around the z_0 axis. At the very end of the reverse joint, the $x_1 y_1 z_1$ coordinate system is defined, with the axis z_1 around which the joint q_2 rotates. The joint angle q_2 represents the angle from the x_1 axis to the x_2 axis in the direction of the right coordinate system. The coordinate system $x_2 y_2 z_2$ is attached to the end of arm 1 (boom) (joint q_2), where the joint q_3 rotates around the axis z_2. The joint angle q_3 represents the angle from the x_2 axis to the x_3 axis around the z_2 axis in the direction of the right coordinate system. The $x_3 y_3 z_3$ coordinate system is attached to the end of arm 2 (stick) (joint q_3) and the direction of the z_3 axis is parallel to the z_2 axis.
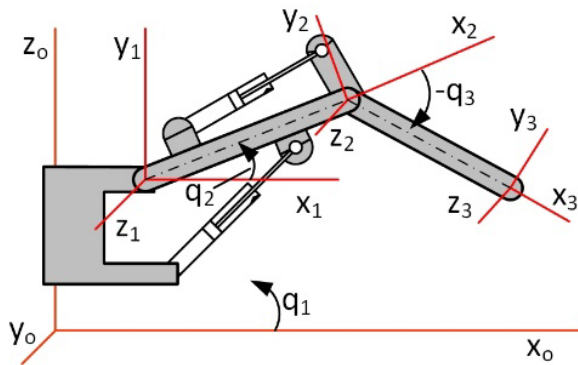
Figure 6: Defining joints and coordinate systems.
Source: own.

Using the joints and coordinate systems defined above, the dynamic equation of the robotic arm is described by the following equation:

$$D\big(q(t)\big)\ddot{q}(t) + h\big(q(t), \dot{q}(t)\big) + c\big(q(t)\big) + B\dot{q}(t) + d(t) = \tau(t) \tag{1}$$

Where is:

$\tau(t)$ - moments generated by hydraulic cylinders;

$D\big(q(t)\big)$ - symmetric inertial n x n matrix;

$h\big(q(t), \dot{q}(t)\big)$ - n x 1 nonlinear vector of Coriolis and centrifugal force;

$c\big(q(t)\big)$ - n x 1 gravitational force vector:

B – diagonal damping matrix;

$d(t)$ – external disturbances involving friction in the joints.

The moments generated by the hydraulic cylinders $\tau(t)$ are a function of the angles of the joints q, while the forces of the hydraulic cylinders F_{opt} act on the joints as a function of the linear displacement of the cylinder $X_{L(i)}$ (t). Moments generated by hydraulic cylinders are related to forces by the following expression:

$$\tau = J \cdot F_{opt} \tag{2}$$

Where J represents the Jacobian matrix that has the following form:

$$J = \begin{bmatrix} \dfrac{\partial x_{L1}}{\partial q_1} & 0 & 0 \\ 0 & \dfrac{\partial x_{L2}}{\partial q_2} & 0 \\ 0 & 0 & \dfrac{\partial x_{L3}}{\partial q_3} \end{bmatrix} \tag{3}$$

$\dfrac{\partial x_{L1}}{\partial q_1}, \dfrac{\partial x_{L2}}{\partial q_2}, \dfrac{\partial x_{L3}}{\partial q_3}$ represent the relationships between the joint angles and the linear displacement of the cylinder. The hydraulic dynamics of each cylinder is defined by the following equations:

$$\frac{V_1}{\beta_e} \cdot \dot{P}_1 = -A_1 \cdot \dot{x} - C_{tm} \cdot (P_1 - P_2) - C_{em1} \cdot (P_1 - P_2) + Q_1 \tag{4}$$

$$\frac{V_2}{\beta_e} \cdot \dot{P}_2 = A_2 \cdot \dot{x} + C_{tm} \cdot (P_1 - P_2) - C_{em2} \cdot (P_1 - P_2) - Q_2 \qquad (5)$$

$$V_1 = V_{h1} + A_1 \cdot x_L \qquad (6)$$

$$V_2 = V_{h2} - A_2 \cdot x_L \qquad (7)$$

Where is:

x_L – displacement of the cylinder;

V_1 - volume of the bore part of cylinder including the volume of the pipe from the valve to the cylinder;

V_{h1} - volume when x_L=0;

V_2 - volume rod part of cylinder piston including the volume of the pipe from the valve to the cylinder;

β_e - modulus of elasticity;

P_1 – cylinder bore surface;

P_2 – cylinder rod surface;

C_{tm} - coefficient of internal oil leakage;

Q_1, Q_2 - flows at the entrance and exit from the cylinder.

The mechanical subsystem model was created in the Matlab-SimMechanics, which is an efficient modelling and simulation tool. This tool uses blocks for modelling bodies and joints with corresponding inputs and outputs where each block defines some physical property such as mass, moment of inertia, possible joint movements, etc. The sensor block provides information about the output movements, while the actuator block defines the inputs. Since the arms of the hydraulic robot are connected to linear hydraulic cylinder, these actuators are modeled as translator joints in the mechanical part of the system.
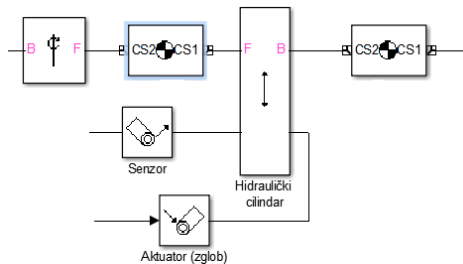
Figure 7: Translator joint of the hydraulic cylinder in the kinematic model.
Source: own.

In order to create a kinematic model of the system, it is necessary to know the masses of the members and the moments of inertia. The following table 4, shows these parameters for hydraulic robotic arm.

Table 4: Masses and moments of inertia of members.

Parameters	Moment of inertia Ixx $[\mathbf{kg \cdot m^2}]$	Moment of inertia Iyy $[\mathbf{kg \cdot m^2}]$	Moment of inertia Ixy $[\mathbf{kg \cdot m^2}]$	Mass
Element 1	388.48	1798.10	1991.41	45
Element 2	568.14	515.50	968.33	32
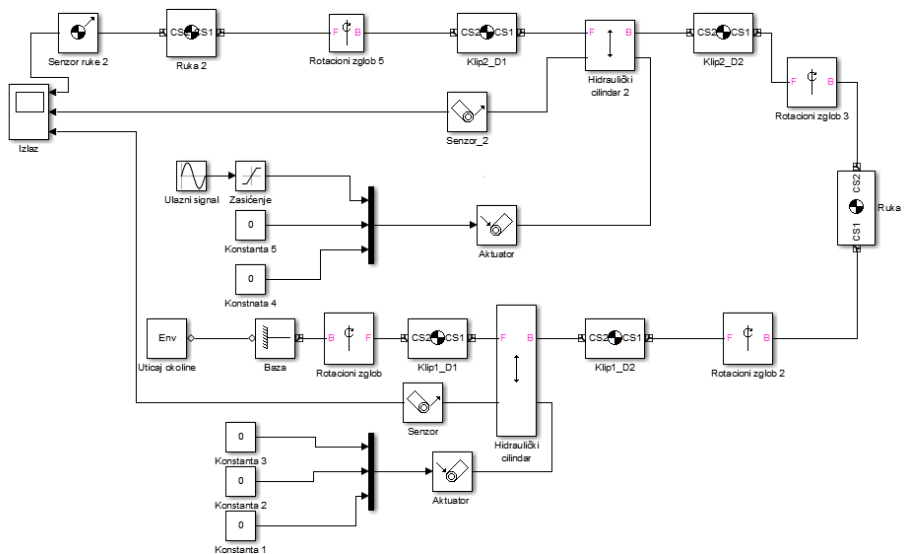
Figure 8: Kinematic model of hydraulic robotic arm.
Source: own.

The Figure 8, show the kinematic model of the hydraulic robotic arm, on which the masses and moments of inertia of the members are defined using the body block, while the hydraulic cylinders are shown using translator (prismatic joints).

The hydraulic subsystem is modelled using the SimHydraulics tool. Hydraulic systems consisting of a hydraulic cylinder controlled by a proportional electric valve. The figure 9, show a hydraulic cylinder modelled in Simhydraulics. It can be noted that the hydraulic cylinder is controlled with 4/3 valve, and with a measuring components.
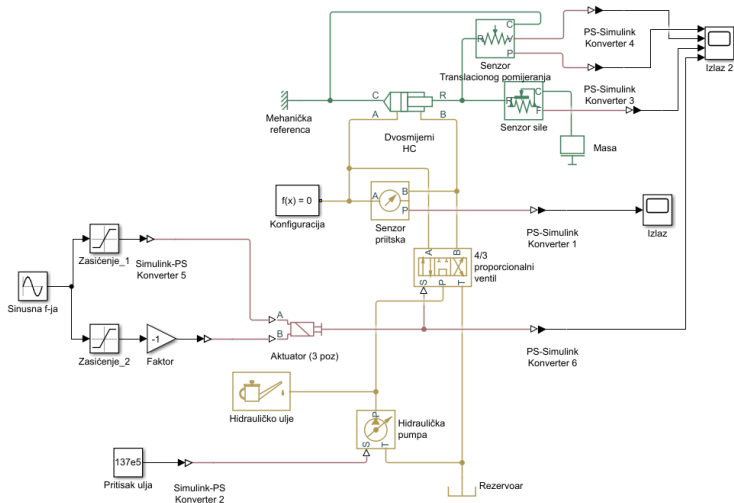
Figure 9: Hydraulic cylinder in Simhydraulics.
Source: own.

In addition to the hydraulic cylinder, the robotic arm also has a hydraulic motor, the model is present on a figure 10.
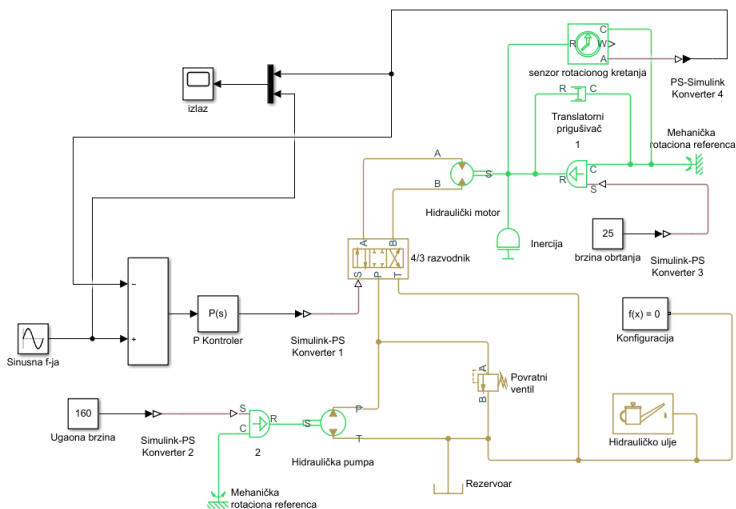
Figure 10: Hydraulic motor in Simhydraulics.
Source: own.

By running the created models in Matlab Simulink, it gets information about the movements of the elements of the hydraulic system. It can also obtain data information according to which the pressures and forces acting on the elements of the system. The following figure shows the diagram of the displacement of the hydraulic cylinder during the movement of the hydraulic robotic arm and hydraulic cylinder pressure change.
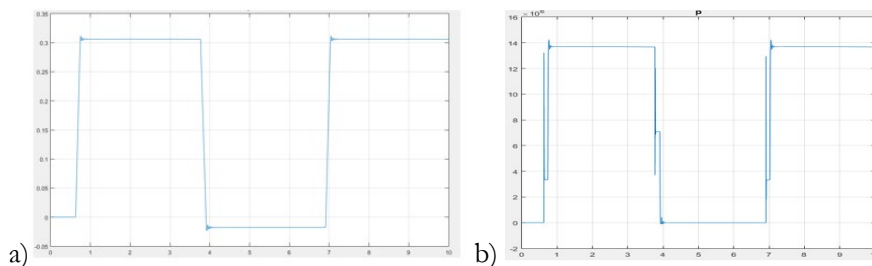
Figure 11: Displacement (a) and hydraulic cylinder pressure change (b).
Source: own.

4   Conclusion

There are many tasks where hydraulic robotic arms have an advantage over classic electric manipulators. Machines in the construction, industry, as well as the control of the movement of heavy loads require high power in relation to weight, rigidity, and short response time, which can be provided by using hydraulic robotic arms. Hydraulic robotic arms (or manipulators) are composed of hydraulic cylinders, hydraulic motors that produce the forces and moments needed to move the joints and are controlled by servo valves, hydraulic pump that provides high fluid pressure in the system, and an electric motor that controls the hydraulic pump. Three types of grippers were designed and presented: gripper with two fingers; three-finger gripper and vacuum gripper. In the end, the components were modelled using Matlab and Cad software, and their movement was simulated. This research presents a simulation model of a mechanism with a hydraulic drive system that performs linear or transversal motion and rotation. The procedure of manual calculation is simplified by creating a simulation model. The provided model gives the force, displacement, velocity, and acceleration of the piston from the hydraulic cylinder. This model-based design is a procedure that allows for the simpler construction of

dynamic systems as hydraulic arm robot and the optimization of hydraulic drive systems based on the results of computational modelling.

References

[1]   H. Mickoski and M. Djidrov (2019). Modeling of mechanism with linear hydraulic drive system. Mathematical Models in Engineering, Vol. 5, No. 3, pp. 73–78.

[2]   A. Osmanović, E. Trakić, S. Čosić, M. Bečirović, (2023): Modeling and simulation hydraulic excavator's arm. XI International Conference "Heavy Machinery-HM 2023", Vrnjačka Banja, 21– 24 June 2023.

[3]   A.Osmanović, E. Trakić (2021). Hidraulika. Tuzla: Off-set.
      L. Dai, Y. Wu, J. Wang, Y. Gong Li, Y. Liu (2011). Modeling and Control of Flexible Hydraulic Robotic Arm. Advanced Engineering Forum (Volumes 2-3), pp. 334-339

[4]   Ziaei K.; Sepehri N. (2000): Modeling and identification of electrohydraulic servos, Mechatronics 10, pp. 761–772.

[5]   B. Yao (2004): Programmable valves: A solution to bypass deadband problem of electrohydraulic systems. Proceedings - IEEE International Conference on Robotics and Automation. 4:3459 - 3464 vol.4.

[6]   W. Lirong, W. Xiaowang, W. Chenglong, Z. Xin (2010). Mechanical-hydraulic integration modeling and simulation of hydraulic support. International Conference on Computer Application and System Modeling, Taiyuan.

[7]   G. R. Reddy (2016). Design and Structural Analysis of a Robotic Arm. Master thesis. Department of Mechanical Engineering, Blekinge Institute of Technology. Karlskrona, Sweden.

[8]   A. Akers, M. Gassman, R. Smith (2006). Hydraulic Power System Analysis, Taylor & Francis Group.

[9]   Cundiff, J. S. (2002). Fluid power circuits and controls: fundamentals and applications. Boca Raton: CRC Press LLC.

[10]   Dieter W., Norbert G., (2008). Hydraulik - Grundlagen, Komponenten, Schaltungen. Springer Verein Deutscher Ingenieure, Berlin.

[11]   Blatnický, M., Dižo, J. (2015). Design and analysis of hydraulic arm of light vehicle. In: Zeszyty naukowe Instytutu Pojazdów: mechanika, ekologia, bezpieczeństwo, mechatronika. - ISSN 1642-347X. - 3 (103), s. 5-13.

[12]   Xu Jiaqi, Yoon Hwan-Sik (2016). A Review on mechanical and hydraulic system modeling of excavator manipulator system. Journal of Construction Engineering, Vol. 2016, p. 9409370.

[13]   K. M. Lynch, F.C. Park (2017). Modern Robotics, Mechanics, Planning and Control, University Printing House, Cambridge, United Kingdom.

[14]   Vacca, A., & Franzoni, G. (2021). Hydraulic Fluid Power - Fundamentals, Applications, and Circuit Design. Hoboken, NJ: John Wiley & Sons, Inc.

[15]   Marghitu, D. B. (2009). Mechanisms and Robots Analysis with MATLAB. London: Springer-Verlag.

Oscillation Problems by the Use of Moog D633 Proportional Control Valves Due to Spool Oscillation and Avoidance by Changing Hose Lengths and Controller Behaviour

Daniel Kriegl, Jörg Edler

Graz University of Technology, IFT, Graz, Austria
daniel.kriegl@tugraz.at, joerg.edler@tugraz.at

The motor is a cyclically controlled hydraulic motor, whereby two cylinders generate a rotary movement from a translatory movement. This is done by shifting two matching screw surfaces to each other. With a weight of 250 kg, a torque of 170 kNm is generated. The two synchronous cylinders are each moved with a Moog D633 proportional control valve in a closed control loop. The exact movement is necessary to be able to precisely adhere to the control times of the cycle-controlled hydraulic motor. After the system had been run in, resonance behavior was observed in several machines, with the pistons and valves vibrating at around 200 to 300 Hz. The valve spools also oscillate at that frequency despite the internally closed control loop. After several measures were carried out, the resonance phenomenon could finally be prevented by changing the hose lengths of the connecting lines and by taking measures on the software side.

1 Intruduction

The motor is a cyclically controlled hydraulic motor, whereby two cylinders generate a rotary movement from a translatory movement. This is done by shifting two matching screw surfaces to each other. This hydraulic motor is installed twice in the boom of a concrete pump placing boom, where it is used to move the last two booms. With a weight of 250 kg, the first one produces a torque of 170 kNm, while the second one, weighing 135 kg, produces around 46 kNm.

Figure 1: Concrete Pump Boom with two hydraulic motors.
Source: own

With the cycle-controlled hydraulic motor [1], [2], two synchronous cylinders are actuated, each controlled with a Moog D633 proportional control valve. A rotary movement is derived from a translatory motion, achieved through the specific tooth geometry. The tooth flanks are shaped as helical surfaces, generating rotational motion when the gears mesh. Notably, the helical surfaces facilitate contact across a surface rather than a line.

With the cycle-controlled hydraulic motor [1], [2], two synchronous cylinders are actuated, each controlled with a Moog D633 proportional control valve. A rotary movement is derived from a translatory motion, achieved through the specific tooth geometry. The tooth flanks are shaped as helical surfaces, generating rotational motion when the gears mesh. Notably, the helical surfaces facilitate contact across a surface rather than a line.

D. Kriegl, J. Edler: Oscillation Problems by the Use of Moog D633 Proportional Control Valves Due to Spool Oscillation and Avoidance by Changing Hose Lengths and Controller Behaviour

89
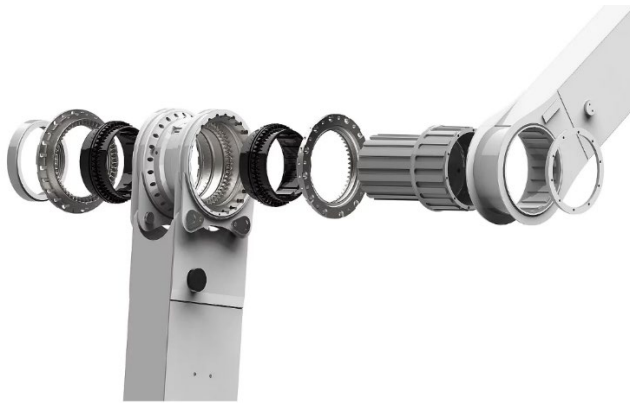
Figure 2: Parts of the hydraulic motor.
Source: own

The two pistons each feature two rows of teeth, with corresponding counter-teeth within the housing. To transmit torque, the pistons are affixed to a shared shaft through splines, preventing relative rotation between the pistons. In the provided Figure 3, one cycle of movement, the pistons are depicted in blue and green, while the housing is shown in red. The four separate images illustrate one of the four cycles through which the load is transferred between the pistons. Within each cycle, the pistons alternate between the two sets of teeth. These teeth are located within the piston chamber, ensuring a continuous flow of pressurized oil for lubrication of the tooth flanks.
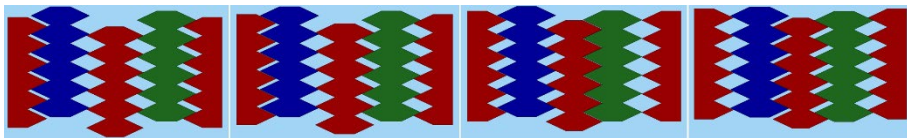
Figure 3: One cycle of movement.
Source: own

The pistons' motion is controlled by two Moog D633 proportional control valves. An LVDT displacement sensor accurately measures the piston's position. This enables closed-loop control, where the valves and displacement sensors work together to move the pistons. Precise movement is essential to maintain strict adherence to the timing of the cycle-controlled hydraulic motor.

The motor receives oil from a constant pressure system at 300 bar. The supply line to the motors spans 30 meters along the boom. A diaphragm accumulator is installed into the supply line to mitigate pressure fluctuations that may arise. The safety-oriented check valves, positioned before the cylinder chambers, are omitted in the provided circuit diagram [Figure 4: hydraulic schematic of the cycle controlled hydraulic motor] to ensure clarity and legibility.
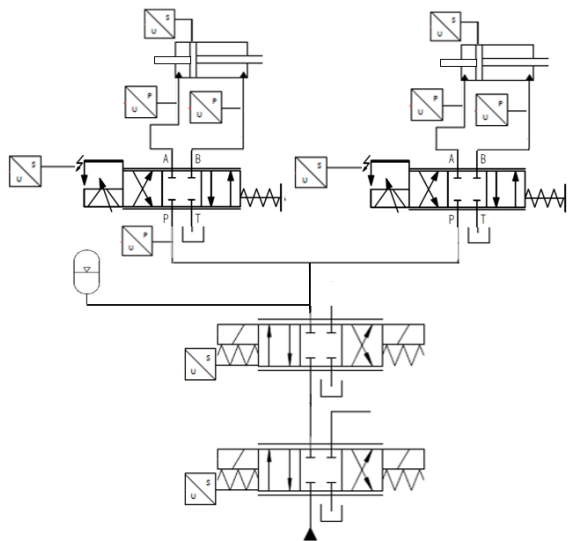
Figure 4: Hydraulic schematic of the cycle controlled hydraulic motor.
Source: own

After the system had undergone a break-in period, resonance behaviour was observed in multiple machines, causing pistons and valves to oscillate at approximately 200 to 300 Hz. This results in highly disagreeable noise and places additional stress on the system's components.

2   The Oscillation of the pistons and valves

2.1   Description of the resonance phenomenon

Under specific operating conditions, a resonance phenomenon arises within the motor. The pistons and proportional control valves oscillate at a frequency of 200 to 300 Hz, displaying a relatively substantial amplitude. This leads to pressure

D. Kriegl, J. Edler: Oscillation Problems by the Use of Moog D633 Proportional Control Valves
Due to Spool Oscillation and Avoidance by Changing Hose Lengths and Controller Behaviour

91

fluctuations that can reach up to 100 bar, even when the load pressure is at 220 bar. The diagram [Figure 5: Plots of the start of oscillation] below illustrates the initiation of an oscillation cycle, depicting the paths and differential pressures of the pistons, along with the supply pressure, valve control value, and the current valve positions.
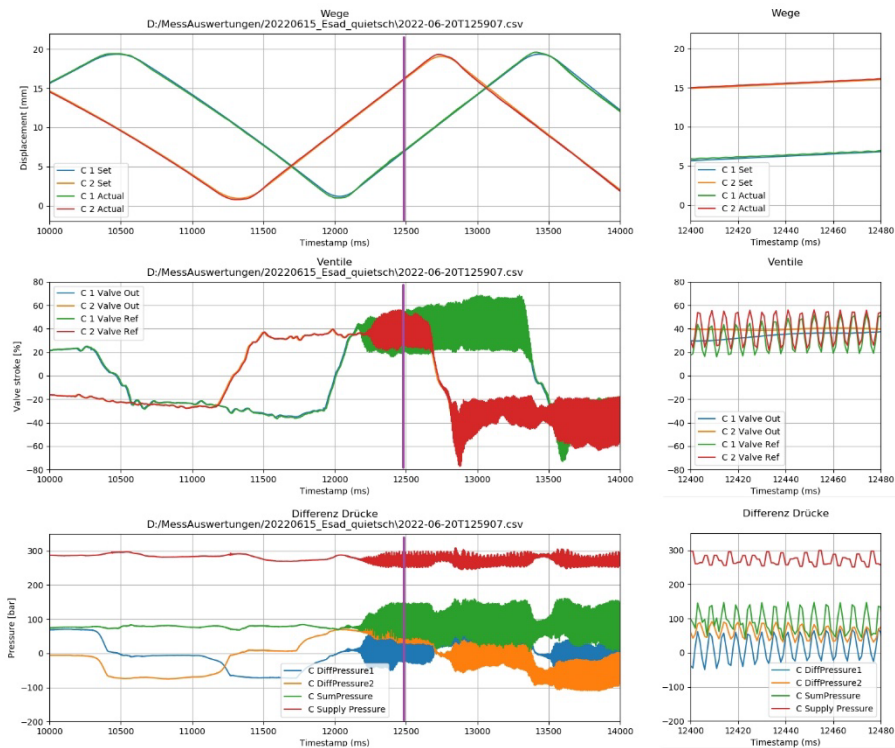
Figure 5: Plots of the start of oscillation.
Source: own

This resonance phenomenon frequently emerges under specific operating conditions. These conditions encompass factors such as oil temperature, torque, speed, and the positioning of the booms relative to one another. The oil temperature must be at least 35 °C; beyond 55 °C, occurrences of this phenomenon are almost negligible. The motor must be subjected to a torque load of no less than 30 %, and the speed must attain 80 % of the maximum speed. The boom's position and torque are somewhat interrelated, with the phenomenon being more prone to manifest in certain boom positions.

Another requirement pertains to the motors' service life. During the initial four months following production, the vibration does not manifest. Subsequently, this behaviour can arise sporadically. It gradually becomes more frequent as the usage duration progresses, eventually occurring regularly after an additional 3 months. This pattern initially hints at running-in and wear-related behaviour. Seal replacements offer temporary relief for approximately 2 months, after which the vibration resurfaces. Interestingly, the dismantling and reassembly process, even without altering components, leads to changes in the behaviour. A certain period elapses before the phenomenon recurs.

2.2   Possible causes

This is obviously a hydraulically oscillating system, with a spring-mass system consisting of a piston and an oil column coming into consideration first. Due to the low mass and the short oil column, however, the natural frequency is many times higher. The seals and the mechanical contacts also have an influence due to possible stick-slip effects, unlockable check valves that may close, resonance of the steel structure or possible excitation from the oil supply.

2.2.1   Excitation through oil supply

The system is powered by an axial piston pump connected to a diesel engine. Despite having 9 pistons and operating at speeds ranging from 1440 to 2100 rpm, the excitation frequency might seemingly match; however, the fluctuations are likely attenuated by the 30-meter hose line and the presence of an accumulator. Various speed tests have failed to reveal any discernible impact on the resonance occurrence.

2.2.2   Closing check valves

The pistons are secured against unintentional movement with hydraulically unlockable check valves. There was a suspicion that these could possibly close in operation. Measurements of the control pressure at the valves have shown that they are constantly open when driving.

D. Kriegl, J. Edler: *Oscillation Problems by the Use of Moog D633 Proportional Control Valves Due to Spool Oscillation and Avoidance by Changing Hose Lengths and Controller Behaviour*

93

2.2.3 Stick-slip effects on the mechanical friction contacts and the seals

The pistons are in mechanical contact with other components, both within the gearing in the oil chamber and on the output shaft featuring splines. Relative movements occur at these junctures, with hydraulic oil serving as lubrication within the oil chamber and grease on the shaft. These contacts exhibit a run-in behaviour, leading to an enhancement of surface smoothness over time. This phenomenon could account for shifts in resonance behaviour over the system's lifespan. However, attempts involving various lubricants on the splined shaft failed to yield any discernible alterations.

The alteration in behaviour subsequent to seal replacement implies that the seal has undergone a run-in process. However, the feasibility of replacing the seal every six months is limited. Modifying the material is equally challenging, as the required testing period would be considerably protracted, and changing materials after several years is not a viable solution either.

2.2.4 Geometric influence

It is striking that it only affects the large motor in the two sizes. The valve block is the same, but the mechanical components have significantly different dimensions. So, there must be a connection here, which unfortunately could not be deduced up to now. The different masses and oil volumes will probably play a role. Due to the circular shape, there are also different ratios between oil volume, ring area, mass and seal lengths compared to the large series.

2.2.5 Accumulator

The size of the accumulator is specified for reasons of space and weight. Although changing the preload pressure and volume did not change anything.

2.2.6 Proportional control valve

Lastly, attention turns to the proportional control valve, which, as evident from the illustration [Figure 6: Bode-diagram Moog D633 with -9dB line], vibrates with notable amplitude and/or potentially triggers the vibration. The Moog D633 valves feature an internal closed-loop control system designed to regulate valve movement,

theoretically capable of damping vibrations. Measurements indicate that the control signal remains vibration-free. The Bode diagram aids in determining the valve's natural frequency, which, at f_e = 30 to 50 Hz, remains distant from the vibration range of 200 to 300 Hz. The natural frequency fluctuates based on oil parameters and valve opening. Vibration-related effects can potentially arise due to electronic control mechanisms.
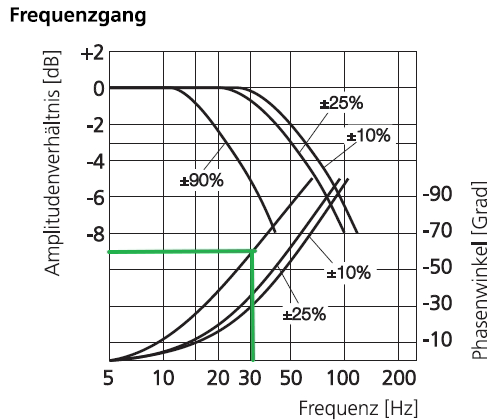
Figure 6: Bode-diagramm Moog D633 with -9dB line.
Source: [3]

In the end, it is likely a blend of valve attributes, piston mass, seal friction, the length of the oil column in the hose, and the presence of the accumulator within the supply line.

2.2.7   Control system

After analysing the measurement data, a reason for the start of the oscillation could be found. A spike can occur when calculating the valve control signal. This comes from a calculation inaccuracy in connection with the control frequency of 1 kHz. The next waypoint of the piston is calculated for the position controller. [4] The current speed is used for the feedforward of the valve controller. The cycles have different calculation methods, which is why the last two waypoints are differentiated according to time to determine the current speed. This can result in a twice as high speed for 1ms and thus a high valve signal. This spike is sufficient as a one-off excitation to start the oscillation.

D. Kriegl, J. Edler: Oscillation Problems by the Use of Moog D633 Proportional Control Valves
Due to Spool Oscillation and Avoidance by Changing Hose Lengths and Controller Behaviour

95

With the help of a software modification, at least this one-off excitation could be prevented, the calculation basis will be changed later for a better speed calculation. The graphic [Figure 7: spike at valve signal] below shows marked where the spikes occurred.
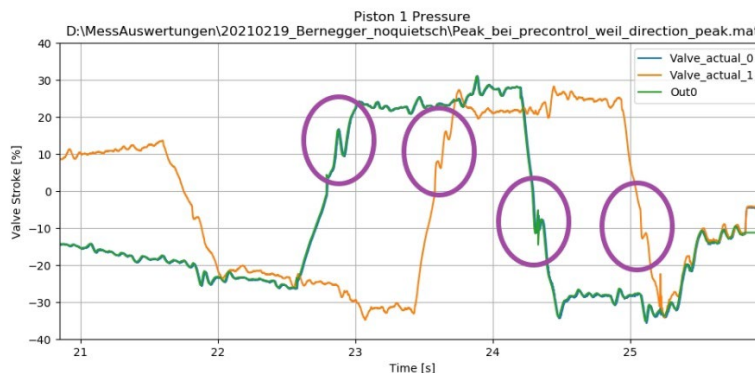
Figure 7: Spike at valve signal.
Source: own

3   Solutions

At the end, two solutions were identified to resolve the issue. Given the dependency on speed, a software adjustment was implemented. Whenever an oscillation surpassing 150 Hz is detected in the present valve position signal, the motor's speed is deliberately reduced. In many cases, initial vibrations generate minimal noise, and a slight speed reduction of 10 % to 15 % often proves adequate. This adjustment remains inconspicuous to users while effectively curbing sustained vibrations. Importantly, this solution could be swiftly executed via remote maintenance across numerous machines worldwide, requiring no physical modifications.

A second solution involved altering the lengths of two hydraulic hoses. After numerous tests, it was discovered that extending one hose per piston effectively detunes the oscillatory system, preventing resonance altogether. Alternate solutions, including mechanical redesign or component replacements, were unfeasible due to the global deployment of approximately 30 machines. Changing the two hoses emerged as a swift and cost-effective resolution. Furthermore, this approach is deemed the most viable and promising solution.
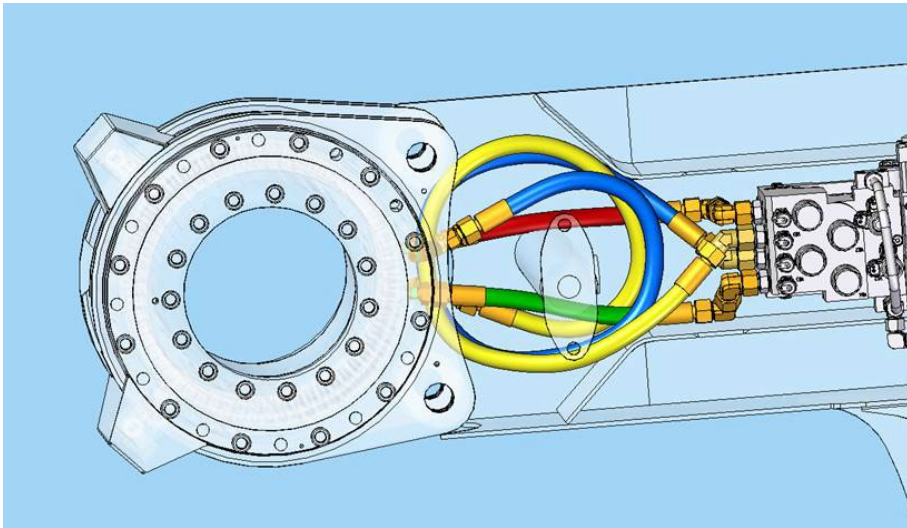
Figure 8: New longer hoses (yellow and blue).
Source: own

References

[1]   Edler J., Morolz K.-H., Jöbstl H. (2018) A new Approach on a Hydrostatic Motor for
       Applications in Mobile Cranes, *Fluid Power Networks: Proceedings 11th International Fluid Power
       Conference.* Aachen, Band 1. S. 27-35 9 S.
[2]   SCHABELREITER J., JÖBSTL H., STEINBAUER R. (2011) Mastaufbau insbesondere für
       eine Autobetonpumpe (Europa Patent EP22776360). Europäische Patentamt
[3]   Moog, Moog-Valves-D633_D634-Catalog-de.pdf, Rev2-04/2009
[4]   EDLER J., KRIEGL D., ULBING M. (2017). Grossraummanipulator mit einem hydraulischen
       Drehantrieb (Internationales Patent Nr. WO2019122280A1). Europäisches Patentamt.

Innovative Mechatronic Systems with Advanced Control Methods

Željko Šitum, Juraj Benić, Branimir Budija,
Borna Hesky, Luka Bačevina, Jerko Đurinović

University of Zagreb, Faculty of Mechanical Engineering and Naval Architecture,
Zagreb, Croatia
zeljko.situm@fsb.hr, juraj.benic@fsb.hr, b220059@stud.fsb.hr, bh220129@stud.fsb.hr,
lb219467@stud.fsb.hr, jd219173@stud.fsb.hr

This article presents four handmade laboratory systems with pneumatic and electric drive which have been designed as educational test models in the field of mechatronic control systems The article first presents a system of pneumatically powered wheelchair, which could lift patients into a horizontal lying position up to the height of the hospital bed, which enables a simple procedure for transferring the patient to the bed. Then, an automated system for mixing liquids in a defined ratio, where the construction solution, component selection, manufacturing and control program are presented. The article then describes the design, construction, and control of a pneumatically driven system for sorting objects according to their colour. The final section of the article describes the design and manufacture of a mobile robot with a pneumatic drive that can move on vertical surfaces. Climbing is achieved using vacuum grippers, and the surfaces on which the robot can move is limited to smooth ones.

1　　Intruduction

The development of modern fluid power systems is moving towards greater inclusion of microprocessors, sensors, and communication components in the final product solutions. Mechatronic engineering, which includes mechanical, electrical and information technologies, the direction of modernization of traditional disciplines such as hydraulic and pneumatic systems and enables their digital transformation and new areas of application [1]. The rapid technological progress of digital technologies, concepts such as the Internet of Things, visual systems, 5G network or artificial intelligence are becoming the subject of scientific research and practical applications in various fields, including the area of fluid power systems [2]. The question arises whether "traditional" techniques such as pneumatic and hydraulic systems can survive in the future digital era and retain their current wide applicability, in terms of the radical demands of digital technologies and energy efficiency? Therefore, the realization of high-performance fluid power systems that would be applied in modern industrial plants requires a symbiosis of mechanical systems with technologies such as microelectronics, sensors, and sophisticated control methods to achieve optimal system behaviour. In many applications, pneumatic drives can be a cheaper alternative to electric and hydraulic systems, especially for small loads, but significant attention should be directed towards more advanced ways of controlling these systems [3]. The use of electronic components for sending and processing signals enables the application of advanced control methods in fluid power systems and their application in industrial and mobile plants that use the principles of modern digital technology. This extends the potential application of these systems to the field of flexible modules that are connected in complex production systems, robotic systems, transportation systems, modern systems in the production of renewable energy sources, etc. [4].

This paper presents several self-made experimental mechatronic systems driven by pneumatic and electric drives, which indicate development trends, and can be used for education in the field of advanced control techniques.

2　　Pneumatically powered wheelchair

This chapter describes the design and manufacture of a pneumatically powered wheelchair which could lift the patient into a horizontal lying position up to the height of the hospital bed, thus enabling a simple procedure for transferring the

patient to the bed. Lifting patients with limited mobility from their wheelchairs and transferring them to the bed is a very demanding activity for the medical staff. Realization of an automated system that enables the easy transfer of patients from a wheelchair to a bed and vice versa would greatly facilitate this physically demanding activity, which is mainly performed by female medical staff. Such wheelchairs should be stable, safe and ergonomic. It is necessary to ensure that structural elements can endure the weight of all components, the weight of the patient, withstand the dynamic loads during lifting, lowering and moving the patient, and the final product should have a simple control.

2.1   Designing and manufacturing of structural parts

The mechanical parts were designed in the SolidWorks software package and then made by hand. In order to reduce the price of the product, for making the lower plate, connecting plate and top plate, as well as the footrest and backrest, wood was chosen that ensures sufficient strength of the structure, Figure 1. Parts like angle profiles for attaching the cylinders, a slider and a telescopic rod for height adjustment were also used.

| a) | b) |
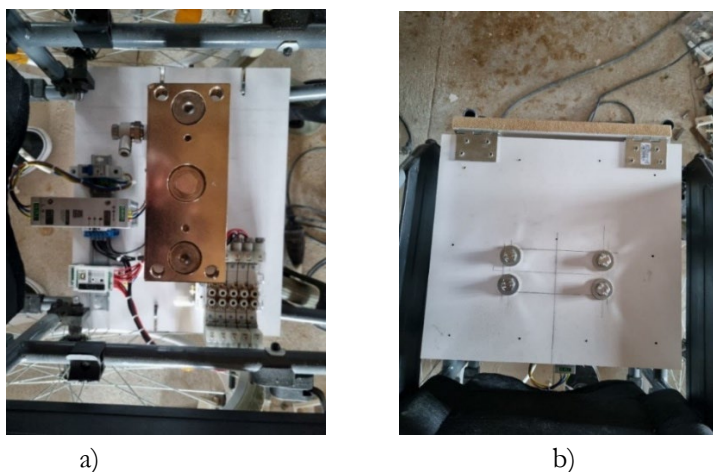
Figure 1: Lifting mechanism, a) components on the lower plate, b) upper plate.
Source: https://repozitorij.fsb.unizg.hr/islandora/object/fsb%3A8493 [5]

The seat is the most loaded part of the system because the components are located on it, and it must have sufficient strength to withstand the weight of the patient during lifting and lowering. The bottom plate and the seat are connected with screws,

and a pneumatic cylinder (SMC MGPM50-250) is attached that allows the patient to be lifted. The footrest enables raising the legs and achieving a horizontal position of the patient together with the backrest, as well as a simpler and more stable transfer from the wheelchair to the hospital bed. The rotational movement of the footrest plate from 0° to 90° is achieved using two pneumatic cylinders placed at an equal distance from the centre of the footrest panel. Rotation is enabled by the hinges, placed between the connecting plate and the footrest plate. To reduce friction and damage the foot plate during the movement of the cylinder piston rod, a nut with a wheel is installed at the end of the piston rod as shown in Figure 2a. The footrest is smoothly placed in a horizontal position by using the wheels. In the case of a fully extended cylinder piston, the height of the wheelchair handgrip limited the transfer of the patient to the bed. For this reason, the handles were removed, and a telescopic rod was installed that has the ability to adjust the height, Figure 2b. This made it possible to pull in and out the rod during raising and lowering the wheelchair.

a)   b)

Figure 2: Made parts for the system operation, a) nut with wheel, b) telescopic rod.
Source: https://repozitorij.fsb.unizg.hr/islandora/object/fsb%3A8493 [5]

All parts on which the patient lies are covered with a 2 cm sponge and then with canvas for a better aesthetic. Additional 4 cm sponges are placed at the bottom of the footrest for better comfort and ergonomics. Also, for better aesthetics of the wheelchair, stainless steel plates with a thickness of 1.2 mm are also attached, which also protect the wooden plates. The back part of the backrest, the lower part of the footrest and the edges of the seat are covered with panels, thus hiding the pneumatic cylinders used to raise the legs.

2.2   Control system

Controllino Mini PLC with software that is fully compatible with Arduino is used as a control device. The basis of the Controllino device is the ATMEGA328P microcontroller, which is actually an integrated chip that controls devices and

processes, stores and executes the program. A valve block with electromagnetic valves (SMC SY5320-5DZ-C6F-Q) is used to control the direction of movement of the cylinders. To adjust the speed of cylinder movement, speed control valves (SMC AS2201F-02-06SA) with a locking rotary knob are used, Figure 3.

Figure 3: Control components.
Source: https://repozitorij.fsb.unizg.hr/islandora/object/fsb%3A8493 [5]

At the beginning of the program, Controllino initializes all necessary variables, then certain pins are assigned the property of input or output pins. When the program is run, the control algorithms are saved in Controllino and executed in an infinite loop where the values of the variables are examined and the given actions are performed. By sending an electrical signal, the positions of the electromagnetic valves are controlled, which determines the direction of movement of the cylinders. Electric signal transmitters send information about the position of the cylinder piston and allow the system to work properly. By using a microswitch, the action of raising and lowering the wheelchair is enabled.

2.3 Description of system operation

The modified wheelchair is used to raise the patient from a sitting position to the height of the hospital bed, Figure 4. The transfer of the patient takes place in the stages of lifting to the working height, moving the patient to the hospital bed and lowering the wheelchair to the starting position. When we place the patient in the

wheelchair, the legs should first be connected using a strap, in order to secure them from unwanted movements and to secure the patient during the lifting process. After that, the patient is raised in a lying position, parallel to the hospital bed. The working height of a hospital bed is usually from 75 to 95 cm. The manufactured wheelchair in its final position, when the piston rod of the lifting pneumatic cylinder is fully extended, has a working height of 95 cm. The telescopic rod for height adjustment allows to reduce the height by 20 cm, and adjust the height to the required value. Using a microswitch mounted on the handle for pushing the wheelchair, raising and lowering operations are initiated.

Figure 4: Functioning of wheelchair.
Source: https://repozitorij.fsb.unizg.hr/islandora/object/fsb%3A8493 [5]

This type of wheelchair system allows the medical staff to transfer patients more easily, but they are still needed to move the patient from a lying position on the wheelchair to the hospital bed and to manually adjust the height of the wheelchair lift to the working height of the hospital bed.

3   Automated system for mixing liquids in a defined ratio

Mixing liquids in a defined ratio is represented in many applications, for example: in production processes for mixing various adhesives and catalysts, in the catering industry for mixing non-alcoholic and alcoholic beverages, in agriculture for the preparation of pesticides, for the preparation of a mixture of fuel and two-stroke oil

and many others. In all the processes mentioned above, there is a need for automated systems for mixing certain liquids. The goal of this project was to create a conceptual device for mixing liquids in a defined ratio that would be easily portable and inexpensive.

3.1 Device construction

The device is structurally designed so that on the front side there is an LCD screen with control buttons and potentiometers, on the left side there is a stand for a container and a glass into which two liquids will be poured and mixed, and two liquid containers with built-in pumps. The back part is adapted to glass containers. Considering that the tanks are heavy enough without liquid, no support is provided for them. Figure 5 shows a 3D model of the device, which was used for the production of structural parts on a 3D printer.
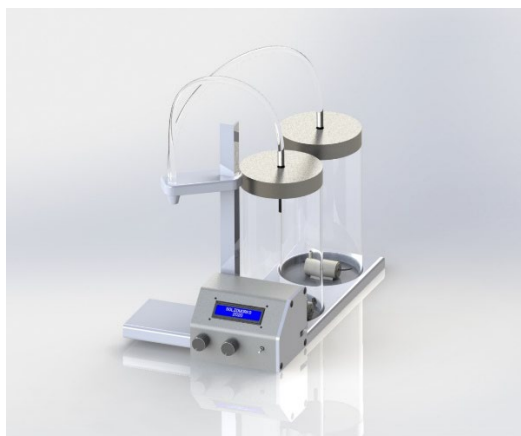
Figure 5: 3D model of the device.
Source: https://repozitorij.fsb.unizg.hr/islandora/object/fsb%3A8460/datastream/PDF [6]

3.2 Control and measuring components of the device

An Arduino Nano microcontroller was used to program the device. This created a simple and cheap platform for connecting a computer to a real device. Initializing specific pins is very easy, as well as sending or receiving data through them. An LCD screen with 16 characters in 2 lines was chosen to display the status and menu on the device, as shown in Figure 6. This screen is widely used as a display of basic

information on simple mechatronic devices, because it is small in size, has good backlighting, and is easy to program and mount on devices.

Figure 6: LCD screen on the device.
Source: https://repozitorij.fsb.unizg.hr/islandora/object/fsb%3A8460/datastream/PDF [6]

In order to reduce the number of outputs on the microcontroller, an I2C adapter is installed that reduces the required number of outputs to only 4 outputs: two for powering the screen and two for I2C communication. The accuracy of the process of pouring liquid into the tank is ensured by using the tank filling sensor in the feedback loop. A weight sensor with strain gauge technology is used for this purpose, Figure 7. Due to the very small changes between the diagonals on the measuring bridge, it is necessary to amplify the signal and convert it into digital form. For this purpose, a 24-bit analogue-to-digital converter (HX711) was used, which has two input channels connected to the diagonals of the bridge.
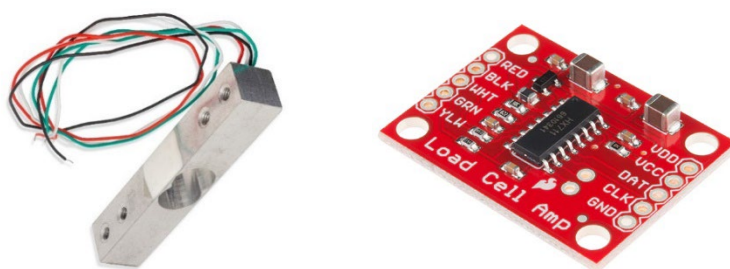
Figure 7: Force sensor with converter.
Source: https://repozitorij.fsb.unizg.hr/islandora/object/fsb%3A8460/datastream/PDF [6]

For the compactness of the device, submersible centrifugal pumps with a smaller nominal flow rate were chosen. In order to protect the Arduino microcontroller from excessive loads by directly connecting the pumps, relays were used to power

the pumps from a separate circuit. The basic technical characteristics of the pumps are: power supply: 3 V to 6 V, pump delivery height: 40 to 110 cm, flow rate: 120 L/h, pump dimensions: diameter 24 mm and length 33 mm.

3.3   Description of system operation

Two glass containers with a volume of 1500 ml containing liquid A and liquid B are located in the rear part of the device. At the bottom of each tank is a submersible centrifugal pump that pushes the liquid through a pipeline to an external tank where mixing takes place. The external tank is on the stand where the mass of the supplied liquid is measured. On the front of the device is an LCD screen that shows the desired ratio of two liquids and the volume of the mixing tank. The ratio and volume parameters are changed using two potentiometers. The mixing process is started by pressing the start button. The final system is given in Figure 8.

Figure 8: Automated beverage mixing system.
Source: https://repozitorij.fsb.unizg.hr/islandora/object/fsb%3A8460/datastream/PDF [6]

4   System for sorting items by colour

Sorting products according to different features is a very common task in automated production lines. Humans usually do not have serious problems with classifying objects based on colour and shape, because they have a developed visual system in their eyes. However, manual sorting of products in industry is an extremely

monotonous process, and the continuous process of manual sorting of products brings problems in quality assurance. On the other hand, when using a machine for sorting objects by colour, various problems can arise, such as insufficient lighting and shadows created by other objects.

Building an educational model of a sorting system using colour detection sensors can be useful for explaining object recognition and sorting technology in various applications.

4.1   System construction

The device has four compartments for sorted items, as shown in Figure 9. Sorting is done using two turntables that are driven by pneumatic cylinders, which rotate depending on the colour of the object. The pivot plates are placed along the edge of the back plate, which ensures that the cylinder does not perform a useless stroke. A wide hole is designed on the back of the box so that turntables can enter and exit without touching the box. The turntables are connected to pneumatic actuators. An electric servomotor rotates the disk and brings the objects individually from the tubular feeder into the scanning position, and then to the hole where they fall onto the turntable. The colour detection sensor is glued to the wooden support. Pneumatic cylinders are attached to aluminium profiles that ensure precise adjustment of the device's operation, Figure 10.
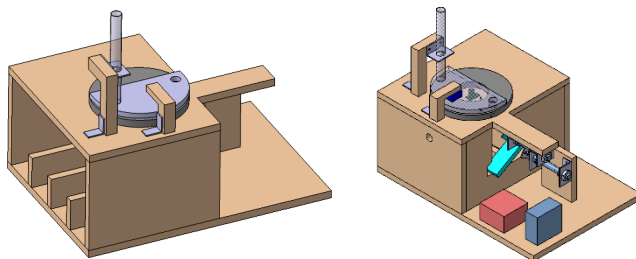
Figure 9: 3D model of the system for sorting items by color.
Source: https://repozitorij.fsb.unizg.hr/islandora/object/fsb:8482 [7]

The supports and the upper turntable are made of a standard aluminum L-profile with dimensions of 20x30x2 mm. The lower turntable is made of wood and has larger dimensions. Two single-acting pneumatic cylinders (SMC CD85N10-30S-B)

controlled by electromagnetic valves (SMC SYJ512-5LOU-M5-Q) are used for rotating the turntables.
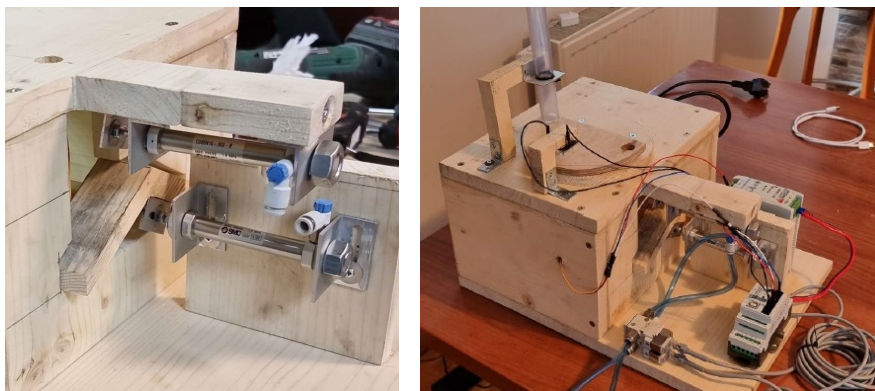
Figure 10: Actuators and turntables.
Source: https://repozitorij.fsb.unizg.hr/islandora/object/fsb:8482 [7]

4.2   Control and measuring components of the system

PLC Controllino Mini was applied as the control device. For the sorting process, a colour detection sensor (TAOS TCS3200) was used, Figure 11. The sensor has 4 groups containing 16 photodiodes each. Three groups have optical filters that do not allow certain wavelengths to pass to the photodiodes. In this way, the intensity of red, blue and green light is detected. The fourth group of photodiodes has no filter. This type of sensors are cheap and easy to integrate into the system.

Figure 11: PLC Controllino Mini and color sensor TAOS TCS3200.
Source: https://repozitorij.fsb.unizg.hr/islandora/object/fsb:8482 [7]

4.3 Description of system operation

The logical commands executed in the control algorithm are as follows:

- the servo motor turns the moving disk to the position under the tubular feeder and the object falls into the hole on the disk,
- the servomotor rotates the disk with the item to the colour sensor,
- the colour sensor reads the state and sends a signal to the Controllino device, where the colour of the object is determined,
- the actuators are placed in one of four possible positions,
- the servomotor rotates the disc to the hole through which the object falls onto the turntable.
- the procedure is repeated.

The algorithm is executed in the control loop, where it is determined which turntables are activated based on the detected colour of the object.

5 *Pneumatic powered wall-climbing robot*

Mobile robots that can move on vertical surfaces leave an intense impression on the observer and represent a demanding engineering task that requires knowledge of constructions, electronics and programming. Such robots should ensure strong adhesion to the wall, carry work tools and equipment, and flexible motion during the execution of specific tasks. Various methods are used to achieve adhesion and movement of robots on vertical surfaces, which include bio-inspired soft robotics, magnetic adhesion systems or the application of vacuum techniques. Application of vacuum is a widely used method for wall-climbing robots, and the main limitation is the requirement for good sealing of vacuum grippers, so such systems are only effective on smooth surfaces.

5.1 Conceptual solutions of a mobile robot

The initial concept in the development of the mobile robot contained six vacuum grippers, as shown in Figure 12. After testing the system, it was seen that four grippers are sufficient to firmly hold the robot on a vertical surface, and this concept was accepted. However, the rubbers on the vacuum grippers were not hard enough

and did not slide well on the vertical surface, which caused difficult movement. Finally, the problem was adequately solved by installing four grippers of a larger diameter with harder rubber.
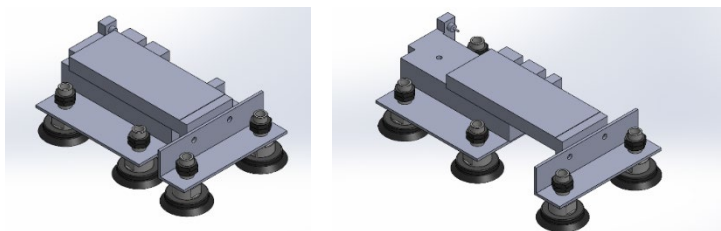
Figure 12: 3D model of the initial concept of the robot.
Source: https://repozitorij.fsb.unizg.hr/islandora/object/fsb%3A8470 [8]

5.2   The main components of the robot

The realized robot for movement on smooth vertical surfaces is driven pneumatically, and holding the robot on a vertical surface is achieved using four vacuum grippers. A pneumatic cylinder (SMC MXS16L-75B-X42) was used as the body of a mobile robot on which vacuum grippers (ZPT63HN-A16) were mounted. Two ejectors (ZH10B-06-06) are used to create a vacuum on the grippers, and their operation is based on the Bernoulli principle. The ejector weighs only 13.6g, which practically means that it can be placed on the air supply pipe. The main components of the robot are shown in Figure 13. Three electromagnetic 5/2 valves (SY3120-5MOU-C6-Q), which are mounted on the connection plate (SS5Y3-20-03-00F-Q), are used to control the direction of movement of the cylinder as well as to control the vacuum in the grippers. The control device PLC Controllino Mini is used to control the movement of the robot. Controllino offers the flexibility of using open-source code, but also ensures the reliability of industrial PLCs.

a)   b)   c)
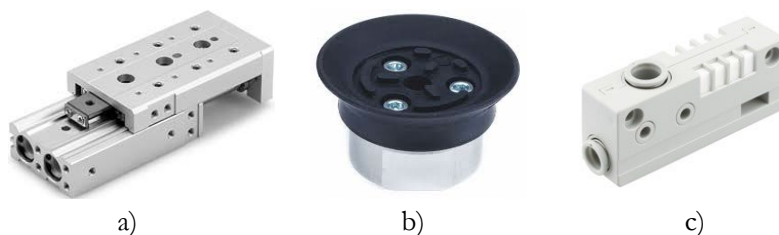
Figure 13: Main components: a) pneumatic cylinder, b) vacuum gripper, c) ejector.
Source: https://repozitorij.fsb.unizg.hr/islandora/object/fsb%3A8470 [8]

5.3   Operation of the mobile robot system

The control of the vacuum grippers and the cylinder is done using the Controllino device, from which the control signals are sent to three electromagnetic valves. By changing the working position of the valves that control the grippers, the vacuum on that pair of grippers is lost and they have the possibility of sliding on the surface. By changing the working position, the valve that controls the cylinder moves to the upper or lower end position. Pneumatic powered wall climbing robot is shown in Figure 14.

Figure 14: *Pneumatic powered wall climbing robot.*
Source: https://repozitorij.fsb.unizg.hr/islandora/object/fsb%3A8470 [8]

6   Conclusion

The paper has presented four handmade experimental systems with pneumatic and electric drive which have been designed as educational test models in the field of mechatronic control systems. The laboratory systems can be used as test models within the field of fluid power drives and automatic control education of mechanical engineering students.

By using such systems, students have the opportunity to learn about mechanical systems construction and control of practical systems built from real industrial components [9, 10]. The educational process, which includes theoretical and

practical applications of different control techniques applied to various mechatronic systems, gives students an insight into the control of real systems.

References

[1] *Scheidl, R., Linjama, M., Schmidt, S. (2012). Discussion: Is the future of fluid power digital? Proceedings of the Institution of Mechanical Engineers, Part I: Journal of Systems and Control Engineering,* 226 (6) 721–723.

[2] Alt, R., Malzahn, J., Murrenhoff, H., Schmitz, K. (2018). A Survey of Industrial Internet of Things in the Field of Fluid Power: Basic Concept and Requirements for Plug-and-Produce. In Fluid Power Systems Technology, Vol. 51968, p. V001T01A015, American Society of Mechanical Engineers.

[3] Bone, G. M. and Ning, S. (2007). Experimental Comparison of Position Tracking Control Algorithms for Pneumatic Cylinder Actuators, *IEEE/ASME Trans. on Mechatronics*, Vol. 12, pp.557-561, DOI: 10.1109/TMECH.2007.905718

[4] Fang Y., Lu Y., Roskilly A.P., Yu X. (2021). A review of compressed air energy systems in vehicle transport. E*nergy Strategy Reviews*, 33, 100583, https://doi.org/10.1016/j.esr.2020.100583.

[5] Budija, B. (2021). Design and fabrication of a pneumatic robotic manipulator. Final year project (in Croatian), University of Zagreb, Fac. of Mech. Eng. and Naval Arch.

[6] Hesky, B. (2021). Automated system for mixing fluids in a defined ratio. Final year project (in Croatian), University of Zagreb, Fac. of Mech. Eng. and Naval Arch.

[7] Bačevina, L. (2021). System for sorting objects based on colour. Final year project (in Croatian), University of Zagreb, Fac. of Mech. Eng. and Naval Arch.

[8] Đurinović, J. (2021). Pneumatic powered wall climbing robot. Final year project (in Croatian), University of Zagreb, Fac. of Mech. Eng. and Naval Arch.

[9] Šitum, Ž. (2017). Fluid power drives in robotic systems. Invited Lecture. *International Conference Fluid Power 2017*, Maribor, Slovenija, 11-23.

[10] Šitum, Ž., Benić, J., Grbić, Š., Vlahović, F., Jelenić, D., Kosor, T., Mechatronic systems with pneumatic drive, *International Conference Fluid Power 2017*, Maribor, Slovenija, 281-293.

DIDACTICS IN I4.0 FLUID POWER SYSTEMS

VITO TIČ

University of Maribor, Faculty of Mechanical Engineering, Maribor, Slovenia
vito.tic@um.si

In the modern industrial environment, we increasingly encounter the challenges and concepts of the fourth industrial revolution, also known as Industry 4.0, where the main emphasis is on automation, digitization and general integration of all elements of the production process, which represents a drastic change in the way products are produced. Consequently, this rapid progress in technologies also applies to the automation and control of fluid power systems, which presents new challenges in the education system and research work performed at universities, where all new technologies and progress in development have to be studied and explored.

1 Intruduction

Industry 4.0 has become an increasingly important topic in recent years and represents the so-called fourth industrial revolution. Industry 4.0 is thus a complex technological system that includes a huge number of concepts of new technologies, which are shown in Figure 1. These concepts include cyber-physical systems (CPS), Internet of Things (IoT), Internet of Services (IoS), robotics, computing in the cloud, cognitive computing and augmented reality, which are the result of technological progress in network connections, data analysis, machine learning, universal connectivity of machines and devices, self-diagnostics, etc. All of the above concepts could be presented together with the term "smart factory". It is characterized by the fact that it includes devices, machines, production modules and products that are capable of independent exchange of information, initiation of actions and mutual control. The latter enables an intelligent production environment. [1-3]
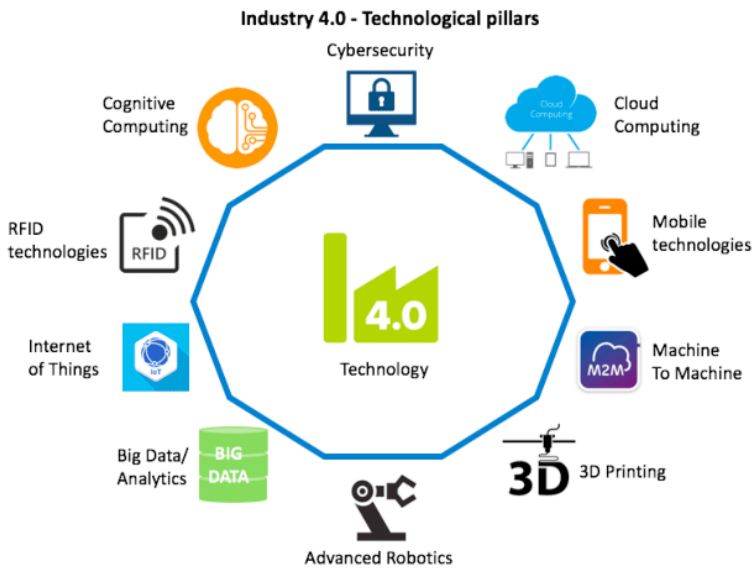
Figure 1: Industry 4.0 core elements [4].

All these key elements and technologies, which are rapidly developing, present a great challenge for the future engineers, as well as for the education system and research work performed at universities, where all new technologies and progress in development have to be studied and explored.

2 Didactics in fluid power automation and Industry 4.0

Didactic systems in fluid power engineering and automation have been increasingly developing in past decades. Basic fluid power system components such as cylinders, valves and simple control systems have been enhanced with modern automation technologies that are part of the I4.0 strategy. Thus, the emphasis is not only on the elemental fluid power elements, but also increasingly on state-of-the-art control technologies and concepts of I4.0.

Figure 2: DLMPS-500C Modular Production System Industry 4.0 [5].

As presented in Figure 2, the market offers various solutions for didactics and research work in the field of fluid power systems, automation and I4.0, from different manufacturers, such as SMC, Lucas Nuelle, Dolang, etc. Their properties and setup mainly vary in complexity and type of used components.

3 Festo CP Lab Cyber physical production system for I4.0

One of the more powerful and sophisticated comprehensive learning and research systems for Industry 4.0 is represented by the Festo CP Lab, which is also available at the University of Maribor. It is a professional and compact cyber-physical system that contains all the components and technologies necessary for in-depth learning and research of digital, fully automated production technologies containing fluid

power systems, as well as the design and programming of digital network plants. CP Lab covers complex, software-related I4.0 topics in the field of mechatronics and automation. [6, 7]

CP Lab consists of individual modules, which represent the stations of real production plants. The mentioned modules can be treated as an independent workstation or they can be connected in different layouts using a circular system, which represents production line that transports workpieces between individual processing stations with the help of a conveyor belt. By combining individual modules, we can create different circulation systems that are adapted to different requirements. The system can also be combined with other systems (e.g. CP Factory) or different manipulators. [6, 7]

Figure 3: Festo CP Lab-408-1.
Source: own.

With the described features, CP Lab represents a compact, expandable, flexible and reconfigurable learning and research system for the study of Industry 4.0. Basically, there are four different configurations of CP Labs offered by Festo, each of which consists of different modules or workstations. Configurations differ from each other primarily in terms of the number of modules they consist of. Thus, there are configurations consisting of four, six, eight or ten workstations. At the university, we have the opportunity to work with the CP Lab 408-1 system, which is shown in Figure 3. The system consists of eight workstations that can be changed and adapted to each other. [7]

3.1 Attainable didactic and research activities

The presented CP Lab 408-1 system enables didactic and research work to be performed on core elements and technologies of all levels of modern production systems in I4.0, ranging from low-level fluid power systems and electrical control systems, to higher level Programmable Logic Controllers (PLCs), Human Machine Interfaces (HMI) and SCADAs, all up to Manufacturing Execution System (MES) and Enterprise Resource Planning (ERP) solutions, as presented in Figure 4.

Figure 4: Modern production system organization [8]**.**

Some of the most significant elements and areas of fluid power systems, automation and integration into I4.0 that are included in CP Lab 408-1 system and offer numerous learning and research activities are:

- basic fluid power systems components,
- additional most commonly used equipment in production lines, such as smart sensors, electro-mechanical axes, industrial printers,…
- pneumatical and electrical drawings,
- industrial control technology using different types of PLCs,
- Human Machine Interfaces (HMI),
- identification and object-related data using RFID technology,
- open communication standards between the components,
- modern manufacturing concepts using Manufacturing Execution System (MES),
- system diagnostics and monitoring of operating status and energy consumption,

   – smart maintenance based on system monitoring,
   – web-based energy monitoring and management,
   – augmented reality (new generation HMI with smart glasses).

Additional to above presented key elements, the system also offers complete system simulation in form of a digital twin using CIROS software package, where most of the above technologies can be tested in virtual environment before they are implemented on the real production system.

3.2   Plausible upgrades

Since the CP Lab 408-1 system is built using state-of-the-art industrial components, the system can be easily upgraded with additional technologies. For instance, the "pick-by-light" operation, which is performed manually by the worker, can be upgraded with automated camera vision system that will perform monitoring of assembled work-pieces. Or, secondly, the system can be expanded using a robot that will stack the final production pieces onto a pallet.

4   Conclusion

As we are facing rapid development of technologies related to fluid power systems and especially their automation and control strategies, as a part of integration in Industry 4.0 concept, we are also imposing greater challenges in didactic and research activities performed at universities. As presented in paper, these technologies cannot be considered separately, since all core elements of I4.0 are linked together. In this manner, the CP Lab 408-1 system offers us sophisticated comprehensive learning and research system for Industry 4.0, on basis which new technologies of I4.0 and fluid power systems can be studied and further enhanced for optimal operation and performance.

References

[1]   Pereira, A. C. and Romero, F., A review of the meanings and the implications of the Industry 4.0 concept. Procedia Manufacturing, 2017, p. 1206-1214

[2]   Ružarovský, R., Holubek, R., Janíček, M., Velíšek, K., and Tirian, G. O., Analysis of the Industry 4.0 key elements and technologies implementation in the Festo Didactic educational systems MPS 203 I4.0, Journal of Physics: Conference Series, Volume 1781, International Conference on Applied Sciences (ICAS 2020) 20-22 May 2020, Hunedoara, Romania

[3]   Roman, Ružarovský & Holubek, Radovan & Janíček, M & Velíšek, K & Tirian, Ovidiu. (2021). Analysis of the Industry 4.0 key elements and technologies implementation in the Festo Didactic educational systems MPS 203 I4.0. Journal of Physics: Conference Series. 1781. 012030. 10.1088/1742-6596/1781/1/012030.

[4]   Saturno, Maicon & Pertel, Vinícius & Deschamps, Fernando. (2017). Proposal of an automation solutions architecture for Industry 4.0. 24th International Conference on Production Research. 2017. Poznan, Poland.

[5]   SMC FAS-200: Automated Flexible Assembly Cell [web]. Available: https://static.smc.eu/binaries/content/assets/smc_cee/trainingsystems/technical_description _english_fas_200-with-siemens-plc.pdf. [Accessed: 20. 08. 2023].

[6]   Festo, Sistemi CP – Celoviti učni obrati I4.0 [web]. Available: https://www.festo.com/si/sl/e/tehnicno-izobrazevanje/koncepti-izobrazevanja/poudarki/ucni-obrati/sistemi-cp-celoviti-ucni-obrati-i4-0-id_32122/. [Accessed: 20. 08. 2023]..

[7]   Festo, CP Lab [web]. Available: https://www.festo.com/si/sl/e/tehnicno-izobrazevanje/koncepti-izobrazevanja/poudarki/ucni-obrati/sistemi-cp-celoviti-ucni-obrati-i4-0/sistem-cp-lab-id_36133/. [Accessed: 20. 08. 2023].

[8]   Rahman, Moksadur & Fentaye, Amare & Zaccaria, Valentina & Aslanidou, Ioanna & Dahlquist, Erik & Kyprianidis, Konstantinos. (2021). A Framework for Learning System for Complex Industrial Processes. 10.5772/intechopen.92899.

FLUID POWER MICROCREDENTIALS - NEW POSSIBILITIES TO ACQUIRE NECESSARY KNOWLEDGE

DARKO LOVREC

University of Maribor, Faculty of Mechanical Engineering, Maribor, Slovenia
darko.lovrec@um.si

Recent events, such as the Covid pandemic, population ageing, the lack of labour, especially in the technical field, and major changes in the field of New Technologies, have also caused urgent changes in the field of Education. Thus, the need to acquire the skills that employers need as quickly as possible emerges as a priority. The solution to this dilemma is offered in the acquisition of so-called microcredits. This also applies to the field of Fluid Power Technology – Hydraulics and Pneumatics. The paper presents the starting points that led to the introduction of microcredits in the field of Fluid Power. One of these is certainly the different implementation of these contents through all levels of formal education, and the offer of additional education, as seen and offered by different stakeholders. The lack of knowledge and the variety of additional offers led to the proposal of accredited microcredits in this field.

1   Intruduction

Knowledge in the field of Fluid Power Technology i.e. Hydraulics and Pneumatics, certainly belongs to special professional knowledge. Within the framework of the regular education system and programmes, these learning contents are certainly not in the "first plan" of learning programmes, even though at least three quarters of all machines and devices use this technique. Generally, the education system everywhere is divided into three basic stages or levels of education: primary, secondary and tertiary education. The same applies to the Slovenian school system, whereby the qualifications obtained through schooling are classified using the Slovenian Qualifications Framework – SQF. The SQF aims to obtain transparency and identification of qualifications at the national and EU levels, where the main objectives of the SQF are to support lifelong learning, connect and coordinate the Slovenian qualifications subsystems, and to improve the transparency, accessibility, and quality of qualifications in terms of the labour market and civil society. [1]

Content related to Hydraulics and Pneumatics is definitely not in the programmes and curricula of primary school education. These contents are starting to be given in the context of secondary education, which is provided by gymnasiums and secondary (vocational) schools. Very few (or almost none) of these contents are present in general programmes of secondary education (general high school). To a somewhat greater extent, they are present in vocational and secondary vocational and professional education. This is very rarely a subject that would devote itself fully to learning the principles and peculiarities of the operation of hydraulic and pneumatic systems and components (and would also have such a title, e.g. Hydraulics and Pneumatics, Pneumatics and Hydraulics, Fluid Power, etc.). Most often, the contents of Hydraulics and Pneumatics are related to other contents, most often from the fields of Automation, Mechatronic systems, Production systems, Robotics, and are given in the context of variously named subjects. These contents are most often found in the Mechatronic Technician or Mechanical Technician secondary professional education programme.

At the level of tertiary education, which is provided by both public and private institutions within the framework of post-secondary and higher education (Faculties and universities), there are more learning contents in the field of Fluid Power. These are more or less comprehensive, independent subjects, or the individual contents of Hydraulics and Pneumatics are included in the learning contents of another subject.

This also depends on the type of study programme and available teaching and professional staff. It is also important here whether the staff are also engaged in research in this field (research projects, implementation projects for industry), or whether it is only a pedagogical presentation of content. It is also important whether there are adequately equipped laboratories, where it is possible to supplement theoretical knowledge with practical exercises and experiments.

Considering all these aspects and influencing factors, these contents are included in the study process in different ways, more or less extensively and with different "passion" in the delivery of these contents. Thus, at colleges and universities, it is usually an optional subject that is devoted entirely to the contents of Hydraulics and Pneumatics, or as already mentioned, the contents are present in the context of other related subjects to e.g. Mechatronic systems or Automation (e.g. where an understanding is required of the principle of the operation of machines, actuators and their control, and the maintenance of these systems).

Thus, later, employees encounter the content of Fluid Power in more detail only in the context of tertiary education. However, this is not necessary, as, in most cases, it is an optional or general optional subject that the student can bypass, depending on the choice of study course. It is usually only one subject, rarely two or more subjects, where the content would be upgraded or supplemented, e.g. Fluid Power I, Fluid Power II, Hydraulic Control Systems, Mobile Hydraulics, Fluidtronics, etc.

Therefore, in the case when an employee needs certain knowledge in the field of Hydraulics and Pneumatics, it is only necessary to acquire this through additional education outside the official school system. This includes a wide variety of training and courses or self-study programmes, from simple understanding of the basics of operation to more specific, specialised knowledge, for example, the dynamics of hydraulic servo systems.

2   Forms, scope and offer of additional education

Additional education in the field of Fluid Power is offered by various companies or institutions. This involves more extensive or shorter training or schooling, with only theoretical, or also with practical knowledge of the subject. A review of the fairly extensive offer in this area reveals a great diversity of providers. These are educational institutions such as colleges, universities or institutes, especially where

there are already laboratories or research groups that deal with this topic in regular teaching and research work. Among the training providers, there are also those who deal only with supplementary education, usually of general content, and when conducting professional training, they are assisted by external providers.

Many training opportunities are also offered by various professional associations and organisations that focus more or less on one topic, e.g. Lubricating and hydraulic fluids and problems in the field of Tribology. Also, companies, manufacturers of hydraulic and pneumatic components and systems offer different trainings or courses. Various courses were (probably initially) aimed at educating customers and users of the company's products, as well as educating its own employees, but later they were also offered to other interested parties.

As an example of the diversity of forms of education, only from the narrower field of Hydraulic Fluids and Lubricants, the various options offered by education providers are given in Table 1.

Table 1: Different offers of education in the field of Lubricants, including hydraulic fluids

Provider:	A	B	C	D	E	F
Nr. of courses	6	4	4	10	2	3
Duration (day)	2 to 3	½ to 1	1 to 2		½ to 1	3
Online training	✓		✓	✓		
Short lessons	✓					
On site	✓		✓		✓	✓
Private online	✓					
Studio recording	✓					
Certificate	✓			✓		

Table 1 shows how different educational opportunities can be, both in terms of the duration of each educational unit and the possible ways of acquiring knowledge. The possibilities are very diverse: From the classic method of education at the provider of education (in his education centre), or at the client (e.g. with users in manufacturing companies), or in the online form of self-learning in the way "anytime and anywhere", as well as the possibility of individual education directly with a mentor in a "one-to-one" way. Thus, the interested party or client can choose the most suitable education form, either in a mixed group of participants, or in a closed group only for their employees, or completely individually, or live, or using the e-education approach.

The offer of additional education in the field of Components and Systems of Hydraulics or Pneumatics is even more diverse and wide. For example, some providers offer comprehensive education in the field of Hydraulics and Pneumatics, which also includes modern controls, carried out in a classic way (lectures, calculations, experiments, independent work...), lasting as long as 8 weeks. [4] With a workload of 8 hours/day and five days a week, this would amount to as much as 320 hours of fluid power education content, which, in the ECTS (European Credit System; 1 ECTS = 30 hours) student workload is a course with 10 ECTS. There is no such comprehensive course in the field of Hydraulics and Pneumatics at any Faculty, and we cannot afford such a scope.

Within field of Hydraulics there are special topics e.g. Design of Industrial Hydraulic Systems, Hydraulic Fluids and their Contamination Control, Hydraulic components, Hydraulic Filters, etc., lasting 15 days, 5 days, 2 days or one day. A similar offer of training is also available in the field of Pneumatics: Pneumatic controls - Basic Level (5 days), Electro-pneumatics and Automation - Basic Level (4 days), Design of Pneumatic Systems (4 days), Pneumatic controls - Advanced Level (3 days), Electro-pneumatics – Advanced Level (3 days), Advanced Pneumatics (4 days) and Advanced Electro-pneumatics (4 days). Apart from this, there are also two training courses related to the use of simulation software in the field of Hydraulics and Pneumatics (Fluidsim-P / Fluidsim-H (2 days), and training related to safe work with such devices – Maintenance and Safety of Hydraulic and Pneumatic Systems (2 days).[4]

A completely different way of approaching education and content related to Fluid Power is independent learning based on following shorter e-lessons thematically, from learning the basics of the operation of the entire system, through the operation of individual types of components of fluid technology, all the way to their maintenance. [5] The entire content is divided into 9 sections, with 30 lectures of 3 h 37 min total length. E-lessons are available via mobile and TV, with full lifetime access and a Certificate of Completion. In this way, the learner can look at the available e-material if necessary. Figure 1 provides an example of a part of the e-lessons` offer and their duration.

Figure 1: Part of the available e-lessons in the field of Hydraulic Basics [5].

The third example of the offer is training offered by companies, manufacturers of hydraulic and pneumatic equipment and systems. The scope of the offered courses and topics, as well as methods of implementation, varies from case to case (e. g. [6] to [10]). Perhaps the Bosch-Rexroth Academy stands out among these, with a very extensive range of educations at three levels, from basic to advanced, and, further, to specialist and targeted [11]. Only at the level of training in the field of Industrial Hydraulics is it possible to choose between thirteen basic training options, from the basics of the operation of hydraulic systems to understanding the operation of individual types of components. It is similar for training related to other thematic areas. As an example, Figure 2 shows the different levels and content of fault-finding training.

Usually these training sessions (at the mother company in Germany) are offered in the German language variant, and in the classic, live way also called "face-to-face". Certain training sessions are also offered in English, and also as e-learning. The training bundles relate to individual fields of expertise and purpose – from Industrial Hydraulics, Pneumatics, Mobile Hydraulics, For Designers, Safety Technology, Maintenance, etc., or are also multidisciplinary and thematically oriented, such as Energy Efficiency, Digital Transformation, Linear Motion, etc.
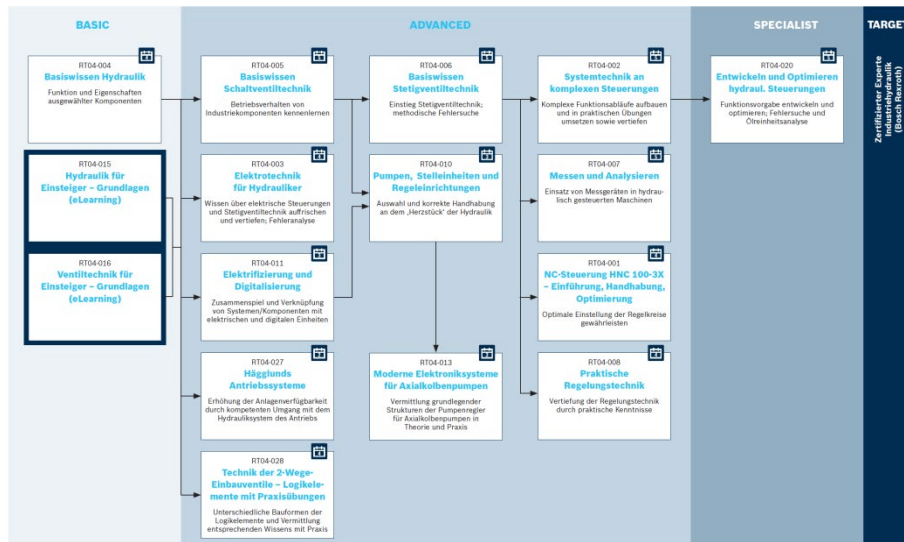
Figure 2: Example of Content Upgrade – Failure Analysis Practice [12]

The choice of training method is also different, from Face-to-face training (Theory combined with a high proportion of practical exercises, in close cooperation with experts), e-learning (at home, at an available time and place), online training (live with experts in a virtual classroom, or via training videos) and as hybrid learning.

The latter option is interesting, which is a combination of all the aforementioned methods – for example, online training for the theoretical part, followed by face-to-face practical training, as it represents an approach to short training courses in the future, and, somehow, according to the current view of the approach to additional education, represents a suitable combination between saving time and the effectiveness of learning about the problem, as well as the time distribution of educational content according to needs.

An overview of the offer of additional education in the field of Fluid Power shows how diverse the offer is, both in terms of the scope of the offer, duration and method of implementation of individual thematic education, as well as in terms of the possibility of upgrading and expanding knowledge, and also in terms of the choice of education method and the demonstration of adopted content through the issuance of Certificates. Certificates can only be of a "confirmation nature", but they can also be generally valid and recognised through professional Associations or

Chambers. Examples of such Certificates, sometimes also called badges, are shown in Figure 3.

Figure 3: Badges for proving certain acquired knowledge in the field of Fluid Power

These Certificates do not confirm that someone has only attended a certain education, but that he has also completed it successfully, with an exam, test or some other way of demonstrating knowledge.

3   Needs for a new educational approach – Mikrocredentials

The industry is facing many challenges today. One of these is the still present lack of manpower, especially in technical professions. Regarding the general staff, many companies still somehow help themselves by hiring foreigners, but the bigger problem is with staff mastering the knowledge and skills related to today's modern technologies (Industry I4.0). There is also a fair gap between the scope and type of necessary knowledge, which the current employees have acquired through their education in the past, and the knowledge and skills that are needed based on the current state of technology: Available vs. necessary.

The problem is even bigger when it comes to specific skills, which include knowledge in the field of Hydraulics and Pneumatics. As presented in Chapter 2, these skills are not necessarily an integral part of compulsory learning content, so employees may or may not have them after completing schooling. However, if they have already encountered these contents during schooling, this knowledge is of varying depth and scope. This is also one of the reasons why various institutions, associations, colleges and manufacturers offer additional training – Chapter 2. The very diverse range of different training courses in this field proves the general "market fact: if there is a need, there is also an offer".

The mentioned facts do not apply only to the field of Hydraulics and Pneumatics, but to various necessary skills that enable various additional qualifications, and, as quickly and efficiently as possible, to acquire knowledge from various fields.

Thus, more than ten years ago, in various countries around the world, e.g. in New Zealand and Japan, and in Canada, Indonesia, America and elsewhere, the idea emerged of the so-called Microcredentials. As an example, the offer of "educational certificates" via the NZQCF portal (New Zealand Qualifications and Credentials Framework) includes more than 340 short courses in various fields, with a duration of 5 to 40 credits (one credit is equivalent to ten national learning hours), which, with microcredits, enables the achievement of ten levels of qualification, from obtaining an individual Certificate (levels 1 to 4) all the way to a Doctorate (level 10). [13]

In response to the ever-changing demands of the labour market, the Mozilla Foundation first proposed microcredits in 2012 as an online verified claim of specific skills or experience valued by employers. Displayed via digital icons on social media platforms such as LinkedIn and Twitter, microcredentials now often contain online 'metadata', such as when, how and by whom learners are assessed – serving to reinforce Microcredential credibility and trustworthiness with employers. However, as the use of Microcredentials continues to grow and mature, the original understanding is now often expanded to encompass much broader applications. These web icons, now known by many nicknames, such as "nanodegrees", "digital badges" and "open badges", can reflect a common understanding or experience that may or may not be relevant in the workplace. As Microcredentials become more common and broadly defined, many labour market stakeholders are working to reach a working consensus on how micro-credentials should be understood and implemented widely in academia and the labour market. [14]

The term Microcredentials has come into force for the mentioned shorter, supplementary education opportunities, which are named differently. There are several definitions for Microcredentials, but they are all more or less similar: »*Microcredentials certify the learning outcomes of short-term learning experiences, for example, a short course or training. They offer a flexible, targeted way to help people develop the knowledge, skills and competences they need for their personal and professional development.*« [15]

The need for changes in educational programmes, adaptation to new needs and ways of imparting knowledge, reducing the gap between existing and necessary knowledge, and the need for retraining of employees, is recognised all over the world, and everyone solves it in their own way.

We also recognised them in Europe, and wrote them into our programmes, agendas and resolutions. Based on this realisation and the need for changes in the education system, the Council of the European Union (EU) adopted the Recommendation on learning for the green transition and sustainable development on 16 June 2022. The recommendation is a Key Policy Statement underlining the key role of education and training in efforts to achieve the goals of the European Green Deal. The accompanying Staff Working Document serves as a handbook for practitioners, providing relevant examples and best practices from across Europe. [16]

These guidelines are followed by all members of the EUR with their national programmes, including in Slovenia: Resolution on the National Programme of Higher Education in Slovenia until 2030, strategic goals in the fields of Social Development and the higher education system are given. [17] The act lists eleven goals that express the need to improve the international comparability and disciplinary plurality of the higher education system. Among them, the closer integration of higher education, research and technological development, the intensification of cooperation between public research institutes and higher education institutions, and the raising of the quality and efficiency of higher education in accordance with the Bologna process, etc. are mentioned, and also the goal that, by 2030, at least 50 % of Slovenian citizens between the ages of 30 and 34 will complete one of the levels of higher education, which is in accordance with EU Acts.

The share of residents in the mentioned age population who have completed tertiary studies successfully (e.g. at a university or a professional institute of higher education) in the last 20 years is 49 %, which is already very close to the target of 50 %. A more detailed analysis of the share by gender reveals that the share of men with such education is lower than 40 % – Figure 4.

It makes sense to improve this proportion, especially for educational programmes that are considered to be "more masculine professions or profiles", e.g. technical professions. Thus, on the one hand, it is necessary to establish an appropriately

updated method of teaching, which will be aimed at students for successful and timely completion of their studies, and, on the other hand, with various forms of additional education, it is necessary to enable those who did not complete regular schooling for various reasons to do so in a flexible way.
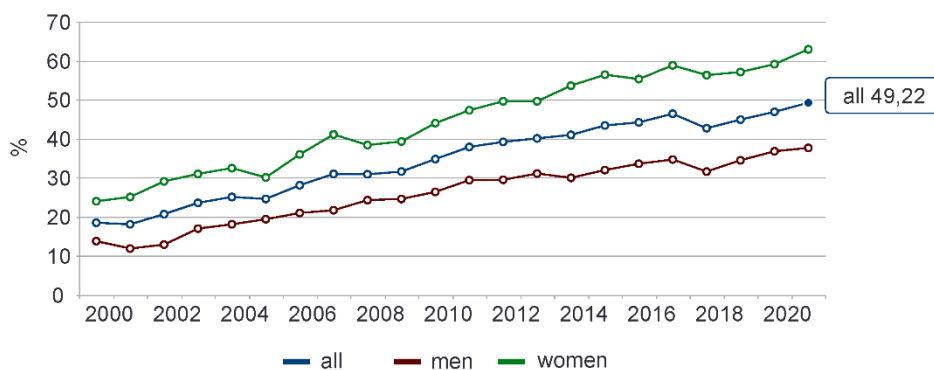

Figure 4: Population with tertiary education by gender in Slovenia [17]

A more detailed picture of tertiary education According to Eurostat data, in 2013 Slovenia exceeded the specific goal of the Europe 2020 Strategy, according to which 40 % of the generation aged 30 to 34 should have attained tertiary education. In Slovenia, this share was 46.9 % in 2020 ([18]). Data from SURS (Statistical Office, Republic of Slovenia) for 2020 show that the share of young people aged 30 to 34 who achieved tertiary education is 40.8%. In 2020/21, 58 % of 19-year-olds participated in tertiary education. The percentage of residents with tertiary education is increasing constantly. According to data from the Statistical Office, the share of Slovenian residents aged 25 to 64 with a tertiary education was 15.3 % in 2002, 23.7 % in 2010, and 30.1 % in 2021. [19]

In view of this situation, and in view of the fact that we are working longer and the knowledge acquired in regular education "years ago" is already outdated, it is necessary to intensify the approach to lifelong learning.

Therefore, the establishment of a functioning system of lifelong learning at the higher education level, including appropriate evaluation and recognition of learning outcomes, is extremely important. Only in this way will the largest possible part of the active population be able to acquire the latest scientific and professional

knowledge. This is especially true in the case of specific professional skills, which also includes knowledge in the field of Hydraulics and Pneumatics.

4   Fluid Power Microcredentials – possibilities and opportunities

Based on the presented starting points and today's needs of industries for modern knowledge, as well as the direction of development of the field of Education given in the previous chapters, the first proposals and pilot implementations have appeared, as well as the related dilemmas of how to deal with Microcredentials in general, and also in the field of Fluid Power. Given that imparting and receiving knowledge must be flexible, uniform, targeted, short term, learner-friendly and accredited, Fluid Power Microcredentials represent a big enough challenge for all stakeholders, especially how to offer the right approach and content format.

The approach to a new way of acquiring the necessary knowledge usually comes from the experience of a regular educational programme, as well as the experience gained through the implementation of various schools and training sessions. The latter were carried out as supplementary education for participants from the industry, which actually belongs to the field of Lifelong Education. In terms of content and structure, micro-evidence must enable both vertical upgrading and horizontal linking of content, and include a modern, usually hybrid method of implementation.

Thus, based on many years of experience in conducting a wide variety of educations/training for participants from the Slovenian industry, we could propose the following Fluid Power Microcredentials as a starting point:

- Basics of hydraulics HID-1,
- Hydraulic drive technology – HID-2 upgrade,
- Servohydraulics HID-3,
- Hydraulics for designers HID-Pro,
- Hydraulic fluids and their maintenance HTN-1,
- Hydraulic fluids and their maintenance HTN-2 upgrade,
- Maintenance of hydraulic systems,
- Pneumatic controls and systems.

Each of the proposed Microcredentials would last/be evaluated with 1 ECTS (30 hours), whereby knowledge can be upgraded vertically and supplemented horizontally. It is also possible to connect horizontally with other contents, for example, related to Tribology and lubricants in general, to Automation, or, e.g., to the design of very complex modern mechatronic systems, where the contents of fluid technology are of key importance.

The following will be required for the implementation of training in the form of Microcredentials:

- Prepare suitable material for each Microcredential, designed according to individual thematic sections, with the possibility of real-time knowledge verification.
- Prepare a workbook for each Microcredential.
- Prepare e-tests to determine prior knowledge and placement in the appropriate level of education, as well as to check acquired knowledge after each chapter and at the end of the completed education.
- Prepare e-materials for the implementation of practical work, by individual chapter, for the purposes of pre-familiarisation with individual practical exercises and experiments,
- Prepare shorter e-lessons related to individual topics for independent learning, and
- Prepare an online tool for monitoring individual progress.

The experience of the online implementation of the pedagogical process, which the recent pandemic forced us to do, will come in handy in this regard.

5   Conclusion

Digital transformation, automation and globalisation not only offer companies opportunities today, but they also present them with new challenges. With a view to the current available workforce and their skill sets, the shortage of skilled workers that can already be observed in many places will intensify. In order to cope with these challenges, the need to retrain staff and upgrade skills is emerging as a priority all over the world. The solution to this problem lies in a change in the approach to

imparting the necessary knowledge and in lifelong learning, which each education provider "sees in his own way". All this is offered by the Microcredentials system.

The solution is offered by the Microcredentials system, whereby imparting and receiving knowledge is flexible, uniform, oriented, short-term, learner-friendly, as well as stackable, wide base, specific oriented, and of course trustful and accredited. We are already facing these challenges in the field of Fluid Power technology i.e. Modern Hydraulics and Pneumatics.

References

[1] Slovenski šolski sistem in Slovensko ogrodje kvalifikacij,
https://www.gov.si/en/topics/slovenski-solski-sistem-in-slovensko-ogrodje-kvalifikacij/,
[2] Terciarno izobraževanje, https://eurydicebrosuravizvrs.splet.arnes.si/terciarno-izobrazevanje/
[3] The Education System in the Republic of Slovenia 2021/2022,
https://www.eurydice.si/publikacije/The-Education-System-in-the-Republic-of-Slovenia-2021-22.pdf
[4] Fluidsys Training Centre, Bangalore , India, https://fluidsys.org/
[5] Prafulla Hatte, The Complete Hydraulic Course, Oil hydraulics systems & fundamentals, hydraulic fluids, control valves, cylinders, circuits construction & analysis,
https://www.udemy.com/course/hydraulics/ :
[6] https://www.eaton.com/us/en-us/markets/eaton-experience-centers/training.html
[7] https://www.moog.com/service-support/services/training-programs.html
[8] https://www.hawe.com/service/trainings/
[9] https://www.festo.com/gb/en/e/solutions/training-and-consulting/our-range-of-courses-id_32832/
[10] https://www.smctraining.com/
[11] https://www.boschrexroth.com/en/us/academy/training/
[12] Bosch-Rexroth Academy trainings – Brochure Bosch Rexroth AG, R999000290/Version 2023-03/DE
[13] https://www2.nzqa.govt.nz/assets/Qualifications-standards/Understanding-NZQF/The-NZQF-brochure.pdf
[14] Employer and Employee Perceptions of Micro-Credentials, Future Skills Centre, April 2023, https://fsc-ccf.ca/wp-content/uploads/2023/06/NAIT_FSC_Report_April2023-1.pdf
[15] European Education Area – Quality education and training for all
https://education.ec.europa.eu/education-levels/higher-education/micro-credentials
[16] EU: Proposal for a Council Recommendation on a European approach to micro-credentials for lifelong learning and employability, Council of the European Union, General Secretariat of the Council, Brussels, 25. May 2022, (2022)
[17] MIZŠ: Resolucija o nacionalnem programu visokega šolstva do 2030 (Uradni list RS, št. 49/22), 19 pages, (available also at: http://www.pisrs.si/Pis.web/pregledPredpisa?id=RESO139), (2022)
[18] SDG Indicators, Republic of Slovenia, Statistical Office, (available at:
https://www.stat.si/Pages/en/goals/goal-4.-ensure-inclusive-and-equitable-quality-education-and-promote-lifelong-learning-opportunities-for-all/4.3-tertiary-educational-attainment)
[19] Eurostat - Participation in lifelong learning increases in 2021;
https://ec.europa.eu/eurostat/web/products-eurostat-news/w/edn-20230130-1

DESIGN GUIDELINES FOR NON-STANDARD PLUGS

ANŽE ČELIK,[1] BORIS JERMAN,[2] FRANC MAJDIČ[2]

[1] Poclain Hydraulics d.o.o., Žiri, Slovenia
anze.celik@poclain.com
[2] University of Ljubljana, Faculty of Mechanical Engineering, Ljubljana, Slovenia
boris.jerman@fs.uni-lj.si, franc.majdic@fs.uni-lj.si

The paper shows and explains activities performed to evaluate mechanical response of non-standard plug because of different loading type. In-depth understanding of plug behaviour helps to setup design guidelines for such components. In the first step, different non-standard plugs have been selected to consider size effect. Then, different materials have been selected in order to evaluate effect of plug material. For the purposes of experimental evaluation, plugs have been modified to allow installation of strain gauges. Thanks to detailed simulation model, mechanical response has been closely observed. Stress field helps to identify areas where design modifications are needed as well as to identify "hot-spots" on plug that affects structural integrity. Experimental activities have been performed with the aim to evaluate induced stresses and preload forces due to tightening torque, contact forces and piloting pressure due to spool shifting, etc. Tests have unrevealed several details regarding mechanical response on plug that have not been known previously.

1   Intruduction

1   Introduction – threaded plugs

From hydraulic point of view, plugs are mainly used to close manufacturing holes (e.g. blanking plugs) and other fluid channels and therefore prevent fluid external leakage. In addition, plugs are also used to limit spool stroke as well as preventing inner parts to leave working domain. See figure 1 for details.
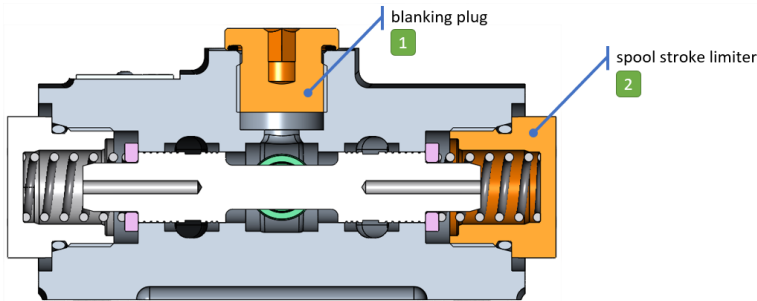

Figure 1: Plugs in different functions
Source: own

Plugs can be purchased from supplier catalogue (i.e. standard plugs, pos. 1 on figure 1) or designed manually (i.e. non-standard plugs, pos. 2 on figure 1). For the later, theory of screw joint is mainly used during the design stage. There are several different norms (e.g. ASTM, ISO, SAE …) and guidelines (e.g. VDI 2230) that support and guide the designer ([1], [2], [3]).

1.1   On threaded plugs used in Poclain

Standard plugs are widely used across many different products (e.g. hydraulic motors, pumps, valves, manifolds …). Different suppliers are used to fulfil production needs. Plug selection is usually done thanks to supplier catalogue data (example on figure 2).

Here, main design parameters are: plug size, working/rated pressure and surface protection. Designer has no need to define plug material or to validate plug integrity (if loads are within customer-defined range). It is supplier responsibility.

T1	D1	L1	L2	S1	Weight g/1 piece	Order code*	PN (bar)[1] CF	A3C
M8×1	12	13.0	9.5	4	6	VSTI8X1OR	630	630
M10×1	13	13.5	9.5	5	8	VSTI10X1OR	630	630
M12×1.5	17	16.0	11.0	6	14	VSTI12X1.5OR	630	630
M14×1.5	19	16.0	11.0	6	20	VSTI14X1.5OR	630	630
M16×1.5	21	17.5	12.5	8	26	VSTI16X1.5OR	630	630
M18×1.5	23	19.0	14.0	8	37	VSTI18X1.5OR	630	630
M22×1.5	27	20.0	15.0	10	58	VSTI22X1.5OR	630	630
M26×1.5	31	21.0	16.0	12	77	VSTI26X1.5OR	400	400
M27×2	32	23.5	18.5	12	95	VSTI27X2OR	400	400
M33×2	38	25.0	18.5	14	148	VSTI33X2OR	400	400
M42×2	48	25.5	19.0	22	233	VSTI42X2OR	400	400
M48×2	55	28.0	21.5	24	336	VSTI48X2OR	400	400

Figure 2: Plug selection from supplier catalogue
Source: [4]

On the other hand, non-standard plugs (figure 3) have to be designed manually (internally) respecting aforementioned norms and guidelines. It is designer responsibility to make a device that satisfy design requirements with respect to integrity, functionality, legislation and regulation. Therefore, there is much more design freedom in the designer's hand but also much more responsibility in comparison using standard plugs.
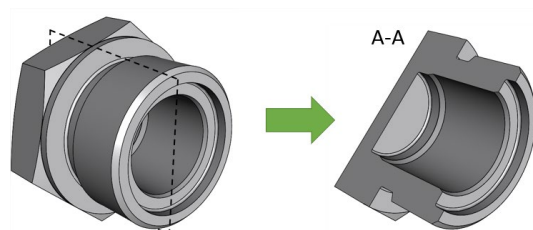

Figure 3: Typical non-standard plug
Source: own

Non-standard plugs are made from different, standardized materials, different sizes (e.g. M8 up to M33), different thread types (e.g. metric, UNF), different sealing solutions (e.g. O-ring seal, ED-seal) and with different surface protections (zinc-coating, painting). For study purposes, the following plugs sizes have been used: M19x1, M27x1,5 and M33x2.

Material is usually selected based on loading scenario: for heavy-duty applications, 42CrMo4 is mainly used, for medium duty applications, 11SMn30 or ETG100 are usually selected. Therefore, those materials have been used for study purposes as well.

1.2   On design method

Currently, non-standard plugs are designed according to theory of screw joint (i.e. VDI 2230) with some modifications and simplifications for plug. Due to plug specific geometry, the calculation of clamping force F_{PM} is simplified to the following equation:

$$F_{PM} = \frac{T_{PR}}{\left\{\frac{d_2}{2} \cdot \tan(\alpha + \rho`) + \mu_P \cdot \frac{d_m}{2}\right\}} \qquad (1)$$

where $T_{PR}, d_2, \alpha, \rho, \mu_P, d_m$ are applied tightening torque, thread diameter, pitch angle, friction angle, friction coefficient under plug head and mean plug head diameter, respectively. See figure 4 for details.
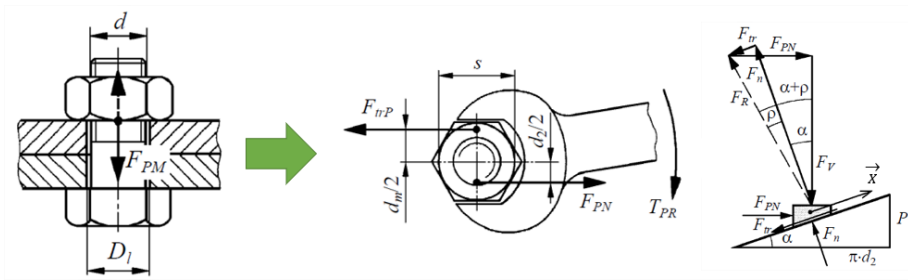

Figure 4: Parameters for calculation of screw preload force
Source: [5]

Beside geometrical parameters that depend on actual plug design, there are also contact parameters (friction coefficients under plug head and between threads). They are unknown, in general, but affect clamping force calculation at most. However, for some predefined scenarios, data are given in corresponding tables.

Materials	coefficient of friction [dimensionless]			
	dry		lubricated	
	static	sliding	static	sliding
Steel (mild) / Steel (mild)	0.74	0.57	-	0.09-0.19
Steel (hard) / Steel (hard)	0.78	0.42	0.05 -0.11	0.029-.12
Steel / Zinc (plated on steel)	0.5	0.45	-	-

Figure 5: Predefined coefficients of friction
Source: [6]

1.3 On denomination convention

For the purposes of this investigation, it makes sense to define common denomination convention for any kind of plug to prevent misunderstanding and confusion. Plug, as a functional device, could be split into different geometrical domains, namely: plug head, body, neck and plug end (figure 6).
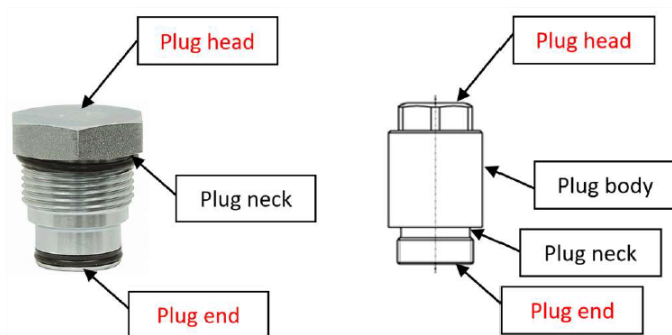

Figure 6: Denomination convention of plug domains
Source: own

Depends on non-standard plug design, plug body is not presented or clearly recognizable in some cases. For the purposes of this investigation, plug is always meant to be a threaded plug.

1.4 On applied loads

The following loads are applied on threaded assembly:

- clamping (preload) force on plug due the tightening torque,
- torsion moment on plug due the tightening torque,
- time-varying load on plug due to the spool-stopping function during the valve piloting action,
- loading due to hydrostatic (piloting) pressure.

Loads have been considered using experiments, numerical simulations and analytical calculations.

2   The scope of investigation

The aim of this investigation is to develop a design method for rapid sizing (fast dimensioning) of non-standard plugs. The method should take into account static and durability (i.e. fatigue) calculation, supported by the available norms. Finally, method should be provided to design team as a tool that allows reliable and straightforward design approach.

For that purposes, in-depth analysis of applied and induced loads as well as corresponding stresses and strains should be examined by means of experimental and/or numerical approach.

3   Experimental approach

There are several physical phenomena on preloaded plugs that have not been studied in detail neither accessible via published papers. Based on Poclain experiences, existing screw joint theory overestimate relationship between applied tightening torque and induced clamping force. Consequently, plug design is usually over-dimensioned in order to satisfy theoretical and/or numerical predictions (e.g. local stresses).

Therefore, significant effort has been made to evaluate mechanical response appropriately and accurately in plug under external loads. Several different experiments have been conducted.

3.1   Measurement of clamping (preload) force

One of those unknown parameters on preloaded plugs is a clamping force. It is induced as a consequence of applied tightening torque. Thus, it is essentially to measure applied tightening torque appropriately and accurately in order to be able to correctly measure clamping force as well.

3.1.1   Customized torque wrench

For such purposes, customized torque wrench for measurements of applied tightening torque with strain gauges attached has been developed internally. See figure 7 and figure 8 for details.
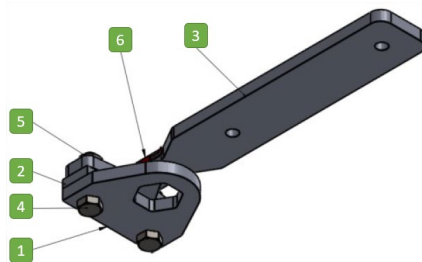
Figure 7: Internally developed torque wrench
Source: own

Positions on figure 7 refer to: (1) replaceable tool, (2), spacer, (3) hand tool, (4), screws, (5) nuts, (6) strain gauges.

Figure 8: Strain gauges on torque wrench
Source: own

The strain gauges have been connected into a full bridge connection type in which two strain gauges have been loaded in tension and two in compression.
All the sensors have been connected with a data acquisition system and a measuring station (both from National Instruments Corporation).

3.1.1 Non-standard plug modifications

Due to the insufficient space available to attach strain gauges and in order to obtain appropriate stresses for strain gauge measurement, non-standard plugs have been redesigned and reworked. The plug neck (part of a shank) has been extended in axial direction to gain space for the strain gauges (figure 9). These extended necks were covered with bushings, which enabled to capture the axial forces including the preload force.

To protect the sensors from mechanical damage, the strain gauges were covered with a purposely designed silicone rubber.

Figure 9: Modified plug M33x2 equipped with strain gauges
Source: own

The appropriate dimensions of modified plugs have been obtained upon multiple finite element (FE) analyses, where stress-deformation states of the valve plugs at maximal expected loads have been simulated. While redesigning the plugs, caution has been paid that the construction changes do not significantly influence mechanical characteristics of the modified plugs with regard to the original plugs.

3.1.1 Calibration of plug force sensor

For calibration of the plug force sensors, a special system has been designed which enables application of tensile axial force on the plugs (figure 10). This system consisted of a lever arm and a bushing for fixation of the valve plugs.
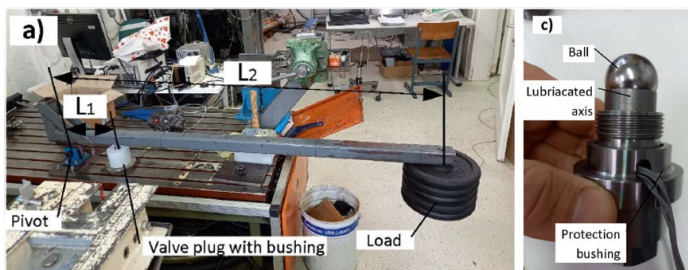

Figure 10: System to calibrate force sensors
Source: own

Figure 10a depicts system for calibration of force sensors on the plugs. The redesigned M33x2 plug with inserted loading axis and a steel ball for appropriate load application is depicted on figure 10c.

As an example, the characteristics of sensors of the M33x2 plug are presented on figure 11 including their approximation functions and R-squared values, which reflect a highly linear characteristic.
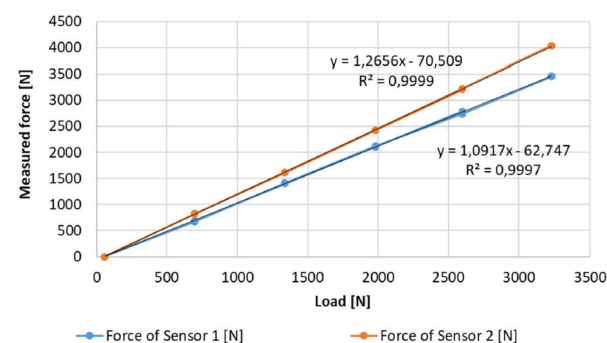

Figure 11: Characteristic of sensors 1a and 2 of the M33x2 plug
Source: own

3.1.1   Clamping force vs. tightening torque

Figure 12 depicts preload force versus tightening torque on plug M27x1,5 for minimal three consecutive fastenings separately (in lubricated and unlubricated conditions). In this figure, there is also the linear approximations (black solid lines) with its functions and R squared value of the average fastening curves.

There is one important feature that could be observed on figure 12: a minor difference of clamping force for lubricated and unlubricated conditions. This is a main difference compare to results of equation (1).

It also makes sense to note that for other two plugs (M19x1 and M33x2), higher scatter observed. However, it should be considered that the European standard EN 13001 assumes the scatter of preload force of ± 23 % when it is applied using known tightening torque or rotation angle.
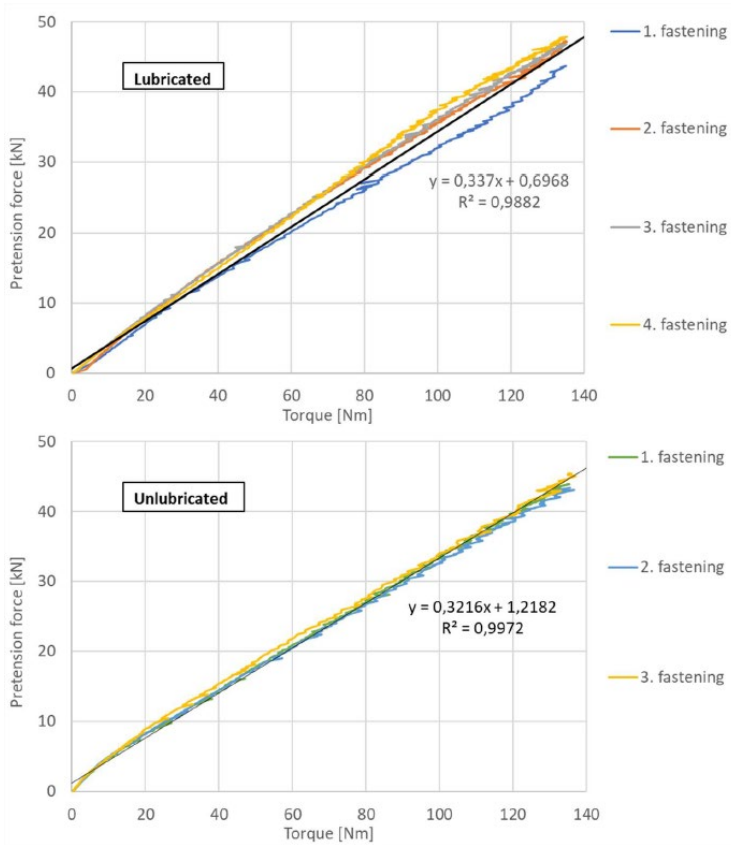
Figure 12: Preload (clamping) forces on the M27x1,5 plug
Source: own

3.2   Measurement of contact (dynamic) force

The next step during the investigation refers to the measurement of dynamic contact forces that are seen by the plug during spool shifting. Two scenarios have been evaluated: dynamic force on the plug head and plug end (refer to figure 6).

3.2.1   On Hydraulic test rig

Forces, acting on the plug have been measured at four different pilot pressures (20, 30, 40, 60 and 80 bar) and for two cases: with and without the counter pressure of 1 bar in the opposite pilot chamber (figure 13). Sampling frequency for all measured quantities is 10 kHz.
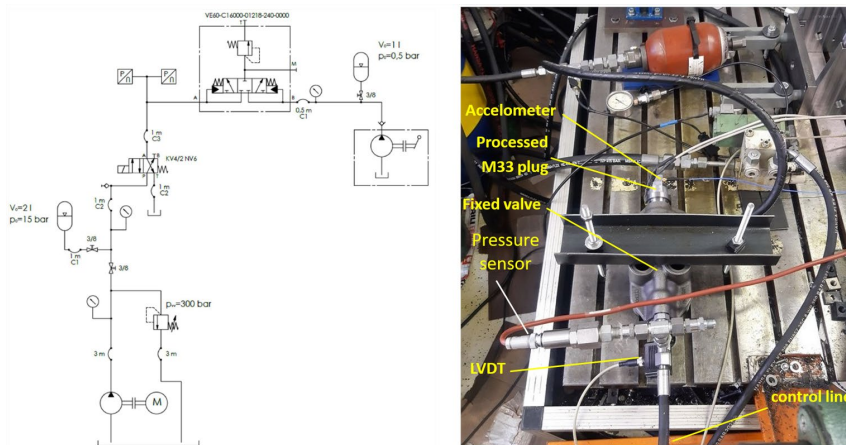
Figure 13: Measurement setup for the spool stroke measurements
Source: own

3.2.2 Dynamic forces at the plug head

Thanks to the plug equipped with strain gauges, the contact forces on the plug have been measured precisely. Figure 14 depicts five consecutive activations and deactivations of the external control valve (piloted with the frequency of 1 Hz). During each activation the preload force in the plug increases from its inactivated static value to its dynamic peak and then decreases to its activated static value and finally goes back to its inactivated static value. During each valve activation the plug head force changes in the similar way.
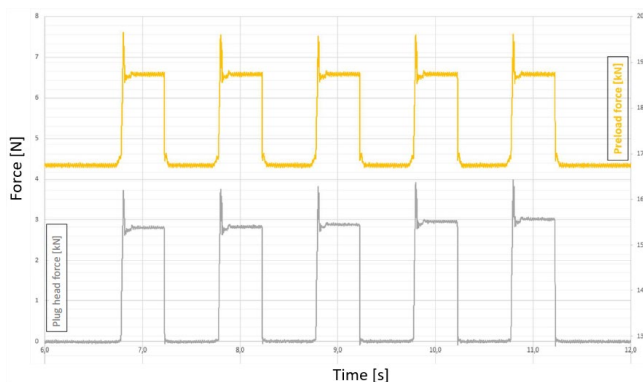

Figure 14: Dynamic forces on plug head for M33x2
Source: own

Several different transient phenomena could be observed from such a graph. One of those is load factor φ. According to VDI2230, the working force in the preloaded bolt (F_{SA}) is reduced by mentioned factor φ in relation to the externally applied force F_A, as introduced by the following equation:

$$F_{SA} = \varphi \cdot F_A \qquad (2)$$

where F_{SA} refers to difference in the preloaded bolt overall tension force before and after the additional force F_A is applied to the screw joint.

For the case considered, the load factor φ is than calculated as:

$$\varphi = \frac{F_{SA}}{F_A} = 0.613 \qquad (3)$$

The values given by equation (3) is much different compared to typical values for screw joint (which is usually between 0.1 and 0.4).

3.2.4   Dynamic forces at the plug end

Similarly, the dynamic forces on the plug end have also been examined in details. Results are not presented hereafter. However, similar trends have been observed and data post-processed in similar way (see figure 15). It is evident that results for all consecutive activations of the valve are almost the same.
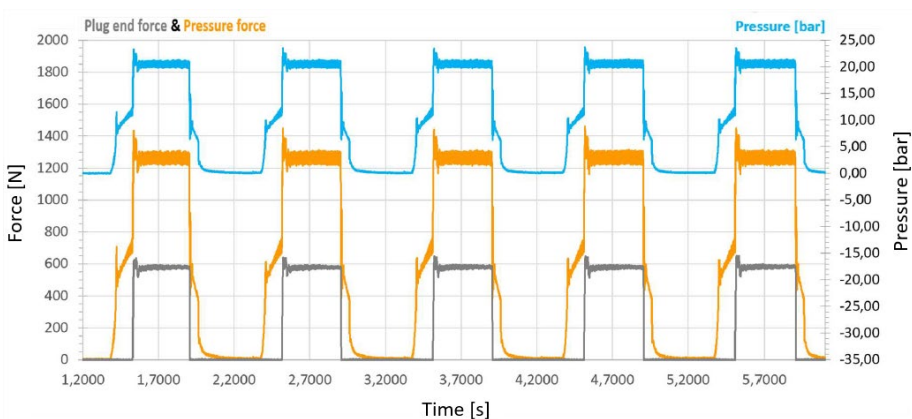

Figure 15: Dynamic forces on plug end for M33x2

Source: own

4 Numerical approach (FEA)

The main purpose of finite element analyses (FEA) on the plugs is to provide the detailed understanding of mechanical response (i.e. stress-strain state) on the plugs. Another important aspect of performed FEA is to compare mechanical response on the original and modified plug design. Then, forces given by measurements executed on the modified configurations can be interpreted for the original configurations. FEA has been performed using the Ansys Mechanical APDL software package.

4.1 Pre-processing stage

For each plug size, two versions of the plug design have been created and analysed (original and modified design). The following assumptions and simplifications have been made:

- axisymmetric model with axial symmetry along the plug longitudinal axis
- 2-dimensional PLANE42 elements with axial symmetry have been used
- plug threads have been modelled with a simplified equivalent circular model (without 3D helix)
- contact between threads on plug and housing has been made using couplings (of adjacent nodal pairs) in the normal direction; contact elements were therefore not used
- other contacts have been made in the same way

Two different materials have been used (namely for the plug and housing) with corresponding elasto-plastic properties. See figure 16 for details.

Material properties							
Element	Denomination (Standard)	W. Nr.	Youngs modulus [GPa]	Poisson ratio [–]	Yield strength [MPa]	Tangential modulus [GPa]	Elongation at break [%]
housing	EN GJS–600–3 (EN 1563)	5.3201	174	0,275	380	1,74	1,0
plug	11SMn30 (+C)[*] (EN 10087)[1]	1.0715	210	0,300	440	2,10	6,0

Figure 16: Material properties
Source: own

Local mesh refinement has been applied on areas of sharp corners, threads, necking etc. See figure 17 for clarity.
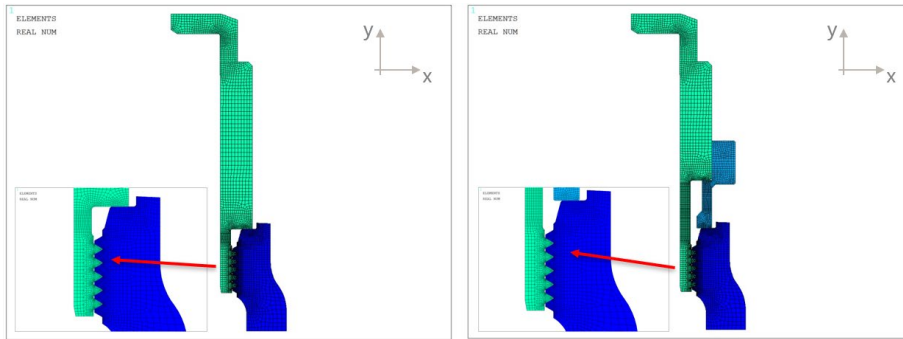

Figure 17: Axisymmetric model of plug M33x2 (left: original plug, right: modified plug)
Source: own

Five different load cases (LC) have been used, namely:

- LC1: inactive valve (spool initial position; preload force and initial spring compression force)
- LC2: active valve (impact on plug head; preload force, maximal spring force and contact force in steady-state piloted spool position)
- LC3: active valve (impact on plug head; preload force, maximal spring force and peak contact force in transient spool position)
- LC5: active valve (impact on plug end; preload force, maximal spring force and contact force in steady-state piloted spool position)
- LC6: active valve (impact on plug end; preload force, maximal spring force and peak contact force in transient spool position)

Impact force of the spool on the plug has been determined for the pilot pressure of 20 bar, which is the typical pilot pressure used in hydraulic closed-loop circuit.

Boundary conditions (in terms of restrain the node displacements) have been prescribed on housing free edge. The relative movement of the contact surfaces in the tangential direction has been considered as free, without taking friction into account.

4.2 Post-processing stage

It is out of the scope of this paper to present and explain the results of each load case separately. Instead, only few typical examples of FEA results are given hereafter. Figure 18 depicts stress-displacement response for plug M33x2 under the LC1 that refers to the simulation of plug tightening. The preload force due to the tightening of plug is modelled by means of temperature contraction on the plug neck in the longitudinal direction (Y axis) only.
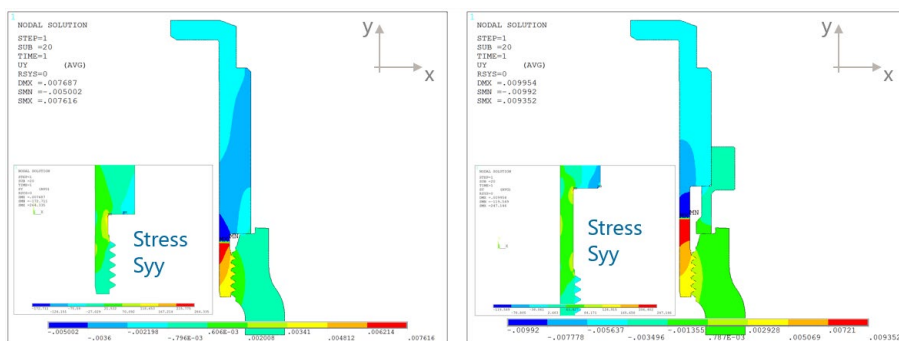

Figure 18: Simulation of tightening on plug M33x2 (temperature contraction)
Source: own

There are several benefits to use FEA in addition to the experimental approach. Mechanical FEA allows to make in-depth review of stresses (among other variables) in the entire component. Further, several different loading scenarios could be simulated relatively quickly and easily. On the other hand, experimental approach gives realistic values of forces, stresses etc. However, it requires more resources (e.g. time, human, cost) and usually enables limited amount of scenarios to test.

5 Design method and tool development

Method for fast dimensioning of the hydraulic plugs has been developed and described on the example of plug M33x2. As first, the fatigue calculation is introduced and after that also the static calculation is included.

5.1   Fatigue design

Fatigue calculations has been performed in accordance with the standard DIN 743 ("Calculation of load capacity of shafts and axles"), because in this standard the adequate details are given, the fatigue data for plug material in question are available and the adequate loadings are considered. The only disadvantage of this standard is that calculations are made for fatigue limit ($2x10^6$ or more loading cycles) whereas the plugs are usually loaded with $5x10^5$ of cycles. By doing so, the calculation stays conservative. The cross-section of the plug neck, containing the transition between the plug neck and plug body have been selected as fatigue critical cross-section (figure 19).
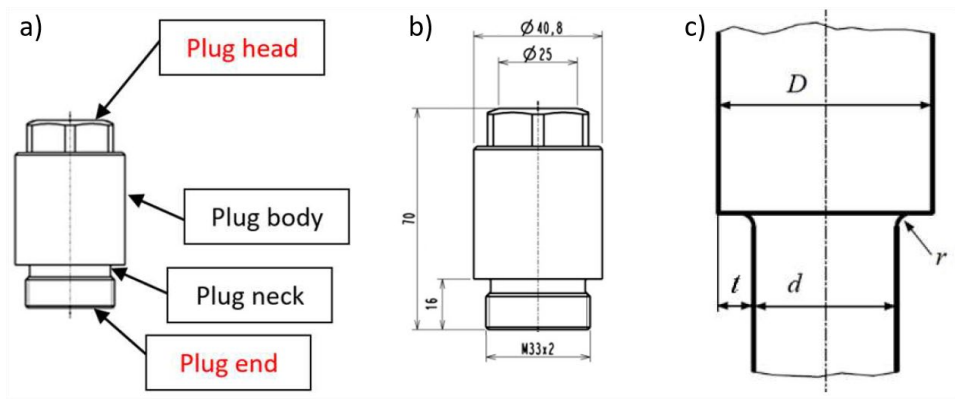

Figure 19: (a) plug parts, (b) plug drawing, (c) sketch of the standard detail
Source: own

5.2   Static design

Static safety factor regarding to yield strength has been calculated. The required minimal yield strength safety factor is defined in appropriate norm ($S_{min} = 1.2$).
In static calculation, the torsion stress cannot be neglected, because the torsion stress due to the plug bolting and preloading can stay in the pug neck during whole lifetime and of course also because the plug must survive the loading case of bolting. Finally, the Excel-based tool has been developed for automatization of developed method for fast dimensioning of the hydraulic plugs (figure 20).

Figure 20: Plug calculation in Excel-based tool
Source: own

6　　Conclusion

The aim of the investigation is to develop a design method for fast dimensioning of hydraulic plugs. The extensive measurements and numerical analyses have been realized on plugs M19x1, M27x1.5 and M33x2. The outputs of these activities enable to develop required design tool. Finally, Excel-based calculation tool was made for simpler, faster and more accurate usage of the developed method.

Extensive experimental approach has been performed which required highly skilled human resources. Some innovative solutions have been developed and implemented (e.g. torque wrench, plug modifications …) that allow precise and repeatable measurements of different variables.

Installation of strain gauges on the plugs allow to measure forces, stresses and strains on the plug neck, plug head and plug end. This has brought new added values to the existing know-how of Poclain development team. In addition, appropriate acquisition system allows to precisely capture transient phenomena during the spool shifting stage.

Main FEM analyses have been completed for modified and non-modified plugs to enable their comparison. As the most important it has been found out that the modifications of the plugs do not affect the measurement results significantly – typical influence is less than 2 %. For static dimensioning of the non-modified plugs,

the loadings measured on the modified plugs can be used without causing relevant deviations.

Method for rapid sizing of hydraulic valve plugs has been developed, based on the analytical approach, as a preferable technique. In the analytical procedure the usage of standard diagrams is partially implemented. Method is based on DIN 743 procedure for shafts and axes from where the static and fatigue strength criteria have been adopted. In addition, method includes scenarios of spool acting on the plug-head and on the plug-end. Finally, Excel-based calculation tool has been made for simpler, faster and more accurate usage of the developed method for fast dimensioning of the plugs.

References

[1]　　https://www.boltscience.com/, last visited on 26.7.2023
[2]　　https://www.bossard.com/global-en/assembly-technology-expert/expert-design/calculation-of-bolted-joint/, last visited on 26.7.2023
[3]　　http://www.vdi2230.de/, last visited on 26.7.2023
[4]　　https://www.parker.com/parkerimages/euro_tfd/cat/english/C150.PDF, last visited on 26.7.2023
[5]　　https://www.scribd.com/doc/257813953/6-Vijacne-zveze#, last visited on 26.7.2023
[6]　　Simcenter Amesim Help, rev. 2021.2

Development of a New Hydraulic Freewheeling Valve HCC-200

Jernej Bradeško

Hydraulics d.o.o., Žiri, Slovenia
jernej.bradesko@poclain.com

This paper presents development of a new hydraulic freewheeling valve HCC-200, intended for activation of two hydraulic motors in rear drive axle of an agricultural combine harvester. Complete development process of the valve was supported by several numerical simulations. Before producing first physical prototypes, polymeric 3D printed models of new components were produced for initial study of production process. First physical prototypes of the new valve were produced in a specific modified version that allowed integration of main spool position monitoring sensor and additional pressure sensor to monitor specific internal chamber of the valve. Both monitored variables are important for evaluation of both valve and system behaviour. Extensive system simulation was performed prior to field test campaign. Simulation results confirmed the functionality of the valve and at the same time identified few potential weak points of the system, for which alternative solutions were provided to customer for the test.

1   Intruduction

New Poclain Hydraulics freewheeling valve HCC-200 was developed for combine harvester application. Combine harvester is a self-propelled agricultural machine that is used to harvest grain crops from farm fields. With its processing system it separates grain and the waste, which is typically shredded and left on field. Grain is collected in tanks integrated into machine.

Combine harvester is operated by an operator, who controls the machine operation from the cab located high in front of the machine for good visibility of the environment. Depending on the configuration of land and harvested fields a machine could be configured for two-wheel drive (2WD) or four-wheel drive (4WD) mode operation.

Figure 1: Typical combine harvester machine
Source: own

Development of a new freewheeling valve enabling shifting between 2WD and 4WD mode of combine harvester is presented in this article. Freewheeling valve controls two motors in the rear wheels of the machine.

1.1   On hydraulic power transmission system

Typical hydraulic power transmission system consists of components, shown in Figure 2. Machines that are using such power transmission system are usually equipped with hydraulic motors, which are connected to variable displacement hydrostatic pump. Often one or more motors (typically on one axle) are intended for on-demand drive function. In this case an additional valve is required, which controls the engagement status of the motor(s).
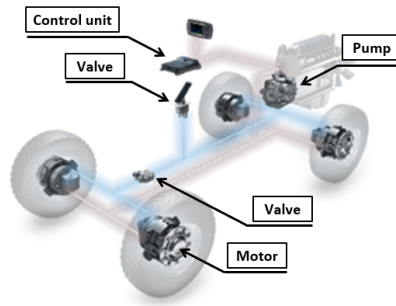
Figure 2: Hydraulic power transmission system
Source: own

Hydrostatic transmission drive is a typical drive type on combine harvester machine. While primary drive is on the front axle, some machines have an option of powered rear axle as well. This is an on-demand feature that utilizes hydraulic motors integrated into wheels of machine rear axle by sharing the same pump flow. Shifting from two-wheel drive mode (2WD) to 4WD mode is done using freewheeling valve.

1.1.1 Freewheeling valve

Freewheeling valve controls engagement status of hydraulic motor in rear driving axle. The name comes from its function, which enables almost free rotation of motors (and wheels respectively) with minimal losses or dragging torque. This is done by draining motor working ports to tank. At the same time motor case is slightly pressurized, which keeps motor pistons retracted and separated from the cam. Hydraulic schematic of basic configuration of freewheeling valve is shown in a Figure 3.

Figure 3: Hydraulic circuit of freewheeling valve (basic configuration)
Source: own

Ports PAR and PAV connect valve to the pump while ports AR and AV connect valve to the motor(s). Port G is fed from charge pump, port F is drained to tank line. G2 port is optional and carries pilot pressure information. Freewheeling valve consists of two main sections; a high-pressu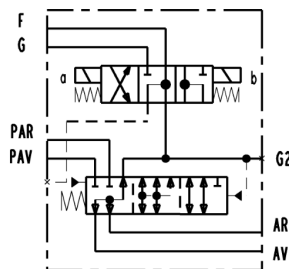re section that connects a main drive pump with the motors and a low-pressure section that allows release of pressure in motors when not being activated and controls motor engagement and disengagement phases.

Figure 4: Freewheeling valve HCC-200
Source: own

While high-pressure section of HCC-200 valve is functionally identical to basic configuration of freewheeling valve there are some differences in low-pressure section of the valve. It features hydraulically piloted directional spool valve and additional solenoid operated directional valve to control pilot pressure for displacement change on hydraulic motor. Valve provides the ability to engage and disengage rear motors regardless of vehicle travel speed, i.e. stationary or on-the-fly shifting.

1.1.2 Radial piston hydraulic motor

Poclain radial piston motor is a high-torque low-speed hydraulic motor that works on cam lobe principle.

Typically for combine harvester application, a dual displacement motors are integrated in the circuit, with control spool valve that shifts between both displacements values when pilot pressure is applied to port Y. Motor ports as shown in Figure 5:

- – A, R: Working ports (feed and return)
- – F: Motor case port (leakage drain and case pressurisation)
- – Y: Displacement control spool pilot port
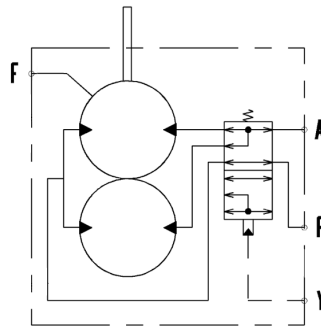
Figure 5: Hydraulic circuit of dual displacement hydraulic motor
Source: own

Two main modes of the motor in 4WD application are:

- – Working mode
  Ports A and R are connected to hydrostatic pump in a closed-loop configuration. Pistons are extracted out of cylinder block and are pressed against the cam. Motor is generating output torque.
- – Freewheeling mode
  Ports A and R are connected to tank line. Slightly pressurized port F sustains certain pressure in motor case that keeps motor pistons retracted inside the cylinder block. Motor can be rotated with minimal dragging torque.
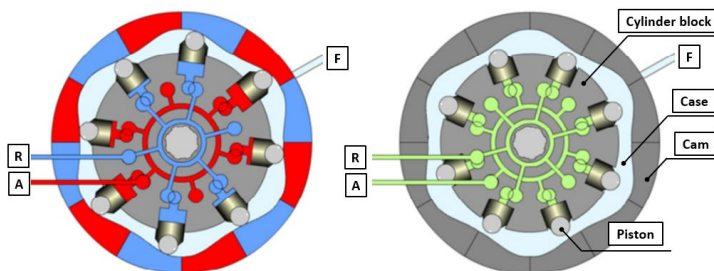
Figure 6: Hydraulic motor in working mode (left) and freewheeling mode (right)
Source: own

2   Valve design and validation process

During the project with combine harvester manufacturer a new freewheeling valve had to be developed because basic (catalogue) configuration of the valve did not meet given system requirements. Due to early implementation date of new valve integration, there was a tight schedule put in place for the team to complete and validate the design of the valve. Several actions were taken to minimize development time and specifically minimize risk of mistakes along the process. Due to short timeline, it was important not to introduce any delay. All common design steps were performed when preparing the design of the new valve:

- 3D concept
- DFMEA (Design Failure Mode Effect Analysis)
- Tolerance stack-up analysis
- Flow analysis (Computational Fluid Dynamics - CFD)
- Structural analysis using finite element method (FEM)
- Functional analysis (1D lumped model simulation)

Apart from usual design steps some specific actions were taken to assure that potential issues are identified and resolved as early as possible – Table 1:

Table 1: Valve design steps

Action	Description	Risk management impact
3D print	Production of new casted components in 3D technology	Early check of tools, fixtures and clamps for machining process
CR inspection	Computed radiography inspection of new castings	Detect potential issues on new parts before launching full validation campaign
Additional sensorics	Integrate spool position monitoring and main spool piloting pressure monitoring. Custom port adaptors produced for testing.	Monitoring of additional valve internal variables. Controlled flow conditions, alignment of test results and simulations.
Functional system simulation	Evaluation of valve and system performance using 1D multiphysics numerical model	Identification of potential critical points. Definition of alternative options.

3 Numerical approach

A significant part of design work was supported by numerical simulations evaluating different aspects of valve characteristics and performance. Some key analyses are presented in this chapter: Structural analysis, Flow analysis, Functional analysis and System integration.

Structural analysis: All main components of the valve were designed from scratch due to specific project requirements. Each of them was calculated for its stress and fatigue lifetime. Most of new components are non-standard and were evaluated by structural analysis using FEM, except for a new compression spring where a standard calculation procedure according to EN 13906-1 was applied.
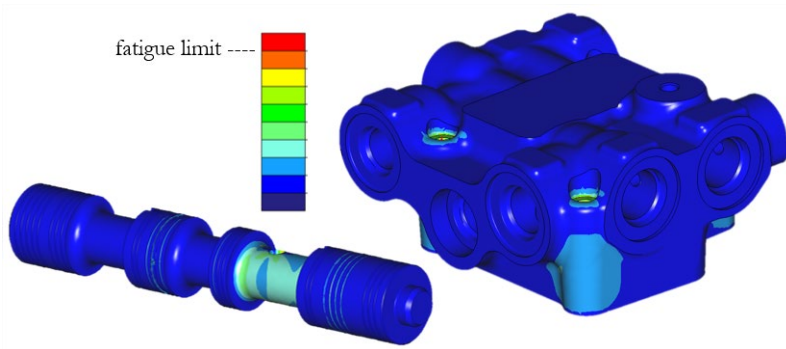
Figure 7: Von Mises stress distribution on spool and pilot housing
Source: own

Flow analysis was performed by CFD simulation tool StarCCM+. Three main focus points of investigation were:

- Pressure drop across main flow lines (main pump to motor)
  This was one of main constraints when designing the valve. Pressure drop directly affects the power consumption on the vehicle during 4WD operating mode. Valve size greatly depends on this requirement.
- Pressure drop (also local at the valve functional internal points) from valve low-pressure section to motor line ports (charge pump to motor and motor to tank)

Pressure drop in piloting lines plays an important role in dynamic 4WD mode engagement and disengagement events. Shift between 2WD and 4WD mode needs to be enabled at any vehicle speed, which requires adequate sizing for both extraction and retraction of motor pistons.

– Flow force on main spool

Flow force can have an important impact on shifting ability of the valve, therefore its understanding is critical to predict valve operating range.

Functional analysis: Numerical evaluation has been performed by commercial simulation tool Simcenter Amesim (2021.2). In the first step, detailed 1D lumped model of a new freewheeling valve has been created and tested for its basic functionality. The model has been tuned so that its response fits the results of flow analysis in terms of pressure drop and flow forces on the spools. Shifting ability of the valve was checked under specified worst case operating conditions (pressure, flow).
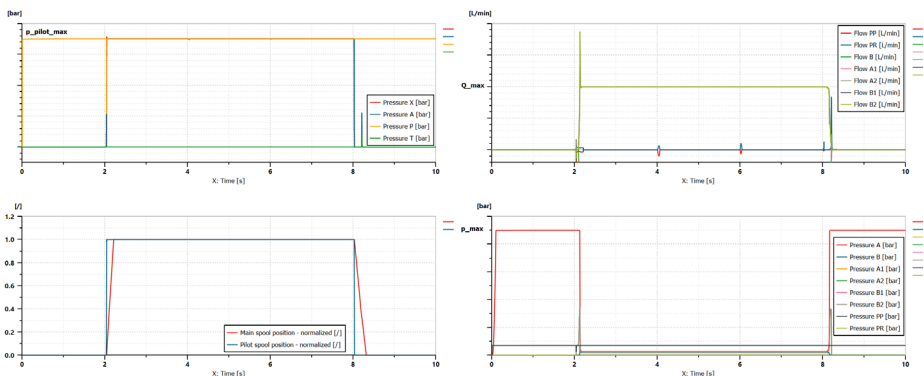
Figure 8: Simulation of valve shifting ability
Source: own

System integration: Based on available data on hydraulic circuit of the machine a system model has been built and valve model integrated into it.

Simulation of system behaviour is important, because new freewheeling valve introduces important functional change in machine 4WD circuit compared to previous circuit configuration. It was therefore deeply investigated and evaluated using functional system simulations.
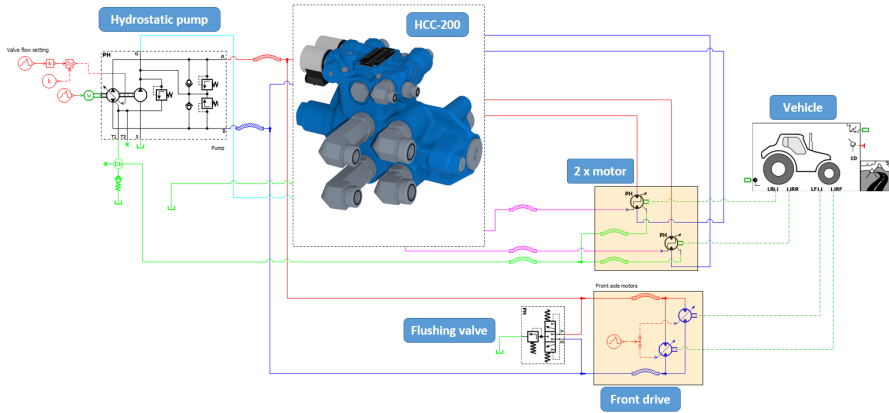
Figure 9: Numerical model of vehicle hydrostatic transmission
Source: own

Due to limited information provided by OEM, the confidence level on simulated system response is limited as well. For that matter some additional sensitivity studies were performed where critical valve parameters were modified and response evaluated for resulting trends. Such modifications were mostly evaluated for their impact on dynamic response of the system, i.e. shifting on-the-fly between 2WD and 4WD mode.
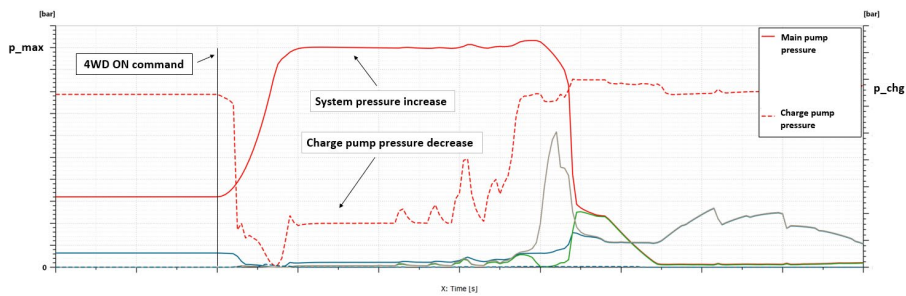
Figure 10: Baseline simulation response of 4WD activation
Source: own

Figure 10 show simulated baseline system response at activation of 4WD. It shows two points that need to be addressed to make system work properly:

- Rapid increase of system pressure at 4WD activation

– Charge pump pressure decrease at 4WD activation

Further analysis identified two important aspects linked to improvement of system response:

– Front drive control
  It is necessary to adjust displacement in front drive when transitioning from 2WD to 4WD mode and back. Timing of this change is critical for good performance and operator's comfort. Understanding the dynamics of valve shifting process is important for control tuning. Impact of valve design parameters variation was studied with simulation.
– Charge pump flow capacity
  New valve utilizes charge pump flow when engaging motors, which is different from customer previous circuit configuration. System impact was evaluated due to high instant draw of oil flow into motors during engagement.

4   Prototype build and testing

A new freewheeling valve has been developed, manufactured and tested internally by Poclain Hydraulics. The design of prototype valve included additional features that were not intended for later serial production design.

4.1   Prototype samples

Two new casted components (raw parts of both housings) were designed during the project. To enable machining of these parts also new clamping tools and fixtures needed to be designed. 3D polymer prints of components were produced for basic demonstration purpose and for an early check of fit between casted parts and the clamping tool delivered by external supplier.

A mistake in one of clamping pins height was detected by this check. With a quick corrective action the clamp has been reworked before first casted parts were delivered and available for machining. No project delay was therefore resulting from clamp issue.

Figure 11: Samples of new castings produced by polymeric 3D print process
Source: own
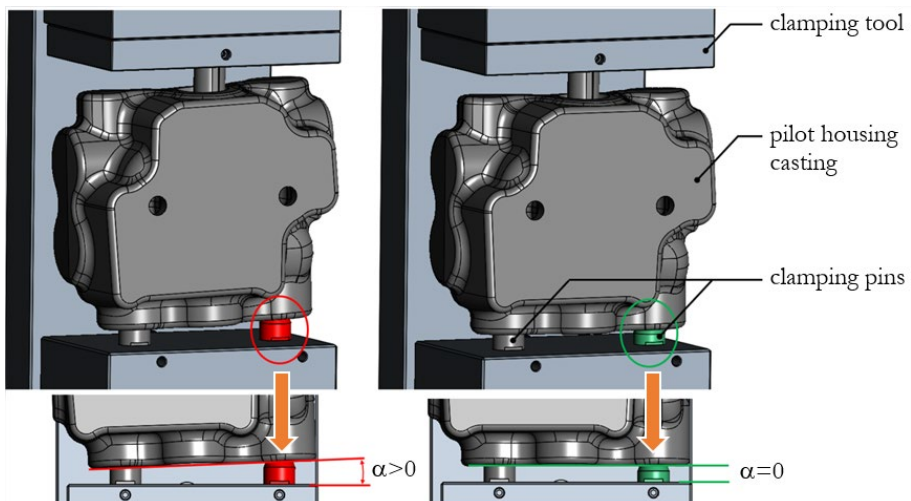
Figure 12: Wrong (left) and correct (right) clamping pin height on clamping tool
Source: own

New casted components of the valve were set for sand casting process. Casting process often requires additional modifications after initial batches in order to reduce risks of porosity, surface defects etc. Non-destructive method of CR was used to inspect the samples before building the valves and launching the validation tests. This assured there were no hidden defects that could be discovered late in testing phase and caused non-representative test results and a need for repeated testing and associated delays.
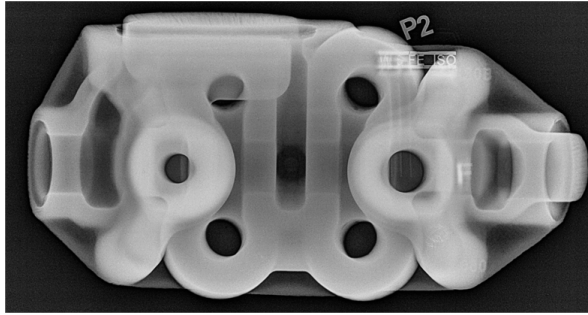
Figure 13: CR inspection of main housing casting
Source: own

Main spool position and its pilot pressure level are two internal variables of the valve that are not monitored on serial production machines. However, experience from previous projects proved that monitoring these variables gives important additional information about status and dynamic performance of 4WD system during its validation. Custom adaptor plug and associated clamps were designed to integrate both spool position sensor and pilot pressure sensor to prototype valve.
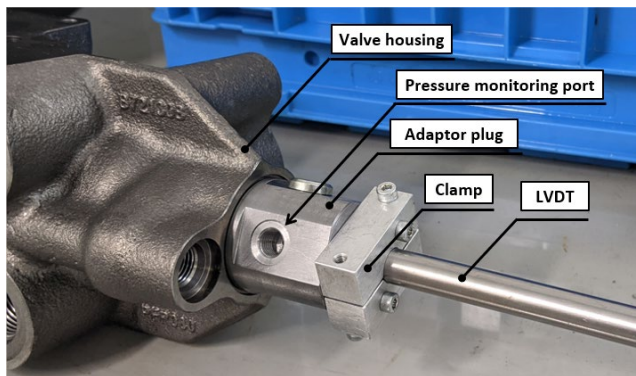
Figure 14: Adaptor plug with LVDT integration and pressure sensor port
Source: own

Custom port adaptors were designed to be installed in valve ports during bench tests. They were designed in a way to assure adequate flow section and diagnostic ports with defined position.

Figure 15: Custom port adaptors
Source: own

Benefits of using such custom adaptors is that they eliminate usage of various fitting types with different flow sections, reductions/expansions and possible local effects that they reflect in measurements. This gives better confidence in measured characteristics of the valve, in particular pressure drop values. 3D model of custom adaptors was used in flow analysis (CFD) as well, therefore a correlation of measured and simulated values was possible for further tuning of functional 1D numerical model.

4.2   Characteristic and endurance bench testing

Prototype samples have been tested on hydraulic test bench to check main hydraulic characteristics as well as structural integrity. Samples were built with additional monitoring features as presented in previous chapter.
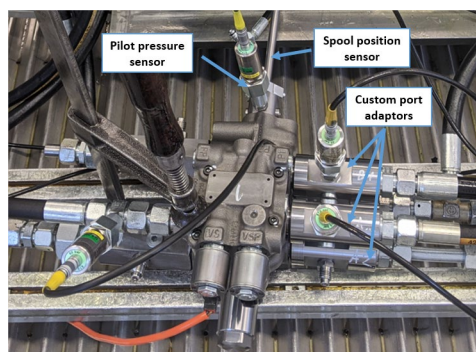
Figure 16: Prototype valve on test bench
Source: own

After in-house bench testing of valve characteristics, the valve has been sent to customer for field testing and final evaluation and validation.

4.3 Customer field testing

Customer has a standard set of procedures and operating modes to test on prototype machine. Apart from that, customer considered proposals resulting from Poclain system simulation and included them into testing plan to evaluate the circuit after integration of the new freewheeling valve. Initial field tests were done with no modification of 4WD system control. Figure 17 shows how measured response of 4WD system during engagement matches well the simulated behaviour in two critical points presented in Chapter 3.2.
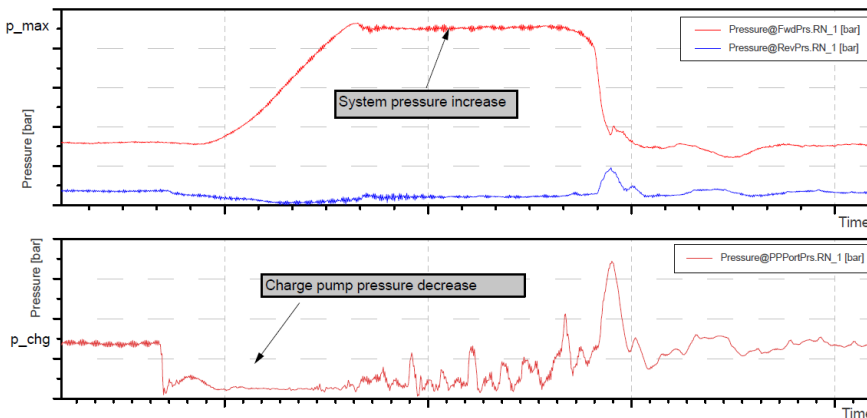
Figure 17: Field test results - initial
Source: own

System simulation suggested change of front drive displacement control to address the rapid system pressure increase at 4WD activation. Modifications were introduced to 4WD system control and the circuit. Repeated field testing resulted in an improved performance, which was detected by machine operators and approved by review of measurement results. Rapid increase of system pressure was replaced by smooth transition during activation of 4WD mode.
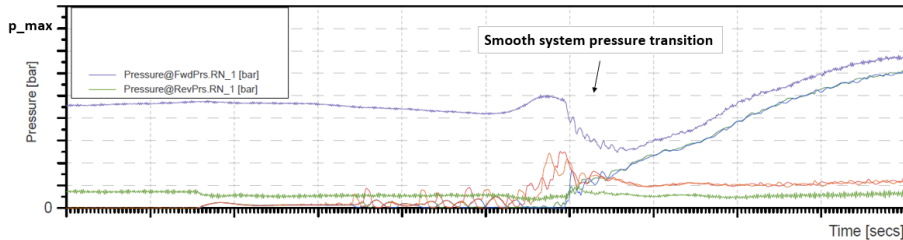
Figure 18: Field test results - modified
Source: own

Drop of charge pressure level at 4WD activation was evaluated more in detail by installing additional pressure sensor to the circuit. It indicated that charge pressure drops low at the valve due to significant distance from charge pump to the valve, but remain at sufficient level on other parts of the circuit. Therefore, it does not affect other functions of the circuit and no modification was required.

5 Conclusion

Project timeline of developing new freewheeling valve was very constrained and represented a challenge for the company. Specific steps were performed to minimize risk of mistakes and issues along the design process and preparation of prototype samples.

Several numerical calculations and simulations evaluated behaviour of the new valve prior to building physical prototypes. System simulations analysed integration of new valve inside 4WD circuit. Few main points were identified that needed specific focus during field test evaluation. Alternative design variants were prepared in case that behaviour of 4WD system would require improvement during field tests.
Eventually, new freewheeling valve was developed and validated on time for implementation on customer machine according project timeline.

References

[1]   Poclain Hydraulics training centre (various internal literature)
[2]   Simcenter Amesim Help, rev. 2021.2
[3]   https://www.poclain-hydraulics.com/applications/agriculture/combine-harvester; last visited on 28.7.2023
[4]   https://poclain-hydraulics.com/products/hydraulic-valves/hydraulic-valves-power-transmission-motion-control/freewheeling-valves/vdf-h15-vdf-h25-freewheeling-valves; last visited on 25.7.2023

[5]   https://poclain-hydraulics.com/systems/mobile-hydraulic-transmission; last visited on 25.7.2023

[6]   https://en.wikipedia.org/wiki/Combine_harvester; last visited on 24.7.2023

3D Printing for

Hydraulic Components

Jan Bartolj

University of Ljubljana, Faculty of mechanical engineering, Ljubljana, Slovenija
jan.bartolj@fs.uni-lj.si

In times of ever-changing requirements and customer demands, engineers are faced with interesting challenge of developing new, sustainable and, above all, flexible production methods when designing and manufacturing products in the modern era. 3D printing is certainly one of the methods that allows designers to incorporate new and innovative solutions into the final designs. While these solutions can be effectively implemented from an energy consumption point of view, they are still hindered by the cost and time factor. Hydraulics is just one of the many areas where 3D printing is demonstrating its full potential and ability to create complex structures and labyrinth-like internal structures. Optimizing parts has never been easier, and this new generation of parts has never been easier to manufacture than with the 3D printer. Using only the material that is absolutely necessary for the strength (existence) of the part offers a great opportunity for material savings.

1 Intruduction

Additive manufacturing (AM) differs from subtractive manufacturing in the very idea of removing material from the initial geometry. Instead of subtracting, as the name suggests, this technique adds material where it is needed. It allows the user to add material only where it is needed from a structural standpoint.3D printing uses a variety of materials such as photo-resistant resins, filaments or powders to create a specific shape of the final part. 3D printing offers the designer almost complete freedom to create new parts. This allows new approaches to create a new generation of products that can offer geometries never before possible with improved properties and performance.

Different types of 3D printing based on manufacturing techniques of material used:

- By manufacturing (fusion, sintering)
- By material (polymers, metals, biomaterials, other…)
- By geometry of base material (powder, particles, pellets, resin, rod, sheet, wire…)

Development is mainly focused on lightweight construction (optimisation), which is needed in all major engineering disciplines:

- Aerospace,
- Robotics,
- Medicine,
- Automotive,
- Agricultural, and more.

2 Various tools and principles for AM-oriented design:

- **Parametrical:** Firstly, designers can create virtual models for 3D printing using CAD software and define all the features of the geometry parametrically. This process is well known, but with additive manufacturing, designers can create completely new features that were previously very difficult or impossible to realise. This is especially true for complex internal structures.

- **Topology optimization and generative design:** Because additive manufacturing is not constrained by the limitations of conventional manufacturing, designers can use modern approaches to design new parts. This could be achieved through topology optimisation, where the computer itself, with sufficient input from the designer, determines the amount and position of material needed. Based on FEA or CFD, designers familiar with both methods should be able to create new parts using these tools. Generative design is a slightly more complicated process that uses artificial intelligence to try to create geometry that meets the requirements specified by the designer.

- 3D scanning: Printing the structure that was 3D scanned is a great tool to copy existing parts and duplicate them, possibly at different scales. 3D scanning of statues and reliefs, for example, is already used in archaeology and restoration. With the knowledge of 3D modelling, there is also the possibility of repairing scanned models (broken pieces, cracks, missing parts…) and printing improved or restored versions of statues, buildings or anything else.

- **Lattice:** The design of parts that contain segments with an intentionally weakened structure in order to minimise the mass of the parts is called lattice design. This type of geometry optimisation, previously almost impossible in traditional manufacturing, allows the designer to reduce the mass of the final product by reducing the amount of material used by creating a specially patterned lightweight structure.
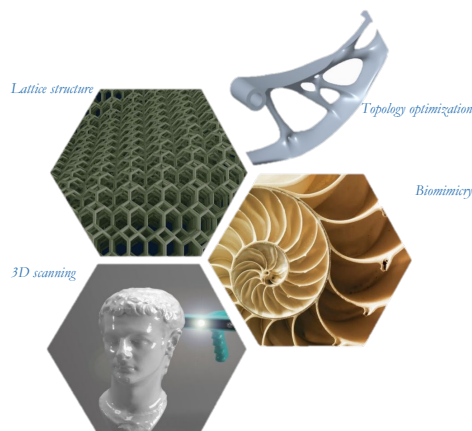
Figure 1: Tools and principles for 3D printing orientated design.
Source: own.

3 Disadvantages of additive manufacturing

As with any manufacturing process, there are some features of AM that can have a negative impact on the parts produced if they are not taken into account. Some of these are listed below:

– Postprocessing

The surface finish obtained directly in AM processes is relatively poor compared to some other manufacturing processes. Usually, the surfaces that come into contact with other parts during operation need to be postprocessed with a milling or grinding machine to meet the required specifications. Chemical treatment is also an option, but it does not usually achieve as smooth finish as fine grinding.

Post-processing includes not only surface treatment, but also the removal of support material and sometimes heat treatment. Since 3D printing in most cases applies heat to the parts, there is a possibility of delayed stress after cooling, which can result in the tensioning of part and its failure. For metals, it is usually necessary to reheat the finished part after printing to avoid cracking.

– Supporting structures

Since the whole idea is to add material where it is needed, this automatically means that the structure cannot be started without support, that being a build plate surface or some other type of disposable structure. In most cases, these structures have to be removed after printing, which drives up the time and cost of post-processing.

– Heat transfer

Most 3D printing processes involve some kind of material heating or warming. This means that the material either melts completely or is partially heated so that it can bond with other layers or the base plate. After the locally heated material has cooled, it usually tends to deform. The deformation or warping of the material is a serious problem that is difficult to solve, either partially or completely. Deformation of the printed parts while printing is still in progress can lead to faulty prints or in some cases seriously damage the machine. In most cases this problem is solved (or

attempted to be solved) by conducting heat into the base structure or supports, but this means that the material must be thermally conductive to some degree.

  – Anisotropy

As the part is printed in layers, the final product will have some anisotropic properties. If the designer is aware of this, it could be used as an advantage, but it could also lead to catastrophic part failures. Metal 3D prints could be subjected to heat treatment, where the part is heated several times to remove most of the anisotropic features, while plastic parts could be chemically treated.

  – Layer adhesion

Another disadvantage of manufacturing parts in layers is insufficient layer adhesion. This refers to the quality of the bond between the layers that are printed on top of each other. Poor layer adhesion can lead to delamination, which is a catastrophic failure of the 3D printed part.

  – Price

When deciding between additive and conventional manufacturing, there is always the concern of price. Relatively high machine costs and possible unprofitability for large series of identical parts or non-optimised geometries still slow down the integration of additive manufacturing machines in small and large industries. In contrast, the high added value of the parts could justify the use of 3D printing almost everywhere.

Most commonly when talking about the cost of AM, there are two arguments that were already mentioned to use AM in production. These are low numbered series and high complexity of parts. Combining the two criteria, even bigger series of extremely complex parts are economical to produce using 3D printing. One of the problems of AM process is that it is almost impossible to decrease production time. Usually, doubling the productivity, using multiple lasers or extruders, drives up the cost of initial investment.
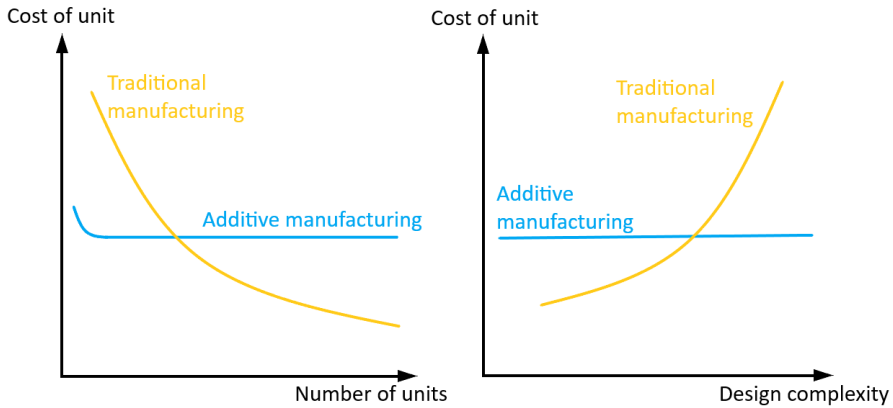
Figure 2: Cost (un)effectiveness of 3D printing based on number of units and complexity of the design.

Source: Busachi et al., 2017: Hopkinson and Dickens, 2003

4   Design rules of additive manufacturing

Design rules of additive manufacturing that designer must follow when constructing parts for AM:

– Overhangs and supports

Overhangs are surfaces that are downward facing, usually at an angle to the vertical line, and in certain circumstances need supports. Most AM techniques allow up to 45 to 50° overhanging angles with 90 being vertical wall and 0 meaning completely horizontal surface.
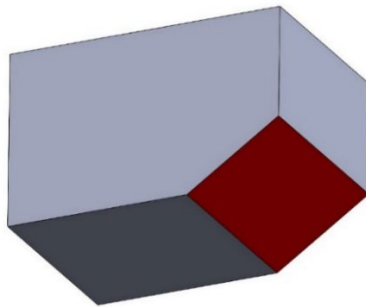
Figure 3: Overhanging surface.

Source: own.

- Wall thickness

Supported and unsupported wall thickness again depends on the particular technique and the machine used. Normally, the lowest achievable wall thickness is 0.2 to 0.3 mm, but is usually in the range of at least 0.8 mm.
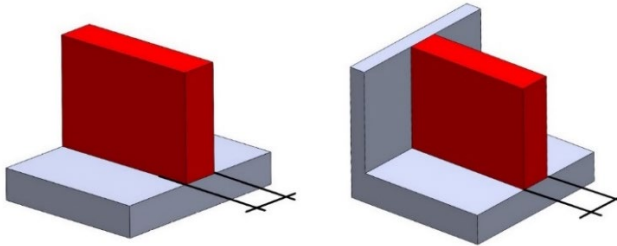
Figure 4: Supported and unsupported wall thickness.
Source: own.

- Pin diameter

The pin diameter and minimum feature size are similar parameters to the minimum wall thickness. It depends on the machine, but the minimum diameter would be 0.4 mm for high precision machines.
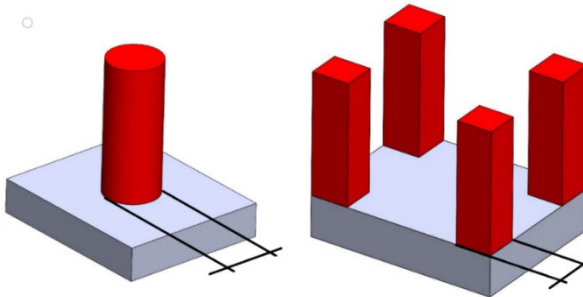
Figure 5: Pin diameter and minimum feature size.
Source: own.

- Bridges

Horizontal bridges or structures connected with an overhang that is not supported should be avoided when designing parts for 3D printing, or redesigned to eliminate any strictly horizontal surfaces to a slope. With FDM machines, the maximum bridge

spacing is 20 mm with sufficient cooling, but with other processes it is almost impossible to create bridges without supports.
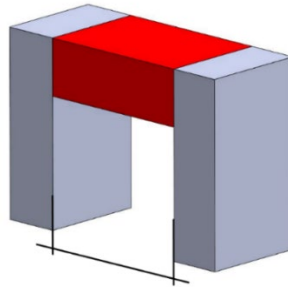
Figure 6: Bridging distance maximum length.
Source: own.

  – Minimum hole diameter

The minimum achievable hole diameter is again related to the characteristics of the machine. Usually it is linked to the nozzle, the diameter of the laser dot, screen resolution or numerically to the computer hardware of the machine and the settings of the slicers.
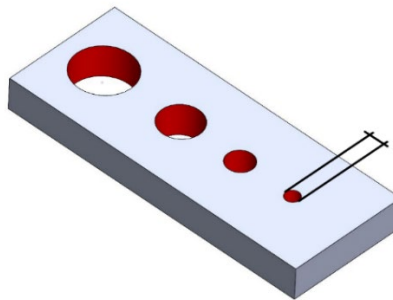
Figure 7: Minimum hole diameter dimension.
Source: own.

  – Unsupported horizontal axis holes

Holes with a horizontal axis, unlike bridges, can be made without supports. Up to a certain diameter, the structure is self-supporting, so it does not need supports. The rule of thumb would be a maximum hole diameter of 10 mm.
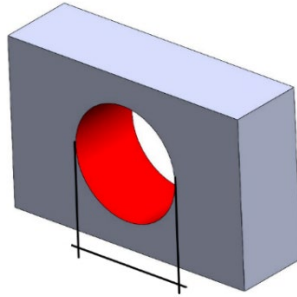
Figure 8: Maximum horizontal axis hole diameter.
Source: own.

– Connecting parts in assembly

Joining parts, either two 3D printed parts or one 3D printed part to others, requires a bit of expertise on specific machine and knowledge of its capabilities. The machine also needs to be calibrated to get the most accurate measurements possible. This is the only way the parts can be joined together, otherwise postprocessing must be performed.
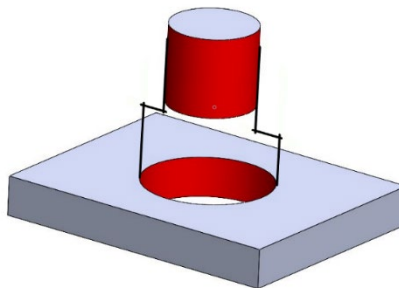
Figure 9: Dimensions for connecting parts.
Source: own.

– Holes for hollow structures

Escape holes are the necessary evil when designing parts for 3D printing with powder or resin. The hole in the structure serves as an extraction port for the material that would otherwise remain trapped inside the hollow structure. It is recommended that the holes are larger than 4 mm in order to remove the resins

sufficiently. When designing hollow structures, the designer must also be aware of internal chambers where resin or powder could become trapped.
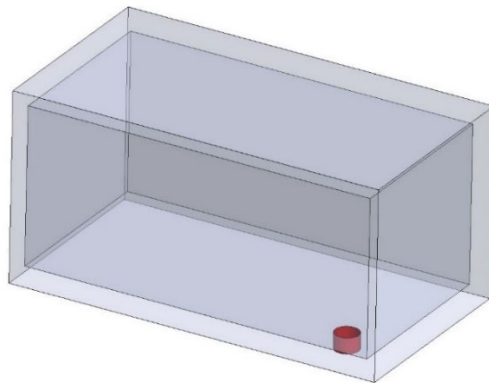
Figure 10: Hole in hollow structure for extracting trapped material.
Source: own.

–   Tolerances

Tolerances are part of a similar issue as fitting parts together and are usually dependent on the machine's capabilities and its calibration. 3D printed parts without and kind of postprocessing are known not to be the most accurate for tight measurements. Surface roughness can also have a big impact on measurements and therefore tolerances.
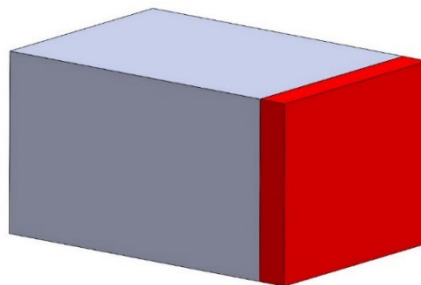
Figure 11: Tolerated dimension with its maximum and minimum possible state.
Source: own.

5 3D print in Hydraulics and pneumatics

It makes sense to 3D print some parts to improve the properties of a particular component and thus of a large system made up of those components working hand in hand with parts made traditionally. It is not about producing the same products as with conventional manufacturing techniques but producing a new generation of parts with the same purpose/functionality but improved performance and properties.

When designing parts for hydraulics and pneumatics, there are certain components where 3D printing makes more sense than others. For example, it would be irrational to 3D print hydraulic hoses for general use. 3D printing lightweight hydraulic valves for aerospace applications or for mobile hydraulic machines, where every gramme counts, makes the whole story of 3D printing much more economical and sensible. So, all in all, it makes sense to improve the properties of parts that are made from a "block" of base material and have a lot of excess volume and mass (or this mass has been removed during the subtraction process in manufacturing) and redesign them to reduce material, production and operating costs to a maximum. This can be achieved by optimising the geometry manually or by using modern software that offers different approaches to solving complex technical requirements for the final part.

Parts that are based on fluid power applications and are worth redesigning for 3D printing are:

- Hydraulic and pneumatic valves
- Hydraulic block
- Collecting manifolds and other types of collectors
- Custom parts for specific use and with special demands for geometry or structure
- Soft structures

Normally, hydraulic valves are casted or manufactured using CNC mills. Casting allows the designer to save some material compared to CNC-milled valves, but even this does not offer as much complexity as 3D printing. AM allows the production of most complex parts and the highest material savings when done correctly, up to 90% in some cases compared to CNC milled valves.
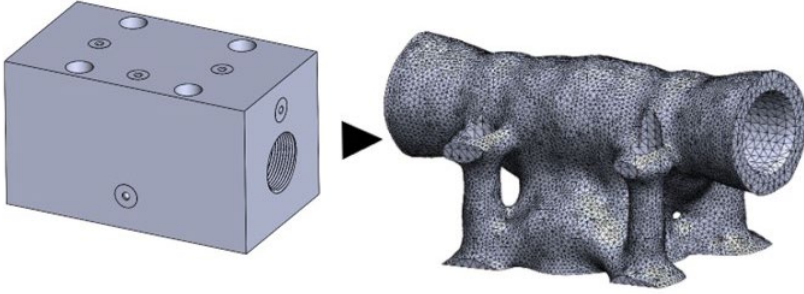
Figure 12: Optimizing geometry of topology optimization.
Source: own.

Hydraulic blocks are in some ways similar to valves on a larger scale. Because 3D printing allows for extremely complex geometries and also only needs to add material where necessary, a 3D printed hydraulic block looks like a bunch of pipes supporting the structures around them. The next step would be to combine valves and hydraulic blocks by integrating valves into the block geometry. This could further reduce the mass of the overall assembled structures.

Figure 13: Hydraulic block optimized to achieve minimum mass requirement.
Source: own.

Printing manifolds of almost any type could also be economical as they add complexity such as hydraulic blocks. In some cases, 3D printing of manifolds and the initial design of manifolds for 3D printing allows designers to use some new features, such as unusual shapes, for the part. Features (bends, shapes, sizes…) that were previously limited by manufacturing technology can now be made with AM.

Figure 14: Hydraulic manifold optimized for efficient flow conditions.
Source: own.

Customised, non-series parts and products in small batches, made for specific purposes and with minor adjustments between parts, could still be the most important factor for the use of AM in almost all industries. In this category we find all kinds of parts that cannot be pressure moulded since big and expensive tools are needed that are rigid and do not offer much flexibility. 3D printing offers exactly that. By making minor corrections to the designs, each part can be unique, while the option to make copies of the same design is still available.

Figure 15: Custom 3D printed manifold.
Source: own.

Soft structures that are designed to deform under pressure to perform specific movements are another example of a field where 3D printing has great potential. The use of soft materials such as TPU or other rubbery polymers is important because pneumatic grippers have complex internal and sometimes external structures that are difficult to achieve with other manufacturing methods. There are always debates about the impermeability of 3D-printed parts, but the same concerns could also apply to silicone or rubber.

Figure 16: Pneumatic soft robotic gripper.
Source: own.

6 Conclusion

All in all AM is a tool that offers great potential to any industry. It is flexible and allows designers to achieve completely new level of complexity of their parts. This parts have very high enhanced value and can easily deliver huge performance increases to the users.

In this article there were only briefly presented some challenges that designers using this technology must know about. Specific values are usually based on machines, software an the experience of each individual user. Presented were also different approaches and disciplines in hydraulics, where 3D printed parts just make sense. Additive manufacturing is and will continue to develop in the future so that it could rival conventional techniques in as many industries as possible.

References

[1] D. Walton, H. Moztarzadeh: *Design and Development of an Additive Manufactured Component by Topology Optimisation.* Procedia CIRP. Vol. 60 (2017), 205-210.

[2] J. Zhu, H. Zhou, C. Wang, L. Zhou, S. Yuan, W. Zhang: *A review of topology optimization for additive manufacturing: Status and challenges, Chinese Journal of Aeronautics.* Vol. 34. Issue 1 (2021), 91-110.

[3] D. Šenica: *Proporcionalni potni ventil za vodno hidravliko: diplomsko delo.* Ljubljana, 2015.

[4] M. Nagode: *Meritev proporcionalnega potnega ventila za vodno hidravliko: diplomsko delo.* Ljubljana, 2019.

[5] EOS: *Material data sheet EOS MaragingSteel MS1.* EOS, Munchen, 2017.

[6] M. Babič: *Razvoj mehkega fluidno-tehničnega robotskega prijemala: diplomsko delo*, Ljubljana, 2022.

[7] C.Y. Yap, C.K. Chua, Z.L. Dong, Z.H. Liu, D.Q. Zhang, L.E. Loh, S.L. Sing: *Review of selective laser melting: Materials and applications.* Appl. Phys. Rev. 2 (2015), 11–16.

[8] Y. Zhu, Y. Yang, P. Lu, X. Ge, H. Yang: *Influence of surface pores on selective laser melted parts under lubricated contacts: a case study of a hydraulic spool valve.* Virtual Phys. Prototyp. 2759 (2019), 1–14.

[9] K.G. Prashanth, B. Debalina, Z. Wang, P.F. Gostin, A. Gebert, M. Calin, U. Kühn, M. Kamaraj, S. Scudino, J. Eckert: *Tribological and corrosion properties of Al-12Si produced by selective laser melting.* J. Mater. Res. 29 (2014), 2044–2054.

DESIGN AND CONTROL OF MINIATURE WATER VESSELS

ŽELJKO ŠITUM, JURAJ BENIĆ, TONI FAIN,
PAVAO KAŠTELAN
University of Zagreb, Faculty of Mechanical Engineering and Naval Architecture,
Zagreb, Croatia
zeljko.situm@fsb.hr, juraj.benic@fsb.hr, tf220038@stud.fsb.hr; pk210825@stud.fsb.hr

This paper presents the design and practical realization of two mechatronic systems designed to float in the water. The first system is a remotely controlled pneumatically powered boat, as an example of ecological and unconventional vessels. The propeller is driven by an air motor that enables the propulsion of the boat. The actuator for steering is a three-position pneumatic cylinder that realizes the three positions of the rudder blade (left-centre-right). Another system is a remotely controlled underwater vehicle or a miniature submarine. The body of the submarine is a watertight chamber containing four ballast tanks, a control unit and batteries. Two servo motors are used to fill and empty water from the ballast tanks, which allows the vessel to sink and surface. The submarine is steered by a servo motor that rotates the rudder blade, and a DC motor that drives the propeller, with the use of a microcontroller.

1   Intruduction

Mechatronics is a highly interdisciplinary field and finds application in almost all branches of technology, even in very specific areas such as marine engineering. Some examples of mechatronic systems used in boats and underwater vehicles include autonomous underwater vehicles (AUVs) that use sensors and control systems to navigate and perform tasks [1], control systems for vessel navigation and attitude or mission control systems for AUVs [2]. The application of microprocessors, sensors, and communication components is widespread in the field of mechatronic systems that are used in underwater vehicles. They are installed to control the vehicle's movement, monitor its environment, or communicate with other systems. Mechatronic systems designed to float in the water are associated with numerous limitations and challenges that must be overcome for proper and reliable operation, such as higher signal delay, significant interference and noise, harsh environment, sealing problems, limited lifetime of the drive without charging, etc. [3].

Pneumatic components are rarely used in mechatronic systems for underwater vehicles. Instead, hydraulic and electric systems are more commonly used. However, there are some examples of mechatronic systems that use pneumatic components. For example, the mechatronic system of a fleet of three autonomous underwater vehicles (AUVs) called Eco-Dolphin uses pneumatic components [4]. Due to their waterproofness, artificial pneumatic muscles may have the potential to be used in mechatronic systems for underwater vehicles as drive actuators or to perform auxiliary actions that need to be performed in water [5]. This paper presents the design and practical realization of two mechatronic systems with pneumatic and electric drive intended for work in a water medium.

2   Pneumatically powered boat

n marine technology, pneumatic systems could be widely used. They can be used as propulsion systems for small boats, kayaks or canoes. Such vessels use compressed air to drive an air engine that drives a propeller or oars. They can also be used on large ships as steering systems, where compressed air drives a pneumatic cylinder that steers the ship's rudder, which turns the rudder blade. In addition, they can be used as ballast systems that use compressed air to inflate and deflate tanks to adjust the ship's stability. They are used in winch and crane systems on cargo ships, as part of diving equipment and many other applications. Remotely operated pneumatic

boats can provide some advantages over traditional electric systems. They can be more energy efficient than electric motors which will result in longer operating times while reducing operating costs. Furthermore, pneumatic systems are more reliable, durable and require less maintenance than electric motors. They are also more environmentally friendly because they do not produce harmful emissions, which makes them suitable for ecologically sensitive areas. Remotely operated inflatable boats are suitable for small-scale operations such as patrolling waterways, monitoring marine wildlife and conducting water quality tests. Therefore, the production of a small boat equipped with electronic components can provide insight into the application of mechatronic principles in systems operating in water.

2.1   Design and construction of the boat

The design requirement was that the boat has enough space for mounting all the necessary components. Next, the components should be arranged to allow an easy flow from the air source to the pneumatic motor to achieve the boat's propulsion and to connect the parts to the boat's construction. Furthermore, it should be taken into account that the compressor, battery and tank are the heaviest and largest components, whose positions on the boat are of crucial importance for the stability of the boat. The hull of the ship was gradually developed, since its shape depends on the elastic properties of the material, the position of the components and the operation of the steering and propulsion systems.
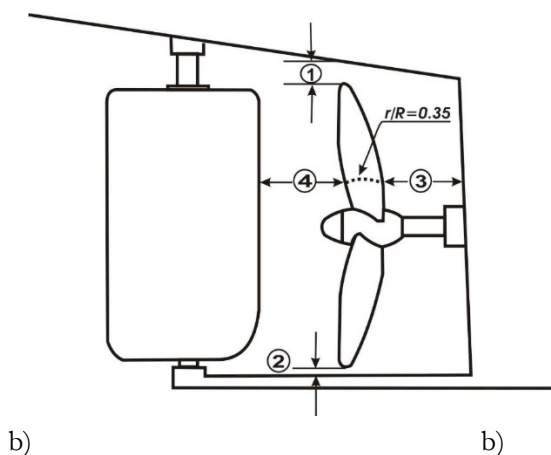
b)   b)
Figure 1: The position of the boat's propeller and rudder.
Source: https://repozitorij.fsb.unizg.hr/islandora/object/fsb:8392 [6]

The size of the components, their shape and placement determined the final form of the boat. The rudder must be positioned behind the propeller and a few centimeters (distance 3 on Figure 1) from the stern in order to achieve the necessary propulsion of the boat, and the rudder blade should be placed at a minimum distance of 15% of the propeller diameter.

a)

b)

c)

d)

e)

f)

Figure 2: Stages of boat hull construction, a) screw connection, b) polyester binding, c) plasticizing, d) coating with cement kit, e) primer coating, f) coating with final paint

Source: https://repozitorij.fsb.unizg.hr/islandora/object/fsb:8392 [6]

The boat must have ribs to ensure structural support and overall stability. According to the rules of shipbuilding, the boat must contain air tanks that provide buoyancy in case of sea entering the boat so that these air chambers keep it above water. The bow part was chosen for the reserve tank. The internal volume of the hull must be 3 times greater than the volume of water whose mass is equal to the mass of the cargo and the boat's hull itself.

The material used to make the hull of the boat was plywood with a thickness of 6 mm. The parts are precisely cut and connected to each other with screws. The contact surfaces of the plywood pieces on the inside and outside were coated with polyester paste. After the binder solidifies, the screws are removed. The bow air chamber is covered with brushed Styrodur which gives a better shape to the boat, which could not be achieved using only plywood.

The next step, after obtaining the final form of the boat, is plasticizing. Through this process, glass wool is placed on the hull of the boat and then a layer of polyester resin is spread over it. This is generally an important step in shipbuilding as it protects the surface from corrosion, water ingress and UV radiation. Also, it adds a new layer of protection and increases strength, gives shine to the boat and makes it more attractive. The hull of the boat is coated with cement putty, which is easy to apply and closes the pores on the vessel. Furthermore, the surface is sanded and the process is repeated until the desired flatness and smoothness of the layer is achieved. The last step in making the boat hull is to apply primer and then the final paint. The primer improves the adhesion between the surface and the final layer. It seals the porous surface and thus ensures that the final layer remains uniform, durable and resistant to moisture. It increases the durability of the boat's formwork and reduces the need for frequent repainting. All stages of making the hull of the boat are shown in Figure 2.

2.1.1 Boat steering system

The initial idea for the realization of the steering system was the use of a two-acting pneumatic cylinder in combination with a proportional valve. However, such a solution would require measuring the position of the cylinder, creating a more complex control algorithm, and would significantly increase the cost of the project. For this reason, a simpler solution was used. For the movement of the boat in three directions (right, straight, left) a three-position cylinder was used that can set the

rudder blade in 3 positions. The steering system is made according to the model given in Figure 3.
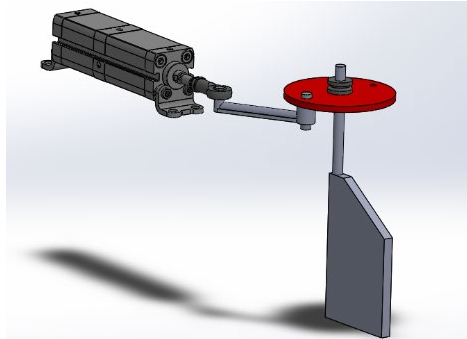
Figure 3: 3D model of the boat steering system.
Source: https://repozitorij.fsb.unizg.hr/islandora/object/fsb:8392 [6]

The piston rod of the cylinder turns the rotary disc which is connected to the boat's rudder blade. The displacement of the piston rod from the middle position to the two end positions is 15 mm, which causes the rotation of the boat's rudder blade by approximately 20°.

2.1.2   Boat propulsion system

There are four problems that had to be solved during designing the propulsion system:

- placing the air motor low enough inside the boat's hull so that the propeller is completely submerged in the water,
- mounting the air motor in a position so that the motor shaft passes through the center of the stern,
- preventing water from leaking through the hole where the shaft passes,
- mounting the 3D printed propeller on the shaft of the air motor.

The first problem was solved by the own weight of the components, which plunges the vessel into the water, with careful selection of the propeller with an outer radius of 51 mm to be within the boat's waterline. For mounting the air motor, an internal and external support is made that holds the air motor in a fixed position. A seal

(semmering) is inserted into the rear support, which does not allow water to enter the interior of the boat. And finally, the air motor shaft is machined so that it can transmit torque from the motor to the propeller. The manufactured parts of the boat propulsion system are shown in Figure 4.
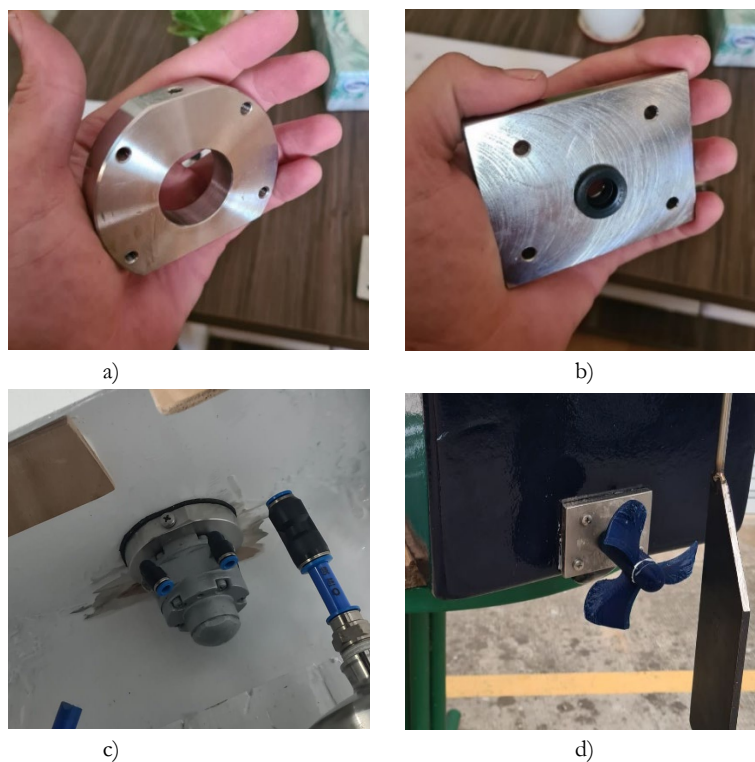
Figure 4: Boat propulsion parts, a) front support part, b) rear support part, c) air motor, d) propeller
Source: https://repozitorij.fsb.unizg.hr/islandora/object/fsb:8392 [6]

2.2   Drive and control components

An air motor (GAST 1AM-NRV-63A) was chosen to drive the boat's propeller. Air motors have many advantages, even compared to electric motors. Air throttling and pressure control are more cost effective compared to electric motor controls and can be overloaded for longer periods without damaging the motor. The characteristics that distinguish air motors are: variable operating speed and output power, they do not heat up significantly during operation, they are ideal for use in extreme conditions (dangerous environments, extreme temperatures, etc.). A three-

position pneumatic cylinder (FESTO ADNM 25-A-P-A-15Z1-30Z2) was chosen as the actuator for steering. The cylinder has 3 three positions where the connecting rod is extended by 0, 15 and 30 mm. It has good corrosion resistance, which is essential for applications in the presence of sea salt. The valve block (FESTO VTUG-10-SH3-S1T-Q6-U-M5S-6K), which contains 12 solenoid 3/2 valves, was used to control the actuators. Each valve is activated by a digital 24 V electrical signal sent by the microcontroller via serial communication. A compressor (VIAIR 400C) was used to supply the system with compressed air. It can produce 1.2 l/s of compressed air when the tank is completely empty and 0.9 l/s when the air in the tank is 5 bar. An air tank (FESTO CRVZS-2) with a volume of 2 litres is placed behind the compressor, and is used for pressures up to 16 bar. The drive components are shown in Figure 5.

a)   b)

c)   d)
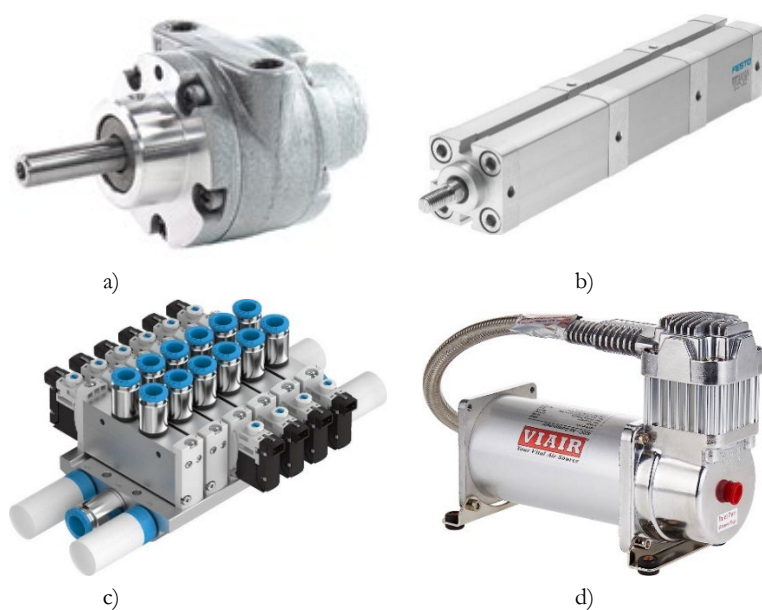
Figure 5: Drive components, a) air motor, b) cylinder, c) valve block, d) compressor
Source: https://repozitorij.fsb.unizg.hr/islandora/object/fsb:8392 [6]

Controllino Mini microcontroller was used as control device. It is programmed using the ARDUINO IDE software package and contains relay outputs that can be used to activate valves without additional electronic elements. It uses an ATmega328P microprocessor and has a USB port for communication with a computer. Bluetooth module (HC-05) is used for wireless control of the boat using a mobile phone or laptop. It has a data mode in which it can send and receive data from other bluetooth

devices. The module requires a +5 V power supply, and its range is less than 100 meters. Two power sources are required for the operation of the entire system. The compressor requires a 12 V DC power supply, and the Controllino can be powered from a 12 or 24 V DC source.

Two batteries were used because the compressor is a big consumer of energy compared to Controllino devices, and in the case of a complete discharge of one battery, the valve would close, although theoretically there could be compressed air in the tank.

2.3   Description of system operation

The program code is transferred to the microcontroller from the laptop using USB communication. The microcontroller initially includes all necessary libraries, defines initial variables, starts serial communication and declares control pins. In the next step, an infinite loop is started in which the values of the variables are constantly examined and it is determined which valve will be activated by an electrical signal. In manual mode, as soon as the operator touches the screen in the application, the programmed task of the boat is interrupted and all control actions are undertaken by the operator, who has the option of moving the boat forward - backward with the option on the mobile phone, Figure 6.

Figure 6: Mobile application for boat control.
Source: https://repozitorij.fsb.unizg.hr/islandora/object/fsb:8392 [6]

Figure 7 shows the developed prototype of a remotely controlled pneumatically powered boat during testing in water.

Figure 7: Pneumatically powered boat in the water.
Source: https://repozitorij.fsb.unizg.hr/islandora/object/fsb:8392 [6]

3   Remote controlled underwater vehicle

Remotely controlled underwater vehicles are used for underwater activities, scientific research, inspection of installations at sea for oil and gas, extraction of shipwrecks from the sea, etc. They can be equipped with different instruments, such as cameras, lights, and manipulators, to collect data or perform a specific task. They can work in deep waters where it is not possible or safe for divers. The goal of this project is to show an example of controlling the depth of the dive and realizing the movement of the vessel in the water. With a sonar or camera upgrade, a vehicle for mapping or recording the underwater surface could be realized.

However, there are many difficulties with remote communications with a vehicle under water. Water absorbs most of the signal wavelengths used in remote-controlled vehicles. For this reason, an underwater cable is often used to connect the vehicle to the control device. The next problem is maintaining the required navigation depth of the underwater vehicle. One solution is to use ballast tanks that can be filled and emptied with water to change the density of the vehicle, causing the vehicle to sink or rise. Manipulating the depth of diving requires knowledge of the static buoyancy of the underwater vehicle (the ability to float in the water at rest). By using ballast tanks, water is introduced into the submarine, which changes its density and enables a change in diving depth. Control of the depth of the underwater vehicle also requires measuring the depth at which the vehicle is located. A pressure sensor will be used for this purpose because the depth can be calculated from the hydrostatic pressure.

3.1   Designing and construction of an underwater vehicle

The hull of the submarine is a watertight chamber, in the form of a cylinder with rounded ends, in which all the parts necessary for the operation of the submarine are located. The main part of the hull is made of a transparent acrylic tube with a diameter of Ø120/114 mm and a length of 340 mm, in which the ballast tanks, control unit and batteries are placed. Figure 8 shows the hull of the submarine in a 3D model. The ballast tanks system is made using medical syringes where the pistons are driven by two servo motors. Each motor drives two pistons at opposite ends of the submarine. This allows manipulating the centre of mass of the submarine and adjusting the pitch. The positions of the pistons inside the cylinders is measured using two linear potentiometers and the data is sent to the microcontroller for controlling the servo motors.
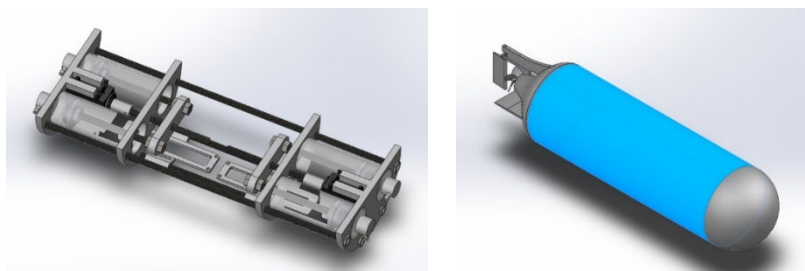
Figure 8: 3D model of ballast tanks and submarine hull.
Source: https://repozitorij.fsb.unizg.hr/islandora/object/fsb:9155 [7]

Servo motors (MPJA MG995) used for filling and emptying ballast tanks have the possibility of continuous rotation. Watertightness between joints is achieved by using suitable seals. There are six contact surfaces on the submarine that require sealing.

3.2   Control of an underwater vehicle

The control unit consists of a microcontroller that is programmed to interpret the input signals from the radio receiver and convert them into suitable output signals for driving the propeller as well as the servo motors for driving the pistons of the ballast tanks. The control system also contains analog or digital inputs for reading signals from the pressure sensor, potentiometer and temperature sensor.
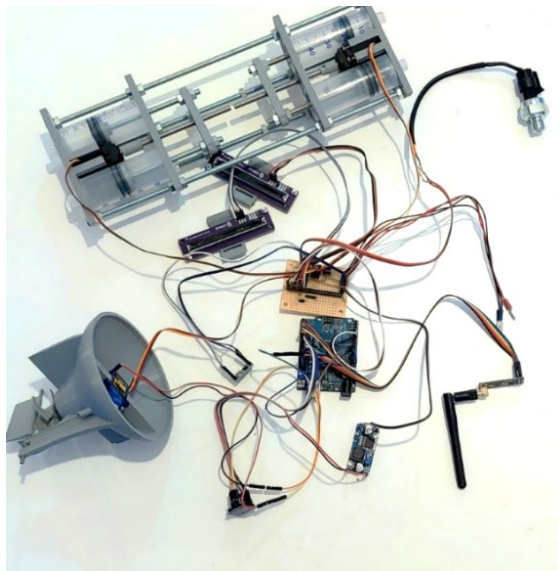
Figure 9: Control electronics with sensors.
Source: https://repozitorij.fsb.unizg.hr/islandora/object/fsb:9155 [7]

An Arduino Uno microcontroller is used for sensor data processing, motor control, wireless communication and PID control. The control device with electronics and sensors is shown in Figure 9. A servomotor (SG90) is used to rotate the rudder of the underwater vehicle, which drives a shaft connected to a lever on the vehicle's rudder, Figure 10.
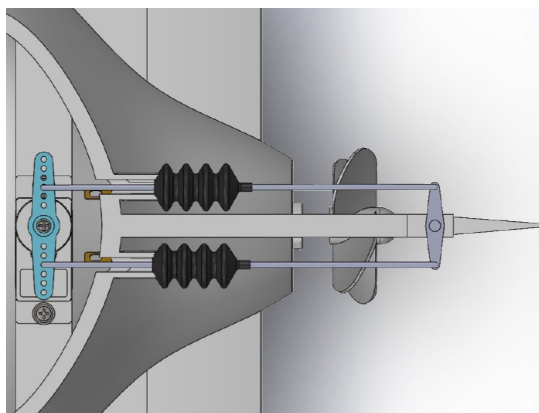
Figure 10: Rudder control.
Source: https://repozitorij.fsb.unizg.hr/islandora/object/fsb:9155 [7]

3.3 Description of system operation

The microcontroller is programmed to perform the tasks of maintaining the required depth, controlling the motors and wireless communication with the transmitter. The submarine has a relatively slow response to changing the diving depth. The reason for this is the large transverse surface of the submarine and the relatively slow rotation of the servo motor, which gives a slow response of the ballast tank. A PID controller was used to achieve the accuracy of the required diving depth and response speed of the submarine, and the operation of the system was checked experimentally. Figure 11 shows the constructed underwater vehicle.

Figure 11: Underwater vehicle.
Source: https://repozitorij.fsb.unizg.hr/islandora/object/fsb:9155 [7]

4 Conclusion

The paper has presented the design and practical realization of two mechatronic systems for floating in the water environment. First, a small boat with a propeller driven by a pneumatic motor was presented. The boat is remotely controlled and has the ability to change the direction of navigation. Then the process of designing and making a remotely controlled underwater vehicle or a miniature submarine was presented. The underwater vehicle has the ability to fill and empty water from the ballast tanks.

These experimental systems can be used as educational test models in the field of mechatronics and automatic control in marine technology. In order for the systems to work properly on water or under water, it is necessary to solve many specific requirements of such mechatronic systems. Such systems clearly demonstrate the possibilities of applying mechatronic and fluid power systems in ship technology. Such innovative works based on mechatronic principles give impetus to students to create new practical works in the future as well [8, 9].

References

[1] Bemfica, J.R., Melchiorri, C., Moriello, L., Palli, G., Scarcia, U., Vassura, G. (2013). Mechatronic Design of a Three-Fingered Gripper for Underwater Applications, *IFAC Proc. Vol.*, Vol. 46 (5), pp. 307-312, https://doi.org/10.3182/20130410-3-CN-2034.00080.

[2] Higuera, C., Sandoval, J., Coria, L.N. et al. (2022). An autonomous unmanned underwater control test vehicle: platform description and experiments. *J Mech Sci Technol* 36, pp. 395–405 https://doi.org/10.1007/s12206-021-1238-0

[3] McPhail, S. (2009). Autosub6000: A Deep Diving Long Range AUV. *J Bionic Eng* 6, pp. 55–62, https://doi.org/10.1016/S1672-6529(08)60095-5

[4] H. Liu *et al.*, (*2015*). The mechatronic system of Eco-Dolphin — A fleet of autonomous underwater vehicles, *International Conference on Advanced Mechatronic Systems (ICAMechS)*, Beijing, China, pp. 108-113, doi: 10.1109/ICAMechS.2015.7287138.

[5] *Fan, J., Wang, S., Wang, Y., Li, G., Zhao, J., & Liu, G. (2022). Research on frog-inspired swimming robot driven by pneumatic muscles. Robotica, 40 (5), pp. 1527-1537. doi:10.1017/S0263574721001247*

[6] Fain, T. (2021). Design and remote control of a pneumatically driven vessel. Final year project (in Croatian), University of Zagreb, Fac. of Mech. Eng. and Naval Arch.

[7] Kaštelan, P. (2021). Design and control of an underwater vehicle. Final year project (in Croatian), University of Zagreb, Fac. of Mech. Eng. and Naval Arch.

[8] Šitum, Ž. (2017). Fluid power drives in robotic systems. Invited Lecture. *Int. Conf. Fluid Power 2017*, Maribor, Slovenija, 11-23.

[9] Šitum, Ž., Benić, J., Pejić, K., Bača, M.M., Radić, I., Semren, D. (2021). Design and control of mechatronic systems with pneumatic and hydraulic drive, *Int. Conf. Fluid Power 2021*, September 16-17, Maribor, Slovenija.

Analysis of Valve Plate Stress in an Axial Piston Pump

Nenad Todić,[1] Maja Andjelković,[2]
Radovan Petrović[3]

[1] University of Kragujevac, Faculty of Engineering, Kragujevac, Serbia
ntodic@gmail.com
[2] University "Union-Nikola Tesla" of Belgrade, Faculty of Information Technology and Engineering, Belgrade, Serbia
maja.andjelkovic@fpsp.edu.rs
[3] University of Kragujevac, Faculty of Mechanical and Civil Engineering in Kraljevo, Kraljevo, Serbia
radovan4700@yahoo.com

Hydraulic pump is the heart of aircraft hydraulic system. Performance degradation based on mixed wear theory of aviation hydraulic piston pumps: its reliability and safety is very important; complicated structure; high pressure; high speed; strong vibration, multi field coupling, high reliability and long life. This paper establish detailed model based on mixed lubrication-wear mechanism. Experiment and validation indicate that the proposed mathematical model can reflect the integrated development process of hydraulic pump. Mechanical analysis of barrel-valve plate covers: film thickness, pressure distribution in different angles, contact pressure considering machined roughness, elastic and plastic deformation, comparison of contact force and fluid force, elastic and plastic deformation, viscosity and deformation compensation.

1   Intruduction

The distribution of pressure in the valve plates of an axial piston pump varies according to the phases of pump operation. The pressure schedule includes suction and discharge phases [1].

In the suction phase, the piston moves, creating a vacuum in the suction chamber. The port on the suction side is open so that the fluid can be sucked from the tank. In valve plates, the pressure is lower in the suction chamber to allow fluid to enter the pump.

The compression phase occurs when the piston moves forward, creating increased pressure in the pump's discharge chamber. The pressure port is open, while the suction port is closed. The pressure in the valve plates is higher in the pressure chamber so that the fluid is pushed through the outlet port to the hydraulic system.

This cycle is repeated during pump operation, creating an alternation between suction and discharge phases. The valve plate pressure distribution is designed to ensure efficient fluid suction during the suction phase and reliable fluid delivery during the push phase. Valve plate openings play a key role in controlling fluid flow direction and pressure distribution in stress analysis [2].

2   Determining the flow sections of the valve plate

The change in pressure is largely influenced by the smallest cross-section of the fluid flow formed by the valve plates and the rotating cylinder block. For simulation calculations, it is important to know the exact size of the flow passage opening on the high and low pressure side, depending on the angle of rotation. Due to the complex geometrical section, an analytical description of the cross-section is not possible. In the past, the cross section was measured and interpolated manually to obtain the surface profile. Using a 3D model of the valve plate, PAK is able to automatically calculate the smallest fluid cross-section for a complete revolution of the cylinder block (Fig. 1). [3]
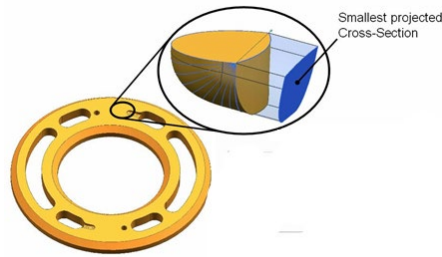
Figure 1: Cross Section Area
Source: own.

3 Systematic research of characteristic parameters

Predicting pump performance for a given design requires a simulation model that describes compressible and viscous fluid flow from the ports through the valve plates to the ventricles. Flow through lubrication gaps, which seal the chambers, must be considered. The change in pressure in the chambers is the result of the basic process of the pump and causes fluctuating forces and moments that lead to oscillating micro-motion of the moving parts of the pump's rotary group.

The influence of suction pressure pu on the gradient of pressure increase in the cylinder is shown in Figure 2 where steeper pressure gradients correspond to higher suction pressures. The size of the pressure pulsations in the pressure chamber is also affected by the suction pressure, in that lower suction pressures correspond to larger pulsations, Figure 3.

The influence of the number of revolutions of the drive shaft n on the flow of high-pressure pressure pulsations in the cylinder during the compression phase was observed, and it was noted that at a higher number of revolutions, larger pulsations appear, as a consequence of the influence of valve dynamics in this phase, Figure 4. The influence of the number of revolutions of the drive shaft on pressure pulsations in the pressure chamber is shown in Figure 5. It is noticed that at a higher number of revolutions, lower pressure pulsations appear in the pressure chamber.
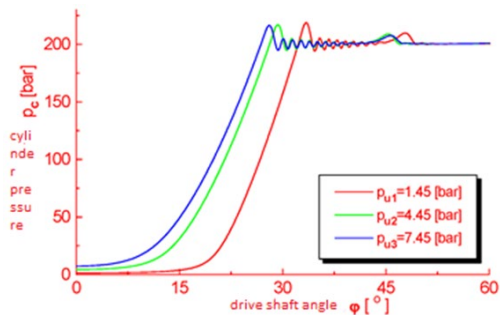
Figure 2: Impact of the suction pressure p_u to the gradient of pressure increase in the cylinder, p_c
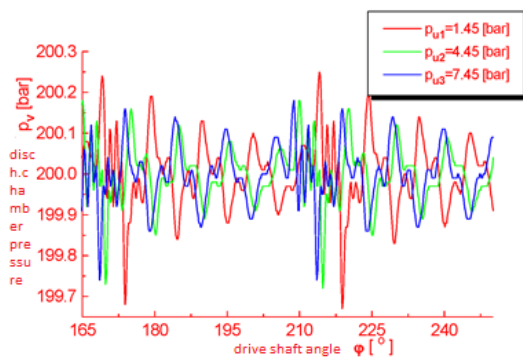
Source: own.

Figure 3: Pressure flow in the discharge chamber p_v during pressure change p_u in the operating fluid

Source: own.
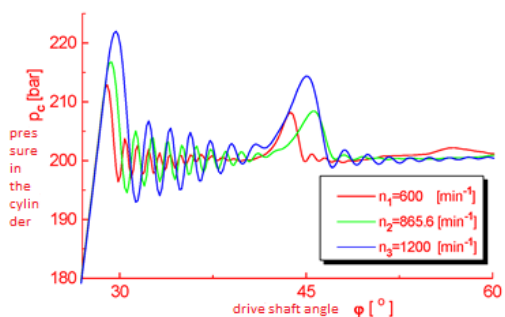
Figure 4: Impact of the number of shaft revolutions nto the pressure pulsations flow in the cylinder, pc in the compression phase

Source: own.
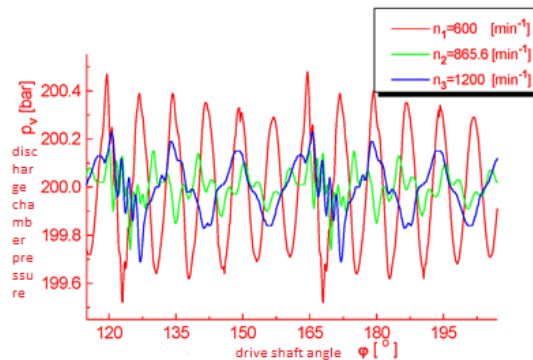
Figure 5: Impact of the number of shaft revolutions n_{to} the pressure pulsation, p_v in discharge chamber
Source: own.

4 Conclusion

Almost all available models are based on measurements, but different methods are applied to obtain an analytical description.

The limit to the achievable accuracy of most of these models is given by the use of a relatively simple analytical expression, while a good fit of the measured curves is usually achieved only in a limited range of operating parameters.

The dependence of all important operating parameters such as pressure difference, velocity, displacement volume and temperature can be easily considered using the PAK software package. The software tool is based on Matlab.

References

[1]   Petrovic R.: „Matematičko modeliranje i identifikacija parametara višecilindričnih klipno-aksijalnih pumpi", doktorska teza, Mašinski fakultet Univerziteta u Beogradu, Beograd 1999.
[2]   R. Petrović, N. Todić "Modeling and experimental research of characteristic parameters hydrodinamic processes of axial piston pumps with constant pressure and variable flow", p. 278 – 285, The 20 th International Conference on Hydraulics and Pneumatics, Prague, September 29 – October 1, 2008.
[3]   R. Petrović, J.Pezdirnik, M.Živković „Mathematical modeling and identification of hydrodinamic processes of a piston radial pump" p.47-58, ISBN=978-961-248-290-9, Mednarodne conference Fluidna tehnika 2011, 15. In 16. September 2011, Maribor, Slovenija

Mud Pump Pressure Pulsation Control Systems

Mihael Cipek, Danijel Pavković, Juraj Benić, Željko Šitum

University of Zagreb, Faculty of Mechanical Engineering and Naval Architecture, Croatia
mihael.cipek@fsb.hr, danijel.pavkovic@fsb.hr, juraj.benic@fsb.hr, zeljko.situm@fsb.hr

Drilling fluid is circulated through the well-bore during drilling operations to transport cuttings from the bottom of the hole to the surface. Hydrostatic high-pressure mud pumps are typically used for this purpose. Triplex pumps, which comprise three pistons mechanically displaced by 120 degrees, are the most common type of mud pump. When more than one mud pump is connected to the common high-pressure line, very high pressure peaks can occur due to asynchronous pump strokes. These pressure peaks can damage high-pressure mud lines and pressure equipment, such as valves and gaskets. They can also undermine well-bore stability. This paper investigates the process of pulsation creation and proposes adequate pressure control systems for pulsations reduction. The proposed systems are based on the use of passive and active control elements.

# 1	Intruduction

Deep drilling operations are required to produce deep wells for the exploitation of hydrocarbons or geothermal energy [1]. A drilling fluid (also called drilling mud) circulating through the well-bore is crucial for this process. Its main purpose is to transport cuttings from the bottom of the hole to the surface through the annulus between the borehole walls and the drill-string. Mud is also used to control the pressure within the well. In particular, the mud pressure must be higher than the well pressure to avoid accidental blowouts, which can have potentially severe consequences for personnel, equipment, and the environment. The mud pressure must also be sufficiently low to avoid accidental fracturing of the well [2].

Mud pumps are used to circulate drilling mud through the well-bore. They are typically reciprocating piston devices, with triplex pumps being the most common type [3]. Triplex pumps have three pistons that are mechanically displaced by 120 degrees [4]. When more than one mud pump is connected to the common high-pressure line, high pressure peaks can occur due to asynchronous pump strokes. These pressure peaks can damage high-pressure mud lines and pressure equipment, such as valves and gaskets. They can also undermine well-bore stability.

One way to reduce these harmful high pressure spikes is to control the phase displacement of individual pumps with respect to each other. This can be done by synchronizing the timing of pump strokes, which leads to equal peak amplitudes. For example, if only one triplex mud pump is connected to a single high-pressure line, there is no possibility of high pressure peaks since all three pistons are mechanically displaced by 120°. However, if two or more triplex pumps are connected to a single high-pressure line, pressure peaks are likely to occur. The dynamics of this system are chaotic, and the angular phase differential between two pumps may be considered quasi-random. This means that there is a much higher probability for pressure peaks to occur in this case [2].

This paper conducts the analysis of pulsation creation and proposes an adequate pressure control systems for pulsations reduction. The proposed systems are based on the use of passive and active control elements.

2   Mud pump system mathematical model

A mud pump is a positive displacement machine consisting of two or more cylinders, each containing a piston or a plunger, which are driven through respective slider-crank mechanisms and a common crankshaft powered by an external source. Rotational speed of the crankshaft, and the number of pistons and their respective dimensions determine a pump capacity. Unlike a centrifugal pump, a positive displacement pump does not develop pressure; it only produces a flow of fluid. The downstream process or piping system produces a resistance to this flow, thereby generating pressure in the piping system and the discharge portion of the pump [5]. Pump flow fluctuates at a rate proportional to the pump speed and the number of cylinders. The amplitude of these fluctuations is a function of the number of cylinders. Generally speaking, the greater the number of cylinders, the lower the amplitude of the flow variations at a specific rotational speed. Mud pumps are capable of producing a variable capacity when coupled to a variable speed drive. Each pump has maximum suction and discharge pressure limits that, when combined with its maximum speed, determine the pump's power rating.

The pump can be subjected to power inputs that are less than its maximum rating, which only results in a slight decrease of its mechanical efficiency. In a positive displacement pump, when pressure exceeds the design limits of the pump, mechanical failure (often catastrophic) may occur unless excess pressure is quickly relieved. For this reason, all piping systems incorporating positive displacement pumps must have discharge pressure relief devices to limit the pressure in the piping system and to avoid pump failure [5].

2.1   Kinematics of piston movement

Mud pump kinematics can be described by a simple slider-crank mechanism. By applying a Cosine law for the aforementioned mechanism, the position of plunger pin from crank shaft centre (corresponds to plunger position) X can be described as:

$$X = r + L - r\,cos\,\theta_{cs} - \sqrt{L^2 - r^2\,sin^2(\theta_{cs})} \qquad (1)$$

where r is the radius of the crank shaft, L is the length of the connecting rod, and θ_{cs} is crank shaft angle. Crankshaft angle is calculated from crankshaft speed ω_{cs} as follows:

$$\theta_{cs} = \int \omega_{cs}\, dt \tag{2}$$

2.2. Isothermal pressure drop

Drilling fluid is compressed within pump cylinders. Volume inside the pump cylinder consists of the dead volume V_0 (volume when plunger is in its top dead centre position) and the changeable (variable) volume ΔV_a which is directly determined by the plunger position ΔX. This volume can be defined as follows:

$$\Delta V_c = V_0 + \Delta V_a = V_0 + \frac{D^2 \pi}{4} \Delta X, \tag{3}$$

where D is diameter of the plunger. Overall cylinder volume in the top dead centre position is $V_{c,min} = V_0$, while in the bottom dead centre position, the total volume is given by the following straightforward relationship:

$$V_{c,max} = V_0 + \frac{D^2 \pi}{4} 2r. \tag{4}$$

On the other hand, the relationship between isothermal pressure drop dp and changeable volume dV is described by compressibility coefficient β, defined as [6-8]:

$$\beta = -\frac{dV}{dp} \cdot \frac{1}{V_{c0}}, \tag{5}$$

where V_{c0} refers to the initial chamber volume.

By applying expression (5) to the volume inside the mud pump cylinder, the pressure drop inside any cylinder (denoted by cylinder number n) can be described as:

$$dp_{c,n} = -\frac{dV_n}{\beta V_{c,n}}, \tag{6}$$

where

$$dV_n = \frac{D^2\pi}{4}dX_n,\tag{7}$$

and $V_{c,n}$ corresponds to the nth cylinder initial volume (at compression starting point).

2.3   Simplified drilling fluid hydraulic circuit

Figure 1 shows the simplified hydraulic circuit of the drilling fluid, which includes the compression of fluid volumes V_{c1}, V_{c2}, V_{c3} inside each of the $n = 3$ cylinders, fluid volume inside the drill string V_{ds}, pressure drop within the drill string Δp_{Dr}, and flow dynamics through the check valves. Figure 1 also shows the mechanical part of the mud pump mechanism. Three pump cylinders are mechanically coupled by a crank shaft (each separated by a $360°/n = 120°$ degree angle). Electric motor(s) propel the crankshaft through power transmission chain and gear with i_{belt} and i_g ratios, respectively.
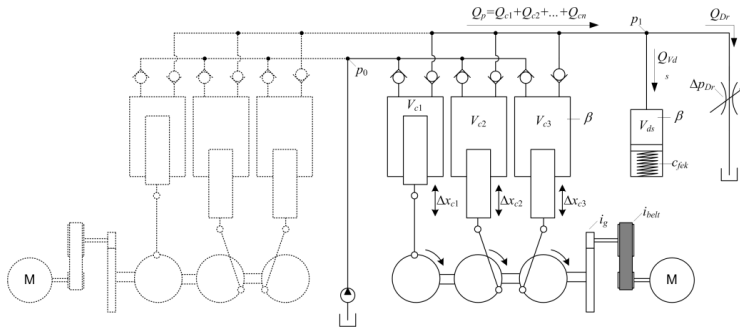
Figure 1: Principal schematic representation of simplified mud hydraulic cycle.
Source: own.

Volumetric fluid flow rate is defined as follows [6]:

$$Q = \frac{dV}{dt}.\tag{8}$$

Volume of the drill string $V_{ds} = l\pi D_{ds}^2/4$ (where l is drill-string length, D_{ds} is its inner diameter) in Fig. 1 is represented as a single chamber, where chamber input/output flow Q_{Vds} can be calculated as the difference of the overall pumping flow Q_p and Q_{Dr} ($Q_{Vds}=Q_p - Q_{Dr}$). Therefore, the pressure drop dp_1 is defined as:

$$dp_1 = -\frac{1}{\beta V_{ds}}(Q_p - Q_{Dr})dt. \tag{9}$$

The bore-hole flow (flow through the drill string) is concentrated within the drilling tool (drill bit) and it is simply represented as a damping (valve) element which can be mathematically described as:

$$Q_{Dr} = K_{Dr}A_{Dr}\sqrt{\Delta p_{Dr}}, \tag{10}$$

where A_{Dr} is cross section area of the flow hole (orifice area). K_{Dr} is damping coefficient which includes mass density of fluid ϱ and the coefficient of discharge for the orifice a_D [20]:

$$K_{Dr} = \alpha_D\sqrt{\frac{2}{\rho}}. \tag{11}$$

Due to the variability and uncertainty of A_{Dr}, a_D and ϱ parameters of the drilling process, they are approximated and lumped together within a fixed parameter $1/k_{ds}$. Following from that, the flow Q_{Dr} can be expressed as:

$$Q_{Dr} = k_{ds}\sqrt{\Delta p_{Dr}}. \tag{12}$$

Fluid flow through check valves can be represented in the form similar to Eq. (10). The high-pressure check valve (discharge valve) within the pumping mechanism is open only if the cylinder pressure $p_{c,n}$ is larger than the pressure inside the drill string (p_1), which gives the following relationship for the check valve flow rate:

$$\begin{aligned} Q_{c,n} &= k_{cv}\sqrt{p_{c,n} - p_1} \quad \text{for} \quad p_{c,n} > p_1 \\ Q_{c,n} &= 0 \qquad\qquad\qquad \text{otherwise,} \end{aligned} \tag{13}$$

where k_{cv} is the lumped damping parameter of the valve. Similar relationship is valid for the low pressure check valve (intake valve). Namely, it is open only if pressure within the cylinder $p_{c,n}$ is lower than the pressure inside intake manifold p_0 (charging pump pressure [9]):

$$Q_{i,n} = k_{cv}\sqrt{p_0 - p_{c,n}} \quad \text{for} \quad p_0 > p_{c,n}$$

$$Q_{i,n} = 0 \qquad\qquad \text{otherwise}. \qquad\qquad (14)$$

While check valves are open the volume of the fluid inside the cylinder changes due to the fluid flow into each cylinder according to:

$$V_{f,n} = \int (Q_{i,n} - Q_{c,n})dt. \qquad\qquad (15)$$

Therefore, the cylinder volume changes from $V_{c,n}$ to the following value:

$$V_{cc,n} = V_{c,n} + V_{f,n} \qquad\qquad (16)$$

wherein the pressure inside the cylinder is $p_{c,n} \approx p_1$ in the case of discharge, while $p_{c,n} \approx p_0$ is valid in the case of intake.

Overall pump discharge flow is given as $Q_p = Q_{c,1} + Q_{c,2} + Q_{c,3}$, while the intake flow is $Q_{ia} = Q_{i,1} + Q_{i,2} + Q_{i,3}$. In the case of additional pumps connected to the same pipeline, pressure p_1 is equal for each pump, while flows of all pumps are added together $Q_{p,all} = Q_{p1} + Q_{p2} + \ldots + Q_{pn}$.

2.4   Mechanical relationships

Mechanical torque produced by the pressure $p_{c,n}$ inside each of the cylinders, and transferred to the crank shaft can be expressed as [10]:

$$m_{c,n} = p_{c,n}\frac{\pi D^2}{4}r\sin(\theta_{cs,n})(1 + \frac{r}{L}\cos(\theta_{cs,n})). \qquad\qquad (17)$$

The corresponding electrical motor torque required to maintain the pumping action can be calculated as follows:

$$m_l = J_{all}\dot{\omega}_m + \frac{\sum_{n=1}^{3}m_{c,n}}{i_{belt}i_g}, \qquad\qquad (18)$$

where $\sum_{n=1}^{3}m_{c,n}$ overall crank shaft torque stemming from the in-cylinder pressure, J_{all} is lumped inertia of crankshaft J_{cs}, drive shaft J_{ds} and motor J_m and can be calculated as:

$$J_{all} = \frac{\frac{J_{cs}}{i_g^2} + J_{ds}}{i_{belt}^2} + J_m. \tag{19}$$

Table 1: Physical parameters of mud pump system.

L [m]	r [m]	D [m]	i_g	i_{belt}	V_0 [m³]
1.28	0.3048	0.14605	3.439	2.3384	0.006
β [Pa⁻¹]	k_{ds}	k_{cv}	J_{cs} [kgm²]		J_{ds} [kgm²]
45.8·10⁻¹¹	1.3·10⁻⁵	0.0004	585.77		34.355

3   Triplex mud pump simulation models

This section presents the simulation models of the individual mud pumps and the overall triplex multiple pump system, implemented within the Matlab/Simulink™ software environment.

3.1   Slider-crank mechanism (Cylinder) sub-model

Figure 2 shows the block diagram of the slider-crank mechanism (Cylinder) sub-model while the corresponding simulation model is implemented within Matlab/Simulink™ software environment. According to mathematical model described above, volume change ΔV_c in the cylinder occurs due to plunger movement, which is calculated by integrating the crank-shaft speed ω_{cs} from the starting angle θ_{cs0}.
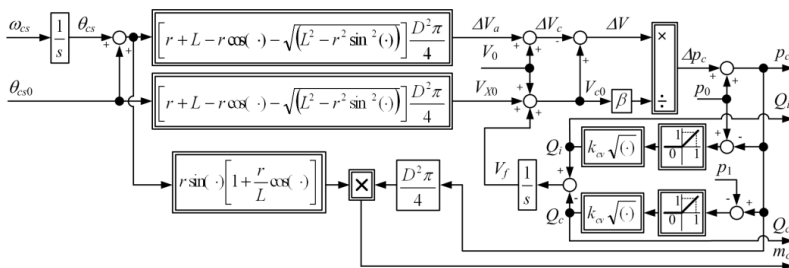

Figure 2: Block diagram representation of Cylinder sub-model
Source: own.

While check valves are closed, overall volume change within the cylinder ΔV is equal to ΔV_c, and the pressure changes according to pressure drop Δp_c relationship. On the other hand, when the cylinder pressure p_c is larger than the pressure inside the

drill string p_1, the high-pressure check valve (discharge valve) opens, which initiates the fluid flow Q_c, and results in a decrease of the fluid volume inside the cylinder by V_f. Finally, when the cylinder pressure p_c is lower than the pre-charge pressure p_0, the low-pressure check valve (intake valve) opens, which results in fluid flow Q_i into the cylinder, and consequent increase of the fluid volume inside the cylinder by V_f.

3.2 Triplex mud pump and drill string pipeline hydraulic system simulation model

Figure 3. shows the block diagram of the triplex mud pump hydraulic system model together with the drill-string pipeline model. Within the triplex mud pump model, the three individual pump pistons are mechanically coupled by a crank shaft (each separated by a $360°/n = 120°$ degree angle). The overall crank shaft torque is the sum total of all cylinder torques $m_{cs} = m_{c,1} + m_{c,2} + m_{c,3}$. Intake and discharge flows of each cylinder are hydraulically coupled, which means that the pump discharge flow is the sum total of all cylinder discharge flows $Q_p = Q_{c,1} + Q_{c,2} + Q_{c,3}$, and pump intake flow is the sum total of all cylinder intake flows $Q_{ia} = Q_{i,1} + Q_{i,2} + Q_{i,3}$. On the other hand, pre-charge pressure p_0, and drill string pressure p_1 are the same for each cylinder.

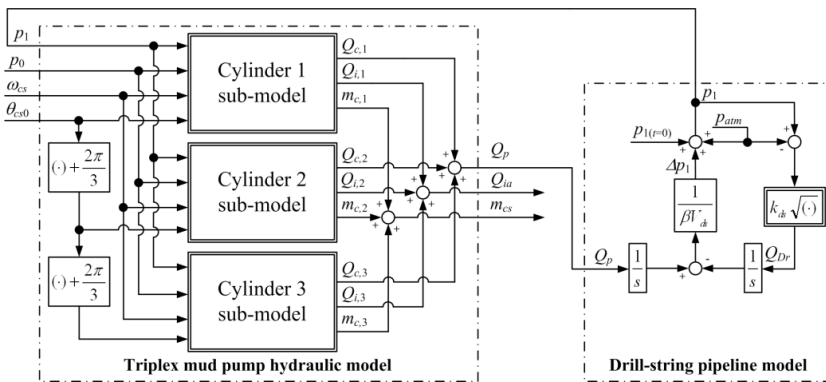**Figure 3: Block diagram representation of Triplex mud pump hydraulic and Drill-string pipeline model.**
Source: own.

Moreover, within the drill-string pipeline model, fluid volume inside the pipeline $V_{ds} = l \times \pi D^2/4$ (l is pipeline length, D is pipeline cross section) is represented by a single chamber, wherein chamber input/output flow can be calculated as the difference of

the overall pumping flow Q_p and bore-hole flow Q_{Dr} (flow through the drill string channelled into the borehole through the drilling tool). Analogously, the volume difference inside the pipeline can be calculated by integrating the flow difference. Finally, based on the aforementioned relationships, the drill string pressure p_1 is then built up due to the volume difference, which is described by well-known pressure drop relationships (see section 2.3). Naturally, atmospheric pressure p_{atm}, and initial drill string pressure $p_{1(t=0)}$ can be included within the drill string model as well, as freely configurable parameters, or as input variables.

3.3   Overall triplex mud pump model

The overall simulation model of the triplex mud pump system, built up from previously described sub-models is shown in Fig. 4, within the framework of speed-controlled DC electrical drive featuring a speed/current cascade control system [11]. The motor controller parameters are determined according to the damping optimum criterion. Block diagram (Fig. 4.) also shows that the motor speed reference ω_{mref} is determined by multiplying the requested pump speed reference ω_{pref} with i_{belt} and i_g power transmission ratios. Negative load torque m_l (crank shaft torque reduced by power transmission ratios $m_l = m_{cs}/i_{belt}i_g$) is added to the motor torque, and the resulting torque difference accelerates the total inertia J_{all} (equation (19)) with the angular acceleration rate $\dot{\omega}_m$, which is used within the model to obtain the motor speed ω_m through integrating the angular acceleration $\dot{\omega}_m$. Pump crank shaft speed is then calculated as motor speed reduced by the overall transmission ratio ($\omega_{cs} = \omega_m/i_{belt}i_g$).
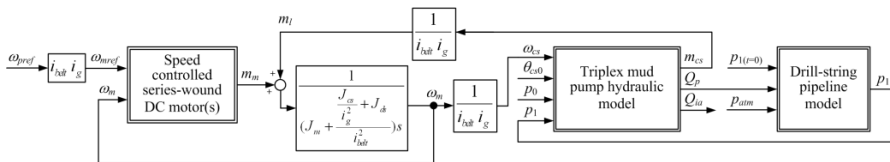
Figure 4: Block diagram of overall triplex mud pump model.

Several independent mud pump models described above can be easily incorporated into an extended multiple pump. In the case when an additional pump is added, intake and discharge flows of all connected pumps are summed together ($Q_{p,all}=Q_{p,1}+Q_{p,2}+…+Q_{p,n}$ and $Q_{ia,all}=Q_{ia,1}+Q_{ia,2}+…+Q_{ia,n}$) while the drill string pressure p_1 and pre-charge pressure are still equal for each pump, respectively.

4   Pressure pulse analysis

Previously defined model of two interconnected mud pumps is simulated for the case of speed reference ω_{cs} of 120 strokes per minute (SPM) and initiating phase angle of first (Master) pump of $\theta_{cs0} = 0$ degrees, while the second (Slave) pump initiating angle has been varied within the range $\omega_{cs1} = 0\ldots120$ degrees with $1°$ increment. Figure 5 shows the pressure pulsation steady-state magnitudes from simulations dependent on the pump phase displacement (crank shaft angle between two pumps). Each sub-plot (Fig 5a-d) represents the results for different amounts of fluid volume inside the drill string V_{ds} (different hydraulic compliance of the system). These results show that the pressure pulsation magnitude generally decreases as the drill string fluid volume capacity increases, and that for the all considered cases the drill string pressure pulsations may be notably reduced if second pump is shifted in phase by $30°$ or $90°$.
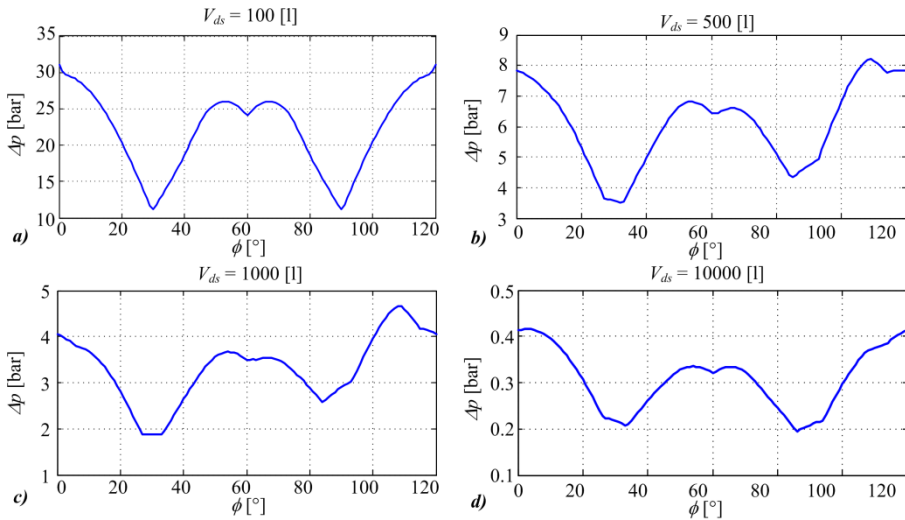
Figure 5: Simulation responses of pressure oscillations for drill-string volume: 100 L (a), 500 L (b), 1000 L (c), and 10000 L (d).
Source: own.

Similar approach to pressure pulsation analysis can be used for the case of three interconnected mud pumps. Again, simulations were carried out for the case of speed reference ω_{cs} of 120 strokes per minute (SPM) and initiating angle of first pump (Master pump) being $\theta_{cs0} = 0$ degrees. The other two pumps have had the

initiating phase angle within the range $\theta_{cs1,2} = 0 \dots 120$ degrees (with 2 degree increments for each point). Simulation results presented in Fig. 6 indicate that pressure pulsations magnitude depends on phase shifts of both auxiliary pumps, and there appear to be eight possible combinations of phase shifts which result in minimal pressure pulsations.
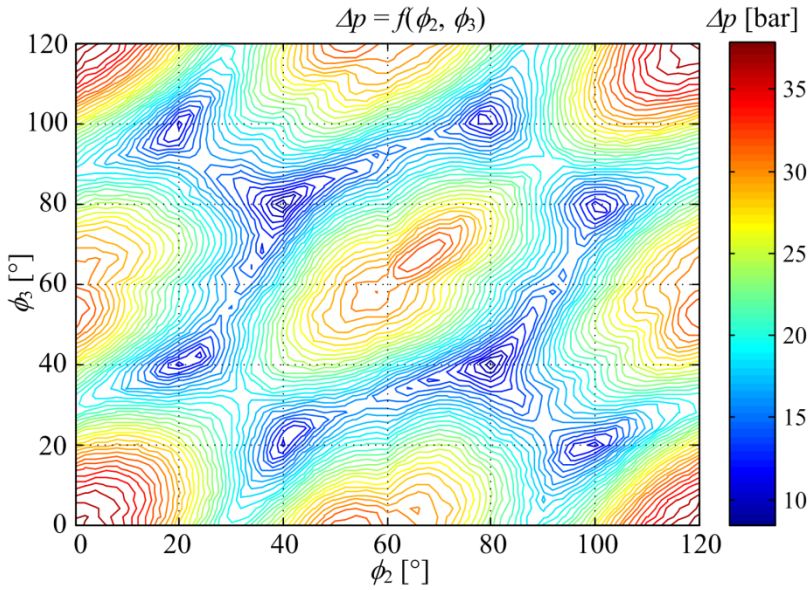
Figure 6: Simulation responses of pressure oscillations for 100 L drill-string volume and three mud pumps

Source: own.

5 Mud pump control system concept

The mud pump control system concept is based on above pressure pulsation analysis for the case of two and three interconnected triplex mud pumps. The pump phase shift controller, shown in Figure 7, uses integrators to measure time intervals between the SPM pulses from the master and slave pumps, while also considering the pump speed reference in order to calculate the phase shift between the master and slave pump. The phase shift result is subtracted from the "optimal" pump phase displacement reference, and the resulting error is multiplied by a proportional gain k_{adhoc}. To avoid possible phase shift overshoots, a saturation block has been also included within the controller, whose output represents the speed reference bias $\angle\omega$, which is added to the speed reference of the slave pump. The controller is extended

by additional rule which utilizes the fact that the angle difference between each piston each stroke amounts to 120° for the considered triplex mud pump. So, for the case when controller estimated phase angle is larger than 120°, this additional rule adds an 120° offset to the phase reference. This additional rule can also be applied in the same way for the phase angle larger than 240°.
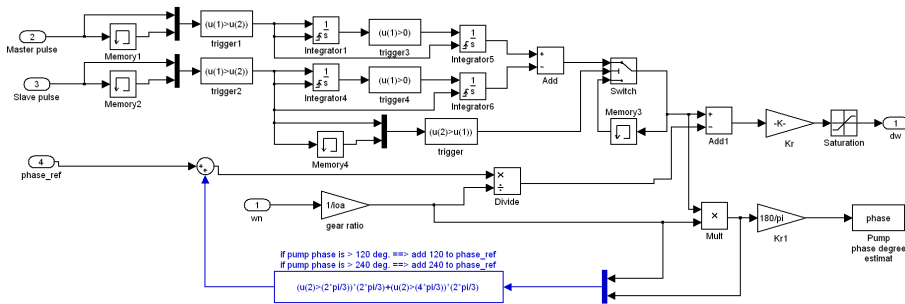
Figure 7: Matlab/Simulink™ representation of simple phase controller.
Source: own.

It is assumed that both pumps are equipped with Stroke Per Minute (SPM) sensor which gives one pulse per one crank shaft revolution, and that electrical motors driving the pumps are also equipped with fast (stiff) embedded speed controller. The above control system can also be applied to three interconnected mud pumps and the drill-string system, as shown in Figure 8.
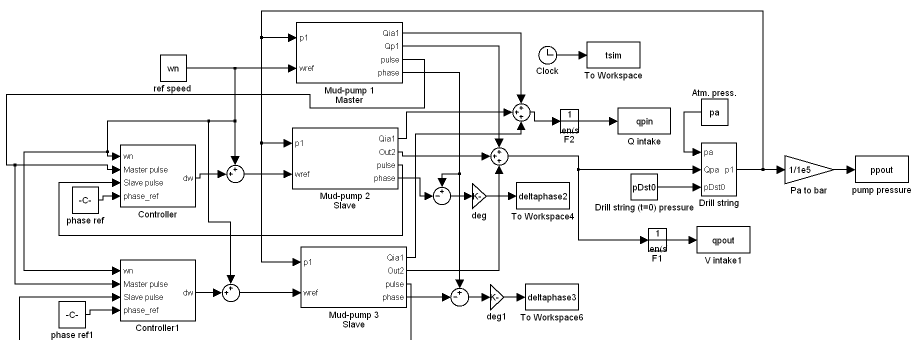
Figure 8: Matlab/Simulink™ implementation of overall "soft-pump" control system of three triplex mud pumps.
Source: own.

In that case, the proposed system possesses two separate phase shift controllers for each slave pump. Each slave pump controller calculates the phase angle of slave pump reference to the master pump angle.

5.1 Simulation results

Figure 9 shows the simulation results of the phase-controlled three mud pump system, with the pumps speed reference ω_{pref} set to 120 SPM ($\theta_{cs0} = 0°$), and the initial drill string pressure set to atmospheric pressure value of 1 bar.
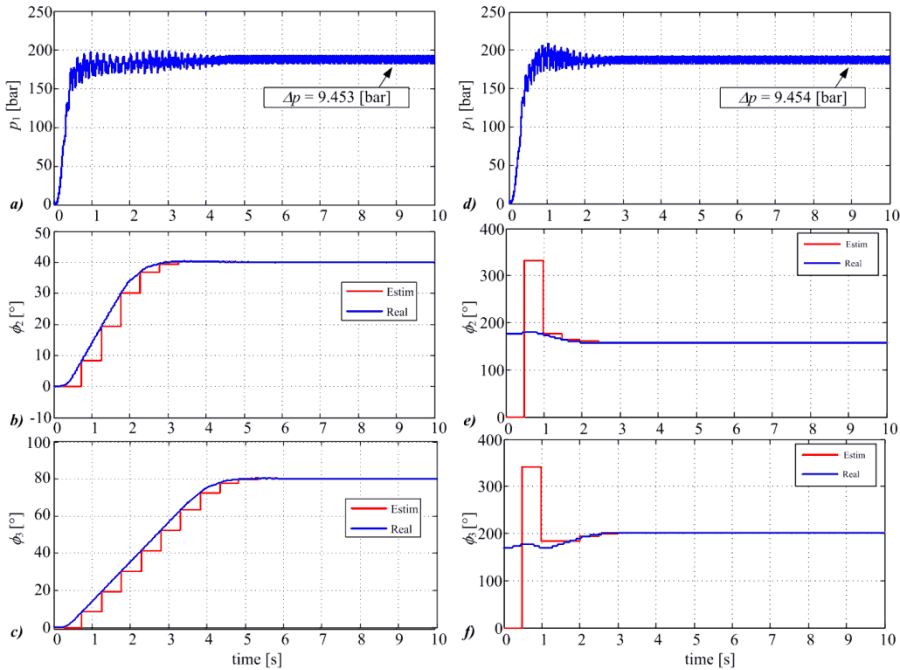
Figure 9: Simulation responses of soft mud pump: pressure (a) and phase of first slave (b) and second slave (c) for all pump starts from 0°, and pressure (d) and phase of first slave (e) and second slave (f) for slave pumps starts phase displaced by 180°.

Left-hand-side sub-plots (Figs. 9a-c) show the simulation responses in the case when slave pumps start in phase with the master ($\theta_{cs1} = 0°$), while right-hand-side sub-plots (Fig. 9d-f) show the case when slave pumps start with half turn phase advance ($\theta_{cs1} = 180°$) with respect to the master pump. For both scenarios, the phase displacement between pumps is brought to the desired (reference) values which correspond to minimal pressure pulsations.

6 Conclusion

Three-piston (triplex) mud pump simulation models are presented and simulated in this study. The simulation results illustrate the dominant flow and pressure pulsation phenomena. The pressure pulsation and phase displacement analyses for the case of two interconnected three-piston (triplex) mud pumps have shown that minimal pressure pulsations occur when master and slave pumps are phase-shifted by a 30° or 90° angle, while in the case of three interconnected pumps, the analysis has shown that eight distinct combinations of phase shifts between individual pumps result in minimum pressure pulsation magnitude. The mud pump pressure pulsation control system concept has also been presented in this study. The proposed controller adjusts the speed reference of the slave pump in order to achieve the required phase shift of 30 degrees for two pumps, while several different combinations are possible for three interconnected pumps in order to achieve the minimum pressure pulsation magnitude.

References

[1]   Pavković, D., Šprljan, P., Cipek, M., Krznar, M.(2021). Cross-axis control system design for borehole drilling based on damping optimum criterion and utilization of proportional-integral controllers. *Optimization and Engineering*, 22, pp 51–81. doi:10.1007/s11081-020-09566-z

[2]   Pavković, D. Current Trends in Oil Drilling Systems R&D with Emphasis on Croatian Oil Drilling Sector – A Review, *Proceedings of the 9th International Conference on Management of Technology – Step to Sustainable Production* (MOTSP 2017), Dubrovnik, Croatia, 2017.

[3]   Guo, B., Lui, G., (2011). Chapter One - Equipment in Mud Circulating Systems, Applied *Drilling Circulation Systems - Hydraulics, Calculations and Models,* pp 3-18. doi:10.1016/B978-0-12-381957-4.00001-2

[4]   National Oilwell Varco: Mud Pumps - 14-P-220 Triplex Pumps, Technical Marketing Sheet, 2016.

[5]   Karassik, I.J., Messina, J.P., Cooper, P., Heald, C.C.(2008). *Pump Handbook*, 4th ed., The McGraw-Hill Companies, Inc.

[6]   Lewis, E.E., Stern, H. (1962). *Design of Hydraulic Control Systems*, The McGraw-Hill Companies, Inc.

[7]   Wilson, D.R., Campbell, M.E., Breed, L.W., Hass, H.S., Galate, J. (1971). *Engineering Design Handbook, Hydraulic Fluids*, Headquarters, U.S. Army Materiel Command.

[8]   Helduser, S. (1998). *Hydraulik und Pneumatik Übungsaufgaben*, Technische Universität Dresden.

[9]   Collier, S.L. (1983). *Mud Pump Handbook*, Gulf Publising Company, Huston.

[10]   Nigus, H. (2015). Kinematics and Load Formulation of Engine Crank Mechanism. *MMSE Journal – Mechanics, Materials Science & Engineering*, ISSN 2412-5954.

[11]   Leonhard, W. (1987). *Control of Electrical Drives*, 1st ed., Springer-Verlag, Berlin.

[12]   Schröder, D. (2007). *ElektrischeAntriebe - Regelung von Antriebssystemen*, 3rd ed., Springer-Verlag, Berlin.

Simulation Analysis of Influential Parameters Effecting the Hydraulic Press Behaviour

Marko Šimic, Denis Janković, Klemen Matoša, Niko Herakovič

University of Ljubljana, Faculty of Mechanical Engineering, Ljubljana, Slovenia,
marko.simic@fs.uni-lj.si, denis.jankovic@fs.uni-lj.si, klemen.matosa@yahoo.com,
niko.herakovic@fs.uni-lj.si

The most common purpose of hydraulic press is to withdraw the desired movement and to generate the force to overcome the movement restrictions. The dilemma is whether changes in component characteristics affect the hydraulic press's behaviour without exception. For this reason, this study investigates how alteration in influencing parameters affect the hydraulic press behaviour. Furthermore, the study considers change in characteristic parameters, such as: valve response time, proportional and integral control parameters, degree of control edge overlap or spool wear in hydraulic valve, extend of the dead volume in cylinder chambers, system pressure and friction characteristics in frame guides. Using a simulation modelling approach, an effective method is proposed to investigate the source of the change and its effect on the discrete hydraulic component. By monitoring the behaviour of the hydraulic press using virtual sensors, the most reflective behaviour of each hydraulic component is described using simulation analysis.

1 Intruduction

The hydraulic presses are widely used for numerous industrial as well as experimental and testing applications. Knowing the hydraulic system behaviour under different circumstances it is crucial to achieve optimal performance of the system. Thus, performing the real-time data analysis and control actions is needed. On the other hand, more and more digital models are used to perform the simulation and optimization of the real systems and processes. Moreover, the measured characteristics in simulation model are performed by the virtual sensors, that are required to develop a digital twins of hydraulic systems (DTHS). Such digital models represent the quasi-replicas of the real systems with the same functionality and behaviour and allows us to perform different working scenarios in advance or in parallel to the real processes. In this way a change in the components characteristics and their effects on the hydraulic system behaviour can be analysed more efficiently.

There are several authors investigating the influence of various causes on hydraulic system behaviour. The authors in [1] proposed acoustic signal-based fault detection of hydraulic piston pump. Researchers in [2] presented hydraulic control valve wear consequently affecting the hydraulic valve response time dynamics. Also, the trend of modern studies concentrates on fault recognition of the systems and leakage occurrence as presented in [3] and [4]. Additionally, researchers expose the importance of considering the nonlinearities in the simulation model resulting from friction dynamics [5], [6], hydraulic oil characteristics [7], hydraulic valve flow and pressure dynamics [8].

Therefore, the paper represents a thorough analysis of the chosen influential parameters of hydraulic components, which can affect the system behaviour. The focus of the investigation is to perform what-if scenarios by using the simulation approach, which allows us to validate and confirm the influential parameters and their minor or major effects on hydraulic system behaviour.

2 The concept of hydraulic system

The concept of servo hydraulic press is proposed as the base for modelling the system (Figure 1). The detail description of the system is presented in previous study [9], the components and their parameters are presented in [10] while the component

parameters of the model are highlighted in section 3. The main components of the hydraulic press are: 1) hydraulic power unit; 2) servo valve MOOG D765; 3) Hanchen servo cylinder (series 320); 4) press frame (Kern Tool Technology, 1113 ISO 3-plate tooling frame); 5) PC and HMI (NI LabVIEW); 6) Moog P-I servo amplifier, G122-829A; 7) position transducer (Messotron Henning GmbH, type: DLH300); 8) pressure sensors (Turck, PT400R).
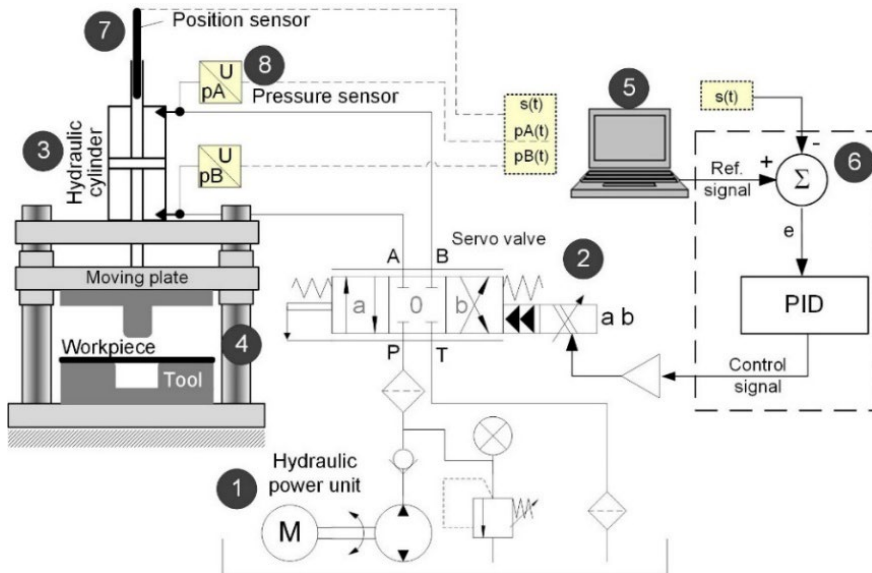
Figure 1: The concept of hydraulic press.
Source: own.

3   Modelling and simulation of hydraulic system

3.1   Modelling of hydraulic system

For the given concept of a hydraulic system (Figure 1), a development of the simulation model is carried out by using the simulation tool DSH^{plus} (Figure 2) representing the quasi-replica of the real hydraulic system [11].

The simulation model structure contains hydraulic, control and mechanical components in order to achieve the same functionality as the real hydraulic system. Hydraulic power unit is simplified involving only the hydraulic pump (01) and

pressure relief valve (02) to achieve proper flow rate and working pressure. Servo valve 4/3 PT1 (03) is used to simulate first order system behaviour in opening and closing regime. Double-rod, double-acting hydraulic cylinder is used (04) with output signal activated to monitor the cylinder velocity (v04) and cylinder stroke (s04) used in closed-loop position control. Mechanical system with spring-damper component (05) and moving mass (06) is added to simulate the stiffness of hydraulic press frame and the mass inertia of the moving parts. Function generator (07) is used to set the position reference (s07). Proportional amplifier (13) is used to convert the reference stroke (s07) from millimetres to reference stroke (s13) as electrical value in Volts. The SUM component (08) and the PI module (09) are used as real Moog P-I servo amplifier G122-829A. The signal limiter (10) is used since Moog servo vale has integrated control electronic that limit the control signal to maximum and minimum signal ±10 V. *P* transfer function module (11) is used to convert and amplify cylinder stroke (s04) in millimetres to output voltage signal (s11) in Volts according to the characteristics of real position transducer amplifier. The detail characteristics of simulation components used from DSH^{plus} library, are presented in Table 1. To generate an external force (s12, system disturbance) the function generator (12) has been added to the model if required in future investigation.
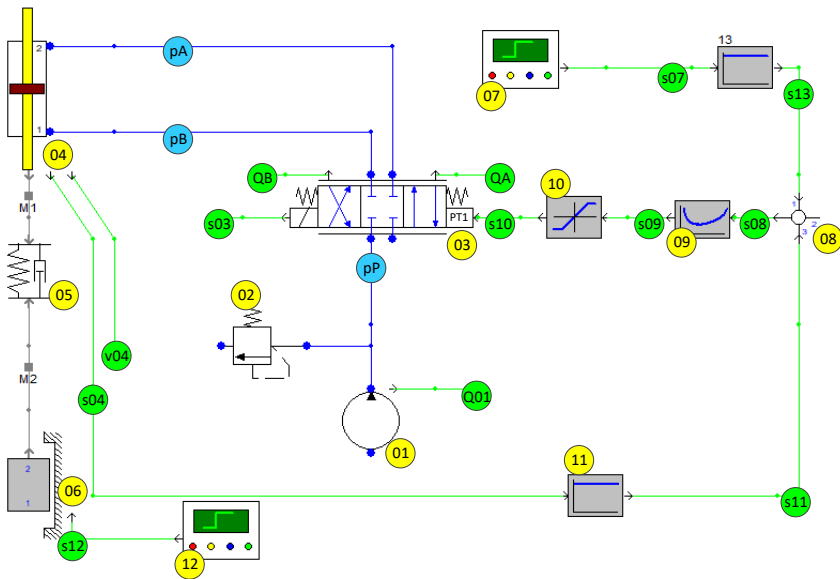

Figure 2: Simulation model of hydraulic closed-loop position control system.
Source: own.

Table 1: Simulation parameters of hydraulic system.

Component	Simulation component and parameters
01–Hydraulic pump	Flow rate: Q= 44 l/min
02–Pressure relief valve	Opening pressure, working pressure: p=100, 150, 200, 250 bar; nominal size: Q=60 l/min (Δp=5 bar).
03–Hydraulic servo valve Moog D765	Type: servo valve 4/3 PT1; nominal size: Q=38 l/min (Δp=70 bar); spool overlap: 1-3%; response time: t=10 ms (100%); input control signal: U=± 10 V; spool stroke: ± 100%; monitoring the spool position s03 and flow rate QA and QB.
04–Hydraulic cylinder, Hanchen, series 320	Type: double-acting, double rod; dimensions: 45/30/200 (piston/rod/stroke); mass of movable parts: m=1 kg; orientation, vertical: 90°; static friction: Ftr_s=10 N; mixed friction: Ftr_m=1 N; dynamic friction: Ftr_d=0,1 m/s; damping: d=10 Ns/mm.
05, 06–mass-spring-damper, to simulate the hydraulic press frame, Kern Tool Technology	Spring stiffness: 287 kN/mm; damping: 1 kNs/m; moving mass: m_1=50 kg, m_2=100 kg (m_3=300 kg); static friction: Ftr_s=20 N; mixed friction: Ftr_m=1 N; dynamic friction: Ftr_d=0,1 m/s; damping: 10 Ns/mm; orientation, vertical: 90°.
07–Function generator	Generation of press cycle, reference position $s(t)$.
08–Sum point	Comparator, factor 1: 1; factor 2: 1; factor 3: -1
09 - PI controller	KP: 1...1000 (P_2=10 set as initial value) KI: 0 (initial setting, analysed during the simulation)
10–Signal limiter	Maximal signal: 10 V; minimal signal: -10 V.
11–Position transducer	Amplifier: proportional gain Kp: 0,05 V/mm.
12–External force generator	Not considered in the analysis, simulation of forming force acting as axial force on hydraulic system.
13–Signal amplifier	Reference signal conversion [mm] - [V].
Hydraulic nodes	pP: 10 l, initial pressure 0 bar; pA: 0,1 l, initial pressure 0 bar; pB: 0,1 l, initial pressure 0 bar.

3.2 Simulation scenarios

The simulation involves detailed analysis of main influencing parameter, which can affect the hydraulic system behaviour (the system response). The influential parameters are:

I. **Servo valve response time (t):** Several time constants are analysed to cover different hydraulic valves: t_1= 5 ms, t_2 = 10 ms and t_3= 20 ms.

II. **P (proportional gain) and I (integral gain):** P_1=5, P_2=10, P_3=15 and P_4=20 are considered for analysis.

III. **Valve spool overlap (z):** Three sizes of the positive valve overlap are considered: z_1=0% (servo valves), z_2=+3% (high-response direct drive servo valves), z_3=+15% (proportional valves).

IV. **Control volumes – nodes pA in pB:** Cylinder chambers, internal channels of the mounting plate or the pipes connected between control valve and the cylinder. The smallest volume $pA_1=pB_1=0.01$ l is considered to simulate the servo valve and mounting plate in the cylinder; $pA_2=pB_2=0.1$ l and $pA_3=pB_3=1$ l volume is chosen to simulate the control valve - cylinder connection via pipes (different diameters and lengths).

V. **Working pressure (pP):** For the analysis, we considered: $pP_1=100$ bar, $pP_2=150$ bar, $pP_3=200$ bar and $pP_4=250$ bar.

VI. **Mass of the moving parts (m):** Proposed scenarios: $m_1=50$ kg (no tooling), and $m_2=100$ kg (with possible tooling).

VII. **Change in friction – guiding system:** The damage of the guiding elements results in friction change (static friction, mixed friction, dynamic friction). Several static and mixed frictions are analysed: $F_1=10$ N, $F_2=100$ N and $F_3=1000$ N.

a)   System step response.

b)   Control signal *s10* and valve opening *s03*.

c)   Flow rate *QA* and *QB*.

d)   Pressure response *pA* and *pB*.
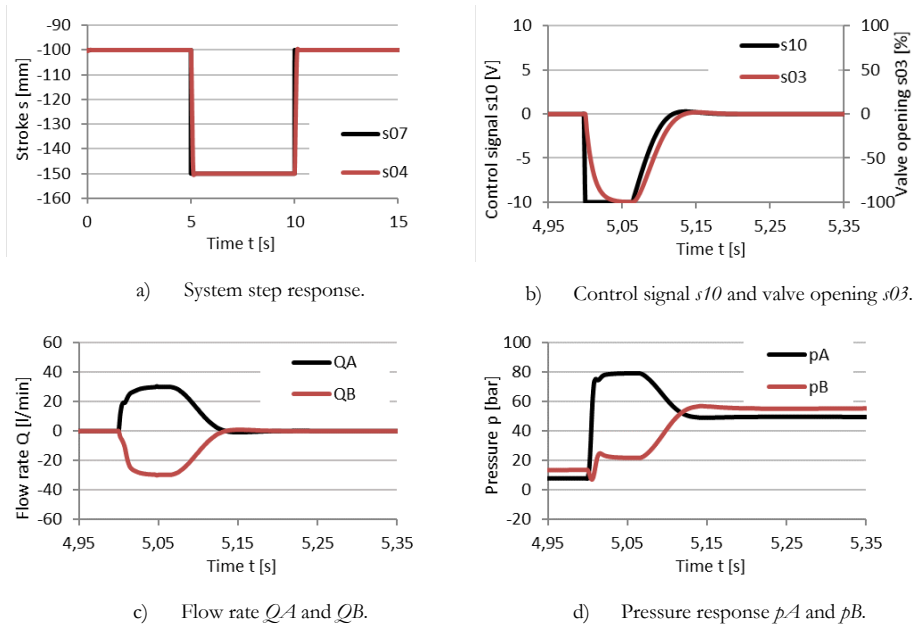
Figure 3: Analysis of hydraulic system behaviour.
Source: own.

In the analysis, we consider the reference step signal, $s_0=-100$ mm (initial cylinder position) and $s_1=-150$ mm (end position). The analysis is focused on system response (Figure 3a) where *s07* represents the reference cylinder position (step position signal)

and *s04* the cylinder position (simulation). For a better understanding, additionally the valve response presented in Figure 3b (s10 – valve control signal and *s03* – valve opening), the valve flow rates *QA* and *QB* (Figure 3c) and the pressure responses *pA* and *pB* (Figure 3d) are analysed.

4   Results and discussion

The results presented in this section show how the change of different parameters of hydraulic components influence the hydraulic system behaviour.

4.1   Influence of servo valve response time

The results show better step response of the system while using high response valve. Response time t_1=5 ms results in stable system response without overshoot, while response time t_3 =20 ms results in overshoot of the system (*O*=3,6 mm) and the settling time t_{stl}=0,17 s.

a)   System step response.

b)   Control signal *s10* and valve opening *s03*.

c)   Flow rate *QA* and *QB*.

d)   Pressure response *pA* and *pB*.
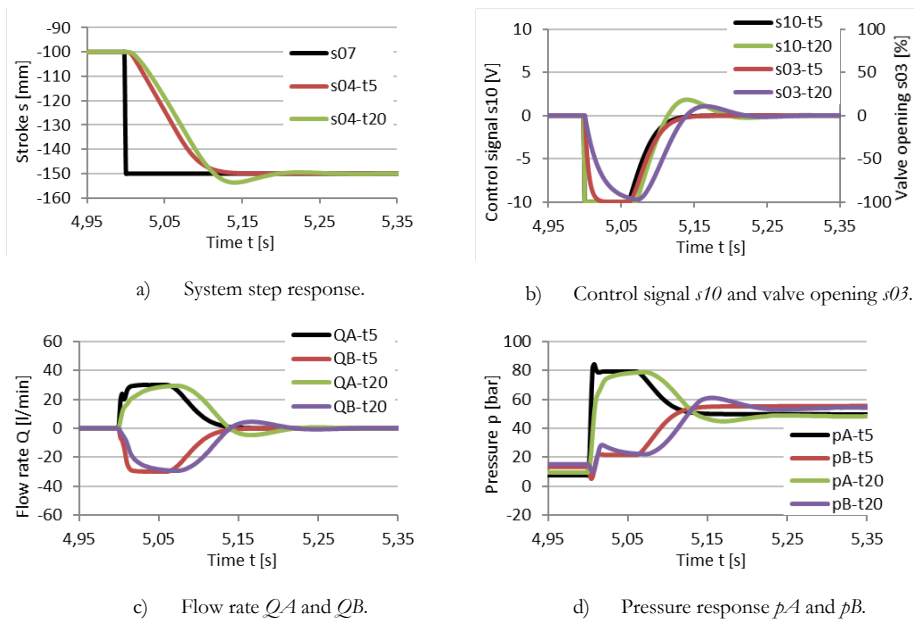
Figure 4: Influence of servo valve response time on system behaviour.
Source: own.

Low dynamic characteristic of the system is the results of low dynamic behaviour of the valve (Figure 4b) and consequently the low dynamics of the flow and pressure characteristics (Figure 4c, Figure 4d). The stable condition without overshoot of the system can be achieved with smaller P (approximately $P=4$).

4.2   Influence of P (proportional gain) and I (integral gain)

Figure 5a shows the response of the system at $P_1=5$ (red curve) and $P_4=20$ (green curve). It can be concluded that a small P results in a poor system response, while a high P results in a fast system response with small overshoot.

a)   System step response.

b)   Control signal *s10* and valve opening *s03*.

c)   Flow rate QA and QB.

d)   Pressure response pA and pB.
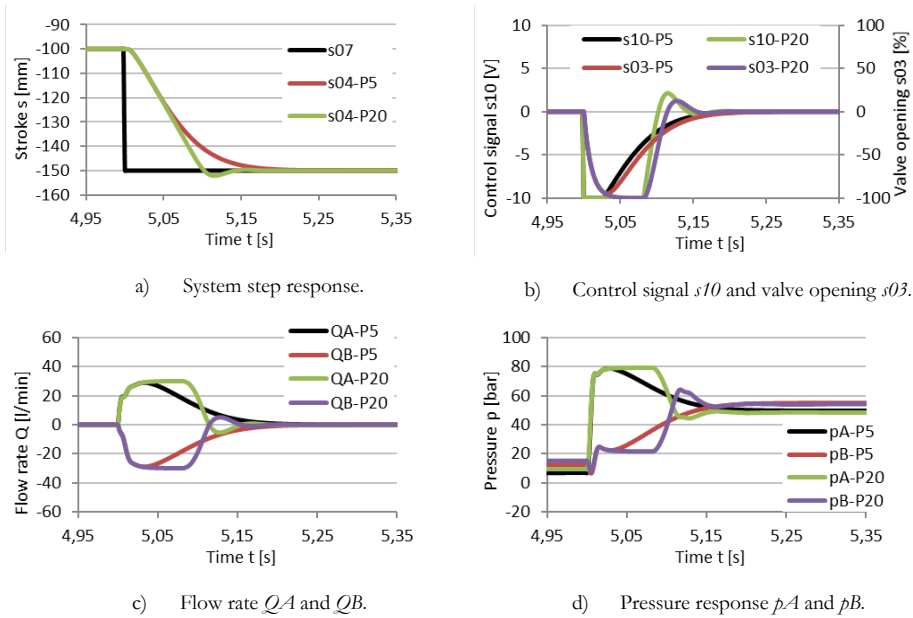
Figure 5: Influence of control parameters P and I on system behaviour.
Source: own.

We can also conclude that we need to find the proper P in order to achieve fast and stable response. By using the valve with time constant $t_2=10$ ms, the optimal $P=8$. While using the valve with time constant $t_1=5$ ms, the optimal $P=17$ resulting in higher response of the system (settling time is reduced by 0,03 s), no overshoot recognized (Figure 6).
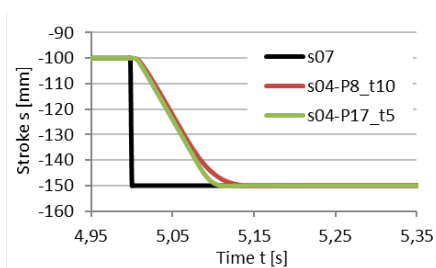
Figure 6: Response of the system at *t*=5 ms, *P*=17 and *t*=10 ms, *P*=8.
Source: own.

The simulation results indicate that *I* gain does not significantly affect the steady-state error (*Δs*). Moreover, the added *I* deteriorates the stability of the system. For the gain *I*=0, the *Δs* at cylinder position *s*=-150 mm is *Δs*=0.003 mm. If the *I* is increased *I*>0.1, the *Δs* is equal to *Δs*>0.01 mm. Based on this, it is recommended to use only the *P* control for the given hydraulic system.

4.3   Influence of valve spool overlap (z)

The increase in the positive valve overlap has a bad effect on the responsiveness of the hydraulic system and at the same time affects the steady-state error. Figure 7a shows a comparison of the system response between a valve overlap 0% (red curve) and +15% (green curve). The steady-state error with a positive overlap of the valve (+15%) is up to 2 mm (*s*=148 mm in Figure 7a). In Figure 7b it is clearly seen that the positive overlapped valve remains open in the overlapped dead zone resulting no flow across the valve and stops the movement of the hydraulic cylinder.

a)   System step response.

b)   Control signal *s10* and valve opening *s03*.
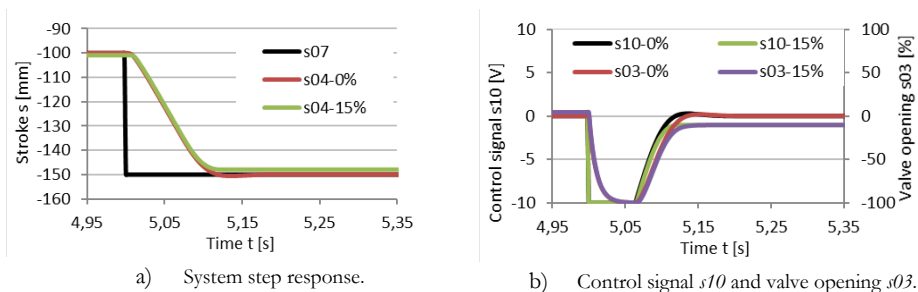
Figure 7: Influence of spool overlap on system behaviour.
Source: own.

All this is also the result of the size of the proportional gain P and the small position error calculated in closed-loop control, which results in a very small valve control signal and small opening of the valve (within the size of valve overlap). The problem of steady-state error can be improved by increasing the proportional gain from $P=10$ to $P=17$.

4.4   Influence of control volumes – nodes pA and pB

The results show that by increasing the volume of pA and pB, the hydraulic stiffness of the system decrease. As a result, the system response is decreased and the higher overshoot appears (Figure 8a). The main cause represents the pressure response (Figure 8d), which is the result of valve behaviour (Figure 8b) and the flow rate (Figure 8c).

a)   System step response.

b)   Control signal $s10$ and valve opening $s03$.

c)   Flow rate QA and QB.

d)   Pressure response pA and pB.

Figure 8: Influence of control volumes on system behaviour.
Source: own.

4.5   Influence of working pressure (pP)

Two working pressures (pP) are taken into consideration, $pP_{min}=100$ bar and $pP_{max}=250$ bar. The increase in pP influence on increase of hydraulic stiffness of the system and therefore on change in pressure distribution at pA and pB (Figure 9d)

and better response of the system (Figure 9a). Change in pressure pP also effects on the flow rate QA and QB (Figure 9c) and thus h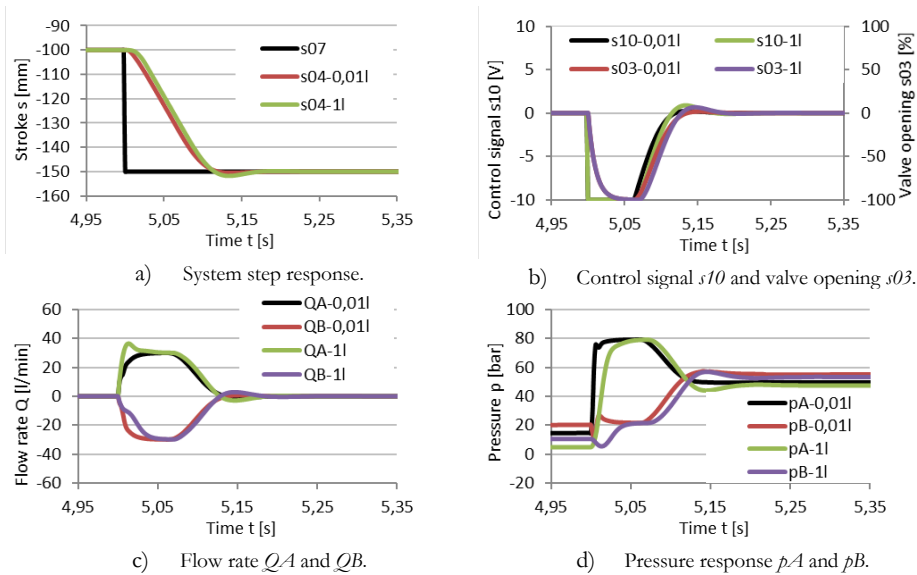ydraulic cylinder velocity, consequently the hydraulic system overshoot. Overshoot of the system can be improved by using higher response valves ($t=5$ ms) or reducing the P gain ($P=5$) while response of the valve remains the same ($t=10$ ms).

a)   System step response.

b)   Control signal $s10$ and valve opening $s03$.

c)   Flow rate QA and QB.

d)   Pressure response pA and pB.
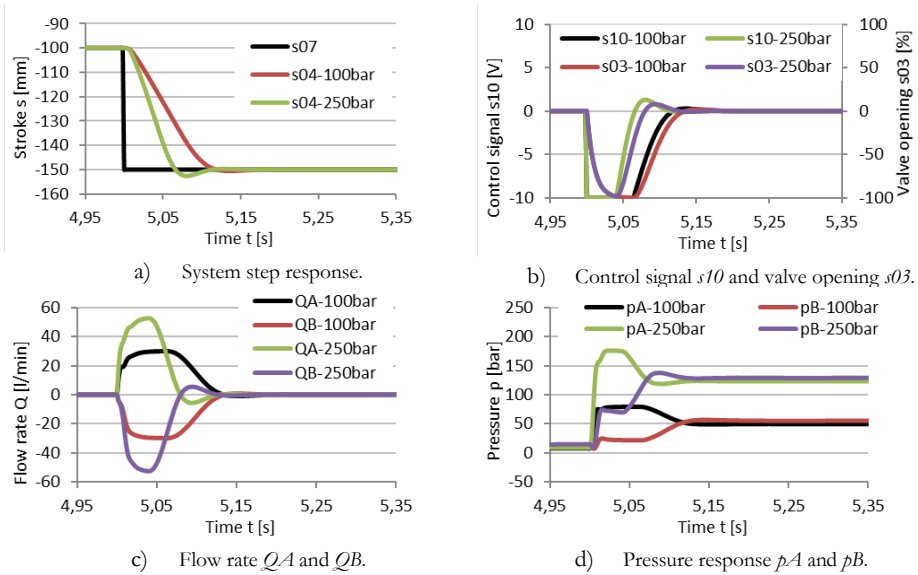
Figure 9: Influence of working pressure on system behaviour.
Source: own.

4.6   Influence of moving mass (m)

Preliminary simulation shows that increasing the mass from $m=50$ kg to $m=100$ kg does not significantly affect the behaviour of the system. The change in system behaviour is seen when the mass exceeds 200 kg (Figure 10a). One example is given by Figure 10, where mass of 300 kg is used and compared with initial system ($m=50$ kg). The main effect can be seen in settle time and system overshoot. The unstable system response can be corrected by changing the working pressure from $pP=100$ bar to at least $pP=200$ bar and a reduction of the P gain from $P=10$ to $P=5$ for the chosen response time $t=10$ ms.

a) System step response.

b) Control signal *s10* and valve opening *s03*.

c) Flow rate *QA* and *QB*.

d) Pressure response *pA* and *pB*.
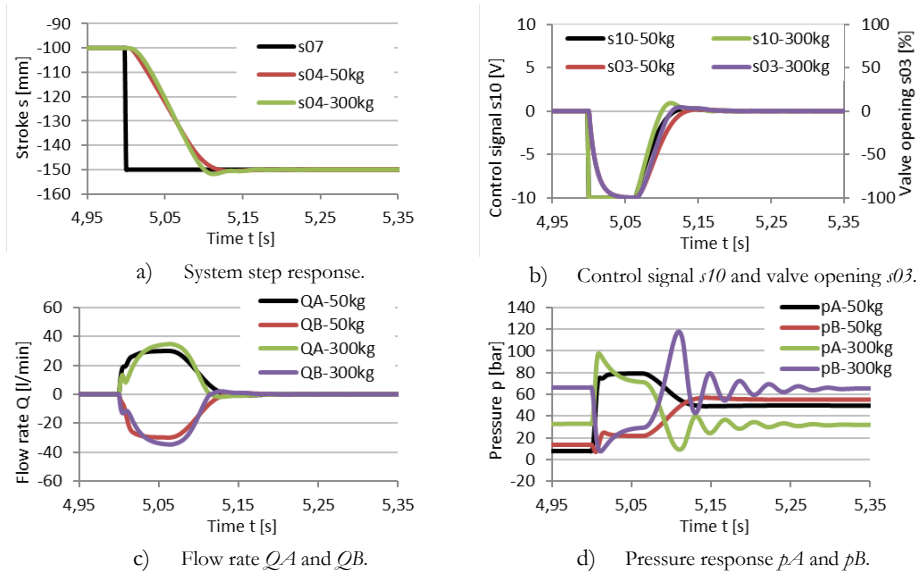
Figure 10: Influence of moving mass (m=300 kg) on system behaviour.
Source: own.

4.7   Influence of change in friction – guiding system

The results from Figure 11 show a small influence of the friction force on change of system behaviour. Nevertheless, higher friction force (*Ftr*=1000 N) leads to lower velocity of hydraulic cylinder (Δv<0,01 mm/s) and small overshoot (Δs<1 mm) of the system (Figure11a). The main difference appears in pressure distribution (Figure 11d) where the pressure difference (*pP-pA* and *pB-pT*) is increased to overcome the additional friction of the system.

a) System step response.

b) Control signal *s10* and valve opening *s03*.

c)   Flow rate *QA* and *QB*.   d)   Pressure response *pA* and *pB*.
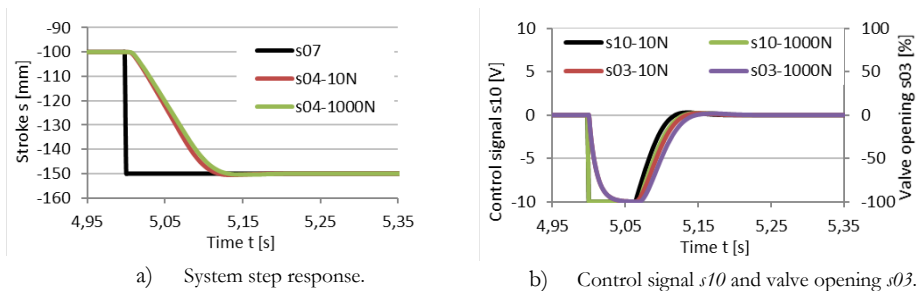
Figure 11: Influence of change in friction on system behaviour.
Source: own.

5   Conclusions

The paper presents a simulation approach to characterise and recognize the most influential parameters of proposed hydraulic system that effects the hydraulic system behaviour. The main contribution of this research is the modelling of the hydraulic system, characterization of the influential parameters for hydraulic system, in depth monitoring and analysis of measured variables, simulation scenarios presentation and simulation analysis performance evaluation with discussion.

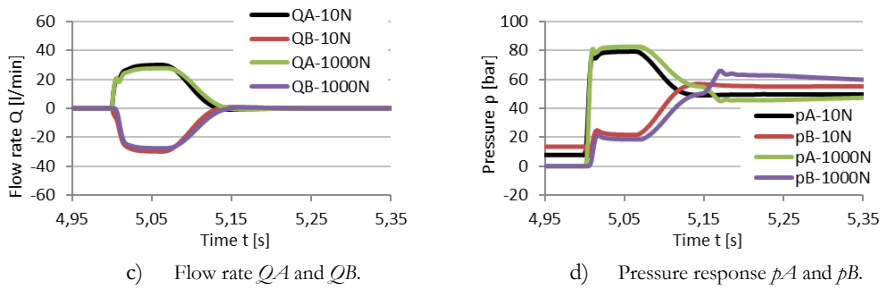–   The results of this study show that the control valve response time has major influence on system behaviour such as system response, size of system overshoot and settling time. The higher the response of valve is the better the system response is achieved, which is logical. In this context we have to take into consideration the proper control parameters, i.e. the proportional gain, to achieve stable condition.

–   The valve spool overlap has minor influence on system response, which can be improved by using larger proportional gain of control unit.

–   The control volume or the dead volume has impact on hydraulic stiffness of the system. The small volume results in higher stiffness of the system and therefore on better system response. The same can be said for the higher working pressure of the hydraulic system. As noted in theory the pressure above 200 bar is recommended to eliminate the effect of hydraulic stiffness.

- The moving mass increase slightly effects on system overshoot and settle time increase. It depends on working pressure, the response of the control valve and control parameters set-up.

- The increase of friction in the guiding elements has minor effect on system behaviour. The major concern is the increase in pressure and thus increase in hydraulic power needed for the given press cycle.

- In our opinion the most influential parameters are the control valve response in combination with the control parameters and working pressure. For these parameters the proper values should be set to achieve fast and stable response of hydraulic system.

Acknowledgments

References

[1]   Y. Zhu, G. Li, S. Tang, R. Wang, H. Su, C. Wang, Acoustic signal-based fault detection of hydraulic piston pump using a particle swarm optimization enhancement CNN, Appl. Acoust. 192 (2022) 108718, https://doi.org/10.1016/j.apacoust.2022.108718.

[2]   X. Liu, H. Ji, W. Min, Z. Zheng, J. Wang, Erosion behavior and influence of solid particles in hydraulic spool valve without notches, Eng. Fail. Anal. 108 (2020) 104262, https://doi.org/10.1016/j.engfailanal.2019.104262.

[3]   X. Ji, Y. Ren, H. Tang, J. Xiang, DSmT-based three-layer method using multiclassifier to detect faults in hydraulic systems, Mech. Syst. Signal Process. 153 (2021), 107513, https://doi.org/10.1016/j.ymssp.2020.107513.

[4]   Y. Guo, Y. Zeng, L. Fu, X. Chen, Modeling and experimental study for online measurement of hydraulic cylinder micro leakage based on convolutional neural network, Sensors 19 (9) (2019) 2159, https://doi.org/10.3390/s19092159.

[5]   Q. Pan, Y. Zeng, Y. Li, X. Jiang, M. Huang, Experimental investigation of friction behaviours for double-acting hydraulic actuators with different reciprocating seals, Tribol. Int. 153 (2021) 106506, https://doi.org/10.1016/j.triboint.2020.106506.

[6]   [4] J.F. Pedersen, R. Schlanbusch, T.J.J. Meyer, L.W. Caspers, V. V. Shanbhag, Acoustic emission-based condition monitoring and remaining useful life prediction of hydraulic cylinder rod seals, Sensors. 21 (18) (2021) 6012, https://doi.org/10.3390/s21186012.

[7]   D. Pochi, R. Grilli, L. Fornaciari, M. Betto, S. Benigni, R. Fanigliulo, Bench testing of sensors utilized for in-line monitoring of lubricants and hydraulic fluids properties, Sensors 21 (24) (2021) 8201, https://doi.org/10.3390/s21248201.

[8]   R. Zhou, L. Meng, X. Yuan, Z. Qiao, Research and experimental analysis of hydraulic cylinder position control mechanism based on pressure detection, Machines 10 (1) (2022), https://doi.org/10.3390/machines10010001.

[9]   Denis Janković, Rok Novak, Marko Šimic & Niko Herakovič, The concept of automatic generation of hydraulic press cycle, page 285, Conference Proceedings, International Conference Fluid Power 2021, DOI https://doi.org/10.18690/978-961-286-513-9.24.

[10]   MATOŠA, Klemen, 2021, Snovanje visoko-dinamične hidravlične testne naprave [na spletu]. Magistrsko delo. Ljubljana : Univerza v Ljubljani. [Dostopano 3 avgust 2023]. Available at: https://repozitorij.uni-lj.si/IzpisGradiva.php?lang=slv&id=129527.

[11]   FLUIDON GmbH, DSH^{plus}, Modelling and simulation of hydraulic and pneumatic systems and components, available at: https://www.fluidon.com/.

Gear Pump Hydraulic Testing and Simulation

Nejc Novak, Ana Trajkovski, Jan Bartolj,
Jan Pustavrh, Franc Majdič

University of Ljubljana, Faculty of Mechanical Engineering, Ljubljana, Slovenia,
nejc.novak@fs.uni-lj.si, ana.trajkovski@fs.uni-lj.si, jan.bartolj@fs.uni-lj.si,
jan.pustavrh@fs.uni-lj.si, franc.majdic@fs.uni-lj.si

Hydraulic systems are increasingly present in all segments of our production chains such as agriculture, construction, transportation and other industrial areas. The key component of every hydraulic system are pumps. With newly developed gear pump testing rig, long-term tests of five gear pumps simultaneously are being tested. One pump is tested with medium test dust, one is tested with real wear particles extracted from a filter and the last three are simulating a real hydraulic system with cleanliness of 20/19/17 according to standard ISO 4406. In addition, simulation in program Automation Studio of durability test of gear pump is presented at different pressure operating points. Findings of this research contribute to sustainable development of hydraulic gear pumps and improving efficiency of whole hydraulic systems.

1   Intruduction

The service life of a hydraulic system is the duration throughout which the system is used economically and efficiently and is able to maintain desired temperatures, pressures, and flow rates. There are numerous parameters that affect efficiency. Among the most important are the hydraulic oil, the temperature and the cleanliness of the oil. One of the most important parameters for oil life is the amount of contaminants in the oil, as well as the influence of pressure, oxidation, pressure, radiation shear, and other oil additives that can trigger a chemical reaction [1–4]. More than 70 % of breakdowns in industry workflow are caused by contaminants in hydraulic fluid, with 60 to 70 % of all breakdowns due to solid particles [5]. For implementing condition-based maintenance of hydraulic components and consequently whole systems the cleanliness of oil is of utmost importance [6–8].

Within the hydraulic system there are a number of particles — some created by wear and tear, others that have entered as contaminants from the surroundings or have existed since the system's inception. The dimensions and composition of these particles exert substantial influence on system performance, particularly when the gaps between moving surfaces closely match the particle size [9]. Particles between contact surfaces and near surfaces promotes wear [10]. Most common wear mechanisms are three body abrasion [11] and erosion [12].

ISO 12103-1 is standard for Arizona test dust that is used for testing filters because it has repeatable distribution of particle size and number [13]. There are four types: A1 ultrafine, A2 fine, A3 Medium and A4 coarse. Medium test dust (MTD) is commonly used for accelerating testing of hydraulic equipment. Test dust is more abrasive than common contaminants found in the hydraulic systems which promote wear of hydraulic components [14]. Volumetric efficiency depends on the decrease of initial flow rate of the pump, usually due to wear of the sealing surfaces of elements in components [15]. Wang et. al [16] predicted the remaining useful life (RUL) of a hydraulic gear pump using an accelerated test of the useful life of a gear pump. This method effectively improved the operating efficiency of the hydraulic system and reduced the frequency of failures Gear pumps were previously studied by Ranganathan et al. [17] and Frith [18] using test dust. It was found that the most influential factors for flow rate degradation were chemical composition, hardness, size distribution, and number of particles that caused wear of critical sealing

elements. There are numerous simulations of gear pump flow rates done by Rundo [19], Casoli [20], Malsavi [21] and others points to the utility of such tools.

The particles inevitably damage every component in the hydraulic system and cause wear. This wear on the sealing surfaces manifests itself in the form of visible leakage, which leads to a reduction in the volumetric efficiency of the system. A review of the literature indicates that particles commonly present in a hydraulic system are less harmful to the system than test dust. There is some evidence that test dust can efficiently accelerate wear to reduce the time required for long-term testing of hydraulic components. However, to determine the acceleration time, parameters such as particle concentration (oil cleanliness), temperature, pressure and others should be considered. In addition, there is no direct correlation in the literature between the effects of wear particles and test dust on hydraulic component wear. Three durability tests were conducted on hydraulic gear pumps in the laboratory: one without additional contaminants, one with wear particles, and one with test dust. The study presents the design and the test rig itself, the simulation of the flow rates of the gear pumps, and the real measurements of the flow rates and the comparison of the volumetric efficiencies of the pumps.

2   Materials and methods

Three hydraulic test rigs were assembled in laboratory. We tested the effect of oil cleanliness in the hydraulic system on the durability of the system itself and compared the effect of wear particles and test dust (MTD) to normal operating hydraulic system without additional contaminants (without adding contaminants). Fig. 1 shows all test conical reservoirs of test rigs (on the left) and hydraulic valves used for the load of the gear pumps (on the right). Initially, 30 L of ISO VG 46 hydraulic oil was added in first unit that was tested without additional contaminants. Other two test rigs had both 13 L of oil in each unit, one was tested with wear particles and the other with test dust. The flow through the gear pump was measured with stopwatch and weighting of oil. Later the flow rate was determined due to the density of ISO VG 46, which is 0,8551 kg/L. Gear pumps have a displacement of 3,5 cm^3/rev. and a maximum pressure up to 290 bar. In the neutral position of the directional 4/3-way valve all ports are closed. The oil temperature of tank, that was used for testing the gear pump without additional contaminant was around 63$\pm$5 ° C. The thermostat was used to control the operation of the cooler set to 70 ° C.

Figure 1: Conical reservoirs (on the left) to prevent the contaminants to settle down and 4/3-way valves with pressure relief valves for the load of the gear pumps (on the right).
Source: own.

The pump (Fig. 2, pos. 1) draws oil from the conical reservoir (Fig. 2, pos. 12), designed as such due to the non-settling nature of particles. This oil is then pushed through the check valve (Fig. 2, pos. 3) into a manually operated 3/2 valve (Fig. 2, pos. 5). Subsequently, it passes through a solenoid-controlled directional valve (Fig. 2, pos. 4). Depending on the valve's position (parallel or diagonal), the oil flows through either working line A or B towards the pressure relief valves (Fig. 2, pos. 7), the cooler (Fig. 2, pos. 10), the priority valve (Fig. 2, pos. 11), and the filter (Fig. 2, pos. 8) back to the reservoir.

The priority valve can be adjusted to maintain a specific pressure differential. This feature allows the valve to either direct oil flow through the filter, ensuring higher cleanliness, or bypass the filter, leading to lower cleanliness levels. The testing process involves setting the system load pressure (the two pressure relief valves) to 220 bar. The hydraulic oil in all three test rigs was initially filtered to achieve cleanliness levels of 16/15/13 or less. Throughout the tests, the temperature was consistently monitored and maintained within the range of 63 ± 5 ° C.

Cleanliness is assessed by manually collecting oil samples, with control of the 3/2 valve at (Fig. 2, pos. 5), and through measurements at the pressure relief valve's measuring connection. Each cycle lasts for 0.5 seconds, during which the solenoid "a" is activated, positioning the spool in the 4/3 directional valve to achieve a parallel configuration. Following this, the solenoid "b" is engaged, returning the spool to its initial diagonal position.
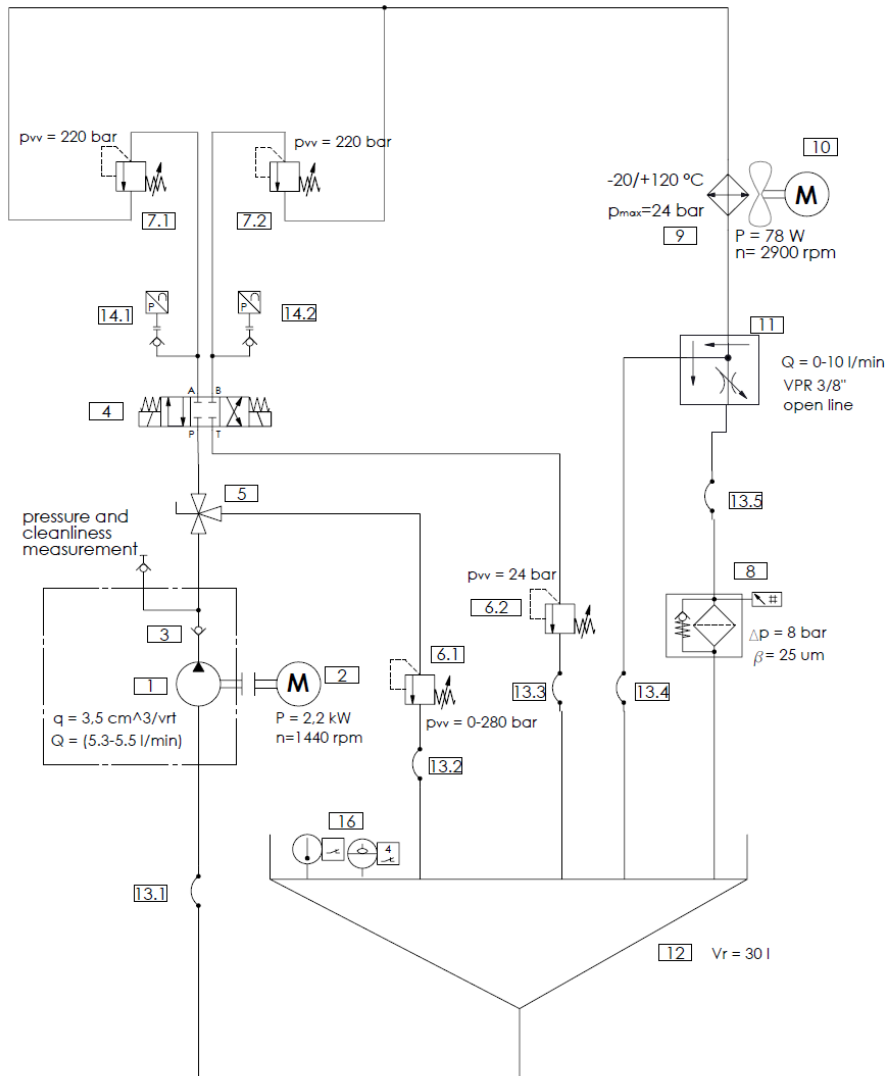
Figure 2: Hydraulic scheme of one test rig for gear pump tested with wear particles and test dust with conical reservoir.
Source: own.

Hydraulic simulation in Automation studio was performed for the gear pump without additional contaminants. The pump flow rate was stable throughout the test. Simulation was designed to simultaneously measure single gear pump at different pressure points (Fig. 3) where the volumetric efficiency curve was specifically defined for the case (Fig. 4).
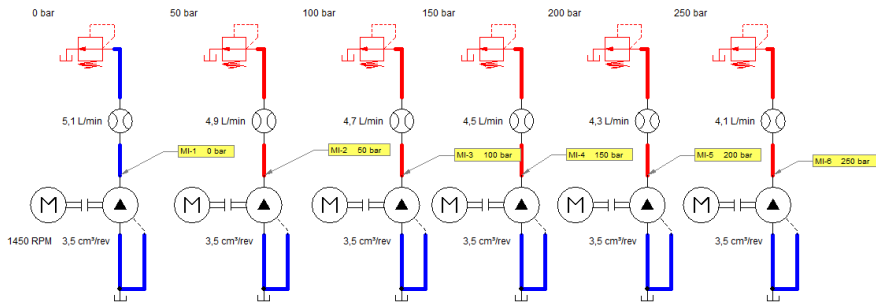
Figure 3: Hydraulic simulation of single gear pump at 5 different pressures (0 bar, 50 bar, 100 bar, 150 bar, 200 bar, 250 bar).
Source: own.
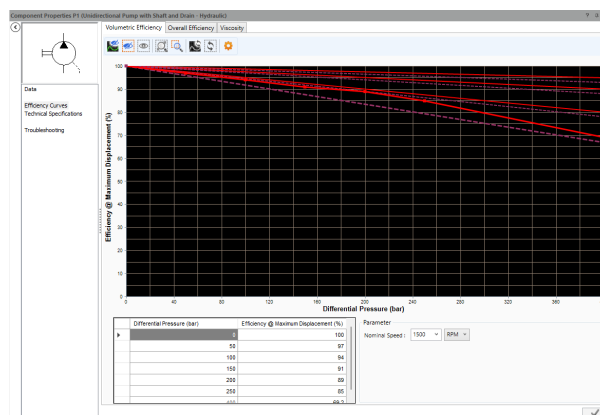
Figure 4: Specifically defined volumetric efficiency curve for simulating gear pump flow rates at different pressure points.
Source: own.

3 Results

Three different conditions of oil contamination were introduced in three separate hydraulic test rigs testing gear pumps with aluminium housings. First, the gear pump without any contamination was tested (Fig. 5). The highest measured flow rate was at a pressure of 0 bar, where the pump was not loaded, and averaged 5.28 L/min. At a pressure of 50 bar, the average flow rate was 5.13 L/min, at 100 bar it was 5.00 L/min, at 150 bar it was 4.85 L/min, at 200 bar it was 4.74 L/min, and at 250 bar the flow rate dropped to 4.75 L/min. The gear pump was tested for 576 hours and the volumetric efficiency did not decrease significantly.
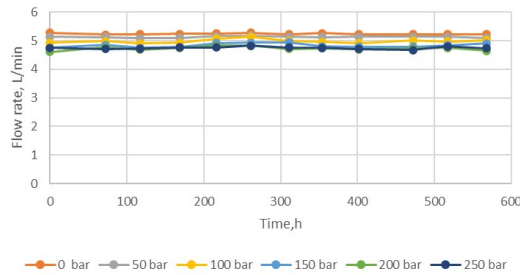
Figure 5: Flow rate of gear pump tested with without the addition of contaminant.
Source: own.

The gear pump tested with wear particles lasted only 19 hours (Fig. 6). At the beginning of the test, we added 8 g of wear particles to 13 L of hydraulic oil, so the concentration of wear particles and oil was 0.615 g/L. At the beginning of the test, the flow rates were similar to the gear pump tested without any additive. The gear pump tested with wear particles had a flow rate of 5.17 L/min at a pressure of 0 bar. At a pressure of 50 bar, the flow rate was 4.99 L/min, at 150 bar 4.81 L/min, at 200 bar 4.66 L/min and at 250 bar 4.57 L/min. After only 19 hours of testing, the flow rate dropped to 4.75 L/min at 0 bar, at 50 bar the flow rate was 2.67 L/min, at 100 bar the flow rate was 0.46 L/min, and at 150 bar and above the flow rate was 0 L/min (not measurable). The oil cleanliness during the test was 22/22/21.
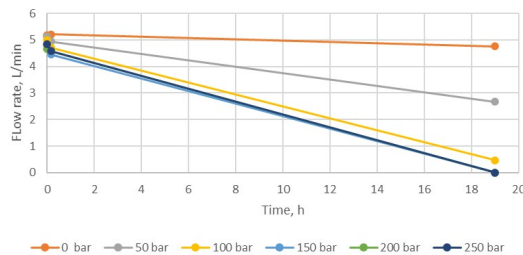
Figure 6: Flow rate of gear pump tested with wear particles with concentration of 0.615 g/L and oil cleanliness 22/22/21.
Source: own.

The gear pump tested with test dust was operated for 70 hours. At the beginning of the test, 0.208 g of test dust was added, resulting in a test dust and oil concentration of 0.016 g/L (Fig. 7). At the beginning of the test, the flow rate at 0 bar was 5.12 L/min. At a pressure of 50 bar, the flow rate was 5.03 L/min, at 100 bar 4.81 L/min, at 150 bar 4.77 L/min, at 200 bar 4.67 L/min and at 250 bar 4.71 L/min. The oil

cleanliness during the test was 21/20/18 and level of impurities in oil increased through time due to wear of components. At the end of the test cleanliness was 22/21/19.
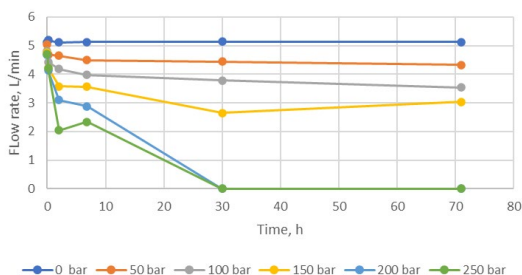
Figure 7: Flow rate of gear pump tested with test dust with concentration of 0,016 g/L and oil cleanliness 21/20/18.
Source: own.

The simulation of the flow rate of the gear pump lasted 5.33 s. The increase of the flow rate depends on the setting of the cracking pressure of the relief valve. Fig. 8 shows that the higher the cracking pressure of the valve, the more delayed is the stabilization of the flow rate and the faster is the transition. The flow rate at 0 bar pressure was 5.07 L/min. At 50 bar the flow rate was 4.88 L/min, at 100 bar 4.68 L/min, at 150 bar 4.48 L/min, at 200 bar 4.28 L/min and at 250 bar 4.09 L/min.
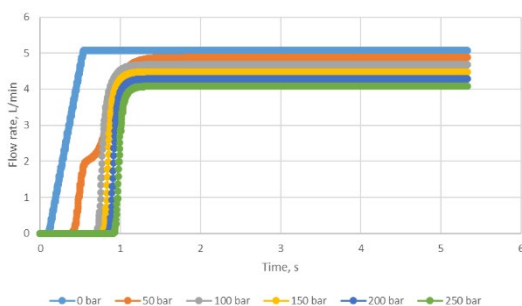
Figure 8: Flow rate simulation of gear pump without additional contaminant.
Source: own.

4   Discussion and conclusion

The difference between three long-term tests of gear pumps is obvious. The gear pump tested without any contamination had a high volumetric efficiency of 100 % at 0 bar, 97 % at 50 bar, 91 % at 100 bar, 89 % at 200 bar, and 85 % at 250 bar.

These efficiencies do not change significantly throughout the test, while the flow rates of the gear pumps tested with wear particles decrease tremendously. In 18 h of operation, the efficiency of the tested gear pump with wear particles drops from 100 % to 92 % at 0 bar, from 99 % to 51 % at 50 bar, from 96 % to 9 % at 100 bar, and from 90 % to zero at the other pressure measurement points (150 bar, 200 bar and 250 bar). In 30 h of operation of the gear pump tested with test dust, the efficiency at 0 bar unusually increased from 99.7 % to 100 % (the reason for this is uncertainty in the measurements), but then dropped from 97 % to 86 % at 50 bar, from 93 % to 73 % at 100 bar, and from 92 % to 51 % at 100 bar. The other efficiencies dropped from about 90 % to zero at both 200 bar and 250 bar.

It can be concluded that the more the gear pump is worn, the greater the differences between the efficiencies at higher pressure. The reason for these phenomena is the higher leakage between the worn sliding/sealing surfaces of the hydraulic elements. In this case, between the housing and the gears. The gear pump tested with wear particles failed after 18 hours and the gear pump tested with test dust failed after 30 hours. Due to the time period between the last measurements, we cannot determine the exact time of failure. When analysing the efficiencies at 100 bar (wear particles 8 %, test dust 73 %) and 150 bar (wear particles 0 %, test dust 51 %), some differences can be observed. It can be assumed that the gear pump tested with wear particles was more damaged (worn) than the gear pump tested with test dust.

Simulating the flow rate of the tested gear pump without additional contaminants shows reasonably comparable results. The simulated flow rates and efficiencies are lower than the real measurements. This is due to the fact that the temperature of the oil is constant at 25 °C. Therefore, the viscosity is higher than in the real environment and the flow rates are slightly lower. Simulating the efficiency curves of hydraulic gear pumps can greatly improve fault diagnosis in the hydraulic system and reduce costs by replacing the gear pump at the most critical time.

References

[1]   Tič V, Tašner T, Lovrec D. Enhanced lubricant management to reduce costs and minimise environmental impact. Energy 2014;77:108–16.
      https://doi.org/https://doi.org/10.1016/j.energy.2014.05.030.
[2]   Mang T, Dresel W. Lubricants and lubrication. John Wiley & Sons; 2007.
[3]   Tič V, Lovrec D. On-line condition monitoring and evaluation of remaining useful lifetimes for mineral hydraulic and turbine oils. 2017. https://doi.org/10.18690/978-961-286-130-8.
[4]   Lovrec D, Kambič M. Hidravlične tekočine in njihova nega. Fakulteta za strojništvo; 2007.

[5]   Zhang Y, Liu Y, Wang Z, Tao Y, Yang L, Li Y. Prediction of Oil Contamination in Aviation Hydraulic System and Active Leakage Strategy. 2022 IEEE 17th Conference on Industrial Electronics and Applications (ICIEA), 2022, p. 578–83. https://doi.org/10.1109/ICIEA54703.2022.10006227.

[6]   Ng F, Harding JA, Glass J. Improving hydraulic excavator performance through in line hydraulic oil contamination monitoring. Mech Syst Signal Process 2017;83:176–93. https://doi.org/https://doi.org/10.1016/j.ymssp.2016.06.006.

[7]   Jardine AKS, Lin D, Banjevic D. A review on machinery diagnostics and prognostics implementing condition-based maintenance. Mech Syst Signal Process 2006;20:1483–510. https://doi.org/https://doi.org/10.1016/j.ymssp.2005.09.012.

[8]   Zio E, Peloni G. Particle filtering prognostic estimation of the remaining useful life of nonlinear components. Reliab Eng Syst Saf 2011;96:403–9. https://doi.org/https://doi.org/10.1016/j.ress.2010.08.009.

[9]   Frith RH, Scott W. Control of solids contamination in hydraulic systems — an overview. Wear 1993;165:69–74. https://doi.org/https://doi.org/10.1016/0043-1648(93)90374-U.

[10]   Esteves PJ, Seriacopi V, de Macêdo MCS, Souza RM, Scandian C. Combined effect of abrasive particle size distribution and ball material on the wear coefficient in micro-scale abrasive wear tests. Wear 2021;476:203639. https://doi.org/https://doi.org/10.1016/j.wear.2021.203639.

[11]   Trezona RI, Allsopp DN, Hutchings IM. Transitions between two-body and three-body abrasive wear: influence of test conditions in the microscale abrasive wear test. Wear 1999;225–229:205–14. https://doi.org/https://doi.org/10.1016/S0043-1648(98)00358-5.

[12]   Osterland S, Müller L, Weber J, Moosavi A, Krahl D. Numerical Prediction and Experimental Investigation of Cavitation Erosion of Hydraulic Components Using HFC. n.d.

[13]   Fletcher RA, Bright DS. Shape Factors of ISO 12103-A3 (Medium Test Dust). Filtration + Separation 2000;37:48–56. https://doi.org/https://doi.org/10.1016/S0015-1882(00)80200-1.

[14]   Novak N, Trajkovski A, Polajnar M, Kalin M, Majdič F. Wear of hydraulic pump with real particles and medium test dust. Wear 2023;532–533:205101. https://doi.org/https://doi.org/10.1016/j.wear.2023.205101.

[15]   Zhang K, Yao J, Jiang T. Degradation assessment and life prediction of electro-hydraulic servo valve under erosion wear. Eng Fail Anal 2014;36:284–300. https://doi.org/https://doi.org/10.1016/j.engfailanal.2013.10.017.

[16]   Wang C, Jiang W, Yue Y, Zhang S. Research on Prediction Method of Gear Pump Remaining Useful Life Based on DCAE and Bi-LSTM. Symmetry (Basel) 2022;14. https://doi.org/10.3390/sym14061111.

[17]   Ranganathan G, Hillson Samuel Raj T, Mohan Ram P V. Wear characterisation of small PM rotors and oil pump bearings. Tribol Int 2004;37:1–9. https://doi.org/https://doi.org/10.1016/S0301-679X(03)00109-9.

[18]   Frith R. A model of gear pump wear due to solids contamination. PhD. Queensland University of Technology, 1994.

[19]   Rundo M. Models for Flow Rate Simulation in Gear Pumps: A Review. Energies (Basel) 2017;10. https://doi.org/10.3390/en10091261.

[20]   Casoli P, Scolari F, Rundo M, Lettini A, Rigosi M. CFD Analyses of Textured Surfaces for Tribological Improvements in Hydraulic Pumps. Energies (Basel) 2020;13. https://doi.org/10.3390/en13215799.

[21]   Malvasi A, Squarcini R, Armenio G, Brömmel A. Design Process of an Electric Powered Oil Pump. Auto Tech Review 2014;3:36–9. https://doi.org/10.1365/s40112-014-0571-4.

EOL Valve Test Bench Automatization

Peter Oblak

Poclain Hydraulics d.o.o., Žiri, Slovenia
peter.oblak@poclain.com

The paper shows the process and examples of transition from manual to automatic testing mode on the test bench which was originally designed for manual testing. Test bench was designed for testing smaller batches of products. It is described what had been changed on the hydraulic circuit, electrical scheme and software side. In the first step hydraulic and necessary electrical modifications were made. When first part of modification was done, the software with automatic tests was updated. Third step was to setup communication between controller and server to synchronize test reports and test procedures, data logs, backups, oil cleanliness information, graphs etc. The software enables simple programming extensions with new features. The test procedure is quickly adaptable for new test procedures which comes when new valve is developed and needs to be tested on the test bench.

1   Intruduction

Test bench for EOL (End of line) testing is a machine where valves assembled in the factory are tested under required test procedures. Usually EOL test is located at the end of the assembly line or somewhere close. EOL test bench consists of hydraulic circuit with pumps, valves, hydraulic blocks, tanks, hoses, measurement equipment and connectors. In electrical cabinet all hydraulic and electrical equipment which needs to be wired are connected to get electrical power supply or acquire the measurements. Electrical cabinet include also controller with touch screen control panel with user interface for managing the software and controlling test bench and test procedures. To ensure safety standards test bench include safety cabinet and compact framework which can be seen on the Figure 1.

Figure 1: Test bench for EOL testing
Source: [2]

Test bench which is introduced in this article was originally designed for manual testing of small batches of the valves. Every valve which comes from the production/assembly line is tested on the EOL test bench to check if valve have any hydraulic or electrical dysfunction or any other damage which can lead to potential error on the customer application. With EOL test for every valve is ensured to deliver high quality product and satisfy customer's requirements.

2   The scope of investigation

To ensure highest possible quality of the product, the decision was to make step forward and upgrade the test bench for testing valves to automatic mode with automatic test procedures. In the sections below it is presented which components have been upgraded or replaced with newer to achieve this goal.

The upgrades were made on hydraulic, electrical and software side. During hydraulic and electrical upgrade, the test bench was out of service for one week. Software upgrade was made in parallel and was implemented when test bench hydraulic and electrical upgrades were ready. During start-up some issues were detected and successfully solved.

The software idea was to use blocks (functions) which can be easily build into the test procedure. With simple blocks, technician can build test programs by themselves with stacking blocks together one by one. The steps are executing in the procedure step by step from the first step to the last step (see Figure 2). In principle individual step is independent from all others. It is possible to merge steps to create partial process which could be a part of the main test procedure (Figure 3). Partial process can be used in several places in the test procedure. It could be also used in other test procedures, not just in one.
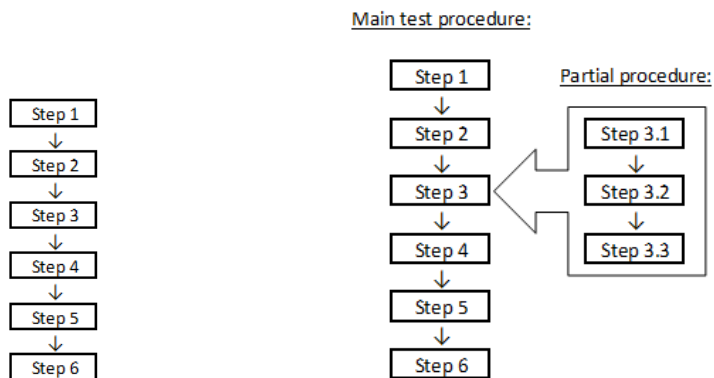
Figure 2: Step by step program execution.
Source: [2]

Figure 3: Step by step test procedure with partial procedures which are included as part of the main test procedure.
Source: [2]

When the requirement for new function arise, the programmer needs to develop new function according to test specifications which are usually given by R&D department. New function could be used in all further test procedures or partial procedures. When all required functions are ready the technologist needs to stack functions to a test procedure and validate test procedure on the test bench to be sure all works fine before test procedure is used in production.

3   Hydraulics modification

For hydraulics upgrades some hydraulic components had to be replaced and some new components had to be added to make possible test in automatic mode. The components which were added are:

- On/off valves instead of manual pipes,
- proportional valves instead of manual settings,
- flow meters,
- particle counter,
- cleanliness measurement (upstream and downstream oil measurement, ISO 4406),
- water cooling system instead of air cooler.

Figure 4: Additional flow meters which are easily to grab and plug into the tested valve.
Source: [2]

Due to lack of space inside the test bench frame it was a challenge to make all required upgrades. When test bench was designed (more than 10 years ago), it was not foreseen that big upgrades would be needed in the future and it was optimized for the current needs. The upgrade required quite a bit of adaptation from the teams which were involved in the upgrade.

Figure 5: Particle counter and oil cleanliness measurement.
Source: [2]

Figure 6: Flow meter mounted on the rail in front side of the test bench.
Source: [2]

4   Electrical modification

Electrical cabinet dimensions were defined for the current needs at the time when test bench was designed. Usually, electrical cabinet is designed to have some additional free space for the future upgrades. In our case there was some additional space, but not enough for all components which were needed to be installed. It was chosen the solution to mount the components on the electrical cabinet door (Figure 7).

Figure 7: New components mounted on the electrical cabinet door.
Source: [2]

5   Software

Software LabVIEW was chosen because it offers many possibilities to adapt the software to specified requirements and needs. For acquiring measurement NI (National instrument) hardware was chosen. It is well known as the best ones and is often chosen for this kind of projects in our company.

Figure 8: LabVIEW - block diagram example.
Source: own.

5.1   User interface

Basic user interface was made to communicate with operator. It has several options to login/logout, automatic testing, manual testing, maintenance mode, basic settings, turn on/off the main motor. Furthermore, the main screen shows essential

information about test bench status such as oil temperature, oil cleanliness, hardware status, log status, reporting status, monitoring, server synchronization etc.
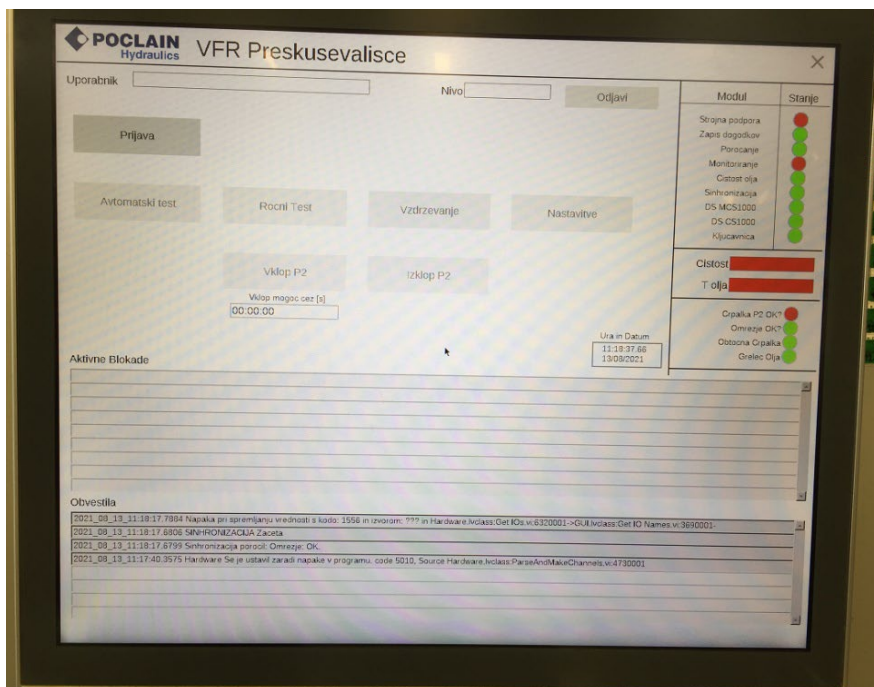
Figure 9: User interface - main screen.
Source: [2]

When click to each key, sub screen appears to operator to manage with test bench and test procedure. To manage with the program, operator can use touch screen, shortcuts on the keyboard, mouse and keypad.

5.2   Manual testing

To have option to test wide range of valves manual test was required. Also, for some valves automatic test does not have sense because it takes more time than manual test. In manual testing some test blockades are disabled (oil temperature range, oil cleanliness …) to have option of test also in case where all conditions are not valid for production testing. In manual operator have wider range of test options which could be useful.

### 5.3	Automatic testing

With development of technology and implementation of standard Industry 4.0 the need for EOL test bench automation becomes more and more important and necessary to reach high reproducibility of the test. With the same test procedure there is no deviation between the tests which may occur if test is manually managed by operator.

Test procedure consists of a set of steps (functions). With set of steps it is possible to make setting on the values, measure the values, capture the graph, analyse the graph or do anything else according to the test procedure. With own development of the functions in LabVIEW it is obtained almost unlimited possibilities to develop customized functions to achieve almost any test procedure requirement.

### 6	Advantages and disadvantages of automatic testing

### 6.1	Advantages

With test automatization the operator's influence on the test report and measurement results is eliminated and could not change test result during the test.

Test reports are generated at the end of every test and are stored on the controller. Every 5 minutes the synchronization between controller and server is triggered and reports with some other files synchronized to the server. If network connection is unavailable the reports are stored on the controller and are synchronized with the server when network connection is established again. After synchronization the original files are deleted on the controller side to release the space for new reports.

To have traceability of the EOL testing the output file is generated at the start of every month. In the output file all major data about tests and test bench are stored. Data structure of the output file can be seen on the Figure 10. This file is used for further analysis and monitoring in different applications.

Test time is important in the way of time consumption and production planning. It is measured how much time the operator spends to test one valve. During automatic testing operator don't need to stay all the time in front of the test bench, it can do other things such as assemble the valves, squatting holes, packing…

```
Preizkusevalisce;Datum;Ura;Operater;Nalog_ID;Sifra;Naziv;Rezultat;Test_Ime;Test_Nacin;Test_verzija;Test_Cas;Olje_Temp;Olje_Nivo;Cistoca
VFR;29/06/2023;11:50:30;Damjan Mohoric;I1R55271621;B55535N;-;GG;B55535N;A;vA1.1;414;52.0°C;12.4/10.1/7.0
VFR;29/06/2023;12:12:34;Damjan Mohoric;I1R55271622;B55535N;-;GG;B55535N;A;vA1.1;437;52.1°C;11.8/9.2/7.0
VFR;29/06/2023;12:21:07;Damjan Mohoric;I1R55271623;B55535N;-;WW;B55535N;A;vA1.1;244;52.6°C;12.7/11.0/7.0
VFR;29/06/2023;12:28:34;Damjan Mohoric;I1R55271623;B55535N;-;GG;B55535N;A;vA1.1;412;50.4°C;13.5/11.7/7.0
VFR;29/06/2023;12:36:36;Damjan Mohoric;I1R55271624;B55535N;-;GG;B55535N;A;vA1.1;413;51.0°C;13.5/11.4/7.8
VFR;29/06/2023;12:44:41;Damjan Mohoric;I1R55271625;B55535N;-;GG;B55535N;A;vA1.1;412;51.8°C;14.0/12.5/8.7
VFR;29/06/2023;12:52:44;Damjan Mohoric;I1R55271626;B55535N;-;GG;B55535N;A;vA1.1;410;52.7°C;13.4/11.7/8.2
VFR;29/06/2023;13:00:43;Damjan Mohoric;I1R55271627;B55535N;-;GG;B55535N;A;vA1.1;409;50.3°C;13.3/11.6/7.0
VFR;29/06/2023;13:08:40;Damjan Mohoric;I1R55271628;B55535N;-;GG;B55535N;A;vA1.1;414;51.7°C;13.5/11.8/7.2
VFR;29/06/2023;12:28:31;Damjan Mohoric;I1R55271623;B55535N;-;WW;B55535N;A;vA1.1;2854;50.5°C;13.5/11.7/7.0
```

Figure 10: Output file example.

Source: own.

In manual testing mode operator have focus on the tested valve all the time during the test. For every test step needs to make some clicking on the keyboard or touch panel. He needs to manually turn on/off motors, valves and set the analogue values. Usually this set values are not set to exact value. Automatic test values are set to exact values every test. Values must be in range and are stored in the report at the end of the test.

Safety is provided with safety devices and is not controlled with test bench software. In our case there is no rotating parts or pressing devices. The only potentially danger is high pressure oil inside the hoses, blocks and valves which are located inside the safety cabinet. These components have high pressure lines where the pressure could reach over 300 bar which can be fatal.

6.2 Disadvantages

In case of NOK test results operator must decide what would be the next action with tested valve. In manual test process are some possibilities where the operator may make wrong decision. During the time it turned out that new operators need training on the test bench and induction period to be able to make the manual test in correct way and to make right decisions.

Test time for some test procedures is longer in automatic mode because it takes some time to measure and analyse the steps, but in manual mode operator can visually check the value and confirm or reject the step.

7 Conclusion

Three main upgrades (hydraulics, electric and software) of test bench were done successfully and test bench works in production for some time.

Next step where the focus will be soon is to test more valves with automatic tests. Some test procedures are in validation phase where separate steps are tested if works properly and in if measurement limits are set correct. Especially big interest is from production side. R&D department is interested to make automatic tests with steps which are adopted to their needs. The software allows us flexibility and adaptability to reach wide range of requirements.

With chosen software concept was achieved the agility and fast reaction to the market needs. It was reached short development time of new steps (functions) and consequently short time to develop new automatic tests for the valve.

References

[1]   Poclain Hydraulics training center (various internal literature)
[2]   Personal photo archive
[3]   Poclain Hydraulics photo archive
[4]   https://www.poclain-hydraulics.com/en/; last visited on 25.7.2023

Implementation of External Matlab Closed-loop Controllers Within Beckhoff Soft-PLC Controller

Vito Tič

University of Ljubljana, Faculty of Mechanical Engineering, Ljubljana, Slovenia
vito.tic@um.si

In the scope of the research, we have designed and implemented the closed-loop position control of the linear axis using a externally-developed controller imported into Beckhoff soft-PLC, which will, further on, allow us to use any position controller. Namely, in the industrial environment, the PID controller is most often used due to its simplicity and robustness. The goal of the research was to replace the PID controller with an external controller, which can also be non-linear, such as fuzzy logic. We have designed the controllers using the MATLAB-Simulink software, from which we have exported the model into TwinCAT 3 environment. We have compared the responses between external position controller and the embedded Beckhoff PID position controller, and then compared the operation of the PID and fuzzy logic controller. Due to high energy density of hydraulic systems and potential risks, the first research was made on small scale electromechanical axis.

1   Intruduction

Fluid power control systems often contain closed-loop position controllers, where the most common used in the industrial environment are proportional-integral-differential (PID) controllers, which meet a wide range of system control needs.

Proportional-integral-differential closed-loop controllers work on the basis of feedback loop principle and are very often used in industrial control systems. When using a PID controller, the error is calculated on the fly with the help of a feedback loop. The latter is calculated between the desired (set) value at the input and the actual value at the output of the system. The controller itself is designed in such a way that it tries to reduce the error with the help of the manipulated variable [1].

In the case of more demanding closed-loop control system, we can detect cases where the use of an established PID controller is not sufficient. For this purpose, non-linear closed-loop controllers, such as e.g. fuzzy logic or neural networks, are gaining prominence. These are much more difficult to implement in industrial controllers, which usually contain already embedded controllers. Therefore, our goal was to design and implement an external position controller developed in the MATLAB-Simulink environment and import it into the TwinCAT 3 programming software (Beckhoff soft-PLC). Due to the limitations of the equipment available, the design and testing was carried out on an electric linear servo axis, where we have compared different types of position closed-loop controllers and their responses to set value.

2   System overview

For the above-described research, we have used Festo FESTO-DGE-25-500 linear axis, which converts rotary motion into linear motion using a toothed belt. The controlled trolley on the linear axis was enhanced to be able to attach up to 5040 g weight in order to change the mass of the control system. To control the linear axis, we have used a Beckhoff AM8113-0F20 servo motor, which has an integrated 18-bit absolute incremental encoder, which allows us to accurately control speed, acceleration and position (Figure 1).
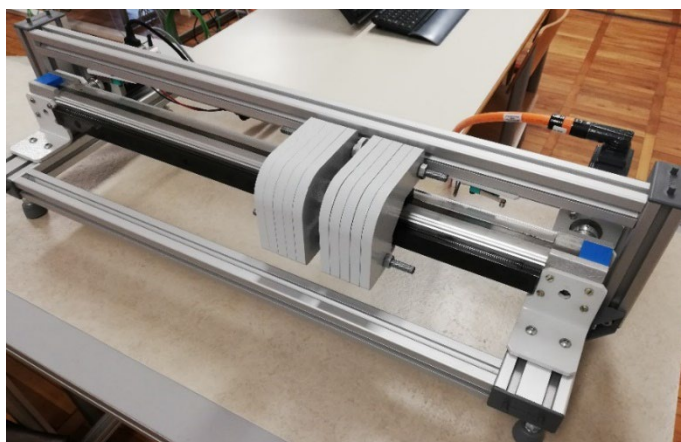
Figure 1: Festo toothed belt linear axis with Beckhoff servomotor.
Source: own.

3   Closed-loop controllers in TwinCAT3

The servomotor is controlled using a closed-loop controller consisting of a trajectory generator and position tracking system. The trajectory generator outputs the position reference (set position) and the speed of change of the position (tangent of the position trajectory) that are fed to the input of the closed-loop position controller. The closed-loop controller uses cascade principle (Figure 2), where the speed and current loops are already set up inside the Beckhoff controller. Our task was to research and implement only various position closed-loop controllers.
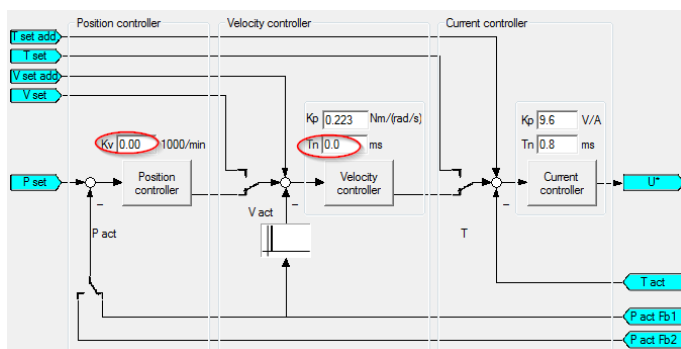

Figure 2: Beckhoff servomotor closed-loop controller in TwinCAT 3.
Source: own.

The proportional-integral-differential controller (PID) works on the principle of a feedback loop, where the error is calculated on the fly with the help of the feedback loop. and contains three parts. These parts are proportional part (P), integral part (I) and differential part (D). Each part contains its own parameter, with the help of which the individual part can be increased or decreased. The influence of the individual part of the controller on its output is interpreted in terms of time. Thus, the proportional part is depended on the current error, the integral part is depended on the accumulation of past errors, and the differential part is depended on the rate of change of the error [2, 3]. The PID controller built into the TwinCAT 3 software is shown in Figure 3.
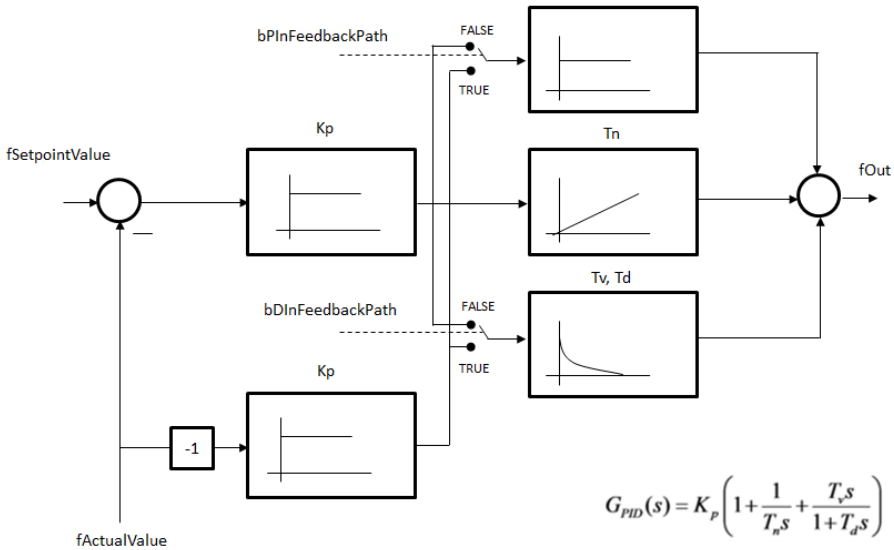
Figure 3: Beckhoff PID controller in TwinCAT 3.
Source: own.

$$G_{PID}(s) = K_p \left(1 + \frac{1}{T_n s} + \frac{T_v s}{1 + T_d s} \right)$$

## 3.1	Setpoint generator

The TwinCAT 3 software has built-in trajectory generator added to the program block for position control. For the calculation of the trajectory, the trajectory generator block requires several inputs: the initial and final position; initial, maximum and final speed; and the acceleration/deceleration, which determine the fastest speed change.

4 Development and implementation of MATLAB – Simulink closed-loop controller

We have designed and implemented PID and fuzzy logic position controller using the MATLAB-Simulink programming environment, in which we can design different types of linear and non-linear closed-loop controllers.

In addition to designing the controllers, we can generate and export the software code of the designed controller, which is suitable for implementation into TwinCAT 3 and can be directly imported into Beckhoff soft-PLC. To begin with, we have created an external PID controller and compared its operation to standard TwinCAT 3 embedded PID controller.

4.1 MATLAB – Simulink PID controller

The PID controller in MATLAB-Simulink was designed using the transfer function, consisting of individual blocks, which were connected into a whole system. The transfer function consists of different blocks such as addition, multiplication, division, delay, input and output block. Figure 4 shows the scheme of the implemented PID controller. The implemented scheme has to be moved into the subsystem in order to generate the export code, which is then imported into Beckhoff programming environment using the *PLCopenXML* standard.
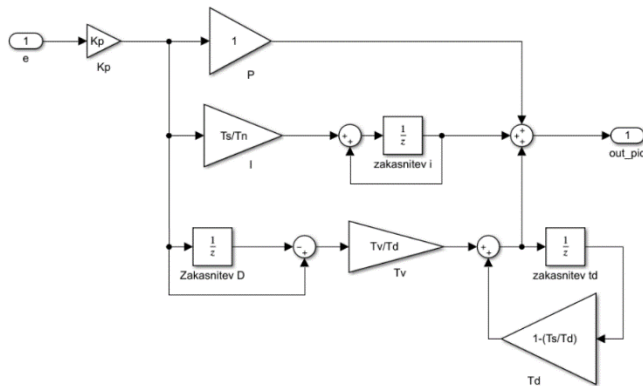

Figure 4: MATLAB – Simulink PID controller.
Source: own.

4.2 MATLAB – Simulink fuzzy logic controller

Fuzzy logic controllers are nonlinear type controllers used in signal processing, pattern recognition, and other control systems. They use soft and blurred quantities, similar to human perception, where the response is far from mathematically precisely defined rules. Thus, it cannot be described by exact equations.

The designed fuzzy logic controller, created in MATBLAB-Simulink, is shown in Figure 5. The transfer function is based on the presented programming blocks. [4, 5]
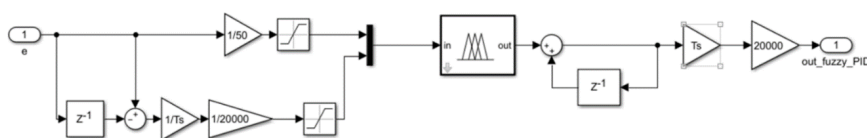

Figure 5: MATLAB – fuzzy controller.
Source: own.

5 Results

The aim of the research was not only the design of external closed-loop controllers, but also their implementation and corresponding tests, where we have compared the responses of TwinCAT 3 and the created external MATLAB-Simulink controllers. In this way, we were able to check whether the axis position system and the controller used were correctly designed and implemented. If we have implemented everything correctly, the response of both systems should be the same.

5.1 Comparison of Beckhoff integrated PID controller and MATLAB – Simulink PID controller

Figure 6 shows the response of the system using integrated Beckhoff PID controller and imported external MATLAB-Simulink PID controller using optimal parameters determined by the Ziegler-Nichols method. The blue line shows the error between the desired (set) value and the actual value of the axis position, the orange shows the generated position trajectory representing the desired (set) value, the red shows the

actual position of the axis, and the green shows the start of the step change. It can be seen from the figure that the operation and the response of the external MATLAB-Simulink PID controller is very similar or nearly the same as TwinCAT 3 embedded controller. In this way, we have confirmed the adequacy of the design of external controllers and their implementation into the TwinCAT 3 Beckhoff environment.

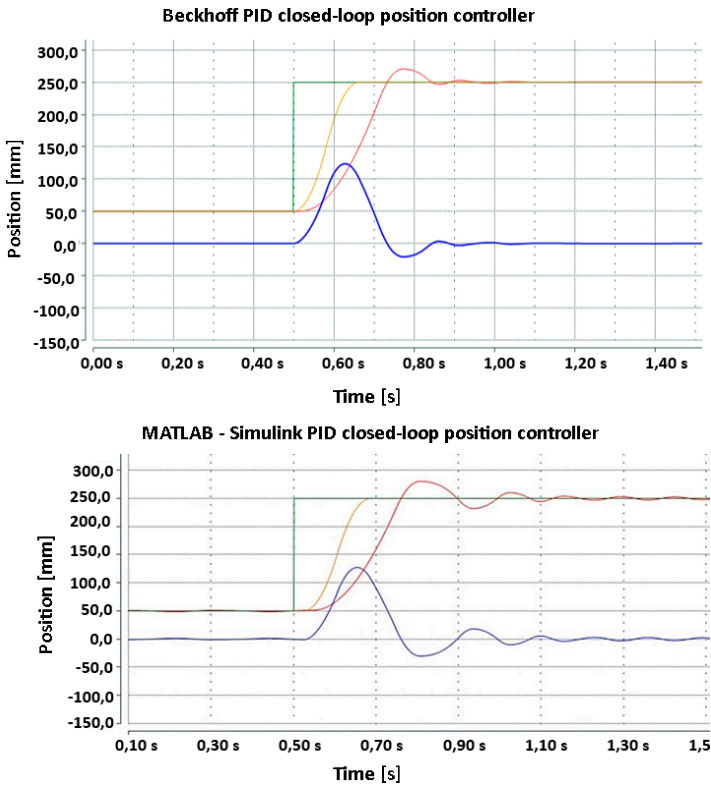**Figure 6: Comparison of Beckhoff integrated PID controller and MATLAB – Simulink PID controller.**

Source: own.

5.2 Comparison of PID controller and fuzzy logic controller

In addition to creating an external closed-loop controller, the goal of our research was to create and implement a fuzzy logic (non-linear) controller. In this way, we were able to define how the two controllers react in different conditions, such as,

for example, a change in the mass of the system. In the below comparison the PID controller was set according to the Ziegler-Nicholson method and additionally fine-tuned manually, and then compared to the designed fuzzy logic controller [5]. The results, presented in Figure 7 and Table 1 show that the PID and fuzzy logic controllers respond very quickly to the step change. We can notice better response from the fuzzy logic controller, which has less overshoot and it is faster when using less precise dead band position deviation. In this case, the difference between the controllers is smaller because the PID controller was optimized for a system without additional mass.
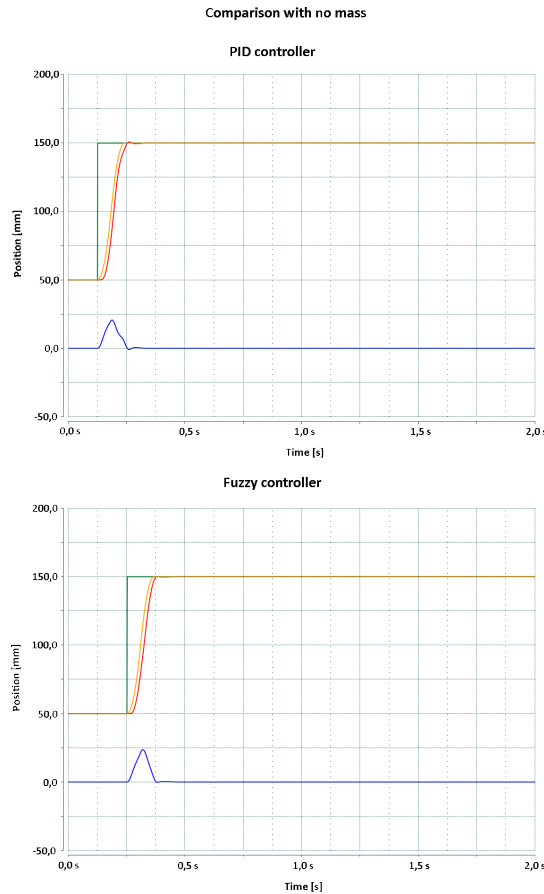

Figure 7: Comparison of PID and fuzzy closed-loop position controller without added mass.

Source: own.

Comparison with mass

PID controller
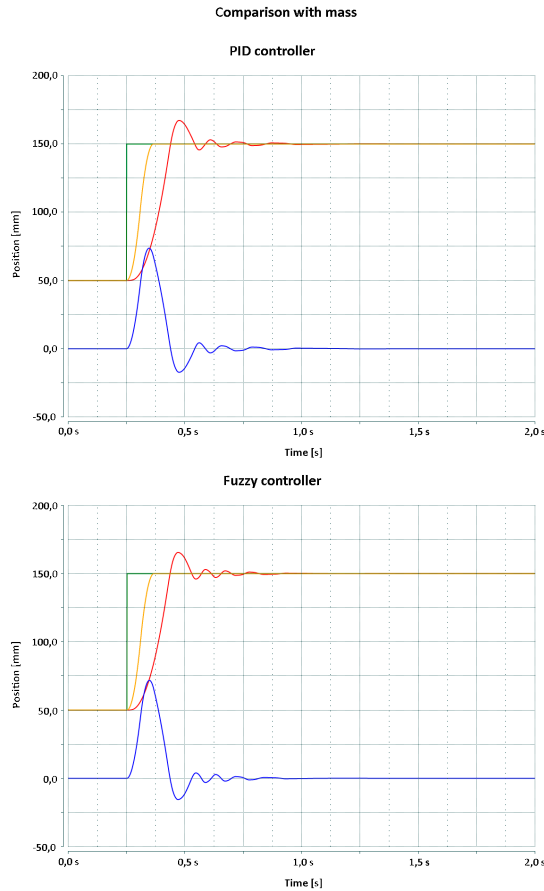
Fuzzy controller

Figure 8: Comparison of PID and fuzzy closed-loop position controller with added mass.

Table 1: Comparison of PID controller and fuzzy logic controller – without mass

		PID	Fuzzy
Dead band position deviation [ms]	0.01 mm	194	197
	0.5 mm	164	122
Maximal overshoot [mm]	Positive	0.84	0.23
	Negative	0.53	0.28
Maximal position deviation [mm]		20.69	23.62

However, when adding additional mass to the system (results in Figure 8 and Table 2), the response of the fuzzy logic controller is better, since the nonlinear controller compensates for the additional mass. The PID controller parameters were defined and optimized without mass, so with added mass it is no longer optimally set.

Table 2: Comparison of PID controller and fuzzy logic controller – with mass

		PID	Fuzzy
Dead band position deviation [ms]	0.01 mm	1033	790
	0.5 mm	682	629
Maximal overshoot [mm]	Positive	17.29	15.55
	Negative	4.32	3.95
Maximal position deviation [mm]		73.67	71.8

The presented results reveal that a well-tuned PID controller can perform the position control operation just as well as a non-linear or fuzzy logic closed-loop controller when the PID parameters are optimized for the application. Major deviations in operation occur when we change the weight of the load, as the controller is not optimized for given load and conditions. Thus, in the case of variable weight of the load, a non-linear or fuzzy logic controller is preferred.

6   Conclusion

In the scope of the research, we have analysed the operation of externally designed and further implemented controllers in the TwinCAT 3 Beckhoff system. Due to the limitations of the equipment available, the design and testing was carried out on an electric linear servo axis, although the final implementation will be done on various fluid power systems.

We have validated the conformity of their operation with an PID controller example. To this extent, we are now able to design various controllers using the MATLAB-Simulink tool and integrate them into Beckhoff industrial soft-PLC controllers.

Further on, the research revealed that the fuzzy logic controller performs better under unsteady conditions, as the latter can compensate for additional changes without changing the parameters. Although fuzzy logic closed-loop controller needs greater processing power due to demanding algorithms, which can be achieved by using high-end soft- PLCs in industrial applications.

Upgrading embedded closed-loop position controller with an external one allows us to use more advanced, more complex, more responsive and faster controllers.

References

[1]   J. K. Åström and T. Hägglund. PID controllers: Theory, design, and tuning (2nd ed.). Instrument Society of Automation, 1995.

[2]   Araki, M. PID CONTROL, Kyoto University, Japan [splet], Dosegljivo: http://www.eolss.net/ebooks/Sample%20Chapters/C18/E6-43-03-03.pdf [Datum dostopa: 14.8.2023]

[3]   PID Control System Analysis, Design, and Technology, University of Glasgow [splet], Dosegljivo: http://eprints.gla.ac.uk/3817/1/IEEE3.pdf [Datum dostopa: 14.8.2023]

[4]   Inteligentne regulacijske tehnike v mehatroniki, Riko Šafarič, Andreja Rojko, Univerza v Mariboru, Fakulteta za elektrotehniko, računalništvo in informatiko, Maribor, november 2007

[5]   G. Komplet, „Razvoj in implementacija zaprto-zančnih položajnih regulatorjev v okolju Beckhoff twinCAT 3 : magistrsko delo", Magistrsko delo, Univerza v Mariboru, Maribor, 2021

Polymers For Sustainable Hydraulic Valves Tested in Water, Glycerol-water Mixture and Hydraulic Oil

Ana Trajkovski, Nejc Novak, Jan Bartolj,
Jan Pustavrh, Franc Majdič

University of Ljubljana, Faculty of Mechanical Engineering, Ljubljana, Slovenia
ana.trajkovski@fs.uni-lj.si, nejc.novak@fs.uni-lj.si, jan.bartolj@fs.uni-lj.si,
jan.pustavrh@fs.uni-lj.si, franc.majdic@fs.uni-lj.si

Engineering polymers such as polyoxymethylene (POM) have proven to have very promising tribological properties and successfully follow high performance thermoplastics. The focus of our research is on testing and analysing POM for very demanding, harsh working conditions of high-speed hydraulic on/off valves. The samples were tested and compared to POM reinforced with 30 % carbon fibres in standard hydraulic oil ISO VG 46, water, and glycerol-water mixture at room and elevated temperature, and at different sliding speeds. The results showed good tribological properties for both polymers when lubricated with glycerol-water mixture, comparable to the results obtained in hydraulic oil but lower than those measured in water. However, the difference decreases at higher temperature. The results also showed an opposite trend of decrease in the coefficient of friction and increase of specific wear rate at lower sliding speed, with a similar trend at higher temperature.

1   Intruduction

The use of low weight and high strength polymers and polymer composites instead of metals, for manufacturing different fluid power elements and components has great potential for reducing components weight and energy losses [1]. Compared to traditionally used steel alloys, the strength-to-density ratio of reinforced polymer composites is 13.5 times that of steel [2]. In the recent study on hydraulic cylinders, the prototype based on the radial stiffness design method and composite structure has reduced weight by 56.86 % while maintaining the same performance as the conventional metal hydraulic cylinder [3]. Additionally, polymer composites have proven to produce very low coefficient of friction and specific wear rate at different loading regimes [4]. By combining the advantages of the new surfaces, materials, and lubrication technologies for friction reduction and wear protection in various equipment worldwide, energy losses caused by friction and wear could potentially be reduced by 18 % in the short term (8 years), or as much as 40 % in the long term [5].

Among different polymer composites, ultra-high performance polymers such as PEEK (Polyetheretherketone), high performance polymers such as PPS (Polyphenylene sulfide), engineering polymers such as POM (Polyoxymethylene), UHMWPE (ultra-high-molecular-weight polyethylene), PA (Polyamides) or commodity polymers such as PE (Polyethylene), PTFE (Polytetrafluoroethylene) have been investigated and analysed with different fillers, reinforcements for different loading conditions and applications [5]. From ultra-high-performance polymers down to commodity polymers, mechanical properties change in contrast to polymer price (representative polymers are compared to AISI 440C stainless steel [4–6] in Table 1).

POM is one of the 'middle range' polymers, with price up to 10 times lower, compared to ultra-high-performance polymers. It has low cost, low weight and low water absorption along with good tribological properties, which makes it one of the most commonly used engineering polymers [7, 8]. It can successfully follow both PPS and PEEK performance when used for gerotor gears, or even follows the performance of the classic metallic pressure relief valve [1].

A. Trajkovski et al.: Polymers For Sustainable Hydraulic Valves Tested in Water, Glycerol-water Mixture and Hydraulic Oil

269

Table 1: Sample properties

Polymer group (representative polymer)	Density [kg/m³]	Young modulus [GPa]	Ultimate tensile strength [MPa]	Operating temperature [∘C]
Ultra-high-performance (PEEK)	~ 1.32	~ 4.2 - 8.1	~ 110	up to 250
High-performance (PPS)	~ 1.43	~ 3.3 - 4.4	~ 75	up to 220
Engineering (POM, UHMWPE, PA)	~ 1.13-1.5	~ 1.7 - 3.3	~ 40 - 80	up to 120
Commodity (PE, PTFE)	~ 2.18	~ 0.5	~ 10	up to 100
Stainless steel representative				
AISI 440 C	~ 8	~ 200	~ 760 - 1960	up to 1100

Usually, polymer composites are tested under dry or water lubricated conditions. However, hydraulic oil is commonly used lubricant for hydraulic applications. Nowadays, green lubricants are becoming mandatory in marine or forestry machinery [9], and extremely wanted in all different sorts of mobile machineries and industries. Typical answer to this quire, is in using pure water, or water with different additives, that correct water extremely low pressure-viscosity coefficient and corrosion problems [10, 11]. Glycerol is another interesting biocompatible alternative, that is main by-product in biodiesel production [12]. Although it has good mechanical and tribological properties, it also has almost 20 times higher viscosity compared to traditional mineral base oils [13]. Such a high viscosity is not particularly desired because there are greater energy losses due to the need for more energy to overcome the thicker lubricating film, resulting in lubricant degradation and possibly early failure of elements or the system. However, glycerol dissolves in water, and both high glycerol freezing point [14, 15], film thickness and viscosity can be controlled with an appropriate amount of water. In this way, even a so-called super-lubricity can be obtained, with a friction coefficient of less than 0.01 [16]. Glycerol aqueous solutions show good results in steel sliding contacts of rolling and sliding bearings [17, 18], under different boundary, mixed and elastohydrodynamic conditions [13, 16, 17]. In recent study of different polymer composites [19], environmentally acceptable lubricant proved to improve tribological properties of polymer-steel contacts. In our recent study, five different polymer composites were compared [20], and glycerol proved to be excellent lubricant, especially for three polymers with higher micro hardness.

The aim of this study is to analyse the tribological properties of pure POM, and to compare the results of polymer-steel contacts in conventional hydraulic oil ISO VG 46, pure water and glycerol + water solution. In addition, the experiments will be performed at room and elevated temperature, as expected in hydraulic applications. And finally, the results will be compared with our preliminary measurements on carbon fibre reinforced POM.

2   Materials and methods

2.1   Test samples

For the chosen type of ball-on-plate tribological tests, POM discs were cut from a 30 mm diameter rod with a thickness of 5 mm. RotoForce-3 automatic sample polishing and preparation machine was used, and samples were polished to a roughness of 0.1 μm. The ball was a commercial bearing ball with a diameter of 25 mm made of hardened AISI 440-C stainless steel. Before starting the test, all samples, clamps and the bath were carefully cleaned.

2.2   Lubricants

Demineralised water was used as the reference lubricant. Glycerol (with ≥ 99.5 % cleanness) was used as the base for the lubricant glycerol + water (G+W). Based on our preliminary experiments, glycerol with 40 % water in the mixture was used, as this mixture allowed the good lubricating properties of pure glycerol to be maintained at room temperature. The third lubricant used in the study is the commercially available, commonly used ISO VG 46 hydraulic oil. The parameters of the lubricants (Table 2) were determined with an automatic viscometer SVM 3001 (Anton-Paar).

Table 2: Lubricants properties

	Kin. Viscosity at 25 °C [mm²/s]	Kin. Viscosity at 80 °C [mm²/s]	Density at 25 °C [g/cm³]	Density at 80 °C [g/cm³]
ISO VG 46	100	9	0.86	0.86
G + W	11.59	2.19	1.17	1.12
W	0.89	0.36	0.99	0.97

A. Trajkovski et al.: Polymers For Sustainable Hydraulic Valves Tested in Water, Glycerol-water Mixture and Hydraulic Oil

271

2.3 Tribological characterization

Measurements were carried out with a Cameron-Plint TE 77 high-frequency tribometer (Figure 1) in reciprocal mode. The average sliding velocity was set to 0.2 m/s and 0.05 m/s (frequency 40 Hz and 5 Hz, respectively, and stroke length 2.4 mm). The load was set to 50 N (90 MPa maximum Hertzian pressure). Before each test, the polymer disc was completely immersed in the selected lubricant. The thermoset was placed in the lubricant bath and a heating element was placed under the bath to check the temperature and keep it constant during the test (at a temperature of 80 °C). Special care was taken to maintain the lubricant level during the test so that the sample and ball were always fully immersed in the selected lubricant. After the final test, the contact sliding surface was marked on the ball using an electric pen.
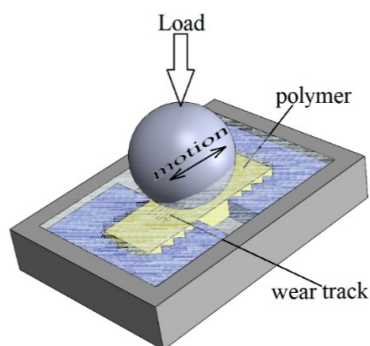

Figure 1: Ball on plate tribo-test scheme
Source: own.

Each test was repeated three times. The tests were conducted for 90 minutes based on preliminary tests that gave a stable value of the coefficient of friction.

2.4 Post-tribological analyses

The wear volume of the disc-like polymer plates was calculated from the dimensions of the wear tracks. The 3D profile of each calotte was determined and characteristic cross-sectional areas at different locations along the wear track were read [20] with digital microscope Hirox HRX-01. Same procedure was also used to determine the shape and dimensions of the wear marks on the steel balls.

3   Results

3.1   Wear and coefficient of friction

The average steady-state coefficient of friction in ISO VG 46 oil, glycerol + water mixture and water are presented in Figure 2.
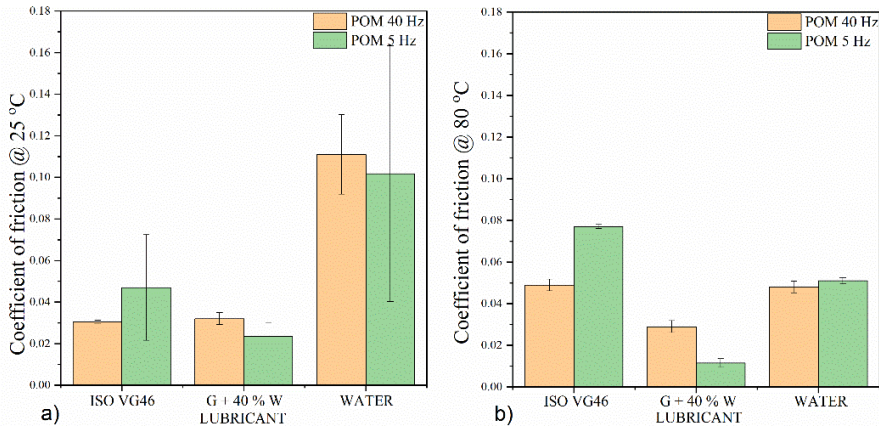

Figure 2: Average coefficient of friction of POM at 40 Hz and 5 Hz in three different lubricants at: a) room temperature 25 ∘C; b) elevated temperature 80 ∘C.
Source: own.

At room temperature (Figure 2a), the results showed comparable values of the coefficient of friction of 0.028 and 0.031 in both ISO VG 46 hydraulic oil and glycerol + water mixture respectively. At lower frequencies, 60 % increase of coefficient of friction was measured in oil, and on contrary slightly lower value (16 % decrease) was measured in glycerol + water mixture. The lowest value was measured in glycerol + water mixture at 5 Hz (0.023). Compared to both oil and glycerol + water mixture case, 4 times higher coefficient of friction was measured in pure water. The highest measured value of coefficient of friction, at room temperature vas measured in water at 40 Hz (0.12). Additionally, the smallest change in measured coefficient of friction value was measured in water, compared to measurement in water at higher frequencies (~ 8 % decrease).

At elevated temperature (Figure 2b) the friction coefficients increased in hydraulic oil, at both measured frequencies, about 70 % increase. The highest measured value

A. Trajkovski et al.: Polymers For Sustainable Hydraulic Valves Tested in Water, Glycerol-water Mixture and Hydraulic Oil

273

at elevated temperature was in oil at lower frequency (0.077). In case of glycerol + water mixture, coefficient of friction showed the smallest change, compared to other two lubricants, namely at 40 Hz around 6.5 % decrease, and at 5 Hz almost 50 % decrease (the smallest measured coefficient of friction, 0.011). In case of water, significant decrease around 55 % of measured coefficient of friction was observed, at both frequencies.

The average calculated values of specific wear, based on analysed wear tracks in ISO VG 46 oil, glycerol + water mixture and water are shown in Figure 3.
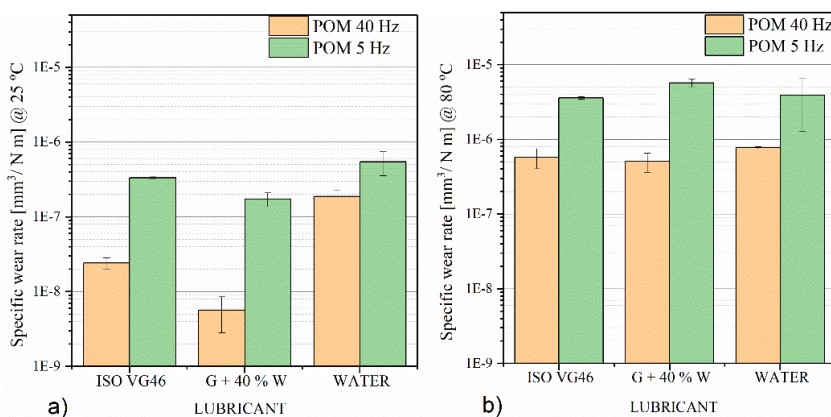

Figure 3: Average calculated specific wear rate of POM at 40 Hz and 5 Hz in three different lubricants at: a) room temperature 25 ∘C; b) elevated temperature 80 ∘C.
Source: own.

At room temperature (Figure 3a), the smallest specific wear rate was measured in glycerol + water mixture (5.68×10^{-9} mm³/Nm) at higher frequency. Slightly higher specific wear rate was measured in oil (2.42×10^{-8} mm³/Nm, ~ 4 times higher compared to glycerol + water mixture). The highest specific wear rate at higher frequency, was measured in water (1.88×10^{-7} mm³/Nm, ~ 33 times higher compared to glycerol + water mixture). At lower frequency, specific wear rate increased, however the difference among lubricant decreased (same ordered of specific wear rate ~ 10^{-7} mm³/Nm).

At elevated temperature (Figure 3b) increased specific wear rate was observed, in all tested lubricants. The highest increase (~ 90 times) was measured in glycerol + water mixture, on contrary lower increase in oil and water (~ 23 to 4.1 respectively).

However comparable specific wear rate was measured for all lubricants ($\sim 10^{-7}$ mm^3/Nm). The same trend was observed at lower frequencies, when comparable specific wear rate was measured ($\sim 10^{-6}$ mm^3/Nm).

3.2   Surface analyses

Polymer worn surfaces were observed with digital microscopy, and selected samples are presented in Figure 4 and 5. The surface appearance, wear track shape and length (~ 3300 µm) are similar in all lubricants and at all tested conditions. However, the narrowest wear track was observed in case of oil at room temperature and at higher frequency (~ 823 µm, Figure 4.I.a). The wear track is not significantly wider in glycerol + water mixture (~ 8 % increase) at room temperature, although the scratches along the sliding direction are much more intense, especially in the middle of the wear scar (Figure 4.I.b). In case of pure water used at room temperature, both wear track width (~ 66.5 % increase), the number and intensity of scratches is significantly higher (Figure 4.I.c).

At elevated temperature, there is no significant difference in wear track width among different lubricants used (~ 1600 µm, Figure 4.II.a-c). This means, that the highest change observed in wear track, due to elevated temperature was observed in oil lubricated case, tightly followed by glycerol + water lubricated case. However, scratches along the sliding direction are not deep and intense in glycerol + water mixture (Figure 4.II.b) as they were in oil (Figure 4.II.a), or even more in water (Figure 4.II.a). This agrees with the smallest specific wear rate in the mixture at 80 °C, and relatively small differences among all three lubricated cases.

At lower frequency (Figure 5.a-c) there was no significant difference in the wear track dimensions among lubricants at both temperatures. At room temperature the wear track width (~ 1148 µm, Figure 5.I.a-c) was wider compared to the tests at higher frequency and room temperature in oil and glycerol + water mixture, and on contrary tighter in case of water. The main difference was observed in wear mechanism since the wear scratches along the sliding direction are the least intense in case of glycerol + water mixture (Figure 5.I.b). They are the most intense and frequent in case of oil (Figure 5.I.a), and the widest and deepest in case of water (Figure 5.I.c). This agrees with the smallest specific wear rate in the mixture, yet there were small differences among different lubricants (Figure 3.a). At elevated

A. Trajkovski et al.: Polymers For Sustainable Hydraulic Valves Tested in Water, Glycerol-water Mixture and Hydraulic Oil

275

temperature, wear track width was comparable among lubricants (~ 1522 µm, Figure 5.II.a-c), and not significantly changed compared to room temperature conditions. Again, the difference was in the scratch's intensity and depth, being the most intense in case of oil and the least intense in case of glycerol + water mixture.
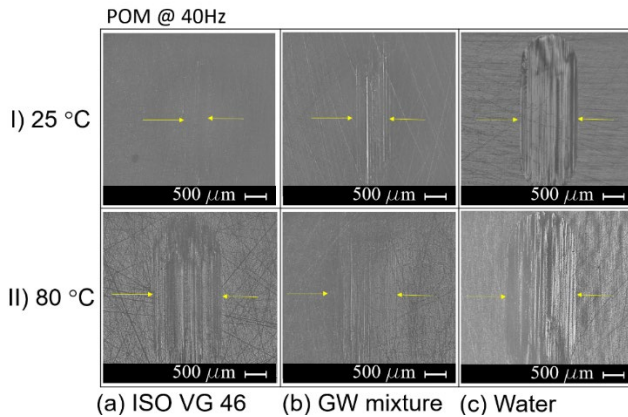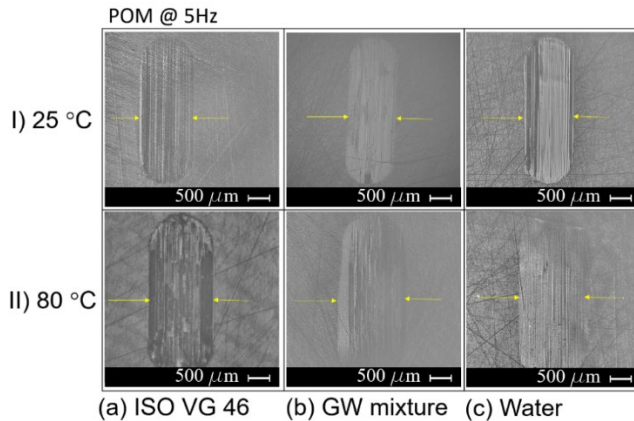

Figure 4: Digital images of POM wear tracks after sliding against still ball at: I) room and II) elevated temperature when lubricated with: a) ISO VG 46 oil; b) glycerol + water mixture; c) water at 40 Hz.

Source: own.

Figure 5: Digital images of POM wear tracks after sliding against still ball at: I) room and II) elevated temperature when lubricated with: a) ISO VG 46 oil; b) glycerol + water mixture; c) water at 5 Hz.
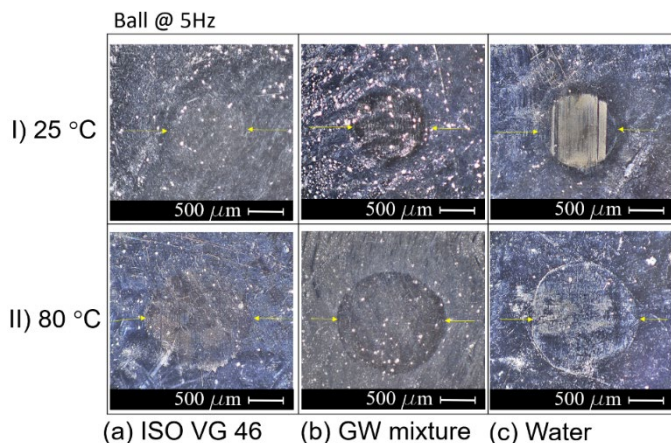
Source: own.

Figure 5: Sample.
Source: own.

Surface analysis showed that at lower frequencies, in the case of all three lubricants, the wear track is also present on the bearing ball (Figure 6) at both temperatures. The transfer film dimensions (almost regular circle) are comparable among lubricants. The width is smaller at room temperature (~ 800 μm, Figure 6.I.a-c), compared to elevated temperature (~ 1300 μm, Figure 6.II.a-c). At room temperature, the scratches were the most intense in water, while at elevated temperature some scratches could be observed in oil.

4   Discussion and conclusion

This study investigated the possibility of using an affordable engineering polymer POM in combination with a glycerol + water mixture as a green lubricant as a potential polymer/steel tribo-pair for hydraulic applications. For reference and comparison, the same contacts were tested in typical ISO VG 46 hydraulic oil and demineralised water, the most widely available green base lubricant. The experiments were performed with parameters that correspond to the seat on-off valves, which could potentially become lighter and have excellent tribological properties. The tests were conducted at room temperature and elevated temperature with the samples fully immersed in the selected lubricant. The tests were performed at two different sliding speeds.

A. Trajkovski et al.: Polymers For Sustainable Hydraulic Valves Tested in Water, Glycerol-water Mixture and Hydraulic Oil

277

Glycerol is an alternative lubricant whose annual production exceeds the demand for the same. Because of its high viscosity, glycerol has already been used in research on steel/steel tribological contacts [18, 21]. Recently, an environmentally friendly commercial glycerol-based lubricant has been used in the literature to study the tribological properties of modern commercial polymer materials and compared with water and dry contact [19]. The glycerol-based lubricant further improved the tribological properties of the observed materials. Our recent study also proved good tribological properties of pure glycerol for five different polymer composites [20]. Among observed composites, POM reinforced with 30 % carbon fibres successfully followed high performance PEEK reinforced with 30 % carbon fibres by tribological performance.

The results of this study show low values of the coefficient of friction of the POM /steel contact when glycerol + water mixture is used as lubricant, at room temperature and elevated temperature and at both frequencies tested. The values of the coefficient of friction were similar when comparing glycerol + water mixture and ISO VG 46 hydraulic oil. At room temperature, the coefficient of friction was about 3.7 times higher for water than for oil and glycerol + water mixture. At elevated temperature, however, the difference was not significant, although the lowest value was measured in the glycerol + water mixture (0.029). At lower frequencies, a similar trend was observed, although the coefficient of friction in oil increased at lower frequencies and, in contrast, decreased in the glycerol + water mixture and in pure water.

The specific wear rate was also lowest in the glycerol + water mixture, especially at room temperature (5.68×10^{-9} mm^3/Nm). However, the results were comparable to those obtained with hydraulic oil. When comparing glycerol + water mixture and oil with water as lubricant, we measured one order of magnitude higher specific wear rate. At higher temperatures, the difference between the lubricants decreased almost completely and an increase in the specific wear rate was observed (the order of $\times 10^{-7}$ mm^3/Nm). At lower frequencies, a higher specific wear rate was observed, which is related to the formation of a transfer film that was present on the steel ball in all tests at lower frequencies. However, at higher temperatures, all specific wear rate values increased and there was no significant difference between the lubricants (the order of $\times 10^{-6}$ mm^3/Nm). Water proved to be a less effective lubricant at both

frequencies and at room temperature compared to a mixture of glycerol and water and oil. At higher temperature, however, the difference decreased significantly.

In our previous study, POM, which was reinforced with 30 % carbon fibres, was tested under similar conditions [20], and in our preliminary study the tests were repeated at elevated temperature. A similar trend was observed in the measured coefficients of friction (influence of water, higher temperature, or lower frequency), but higher values were measured overall for pure POM than for POM reinforced with 30 % CF. In contrast, lower values of specific wear rate were observed for pure POM compared to reinforced POM. This effect is probably due to the fact that in the case of reinforced POM the carbon fibres carry most of the applied load, but at the same time the thinning of the fibres indicates a fracture of the POM matrix and a higher wear rate [22]. However, further elemental or spectroscopic analysis of the worn surfaces is required to discuss the difference in detail. Based on the current measurements, pure POM gives excellent tribological results in both hydraulic oil and a glycerol-water mixture and can be considered as a potential material or even a combination of material and lubricant for hydraulic applications where low load and high frequency are expected.

References

[1]   Stryczek J, Banaś M, Krawczyk J, Marciniak L, Stryczek P. The Fluid Power Elements and Systems Made of Plastics. Procedia Eng 2017;176:600–9. https://doi.org/10.1016/J.PROENG.2017.02.303.

[2]   Elasswad M, Tayba A, Abdellatif A, Alfayad S, Khalil K. Development of lightweight hydraulic cylinder for humanoid robots applications. Https://DoiOrg/101177/0954406217731794 2017;232:3351–64. https://doi.org/10.1177/0954406217731794.

[3]   Li Y, Shang Y, Wan X, Jiao Z, Yu T. Design and experiment on light weight hydraulic cylinder made of carbon fiber reinforced polymer. Compos Struct 2022;291:115564. https://doi.org/10.1016/J.COMPSTRUCT.2022.115564.

[4]   Panin S V., Alexenko VO, Buslovich DG. High Performance Polymer Composites: A Role of Transfer Films in Ensuring Tribological Properties—A Review†. Polymers (Basel) 2022;14:975. https://doi.org/10.3390/POLYM14050975/S1.

[5]   Friedrich K. Polymer composites for tribological applications. Advanced Industrial and Engineering Polymer Research 2018;1:3–39. https://doi.org/10.1016/J.AIEPR.2018.05.001.

[6]   tribology-abc 2023. https://www.tribology-abc.com/ (accessed August 3, 2023).

[7]   Siddiqui MSN, Pogacnik A, Kalin M. Influence of load, sliding speed and heat-sink volume on the tribological behaviour of polyoxymethylene (POM) sliding against steel. Tribol Int 2023;178:108029. https://doi.org/10.1016/J.TRIBOINT.2022.108029.

[8]   Matkovič S, Pogačnik A, Kalin M. Wear-coefficient analyses for polymer-gear life-time predictions: A critical appraisal of methodologies. Wear 2021;480–481:203944. https://doi.org/10.1016/J.WEAR.2021.203944.

A. Trajkovski et al.: Polymers For Sustainable Hydraulic Valves Tested in Water, Glycerol-water Mixture and Hydraulic Oil

279

[9] Deuster S, Schmitz K, Widomski K, Barnat-Hunek D, Musz-Pomorska A. Bio-Based Hydraulic Fluids and the Influence of Hydraulic Oil Viscosity on the Efficiency of Mobile Machinery. Sustainability 2021, Vol 13, Page 7570 2021;13:7570. https://doi.org/10.3390/SU13147570.

[10] Strmčnik E, Majdič F. Comparison of leakage level in water and oil hydraulics. Research Article Advances in Mechanical Engineering 2017;9:2017. https://doi.org/10.1177/1687814017737723.

[11] Jeng Y-R, Tsai P-C, Chang C-M, Hsu K-F. materials Tribological Properties of Oil-in-Water Emulsion with Carbon Nanocapsule Additives n.d. https://doi.org/10.3390/ma13245762.

[12] Zhang T, Liu C, Gu Y, Jérôme F. Glycerol in energy transportation: a state-of-the-art review. Green Chemistry 2021;23:7865–89. https://doi.org/10.1039/D1GC02597J.

[13] Chen Z, Liu Y, Zhang S, Luo J. Controllable superlubricity of glycerol solution via environment humidity. Langmuir 2013;29:11924–30. https://doi.org/10.1021/LA402422H.

[14] Liu C, Qiao Y, Lv B, Zhang T, Rao Z. Glycerol based binary solvent: Thermal properties study and its application in nanofluids. International Communications in Heat and Mass Transfer 2020;112:104491. https://doi.org/10.1016/J.ICHEATMASSTRANSFER.2020.104491.

[15] Trejo González JA, Longinotti MP, Corti HR. The Viscosity of Glycerol−Water Mixtures Including the Supercooled Region. J Chem Eng Data 2011;56:1397–406. https://doi.org/10.1021/JE101164Q.

[16] Ma Q, He T, Khan AM, Wang Q, Chung YW. Achieving macroscale liquid superlubricity using glycerol aqueous solutions. Tribol Int 2021;160:107006. https://doi.org/10.1016/J.TRIBOINT.2021.107006.

[17] Shi Y, Minami I, Grahn M, Björling M, Larsson R. Boundary and elastohydrodynamic lubrication studies of glycerol aqueous solutions as green lubricants. Tribol Int 2014;69:39–45. https://doi.org/10.1016/J.TRIBOINT.2013.08.013.

[18] Björling M, Shi Y. DLC and Glycerol: Superlubricity in Rolling/Sliding Elastohydrodynamic Lubrication. Tribol Lett 2019;67:1–8. https://doi.org/10.1007/S11249-019-1135-1/FIGURES/2.

[19] Somberg J, Saravanan P, Vadivel HS, Berglund K, Shi Y, Ukonsaari J, et al. Tribological characterisation of polymer composites for hydropower bearings: Experimentally developed versus commercial materials. Tribol Int 2021;162:107101. https://doi.org/10.1016/J.TRIBOINT.2021.107101.

[20] Trajkovski A, Novak N, Pustavrh J, Kalin M, Majdič F. Performance of Polymer Composites Lubricated with Glycerol and Water as Green Lubricants. Applied Sciences 2023;13:7413. https://doi.org/10.3390/APP13137413.

[21] Habchi W, Matta C, Joly-Pottuz L, De Barros MI, Martin JM, Vergne P. Full film, boundary lubrication and tribochemistry in steel circular contacts lubricated with glycerol. Tribol Lett 2011;42:351–8. https://doi.org/10.1007/S11249-011-9778-6/FIGURES/6.

[22] Zhang L, Qi H, Li G, Zhang G, Wang T, Wang Q. Impact of reinforcing fillers' properties on transfer film structure and tribological performance of POM-based materials. Tribol Int 2017;109:58–68. https://doi.org/10.1016/j.triboint.2016.12.005.

AIR RELEASE OF USED HYDRAULIC MINERAL-BASED OILS

MILAN KAMBIČ,[1] DARKO LOVREC[2]

[1] Olma d.o.o., Ljubljana, Slovenia
milan.kambic@olma.si
[2] University of Maribor, Faculty of Mechanical Engineering, Maribor, Slovenia
darko.lovrec@um.si

The presence of air in the hydraulic system or in the hydraulic fluid itself, either in its elementary form e.g., as an air pocket or bubble, or in the form of dissolved air, causes much inconvenience. This is manifested in the form of unwanted operation of the hydraulic system, causing accelerated ageing of the fluid, especially mineral oil. Apart from knowing the measures to prevent air intrusion into the hydraulic system, it is also important to know the tendency of each type of hydraulic oil to foam and its air release property. A discussion of the air release property of mineral oil usually refers to different types of fresh hydraulic oils. How this property is reflected and changes in the case of already used and chemically degraded hydraulic oils is discussed in the present paper.

1   Intruduction

Air in the hydraulic fluid, in its elemental form as an air pocket or air bubbles, is certainly a very undesirable, annoying and aggressive contaminant that causes a whole range of inconveniences. From a mechanical point of view, it causes increased compressibility and too elastic operation of the hydraulic system, and, from a chemical point of view, it causes faster ageing of the hydraulic oil.

In addition to the increased compressibility of the fluid and the resulting effect on the stiffness of the hydraulic components and the entire system, slower reaction times, as well as the occurrence of oscillation in the system in a mechanical sense, air causes a whole range of other inconveniences. For example, due to the incomplete filling of the pump chamber, it also affects the reduction of the actual flow of the pump and, thus, lowers volumetric efficiency, increased heating of the pump and noise, the occurrence of cavitation and the related wear of the material, a worse lubricating effect of the liquid and a reduced load capacity of the lubricating film, the diesel effect and damage to seals and smooth surfaces, etc. Apart from that, the present air also has a negative effect on accelerated oxidation (ageing), e.g., the hydraulics, causing the formation of deposits in the tank and on the components (sludge and varnishing).

Considering the whole range of negative effects, air is undesirable in the hydraulic system and is treated as a very "aggressive" contaminant and its presence in the hydraulic system is prevented and reduced. Therefore, it is necessary to remove it and ensure that it does not enter the hydraulic system in various ways.

In the literature, we can find a whole range of different tips and recommended measures to prevent air from entering the hydraulic system (aeration) or the formation of air in the system itself. The correct design of the shape and interior of the tank, care for flawless sealing of the hydraulic connections, is definitely one set of measures. The second set of measures refers to the possibilities of air extraction. In connection with this, it is certainly necessary to vent the system carefully during the first start-up of the hydraulic system, as well as measures for the effective elimination of air bubbles. Of course, if air bubbles have already appeared in the system, e.g., in the tank, we must prevent them from accessing the suction port of the pump in any way.

When we talk about air inside a hydraulic system, we must not only think of air in its elementary form, of air bubbles. We also have to think about the non-negligible proportion of chemically dissolved air in the oil, under certain conditions, can be released from the oil and appear in its elemental form, as an air bubble.

Chemically bound, dissolved air in the hydraulic fluid itself and its negative effect are mentioned much less, although we know that in mineral hydraulic oil there is from 7 % to 9 %, or even a few more percent, of dissolved air. Dissolved air cannot be seen with the naked eye, and since it is not present and visible in its elemental form as an air bubble, it does not cause the mentioned harmful effects directly in this form. Therefore, in this form, it is of secondary importance, and affects the operation of the device and the condition of the oil. The situation changes when, due to a change in pressure, the pressure in a local part of the hydraulic system falls below the value of the vapour pressure (a certain negative pressure), the dissolved air is released as an air bubble.

2 Mechanism of air bubble release

The presence of air in various forms and in fluids has long been the subject of many studies. The same applies to studies related to the knowledge of the physical background of air generation and release, as well as their influence on the operation of the hydraulic system. The findings were summarised by many other authors. ([1] to [11])

When air bubbles appear, regardless of the cause of their origin, we must remove them from the hydraulic system as quickly as possible. The efficiency of the elimination of air bubbles depends on many factors: on the shape and dimensions of the tank, on the flow conditions in the tank, on how the hydraulic fluid is returned back to the tank, on the operating conditions in the hydraulic system, e.g. the operating temperature, and also from the type of hydraulic fluid installed, most often hydraulic mineral oil.

At the same time, we must not forget the presence of other contaminants, such as water and solid contaminants, and the degree of fluid degradation, which all affect the effectiveness of the released air additionally.

2.1   Solubility of gases in oil

As mentioned, in addition to aeration, the proportion of dissolved air is important. In general, lubricating oils, including hydraulic oils, can dissolve significant amounts of gases (here, air). In addition to the type of base oil, the amount essentially depends on the pressure and the temperature. The degree of refinement of a mineral oil, the viscosity and the presence of active ingredients do not have a pronounced influence on the air solubility. The Henry-Dalton law applies to the dissolved gas volume in ml:

$$V_{Gas} = \alpha_V \frac{V_{Oil}\ p_2}{p_1} \qquad\qquad [ml] \qquad\qquad (1)$$

Table 1 gives approximate values of dissolved air in percentages, typical for different lubricating oils under normal conditions (20 °C and 1013 mbar). [6]

Table 1: Dissolved air in the lubricating oil

Fluid type	Bunsen coefficient
Mineral based oil	0.07 to 0.09
Silicone oil	0.15 to 0.25
Phosphate ester	About 0.09
Vegetable (bio) oil	About 0.09
Water	About 0.0187

The values listed in Table 1 show that the volume content of air in mineral hydraulic oils is between 7 % and 9 %. The Bunsen coefficient gives the volume ratio between the amount of gas dissolved in a fluid under normal conditions and the volume of the fluid. The dissolution of air bubbles when the pressure increases requires a certain amount of time. For mineral oils with a low viscosity (around 10 mm²/s at 40 °C) and 20 bar, this amounts to around 20 s. An oil with a higher viscosity, 40 mm²/s at 40 °C, requires around 60 s. [6] With increasing pressure, the solubility of air in mineral oil increases according to Henry Dalton's law.

For mineral oil products, the solubility of various gases can be calculated according to the ASTM method D 2779. It is only necessary to know the density value of the petroleum product and the type of dissolved gas.

Standard ASTM D 3827 specifies a calculation method that applies not only to mineral oil products, but also to other organic fluids (synthetic oils). The separation of air bubbles when depressurising occurs much faster than the gas absorption when the pressure increases.

The solubility of air decreases with the increasing viscosity of a base oil, i.e. with increasing average molecular weight, Table 2. [12].

Table 2: Dissolved air in the lubricating oil

Average molecular mass [g/mol]	Volume content of air [%]
670	7.83
610	7.92
570	8.43
530	8.78
400	9.03

Note: The density and molecular weight of a chemical are directly proportional to each other, and the density and volume of a chemical are inversely proportional to each other. As the molecular weight of a chemical increases then the density of the chemical increases.

2.2   Finely distributed air in the lubricating oil

In addition to dissolved air, lubricating oils can absorb additional amounts of air, distributed finely as the disperse phase during operation. This distribution of air in oil is often called aero-emulsion, air emulsion or also spherical foam. Air-in-oil dispersions are undesirable for the operation of hydraulic systems in almost all cases, since a number of (already mentioned) disadvantages arise from the presence of free air. [13], [14], [15]

Air dispersed in oil leads to an increase in viscosity, which can be estimated using the following approximation equation ([16]):

$$\eta_{Air} = \eta_{Oil} + \eta_{Oil} \cdot 0.0015 \cdot X \qquad (2)$$

The equation shows that a volume content of 10 % air in the oil leads to a viscosity that is around 15 % higher.

The distribution of undissolved air in the lubricant can be reduced by the already mentioned design measures, and/or by the composition of the oil. The constructive possibilities include the following measures, some of which have already been mentioned, such as: Low oil circulation number due to large oil volume, low height of the oil tank, long distances between the oil entry point in the tank and the intake line, air release devices provided, attach the intake manifold as low as possible below the surface and avoid sharp edges of the deflections in the system.

The material factors of hydraulic oil, which play an important role in the elimination of air, are: The degree of refining of the mineral oil, the viscosity and the presence of certain active ingredients, e.g., the presence of water, oil ageing products, and also the cleanliness level of the oil.

All of these influential factors also affect the speed and efficiency of the elimination of air bubbles from the fluid.

2.3   Air release mechanism

The theoretical rise time of an air bubble in clean mineral based oil can be calculated with a good approximation using Stok's law. It is proportional to the kinematic viscosity of the fluid, and inversely proportional to the square of the bubble`s diameter. The buoyancy force of an air bubble is expressed as [11]:

$$F_{\text{Buo}} = \frac{4}{3}\pi \, (\rho_{\text{Fl}} - \rho_{\text{Air}})r^3 g \quad [\text{N}] \tag{3}$$

Consideration of the drag force in the motion of spherical bodies, according to Stokes, for very small Reynolds numbers:

$$F_{\text{Drag}} = 6 \, \pi \, \eta \, v \, r \quad [\text{N}] \tag{4}$$

leads to an expression for the rate of rise of the air bubble:

$$v = \frac{2}{9} \, (\rho_{\text{Fl}} - \rho_{\text{Air}}) \, \frac{r^3 \, g}{\eta} \quad [\text{m/s}] \tag{5}$$

Here, in equations (3), (4) and (5), r represents the radius of the bubble, ρ_{Fl} the density of the fluid, and ρ_{Air} the density of the air.

According to research by Hayward [16], the most commonly encountered bubble diameter is 0.25 mm to 0.5 mm. The operating viscosity for most industrial hydraulics is between 20 mm²/s and 30 mm²/s. According to this, the time it takes for a bubble to rise a metre in still oil is theoretically about 6 to 9 minutes on average. Since the viscosity of a hydraulic fluid depends very much on the temperature, the air bubbles rise faster at higher temperatures due to the lower viscosity. The actual rise time is considerably longer, depending on the type of oil, impurities/contaminants and water content, so this fact should be taken into account sufficiently when designing the oil tank.

Based on the Stokes equation, it can be seen that the rate of bubble rise decreases as the bubbles become smaller, Figure 1.
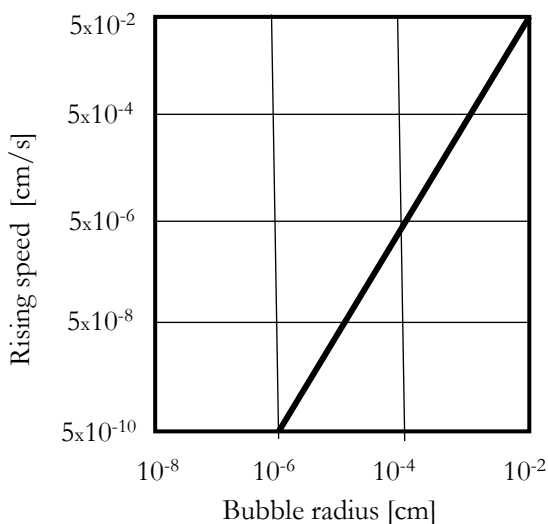
Figure 1: Rising speed of air bubbles depending on the bubble radius.
Source: own.

The ability of a fluid to remove dispersed air bubbles is called air release capacity – LAV (The commonly used abbreviation LAV for air release capacity originated from the German language: Luftabscheidevermoegen). Apart from the abbreviation LAV, the abbreviation ARV - Air release value is also often used for the same purpose.

The LAV of mineral oils is affected by viscosity, temperature and the presence of additives. Based on Stoke's law for the effect of viscosity, the higher the value of viscosity, the slower the air release. A general relationship that applies to all base oils cannot be given, because, depending on the origin and refining process, there is a different interfacial tension, and, thus, a different bubble size, Figure 2.
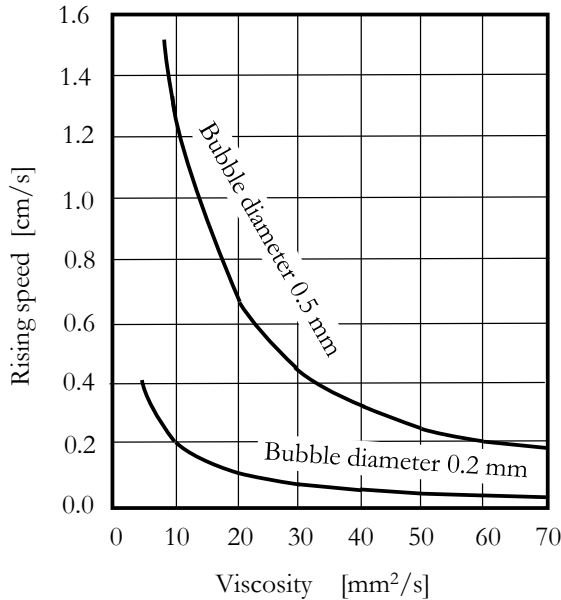
Figure 2: Theoretical rising speed of air bubbles of different diameters, depending on their viscosity.
Source: own.

The viscosity value is influenced greatly by the temperature of the oil. As the temperature increases, and, consequently, the viscosity decreases, the LAV behaviour improves.

All active ingredients that reduce the surface tension of the liquid have a negative effect on the LAV. In the case of corrosion inhibitors, detergents and oxidation inhibitors, this effect is generally neglected.

3   LAV Method of various hydraulic fluids

The standardised method for determining the LAV is the so called Impinger-method according to the DIN 51 381 Standard. For this purpose, air is blown through a capillary into the oil in an Impinger gas washing bottle at a defined temperature for

seven minutes. The release of the dispersed air is monitored with a hydrostatic balance, by measuring the density until the value of the air-bubble-free sample is reached. The LAV is given in minutes for the time after which the oil still contains 0.2 % by volume of dispersed air.

There are several standard and non-standard methods for determining foaming, air content and its elimination, and they are more or less similar (see [17]). Today, the most widely used method of determining LAV is according to the ASTM D 3427-19 Standard. The test procedure is performed under a standardised set of test conditions, and hence permits the comparison of the ability of oils to separate entrained air under conditions where a separation time is available. [18]

According to the ASTM D 3427-19 Standard, the time required for the fluid to release the contained air is measured at different temperatures, at 25 °C, 50 °C and 75 °C. For the practitioner, the most interesting is certainly the performance of the test at 50 °C, which is considered as the recommended operating temperature, at which the hydraulic device also operates most of the time.

Depending on the composition of the hydraulic fluid, both in terms of base stock and the additive package it contains, the air release properties can vary substantially. Figure 3 shows a range of air release values associated with different mineral oil types. [19], [20]

	Oil	Grade	Minutes to 0.2% vol. air	
			25°C	50°C
A	Hydraulic	ISO 32	—	3
B	Turbine	ISO 32	4	2
C	Hydraulic	ISO 46	—	6
D	Turbine	ISO 46	7	3
E	Turbine	—	10	5
F	E + 1.0% oil J		10	5
G	E + 0.5% water		56	—
H	Hydraulic	ISO 100	—	13
I	Turbine	ISO 100	14	6
J	MIL-L-2104B diesel	SAE 30	77	—
K	J + 0.5% water		115	—

Figure 3: Air release properties of various oil. [19]

When it comes to air bubbles in oil, the results usually refer to fresh hydraulic oils or other types of hydraulic fluids. However, it is (almost) not stated anywhere precisely, and possibly given a limit value, how it is with the elimination of air bubbles in variously degraded used oils.

4   Air release properties of used mineral hydraulic oils

It is true that the air release of diverse types and the composition of fresh oil is undoubtedly important, but in most cases of industrial use, there is a much larger amount of used oil in hydraulic systems than fresh oil. There is also no guarantee that efficient air release of fresh oil will ensure efficient air release when the same oil will be degraded. For this reason alone, it makes sense to look for correlations between different levels of oil degradation and changes in the physical-chemical properties of the oil and the ability to eliminate air. The degree of air release could, perhaps, be one of the parameters on the basis of which we could judge the suitability of further use.

The air release capacity and the tendency to foam are influenced negatively by contaminants such as particles and water, as well as oil products, e.g., by the increase in viscosity as a result of oil oxidation and additive consumption. Also, the mixing of different types of oil has an effect on the air release capacity and the tendency to foam, e.g., by the entry of incompatible additives. Contaminants can arise from both external and internal sources. Examples of external sources can be other types of oil, other fluids, e.g., water, and dirt. The presence of water can reduce viscosity, since it becomes emulsified. Figure 3 includes some examples of the adverse effect on air release of small amounts of water.

Also, the products of the thermal degradation process or oil ageing lead to a change in viscosity and density. The same applies to acidic oxidation products, which, in turn, lead to changes in LAV. [19]

4.1   LAV of accelerated aged oils

In order to determine changes in the physical and chemical properties of variously degraded mineral hydraulic oils, we used our own developed procedure for accelerated thermal ageing of the oil, the so-called dry thermal test. The test is similar to the TOST test, where, at an elevated temperature (150 °C), the presence of copper

and oxygen in the air in the role of catalysts or accelerators of thermal oil degradation led to faster oil degradation. More details on the procedure and test execution can be found in [21]. The thermal loading of the sample lasted for a certain number of hours, after which all those physical-chemical properties were measured, which are usually changed due to degradation and could also affect the LAV. The results are summarised in Table 3. Hydraulic mineral oil of the HL type and viscosity class ISO VG 46 was used for the test.

Table 3: Results of the analysis of samples after hours of accelerated ageing

Hydraulic oil HL ISO VG 46	HL 0	HL 40	HL 60	HL 110
Testing time [h]	0	40	60	110
Colour [-]	2.0	6.0	> 8.0	> 8.0
Density @ 20 °C [kg/m³]	876	876	877	879
Viscosity @ 40 °C [mm²/s]	46.45	48.35	49.30	62.18
Viscosity @ 100 °C [mm²/s]	6.91	7.06	7.18	8.08
Neutralisation No. [mg KOH/g]	0.54	0.65	0.72	1.9
FT-IR Oxidation [-]	0.31	0.43	0.64	2.30
LAV @ 50 °C [min]	**5.7**	**6.1**	**5.8**	**6.1**
Foaming - Sequence I [ml/ml]	**0/0**	**20/0**	**0/0**	**610/0**
Foaming - Sequence II [ml/ml]	**30/0**	**20/0**	**10/0**	**30/0**
Foaming - Sequence III [ml/ml]	**0/0**	**0/10**	**0/0**	**570/50**
Electrical conductivity [pS/m]	607	853	1121	9219

Table 3 shows clearly those physical-chemical parameters and their values that are at the forefront of consideration - LAV and foaming. Increasing values for viscosity, neutralisation number, FT-IR oxidation and also values for colour and electrical conductivity, show clearly the degree of oil degradation as a result of thermal stress under the influence of the ageing process accelerators.

It is evident and interesting from the results that, after the accelerated thermal ageing of the oil, the value of the LAV had hardly changed (small fluctuations in the value are a possible result of the precise assessment of the determination of the end of the test - the difference in times amounts to 6%). In principle, changes in LAV coincide with changes in density, which changed minimally. However, the viscosity of the aged oil changed significantly, and the foaming of the oil worsened a lot.

Since accelerated thermal ageing of the oil was used in this case, in which no noteworthy changes in LAV were detected, it is certainly reasonable to check whether a similar pattern of changes also occurs in "naturally" aged oils - after a certain period of operation. It should be noted that the hours of the accelerated

thermal degradation process are equivalent to several months, or even years, of naturally degraded oil.

4.2 LAV of naturally aged oils

Similar changes in the quantities mentioned in the previous chapter can also be expected in the case of naturally aged oil, on a real hydraulic device, except that the time of appearance of the change is significantly longer (several tens of days, or even months).

Monitoring of the state of the physical-chemical parameters of hydraulic oils in industrial use is usually carried out at certain time intervals, usually every two months. In this case, the test operator usually does not know the actual number of operating hours during this period, so there may be deviations or less credible results. Also, other operating parameters, such as, e.g. ambient temperature, ambient humidity, or something else.

Table 4 shows only some of the parameters of an otherwise wide range of comprehensive analysis for the case of naturally degraded oil and a two-month sampling interval for a period of eight months. The values for LAV and foaming are in the foreground. ISO VG 46 hydraulic mineral oil was used as the oil.

Table 4: Comparison of viscosity, foaming, and air release properties of naturally degraded hydraulic oils

Sample	Hydraulic oil ISO VG 46					
Date	9.2022	11.2022	1.2023	3.2023	2.2023	7.2023
Density @ 20 °C [kg/m³]	871	871	871	871	871	871
Viscosity @ 40 °C [mm²/s]	45.76	46.43	46.48	46.60	46.31	46.59
Viscosity @ 100 °C [mm²/s]	7.199	6.859	6.886	6.963	6.939	6.976
LAV @ 50 °C [min]	6.3	4.8	4.7	5.4	4.4	4.4
Sequence I [ml/ml]	0/0	0/0	0/0	0/0	190/0	430/0
Sequence II [ml/ml]	70/0	20/0	40/0	50/0	30/0	30/0
Sequence III [ml/ml]	20/0	20/0	0/0	270/0	30/0	480/0

Even in the case of naturally aged oil, it turned out that the LAV value changes very little, but the foaming much more. The release of air depends much more on the type of fluid, basic physical-chemical values such as density and viscosity, and also on the type of additives present.

6   Conclusion

The operation of the hydraulic system is certainly influenced by the type of built-in fluid and its basic material properties, such as density and viscosity, temperature behaviour, type of additives and base fluid, and more, as well as the presence of air and its ability to be released. As is known, the air present in the hydraulic fluid causes a whole range of negative effects, from a direct effect on the dynamic behaviour of the system, to an indirect effect on the faster ageing of the fluid, for example hydraulic mineral based oil. For this reason, the fluid's ability to eliminate air from the system as quickly as possible is one of the important properties that may not be given enough detail. The latter property is determined by a standard test to determine the air release.

The paper presents the mechanisms that affect air release, and summarises some findings from some previous studies. Typically, these findings apply to unused, fresh hydraulic oils. In the continuation of the paper, the focus of discussion is on the ability to release the air of used, already degraded hydraulic oils. The results related to the efficiency of air release and the occurrence of foaming are shown for two cases: for the case of accelerated thermally degraded oil, and for the case of naturally degraded oil under real industrial operating conditions.

Both in the case of oil with accelerated ageing and naturally aged oil of the same type, it was found that the LAV value changes very little, but it foams much more. Based on this, we can conclude that the type of liquid, especially its density and viscosity, as well as the type of base oil, have a much greater impact on LAV.

References

[1]   Hayward, A.T.J. (1961). Aeration in Hydraulic Systems - It's Assessment and Control, *Proc. Inst. Medi. Eng. Conf. Oil Hydraulic Power and Control*, Instn. Mech. Engrs., 216-224.
[2]   Hayward, A.T.J. (1963). How to keep Air Out of Hydraulic Circuits. *A publication of the National Engineering Laboratory*, East Kilbride, Glasgow.
[3]   Magorien, V. G. (1968). How Hydraulic Fluids Generate Air. *Hydraulics & Pneumatics*, 104-108.
[4]   Fowle, T.I. (1981). Aeration in Lubrication Oils, *Tribol. Int.*, 14, 151-157
[5]   Staeck, D. (1983). Gases in Hydraulic Oils. Tribologie & Schmierungstechnik, Vol 34, No. 4, 201-207.
[6]   Hamann, P. W., Menzel, O., Schroeder, H. (1978). Gase in Ölen. *Fluid*, 12, Nr 9, 24-28.
[7]   Claxton P.D. (1972). Aeration of Petroleum Based Steam Turbine Oils. *Tribology*, February, 8-13.

[8]   Tsuji, S., Katakura, H. (1978). A Fundamental Study of Aeration in Oil 2nd Report. The Effects of the Diffusion of Air on the Diameter Change of a Small Bubble Rising in a Hydraulic Oil, *Bulletin of the JSME*, 21 (156), 1015-1021, https://doi.org/10.1299/jsme1958.21.1015.

[9]   Blok, P. (1995). The Management of Oil Contamination, Koppen & Lethem, Aandriftechnieck B.V. Neederland, ISBN: 9090084584.

[10]   Suzuki, R. (2019). Removing Entrained Air in Hydraulic Fluids and Lubrication Oils. *Machinery Lubrication,* Noria Corporation, www.machinerylubrication.com/Read/373/entrained-air-oil-hydraulic

[11]   Möller, U.W., Nassar, J. (2002). *Schmierstoffe im Betrieb*, Springer-Verlag Berlin Heidelberg, ISBN 978-3-642-62620-3, pages 873.

[12]   Hörner, D. (1980). Luft-Aufnahme und-Abgabeverhalten (LAAV) von Getriebeölen und Hydraulikflüssigkeiten. *Mineralöltech* 25 Nr. 6: 1–23.

[13]   Hofer K. (1978). Luft im Öl. *Betriebstech.* 16 Nr 11: 29–30.

[14]   Magorien, V.G. (1980). Keeping air out of hydraulic systems. *Mach. Design.* 52 Nr 18: 71–76.

[15]   Fowle, T.J. (1981). Aeration in lubricating oils. *Tribology Int.* 9 Nr 6. 151–15.

[16]   Hayward, A.T.J. (1962). The viscosity of bubbly oil. *J. Inst. Pet.* 48 Nr 461, 156–164-

[17]   Totten, G.E., De Negri, V.J. (2011). Handbook of Hydraulic Fluid Technology, *CRC Press*; 2nd edition, 982 pages.

[18]   ASTM D3427-19. (2020). Standard Test Method for Air Release Properties of Hydrocarbon Based Oils, *ASTM International*, West Conshohocken, PA, last Updated: Jan 22, 2020.

[19]   Phillips, W. D. (2006). The high-temperature degradation of hydraulic oils and fluids, *Journal of Synthetic Lubrication*, 23: 39–70, Published online in Wiley Interspine, daoi: 10.1002/jsl.11.

[20]   Jackson, T.L. (1981). Hydraulic oil blackening. *Proc. 6th Int. Fluid Power Symp.* Cambridge, April, Paper B1.

[21]   Tič, V., Lovrec, D. (2017). On-line condition monitoring and evaluation of remaining useful lifetimes for mineral hydraulic and turbine oils. 1st ed. *University of Maribor Press,* ISBN 978-961-286-130-8. doi: 10.18690/978-961-286-130-8.

Air Release of Used Hydraulic Mineral-based Oils

Maja Vidmar, Aleš Hrobat, Milan Kambič

Olma d.o.o., Ljubljana, Slovenia
maja.vidmar@olma.si, ales.hrobat@olma.si, milan.kambic@olma.si

Among the properties of oil, air release and foaming tendency are very important. This is mainly because oil fills are getting smaller and the associated circulation times are getting shorter. The oil has less and less time to release air in the tank before it is recirculated. When we use additives to reduce the tendency of the oil to foam, we usually also decrease the rate at which the air is released from the oil. It is therefore a challenge for lubricant manufacturers to harmonise these two properties. This paper will present measurements of both foaming and air release from the oil. Requirements for fresh hydraulic oils will be given as a point of reference. The influence of different viscosity grades of fresh mineral hydraulic oils will be shown. The results of the measurements on different types of base oils will be presented.

1   Intruduction

Hydraulic fluid is an essential component of hydraulic system that is often overlooked. Besides the main purpose of power transmission, it also performs various other functions, including reducing friction and wear, preventing leakage, removing heat, flushing away wear particles and contaminants, and protecting surfaces from rust and corrosion. The oil quality required for hydraulic systems depends on the specific application and components used [1]. Viscosity, viscosity index, wear protection, oxidation stability, antifoam and air separation characteristics, demulsibility, rust protection, and compatibility are important characteristics of hydraulic fluids.

Air release and foaming tendency are critical properties of hydraulic oils, especially as oil fills are getting smaller and circulation times are getting shorter. Lubricant manufacturers face the challenge of balancing these two properties.

This paper presents measurements of both foaming and air release from the oil, along with requirements for fresh hydraulic oils as a reference point. The influence of different viscosity grades of fresh mineral hydraulic oils will be shown, as well as the results of measurements on various types of base oils, including used hydraulic oils.

2   Air content in oil and its consequences

Hydraulic devices typically have proportions of undissolved air around 5 vol. % up to 10 vol. % in size. This applies particularly to mobile hydraulics. Often, the fluid cannot remove air bubbles, impurities and cool down, which can cause oil to foam excessively. Air can get trapped inside the device for various reasons and in different forms. The trapped air can be seen by the naked eye, forming a foam or tiny air bubbles. Alternatively, it can be dissolved in a liquid and remain "invisible". The "invisible" (dissolved) air could be also detected in the form of bubbles when the operating conditions change (e.g., pressure), which is also closely related to the design of the individual hydraulic components [2], [3].

The most common causes of the air presence in the oil are certainly the intrusion of air through leaky places (so-called aeration), unsuitable design of the components of the hydraulic system (e.g., tank, pipe network, valves and valve blocks...) or significant inappropriate changes in the operating point related to the design of the hydraulic devices.

Foams that appear on the surface of the liquid in the tank are not directly dangerous and do not affect the compressibility of the hydraulic fluid. Air bubbles that are in the fluid itself are threatening, which leads to various consequences. Thus, the presence of air bubbles in the device primarily affects the compressibility or fluid stiffness, which in turn has a greater or lesser impact on the operation of the hydraulic device itself, such as the accuracy of actuator movement, the occurrence of oscillations, the transmission of signals, the need to change the settings of the regulator parameters, etc.

Air-containing hydraulic oil impairs the lubricating abilities of the oil itself and has an adverse effect on the ageing of the oil. That often leads to premature oxidation of the oil or even to its burning, destruction of seals and consequent leakage, besides this cavitation could occur on the pump and other elements [3], [4].

3   The influence of base oil and additives on foaming

Base oils typically have a low foaming tendency and good stability, though this can vary based on the source of the crude oil and its processing. Studies indicate that there is a direct correlation between foaming tendency and surface tension. If the foam is generated mechanically, using synthetic oil may help decrease the impact of foaming.

- Polyalphaolefin (PAO) and hydrocracked oils have a lower tendency to foam due to their high surface tension compared to petroleum hydrocarbons.
- Organic esters without additives do not foam, but they are easily contaminated or affected by additives.
- Polyglycols (PG) can be challenging to classify due to their ability to absorb water, which may affect their foaming behaviour.

Foam production is highest in base oils with a viscosity of 280 mm²/s, as noted in reference [5]. Lower or higher viscosity can decrease foam amount and stability.

A commonly used additive in detergent oils to prevent foam is based on silicone, specifically polydimethylpolysiloxane (PDMS). Silicones have a low surface tension and tend to gather at the interface of air and oil. To be effective in preventing foam, the silicone must be insoluble in oil and the particles should be less than 5 to 7 microns for long-term performance. The way antifoam additives work is by contacting a bubble's film and spreading around it, thinning the bubble wall until it ruptures. One property of silicones is their higher density compared to surrounding fluids, which slows the ascent of bubbles to the surface. Figure 1 illustrates the effects of silicone on air release, showing that silicone reduces the number of bubbles formed but may also retain them longer during a settling phase.
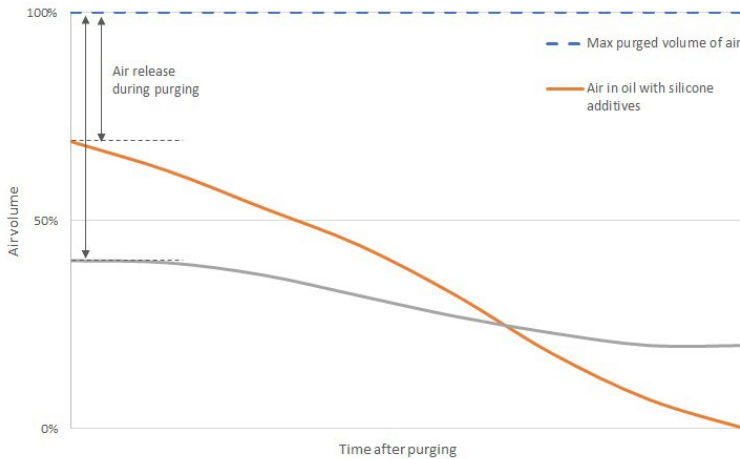
Figure 1: Device for determining air release.
Source: own.

4   Measurements of air release and foaming

In order to prevent or reduce the negative effects of air in oil, it is important for the oil to quickly separate any excess air. This behaviour is known as air release property and is determined in the laboratory. Factors such as the type of base oil, additives, viscosity, and temperature can influence the air release value (ARV; also, using the

abbreviation from German, LAV). Additionally, impurities and mixtures can affect the size of air bubbles. Comparing the ARV of used oil to that of fresh oil or a previous analysis can help determine the cause of operational failures or damage, as well as provide insight into continued usage. By examining other analysis values, conclusions can often be drawn regarding why the ARV value has deteriorated.

To determine the ARV using ISO 9120 and ASTM D3427 standards, the air is discharged into a 200 ml sample of the oil being analysed. The time it takes for the air to separate from the oil until only 0.2 vol. % remains is measured in minutes. Preheated air is discharged through a nozzle at a fixed pressure for a specific period of time, and the dispersed air bubbles gradually escape the oil due to its density. This process is recorded graphically until the volume no longer changes. The time from when the air intake is switched off until the density no longer changes is known as the air release time [6]. The device used for determining air release is depicted in Figure 2.

Figure 2: Device for determining air release.
Source: own.

The measurements were carried out in accordance with ASTM D3427. To ensure a proper comparison, all samples were measured at 50 °C regardless of their viscosity.

To assess the foaming properties of hydraulic oils, a few standards can be used, such as ASTM D892, DIN 51566, and IP 146. The ASTM D892 method was utilized to measure the foaming of the samples. This method involves determining the foaming characteristics of lubricating oils at 24 °C and 93.5 °C. The measurements were

performed using Linetronic Technologies device LT/FB - 192000 [7], shown in
Figure 3.

Figure 3: Device for determining foaming properties of lubricating oils.
Source: [7]

The measurement process begins with 190 ml of the sample being heated to a
particular temperature in two parallel measurements, based on the sequence.
Preheated air is discharged via a spherical, porous stone into the sample of oil. This
leads to an air in oil dispersion in the form of fine bubbles which rise to the surface
and create a layer of foam. The foam volume is measured immediately after the air
is switched off and again after 10 minutes. Table 1 outlines the specific parameters
for temperature, airflow, and aeration time for each sequence.

**Table 1: Parameters of temperature and aeration time for each sequence for determination
foaming characteristics of lubricating oils**

Sequence number	Temperature / °C	Air flow / ml/min	Aeration time / min	Waiting time/ min
I.	24			
II.	93.5	94	5	10
III. (sample from II.)	24			

To ensure that the oil can be used for an extended period, it is essential to have good
output values. Therefore, it is important that the air release and foaming properties
of newly bought hydraulic oils do not exceed the limit values mentioned in Table 2.

Table 2: Requirements for foaming and air release properties of fresh hydraulic oils

Hydraulic oil type	Requirements				
Designation according to DIN	HLP 22	HLP 32	HLP 46	HLP 68	HLP 100
Designation according to ISO	ISO VG 22	ISO VG 32	ISO VG 46	ISO VG 68	ISO VG 100
ARV_{max} at 50 °C / min	5	5	10	13	21
Foaming$_{max}$ /ml 24 °C (sequence I.) 93.5 °C (sequence II.) 24 °C (sequence III.)	150/0 75/0 150/0				

Source: DIN 51524-2

5 Foaming and air release of fresh hydraulic and base oils – results

The fresh hydraulic oils have been prepared according to a formulation that meets the requirements of ISO VG.

For purpose of comparison, hydraulic oils were prepared using common base oils SN 150 and SN 600 from two different producers (Base oil A and Base oil B). The requirements of ISO VG were achieved using the same amount of additives, widely familiar to experts in the field.

Table 3 compiles the findings for foaming and air release, alongside viscosity measurements at 40 °C and 100 °C, along with the viscosity index.

Figure 4 depicts the relationship between air release time at 50 °C and viscosity grade in the form of a graph.

Figure 5 represents the foaming characteristics of hydraulic oils as a function of viscosity grade.

In Table 4 viscosity, foaming and air release properties of base oils A and B are shown.

Table 3: Comparison of viscosity, foaming, and air release properties between hydraulic oils based on two different base oil sources

Hydraulic oil type according to ISO		Base oil A				
		VG 22	VG 32	VG 46	VG 68	VG 100
Viscosity / mm²/s	40 °C	22.22	32.65	47.23	69.37	100.7
	100 °C	4.418	5.565	7.050	9.007	11.37
Viscosity index		108.5	107.7	106.5	103.8	98.96
ARV at 50 °C / min		1.2	2.2	5.5	10.0	16.7
Foaming[1] / ml	I.	150/0	50/0	20/0	10/0	10/0
	II.	10/0	20/0	20/0	10/0	40/0
	III.	140/0	30/0	20/0	10/0	10/0
Hydraulic oil type according to ISO		Base oil B				
		VG 22	VG 32	VG 46	VG 68	VG 100
Viscosity / mm²/s	40 °C	22.07	32.36	49.78	69.06	100.5
	100 °C	4.407	5.526	7.273	8.941	11.30
Viscosity index		109.1	107.2	105.6	102.9	98.18
ARV at 50 °C / min		1.2	1.6	5.1	9.4	15.3
Foaming[2] / ml	I.	150/0	20/0	20/0	30/0	30/0
	II.	20/0	20/0	20/0	20/0	70/0
	III.	150/0	30/0	50/0	30/0	30/0
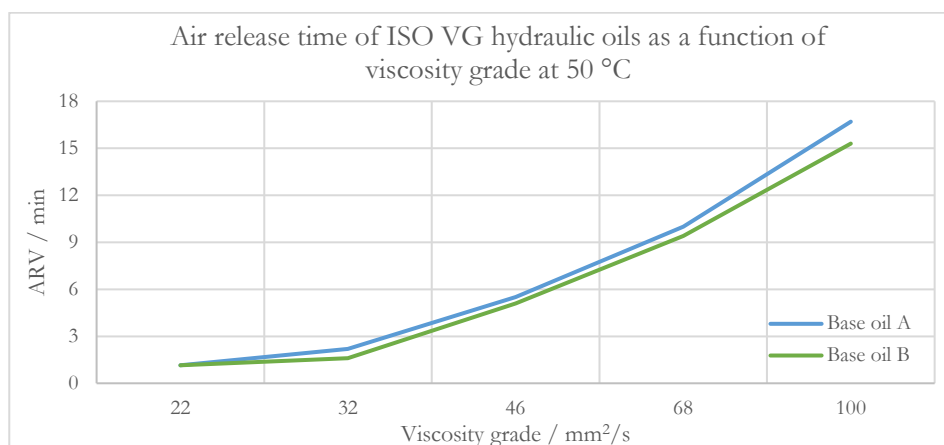
Figure 4: The relationship between air release time and viscosity grade of hydraulic oils.
Source: own.

---

[1] The results of foaming are given in format [at the end of aeration / after 10 minutes].
[2] The results of foaming are given in format [at the end of aeration / after 10 minutes].
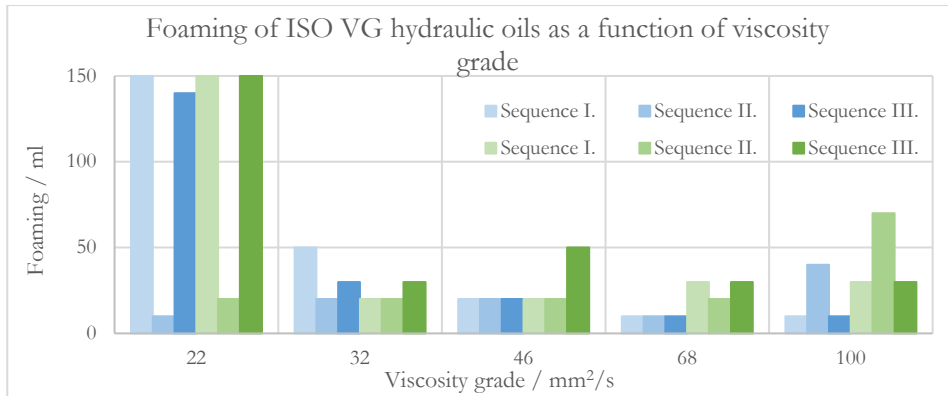
Figure 5: Foaming characteristics of ISO VG hydraulic oils as a function of viscosity grade. Results of hydraulic oils based on base oils A and B are presented with blue and green columns, respectively.

Source: own.

Table 4: Viscosity, foaming and air release properties of base oils A and B

		Base oil A	
		SN 150	SN 600
Viscosity / mm²/s	40 °C	30.00	111.6
	100 °C	5.243	12.07
Viscosity index		105.5	97.30
ARV at 50 °C / min		1.1	17.8
Foaming[3] / ml	I.	370/0	160/0
	II.	30/0	80/0
	III.	370/0	220/0
		Base oil B	
		SN 150	SN 600
Viscosity / mm²/s	40 °C	31.94	111.0
	100 °C	5.441	11.94
Viscosity index		105.0	96.05
ARV at 50 °C / min		1.5	11.5
Foaming[4] / ml	I.	390/0	580/20
	II.	30/0	60/0
	III.	390/0	530/20

In Figure 6 the results of air release time and foaming for base oils A and B are presented as a function of initial viscosity grade (SN 150 and SN 600).

---

[3] The results of foaming are given in format [at the end of aeration / after 10 minutes].
[4] The results of foaming are given in format [at the end of aeration / after 10 minutes].
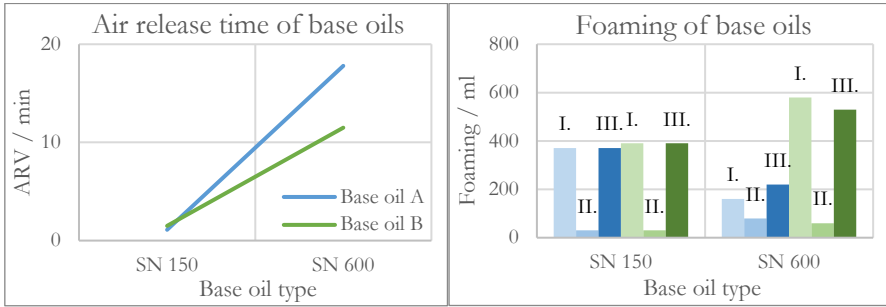
Figure 6: The relationship between air release time and viscosity grade of base oils (left) and foaming characteristics by sequences of base oils (right). Results of base oil A and B are presented with blue and green curve/columns, respectively.

Source: own.

From the results collected in Tables 3 and 4, presented in Figures 4, 5, and 6, it can be concluded that the air release time is a function of viscosity grade – the higher the viscosity, the more difficult it is for the oil to release the air trapped in a sample. The results are comparable with air release values for base oils, which were used to prepare ISO VG hydraulic oils. If we compare hydraulic oils in general based on the base oil, from which they were prepared, we can observe that the higher the air release value for base oil, the higher the air release of hydraulic oils based on the same base oil.

Foaming as a function of viscosity grade does not show the same trend as an air release. Based on the results of foaming of base oils, we cannot observe the same trend for hydraulic oils. Hydraulic oils tend to foam extensively at low viscosity grades, while the effect is barely noticeable at viscosity grades from 32 mm²/s to 68 mm²/s and slightly higher at viscosity grade 100 mm²/s.

It can be concluded that the air release of hydraulic oils is strongly correlated with the air release of base oils and initial viscosity while the same cannot be confirmed in the case of foaming tendency.

6   Summary

Air release time and foaming tendency were checked on fresh hydraulic oils of several viscosity grades prepared from two different base oils. Air release value (ARV) was measured at 50 °C for comparative purposes, regardless of the initial

viscosity of hydraulic oils. The results of ARV confirmed the relationship between base oils and hydraulic oils made from those base oils. The ARV strongly depends on the viscosity grade of hydraulic oils – the higher the viscosity, the more difficult it is for oil to release trapped air. The same trend was not observed at foaming – higher values were determined at samples of hydraulic oils with low viscosity, while the foaming tendency decreased at viscosity grades from 32 mm²/s to 68 mm²/s and slightly increased at viscosity grade 100 mm²/s.

It can be concluded that the air release of hydraulic oils is strongly correlated with the air release of base oils and initial viscosity value, while the same cannot be confirmed for foaming.

Examining the hydraulic oils in use reveals that the propensity for alterations in foaming characteristics becomes more apparent after a specific period of utilization. Nevertheless, the air release value (ARV) does not exhibit such heightened sensitivity in this particular case.

Further investigation will be performed, starting with more base oils from different producers and with other types of hydraulic oils.

References

[1]   Pirro, D. M. & Wessol, A. A. (2001). *Lubrication fundamentals*, 2nd ed. Marcel Dekker, Inc.
[2]   Lovrec, D. & Tič, V. (2022). Stisljivost hidravličnega olja in vpliv zraka. *Ventil*, 6, 492-498.
[3]   Kambič, M. (2023). Izločanje zraka iz olja in penjenje. *IRT3000*, 66-68.
[4]   Lovrec, D. (2016). Vzroki za prisotnost zraka v hidravličnem sistemu. *Ventil*, 4, 310-317.
[5]   Normalab (2023, March 30). *Air release properties of petroleum oil*.
      https://www.normalab.com/en/produit/arv-tech/
[6]   OelCheck GmbH (2023, July 12). *Air and foam in oil*. https://en.oelcheck.com/wiki/air-and-foam-in-oil/
[7]   Linetronic Technologies (2023, August 3). *Foaming Characteristics of Lubricating Oils*.
      https://www.lin-tech.ch/english/fb190000eng.html

Cleanliness of Valve Components – Research of Basic Washing Parameters Through Measuring Dynamic Surface Tension of Liquids

Sven Burnik

Hydraulics d.o.o., Žiri, Slovenia
sven.burnik@poclain.com

The simplest way to control the quality of solution baths in water-based industrial washing is to track the concentration of detergent advised by detergent suppliers. Usually this is made indirectly by titration of total alkalinity of bath. These suggested limits of detergent concentration are usually relatively wide. Additionally, this method can sometimes give an incomplete picture of bath possibility to remove impurities. More detailed information about effectiveness of cleaning solutions could be given by measuring dynamic surface tension. In this paper, some basic measurements of dynamic surface tension done in real process are presented and discussed. Based on the results future developments of washing control and optimization of process parameters are foreseen.

1 Intruduction

Cleanliness of valve components is usually specified only in terms of technical cleanliness specification. In most cases it consists of total mass of impurities extracted from the part surface and the maximum size of the biggest particle found during analysis.

To provide a technical cleanliness value of a component a special method was developed. These analyses are relatively long so we cannot perform these tests on each component during mass production, but we rather rely on statistical process control. Furthermore, these analyses are usually done at final washing steps but not necessarily reflecting bad washing. The analyses are representing the whole manufacturing process of component, and not only washing itself. Often the root causes for impurities found on cleanliness test lie outside of the washing process steps.

To find root causes outside of washing steps, the best practice is that we run the washing process at best possible level or at least it must be as constant and controlled as possible.

Many parameters influence on washing efficiency. One of them is definitely the cleaning agent used in the process.

A cleaning agent for industrial, aqueous cleaning processes consists of builder and surfactant components. The cleaning process causes both components' concentrations to be used up differently due to different absorption of contamination particles and the carry-over effect. Dosing according to the consumption is necessary for ensuring high process reliability.

One possibility for controlling the cleaning agent concentration is titration of total alkalinity. But this method does not give you any insight of washing media contamination or/and its effectivity.

Additional or alternative method for washing media control is measuring surface tension with the bubble pressure method. This method is the most effective way of inspecting washing active surfactants. [1]

S. Burnik: Cleanliness of Valve Components – Research of Basic Washing Parameters Through Measuring Dynamic Surface Tension of Liquids

309

2 Surfactants

2.1 Dynamic surface tension

The following image shows the correlation between surfactant concentration and surface tension. Application-specific dosages of surfactant components are made possible by determining the limit and target values related to an individual cleaning process. [1]
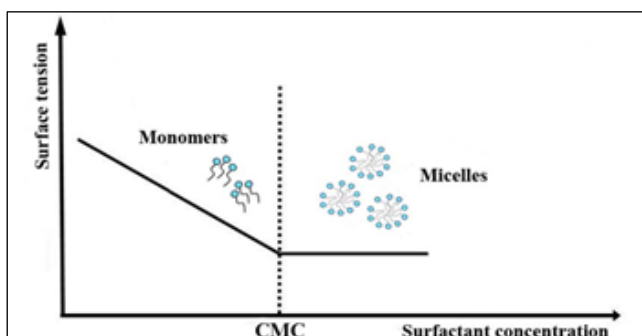
Figure 1: Correlation between surfactant concentration and surface tension.
Source: Pacwa-Plociniczak et al., 2011, CC-BY

2.2 Critical Micelle Concentration (CMC)

Critical Micelle Concentration (CMC) values are important indicators when considering which surfactant will provide optimal performance benefits for your formulation.
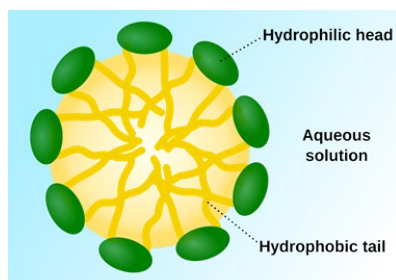
Figure 2: Agglomerates of surfactant molecules inside the liquid.
Source: SuperManu, Wikipedia.org, CC-BY-SA, 2007

When a certain amount of surfactant is added to water, the molecules will begin to form micelles. These consist of agglomerates of surfactant molecules inside the liquid and facilitate washing by storing hydrophilic substances (fats, oils, etc.) within the agglomerates.

The CMC value indicates the amount of surfactant required to reach maximum surface tension reduction. Expressed in wt/%, the lower the CMC, the less surfactant required to effectively emulsify, solubilize, and disperse soils at the surface. In sum, CMC measures the efficiency of surfactants. [2]
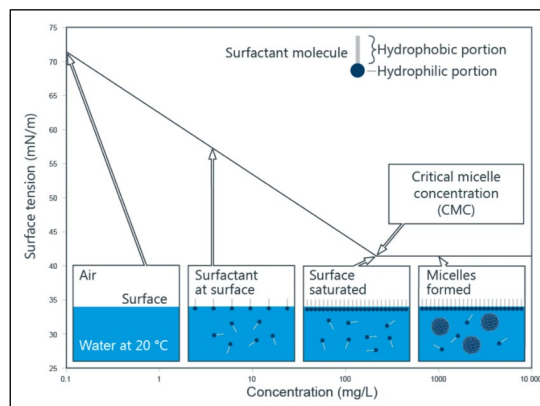
Figure 3: Surface tension of a surfactant solution with increasing concentration, formation of micelles.
Source: own.
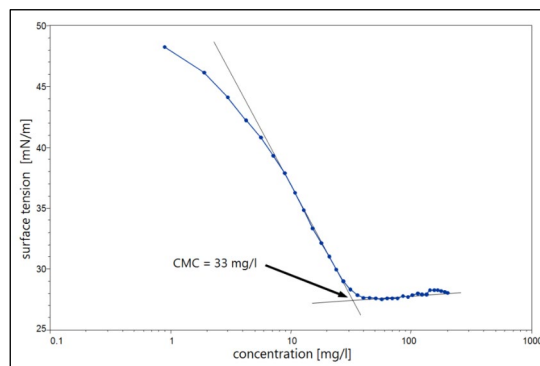
Figure 4: Determination of the CMC with a tensiometer.
Source: own.

S. Burnik: Cleanliness of Valve Components – Research of Basic Washing Parameters Through Measuring Dynamic Surface Tension of Liquids

311

3   CMC Study in real process

To define the state of our current process, we first investigated CMC value of our detergent. We made series of test in laboratory and in real process with an industrial washing machine. We found some significant difference between laboratory environment and real process. In laboratory the CMC value was achieved at around 1.5 % to 1.7 % of detergent concentration.
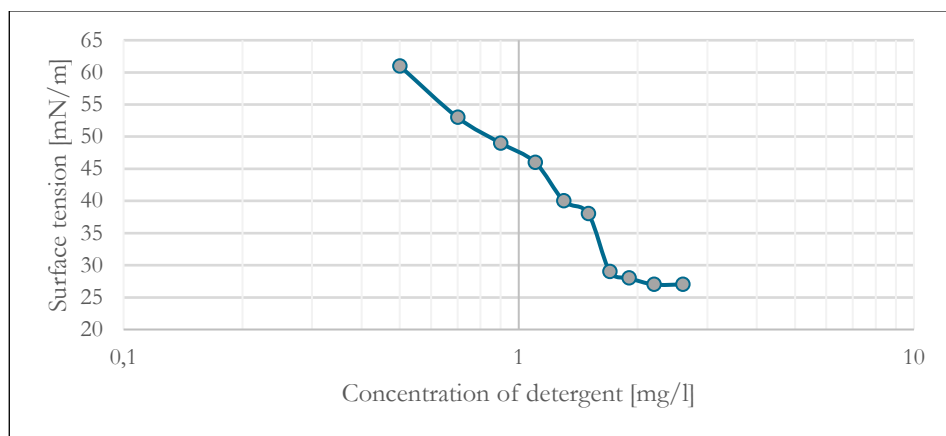
Figure 5: CMC in laboratory condition

Source: own.
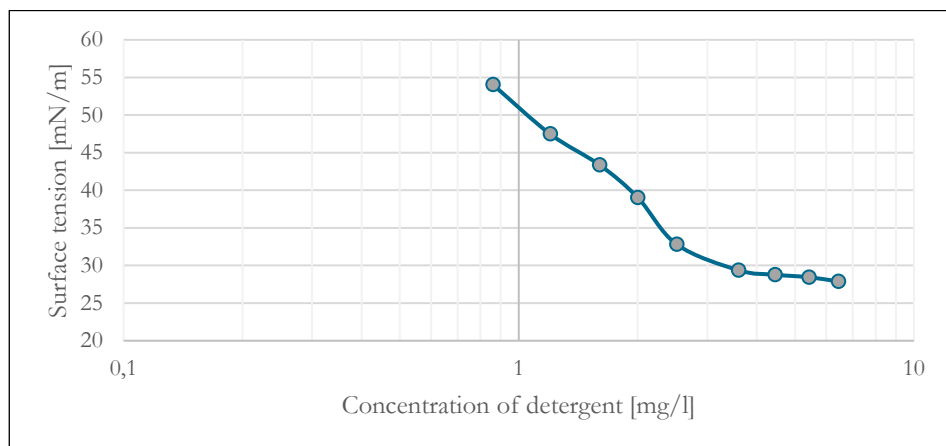
Figure 6: CMC at washing machine

Source: own.

In real process, the CMC value was higher – around 2.5 % to 3.0 % of detergent concentration. This means that we needed to have at least 3.0 % of detergent in our washing baths to reach the most effective cleaning. Adding more detergent was not improving the process. By adding more detergent, we only got an undesirable effect of excessive foaming.

4   Dynamic surface tension in real process

Since such a big difference between laboratory conditions and conditions in real process was observed, we decided to make further analysis on solutions taken directly from our process. Additionally, we know that surfactants activity is very much dependent on temperature. So, each sample taken from the process was measured instantly. Then we took measurements of the same sample during cool down phase to get an insight on this temperature dependency.

From figure 7, we can get similar conclusion about CMC value as in CMC study in previous chapter. We can see that adding more than around 3 % concentration of detergent does not improve the process anymore. The lowest surface tension reached is slightly below 30 mN/m.
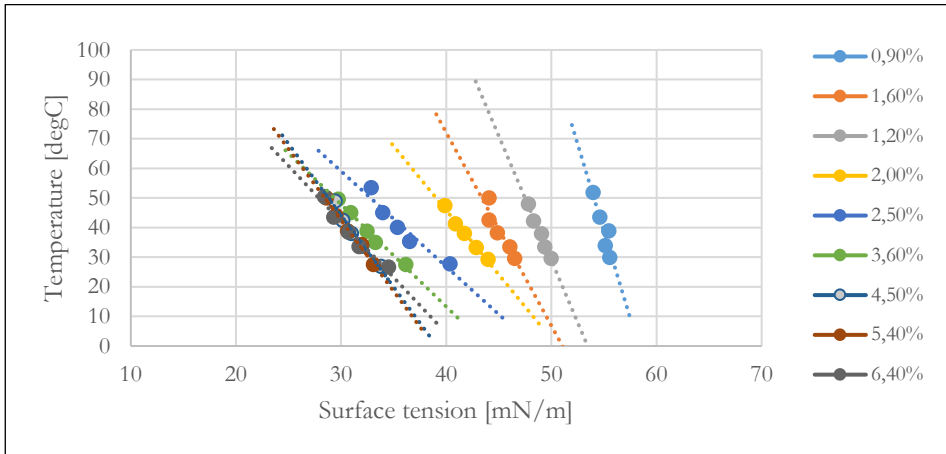
Figure 7: Surface tension in washing tank
Source: own.

S. Burnik: Cleanliness of Valve Components – Research of Basic Washing Parameters Through Measuring Dynamic Surface Tension of Liquids

313

In addition to the previous chapter, we can see another phenomenon in figure 7. The temperature dependency is significantly bigger at higher concentration. But it reaches its limits at CMC values when temperature dependency also loses its linear progression.

4.1   'Ageing' of washing media

In aqueous media industrial washing process, we reach a point when washing media is so contaminated that we need to empty the washing tanks and setup a new solution with fresh water and detergent.

Figure 8 presents washing media surface tension in first two weeks after new setup is presented by days. Concentration measured by titration was relatively constant – from 2.4 % to 2.5 %. On the other hand, we can see some significant difference in surface tension.
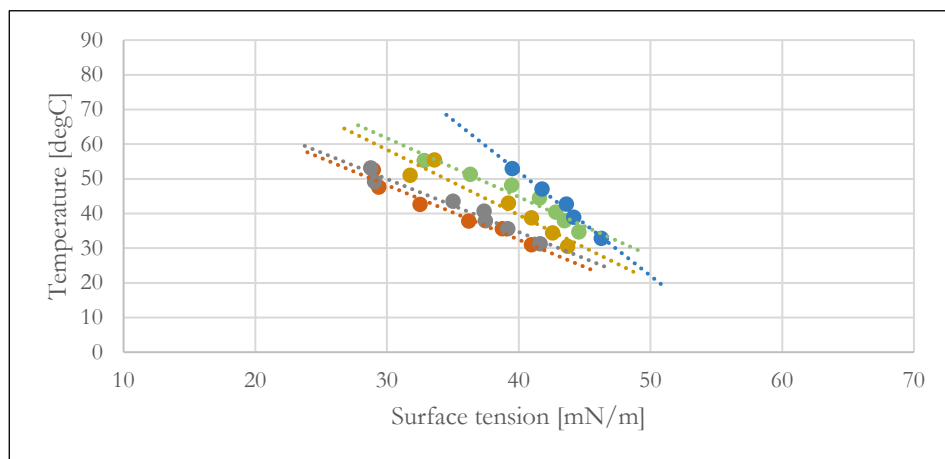
Figure 8: Relatively fresh washing media (1st and 2nd week after new setup)
Source: own.

After 2 to3 weeks the dynamics in our washing media changes. At the same concentration limits we get less temperature dependency but also some significantly higher values of surface tension at operating temperatures (approx. 60 °C).
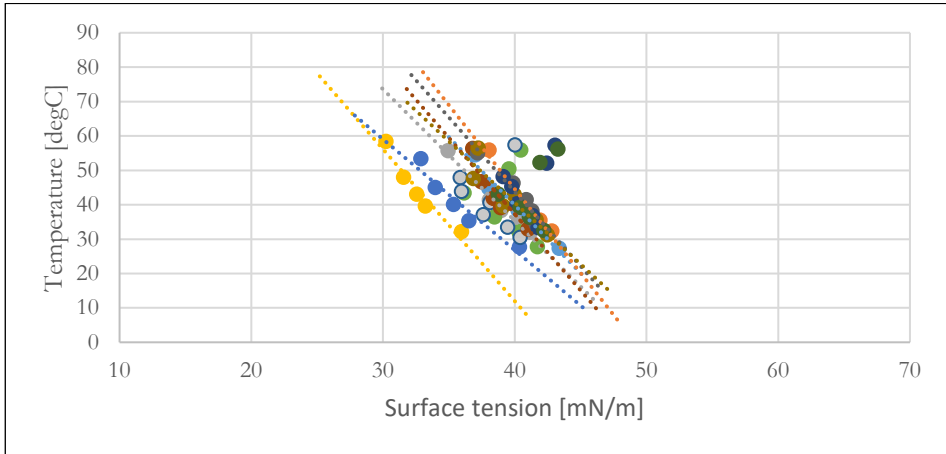
Figure 9: Washing media after weeks of operating (3rd-5th week after fresh setup)
Source: own.

4.2.   Oil separator

One of the biggest contaminants in industrial washing media is oil. During washing of parts different kind of oils are removed from its surface. The oil contaminants are emulsified into washing media. For further effective washing these oils needs to be removed from washing media as much and as fast as possible. To do this an oil separator is usually added to the washing machine.
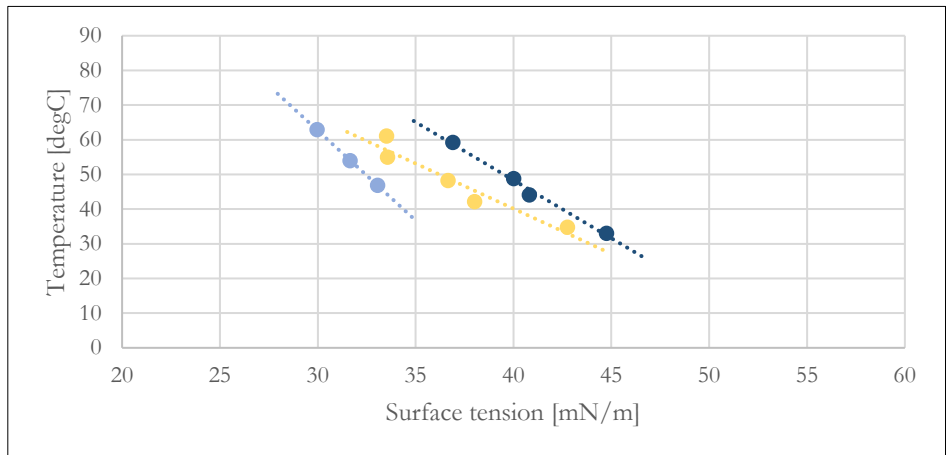
Figure 10: Role of oil separator in surface tension of washing media
Source: own.

S. Burnik: Cleanliness of Valve Components – Research of Basic Washing Parameters Through Measuring Dynamic Surface Tension of Liquids

315

In previous chapter we saw that our media is losing its effectivity through weeks of operating. One of possible cause for this is how effectively the oil removal process is set.

The samples shown on figure 10 were taken at some special periods in our process.

The yellow line represents a normal working without taking any focus on oil separator. The blue lines are representing two extremes found in our process. The light blue values were taken after careful continuous oil removal. When the oil separator was not doing well due to some excessive flows, we got values represented with dark blue colour.

5   Conclusions

In comparison to technical cleanliness test or titration of total alkalinity, measuring of dynamic surface tension of washing liquids gave us a faster and more precise data about quality of our washing process.

We managed to adjust parameters such as dosing of detergent, temperature of washing liquid etc. much faster than we would only by using previous methods. We got an insight into 'ageing' of washing liquids and when to setup a new, fresh liquid without relying only on daily period set by experience. Intake of oil and other oily contaminants are changing a lot and if we rely only on daily set period, we can sometimes make a fresh setup too soon or too late.

With these basic measurements we also found out that our oil separator was not working effectively. When the washing liquids were fresh, we did not detect bigger deviations but in few weeks, we found some significant deviations at operating temperatures. By detailed checking of possible root causes and measuring of dynamic surface tension we found out that oil separator was one of the main contributors to less efficient performance (deviations at operating temperatures mentioned in chapter 4.1.).

Together with two other control devices which are tracking only oily, greasy, etc. contaminants in washing liquid and on parts surface, a detailed analysis were made on one specific detergent with working on one specific washing machine. We

compared data with other detergents and washing machines in production where we got some significant differences. By this we could set some approximate limits for each device. Based on this research a standard on a group level was issued. It includes suggestions for regular control of washing process to achieve the desired technical cleanliness level.

All this detailed data gathered on one washing detergent and on one type of washing machine will be used in future when testing other detergents and washing machines. Validation of both will be much shorter and less risky than validation only by using methods of technical cleanliness test and titration of total alkalinity.

References

[1]   https://www.sita-process.com/applications/industrial-parts-cleaning-liquids-media/inspecting-and-monitoring-the-surfactant-component-of-a-cleaning-agent/; last visited on 1.6.2023
[2]   https://www.jrhessco.com/critical-micelle-concentration-measuring-surfactant-efficiency/; last visited on 1.6.2023

Conference sponsors

General sponsor
HAWE Hidravlika d.o.o.

Social event sponsor:
POCLAIN Hydraulics d.o.o.

Round table sponsor:
NOO
University of Maribor, Ministry of Higher Education, Science and Innovation

Conference organization has been sponsored by:
OLMA d.o.o.
LA & CO d.o.o.
FESTO d.o.o.
BECKHOFF Avtomatizacija d.o.o.
TESNILA Bogadi d.o.o.
TIMTEC Defence d.o.o.
IPRO Ing d.o.o.

Media sponsors:
VENTIL   UM Press   IRT3000

We would like to thank all the sponsors for their support and contribution to the organization of the conference!
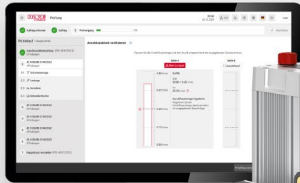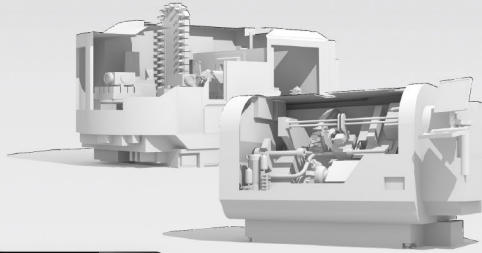
Nothing moves without us.
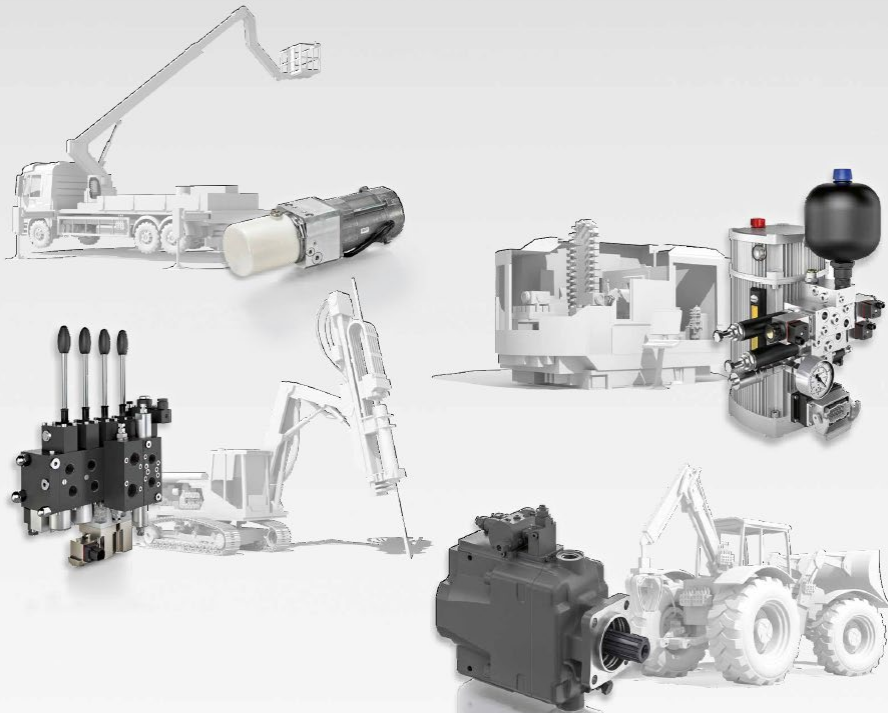
When great things are being moved with hydraulics, HAWE is involved.

HAWE Hydraulik is a leading manufacturer of technologically advanced, high-quality hydraulic components and systems. HAWE products are used wherever high quality, high power and maximum precision is required - whether in machine tools, construction machinery or wind turbines.

www.hawe.com

HAWE HYDRAULIK

S pravim mazivom
ne spodrsava

OLMA
www.olma.si

Olma d.o.o., Poljska pot 2, 1000 Ljubljana,
tel.: (01) 58 73 600, e-pošta: order@olma.si

Certified Excellence

rexroth

A Bosch Company
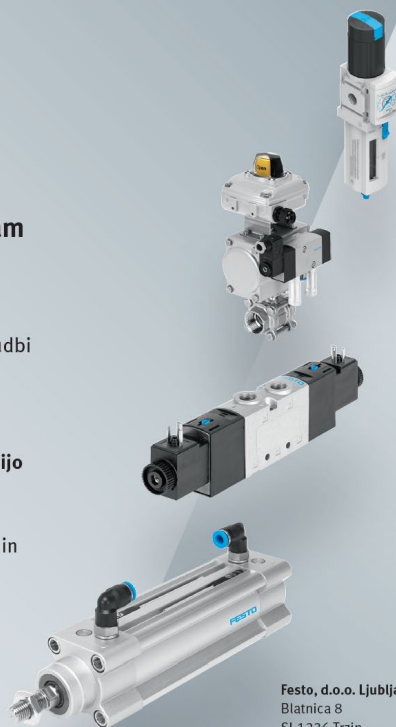
EtherCAT in tehnologija PC krmilnikov: New Automation Technology

EtherCAT in tehnologija PC krmilnikov postavljata standarde po svetu:
- vse komponente za industrijske računalnike, V/I periferijo, pogonsko tehniko in avtomatizacijo
- uveljavljeni mejniki v avtomatizaciji na globalni ravni: Lightbus, V/I moduli, programska oprema TwinCAT
- maksimalna skalabilnost in odprti sistemi za avtomatizacijo
- na osnovi visoko zmogljivega področnega vodila EtherCAT
- združevanje ključnih funkcij naprave ali sistema na eni krmilni platformi
- univerzalne rešitve za avtomatizacijo za prek 20 različnih tipov industrije: od CNC obdelovalnih strojev do pametne avtomatizacije zgradb

Skenirajte za
več informacij
o sistemu
Beckhoff

New Automation Technology **BECKHOFF**

mikroDOKAZila

– DA STE NA PRAVI POTI –

Univerza v Mariboru

Fakulteta za strojništvo

KOMPETENCE

SPRETNOSTI

OKREPITE SE

PRIJAVI SE ZDAJ!

S CENTROM ZA VSEŽIVLJENJSKO UČENJE FS UM

cvu.fs@um.si

+386 (2) 220 7700

www.fs.um.si

MIKRODOKAZILA

Pripravljamo nabor pilotnih izobraževanj, z namenom izobraziti in opremiti posameznika s specifičnim znanjem, veščinami in kompetencami.

IZOBRAŽEVANJA ZA PODJETJA PO MERI

Podjetjem omogočamo pripravo učnih modulov, ki neposredno naslavljajo potrebe poslovnega procesa. Zaposlene opremimo z znanjem, spretnostmi in kompetencami, katere lahko takoj uporabijo na delovnem mestu. Praktični del izvajamo na najsodobnejši tehnološki opremi ali po dogovoru na opremi naročnika.

NAČRT ZA
OKREVANJE
IN ODPORNOST

Univerza v Mariboru

REPUBLIKA SLOVENIJA
**MINISTRSTVO ZA VISOKO ŠOLSTVO,
ZNANOST IN INOVACIJE**

**Financira
Evropska unija**
NextGenerationEU

- **Strokovni in znanstveni prispevki**
- **Iz prakse za prakso**
- **Ventil na obisku**
- **Novice - zanimivosti**
- **Aktualno iz industrije**
- **Novosti na trgu**
- **Podjetja predstavljajo**
- **Ali ste vedeli**
- **Dogodki**

Spoštovani!

Ventil je znanstveno-strokovna revija in objavlja prispevke, ki obravnavajo razvojno in raziskovalno delo na Univerzi, inštitutih in v podjetjih s področja fluidne tehnike, avtomatizacije in mehatronike. Revija želi seznanjati strokovnjake z dosežki slovenskih podjetij, o njihovih izdelkih in dogodkih, ki so povezani z razvojem in s proizvodnjo na področjih, ki jih revija obravnava. Prav tako želi ustvariti povezavo med slovensko industrijo in razvojno in raziskovalno sfero ter med slovenskim in svetovnim proizvodnim, razvojnim in strokovnim prostorom. Naloga revije je tudi popularizacija področij fluidne tehnike, avtomatizacije in mehatronike še posebno med mladimi. Skrbi tudi za strokovno izrazoslovje na omenjenih področjih.

Revija Ventil objavlja prispevke avtorjev iz Slovenije in iz tujine, v slovenskem in angleškem jeziku. Prispevkom v slovenskem jeziku je dodan povzetek v angleščini, prispevki v angleščini pa so objavljeni z daljšim povzetkom v slovenskem jeziku. Člani znanstveno strokovnega sveta so znanstveniki in strokovnjaki iz Slovenije in tujine. Revijo pošiljamo na več naslovov v tujini in imamo izmenjavo z drugimi revijami v Evropi. Revija je vodena v podatkovni bazi INSPEC.

Štiriindvajsetletno izhajanje revije Ventil pomeni, da je v prostoru neprecenljiva za razvoj stroke. Uredništvo si skupaj z znantveno strokovnim svetom prizadeva za visokokvalitetno raven in relevantnost objav, ki bosta v prihodnosti vse napore usmerila v to, da bo kvalitetna raven še višja. V ta namen vključuje v znantveno strokovni svet priznane znanstvenike, raziskovalce in strokovnjake, ki s svojim znanjem vspodbujajo vsak na svojem področju objavljanje rezultatov razvojnega in raziskovalnega dela. Uredništvo spremlja razvoj stroke in znanstveno raziskovalno delo doma in v vtujini preko konferenc, delavnic in seminarjev ter z izmenjavo tuje periodike.

Revija je priznana v tujini, še posebno na področju fluidne tehnike, kar želimo doseči tudi na področju mehatronike in avtomatizacije. Preko objav v reviji se promovirajo dosežki slovenske znanosti in industrijske proizvodnje. Revija je in bo tudi v prihodnje prostor za predstavljanje kvalitetnih razvojnih in raziskovalnih dosežkov slovenske industrije in raziskovalne sfere na področju fluidne tehnike, avtomatizacije in mehatronike.

Uredništvo

International Conference Fluid Power 2023

Darko Lovrec, Vito Tič (eds.)

University of Maribor, Faculty of Mechanical Engineering, Maribor, Slovenia
darko.lovrec@um.si, vito.tic@um.si

The International Fluid Power Conference is a two-day event, intended for all those professionally involved with hydraulic or pneumatic power devices and for all those, wishing to be informed about the 'state of the art', new discoveries and innovations within the field of hydraulics and pneumatics. The gathering of experts at this conference in Maribor has been a tradition since 1995, and is organised by the Faculty of Mechanical Engineering at the University of Maribor, in Slovenia. Fluid Power conferences are organised every second year and cover those principal technical events within the field of fluid power technologies in Slovenia, and throughout this region of Europe. This year's conference is taking place on the 20th and 21sr September in Maribor. The main focus of this year's contributions is on the components and system development in the field of fluid power technology.

University of Maribor

Faculty of Mechanical Engineering

FT2023